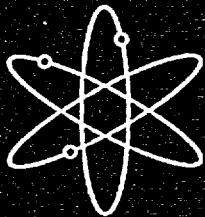


# Fatigue Analysis of Components for 60-Year Plant Life



**Pacific Northwest National Laboratory**



**U.S. Nuclear Regulatory Commission  
Office of Nuclear Regulatory Research  
Washington, DC 20555-0001**



**AVAILABILITY OF REFERENCE MATERIALS  
IN NRC PUBLICATIONS**

**NRC Reference Material**

As of November 1999, you may electronically access NUREG-series publications and other NRC records at NRC's Public Electronic Reading Room at [www.nrc.gov/NRC/ADAMS/index.html](http://www.nrc.gov/NRC/ADAMS/index.html).

Publicly released records include, to name a few, NUREG-series publications; *Federal Register* notices; applicant, licensee, and vendor documents and correspondence; NRC correspondence and internal memoranda; bulletins and information notices; inspection and investigative reports; licensee event reports; and Commission papers and their attachments.

NRC publications in the NUREG series, NRC regulations, and *Title 10, Energy*, in the Code of *Federal Regulations* may also be purchased from one of these two sources.

1. The Superintendent of Documents  
U.S. Government Printing Office  
P. O. Box 37082  
Washington, DC 20402-9328  
[www.access.gpo.gov/su\\_docs](http://www.access.gpo.gov/su_docs)  
202-512-1800
2. The National Technical Information Service  
Springfield, VA 22161-0002  
[www.ntis.gov](http://www.ntis.gov)  
1-800-553-6847 or, locally, 703-605-6000

A single copy of each NRC draft report for comment is available free, to the extent of supply, upon written request as follows:

Address: Office of the Chief Information Officer,  
Reproduction and Distribution  
Services Section  
U.S. Nuclear Regulatory Commission  
Washington, DC 20555-0001

E-mail: [DISTRIBUTION@nrc.gov](mailto:DISTRIBUTION@nrc.gov)  
Facsimile: 301-415-2289

Some publications in the NUREG series that are posted at NRC's Web site address [www.nrc.gov/NRC/NUREGS/indexnum.html](http://www.nrc.gov/NRC/NUREGS/indexnum.html) are updated regularly and may differ from the last printed version.

**Non-NRC Reference Material**

Documents available from public and special technical libraries include all open literature items, such as books, journal articles, and transactions, *Federal Register* notices, Federal and State legislation, and congressional reports. Such documents as theses, dissertations, foreign reports and translations, and non-NRC conference proceedings may be purchased from their sponsoring organization.

Copies of industry codes and standards used in a substantive manner in the NRC regulatory process are maintained at—

The NRC Technical Library  
Two White Flint North  
11545 Rockville Pike  
Rockville, MD 20852-2738

These standards are available in the library for reference use by the public. Codes and standards are usually copyrighted and may be purchased from the originating organization or, if they are American National Standards, from—

American National Standards Institute  
11 West 42<sup>nd</sup> Street  
New York, NY 10036-8002  
[www.ansi.org](http://www.ansi.org)  
212-642-4900

The NUREG series comprises (1) technical and administrative reports and books prepared by the staff (NUREG-XXXX) or agency contractors (NUREG/CR-XXXX); (2) proceedings of conferences (NUREG/CP-XXXX); (3) reports resulting from international agreements (NUREG/IA-XXXX); (4) brochures (NUREG/BR-XXXX), and (5) compilations of legal decisions and orders of the Commission and Atomic and Safety Licensing Boards and of Directors' decisions under Section 2.206 of NRC's regulations (NUREG-0750).

**DISCLAIMER:** This report was prepared as an account of work sponsored by an agency of the U.S. Government. Neither the U.S. Government nor any agency thereof, nor any employee, makes any warranty, expressed or implied, or assumes any legal liability or responsibility for any third party's use, or the results of such use, of any information, apparatus, product, or process disclosed in this publication, or represents that its use by such third party would not infringe privately owned rights.

**NUREG/CR-6674  
PNNL-13227**

---

---

# **Fatigue Analysis of Components for 60-Year Plant Life**

---

---

**Manuscript Completed: May 2000  
Date Published: June 2000**

**Prepared by  
M.A. Khaleel, F.A. Simonen, H.K. Phan, PNNL  
D.O. Harris, D. Dedhia, EMT, Inc.**

**Pacific Northwest National Laboratory  
Richland, WA 99352**

**Subcontractor:  
Engineering Mechanics Technology, Inc.  
San Jose, CA 95129**

**S.K. Shaukat, NRC Project Manager**

**Prepared for  
Division of Engineering Technology  
Office of Nuclear Regulatory Research  
U.S. Nuclear Regulatory Commission  
Washington, DC 20555-0001  
NRC Job Code W6671**



## Abstract

Recent data indicate that the effects of light-water reactor environments can significantly reduce the fatigue resistance of materials. To assess the significance of proposed revisions to design fatigue curves and to compare the expected probability of fatigue failure at a 60-year plant life versus a 40-year plant life, probabilistic fatigue calculations for a sample of components in the reactor pressure boundary were performed at Pacific Northwest National Laboratory. Probabilities of fatigue failures and associated core-damage frequencies were estimated for RPV and piping components of five pressurized water reactor and two boiling water reactor plants. These calculations were made possible by the development of a new version of the pc-PRAISE probabilistic fracture mechanics code that has the ability to simulate the initiation of fatigue cracks in combination with a simulation of the subsequent growth of these fatigue cracks. The calculations indicate

that the critical components with the highest probabilities of failure can have through-wall crack frequencies for the water environment that are on the order of about  $5 \times 10^{-2}$  per component per year. However, these components with the highest fatigue usage show little or no increase in the failure frequency from 40 years to 60 years. Other components with lower failure probabilities can have their failure frequencies increased by a factor of about 10 over this same 20-year time period. In contrast, changing to a reactor water environment from an air environment increased the calculated failure probabilities by a factor of about 100. Contributions to core damage frequencies were also estimated for each of the vessel and piping components. The maximum calculated contributions were on the order of  $10^{-6}$  per year. An appendix to this report describes sensitivity calculations that evaluate the effects of the many uncertainties of concern.

# CONTENTS

	Page
1 INTRODUCTION .....	1.1
2 PLANTS AND COMPONENTS CONSIDERED .....	2.1
3 METHODOLOGY FOR THROUGH-WALL CRACK CALCULATIONS .....	3.1
4 FATIGUE CRACK INITIATION MODEL .....	4.1
4.1 Low Alloy and Carbon Steels in Water and Air .....	4.1
4.2 304 and 316 Stainless Steels in Water .....	4.2
4.3 304 and 316 Stainless Steels in Air .....	4.2
4.4 316NG Stainless Steel in Water .....	4.2
4.5 316NG Stainless Steel in Air .....	4.3
4.6 Implementation of Crack Initiation Model .....	4.3
4.7 Treatment of Size Effects .....	4.5
5 FATIGUE CRACK GROWTH MODEL .....	5.1
5.1 Fatigue Crack-Growth Model .....	5.1
5.2 Stress Intensity Factor .....	5.1
5.3 Fatigue Crack Growth for Carbon and Low Alloy Steel Materials .....	5.2
5.4 Fatigue Crack Growth for Stainless Steel Materials .....	5.3
5.5 Treatment of Through-Wall Stress Gradients .....	5.3
5.6 Calculation of Through-Wall Crack Frequency .....	5.4
6 CONDITIONAL PROBABILITIES OF SMALL AND LARGE LEAK RATES .....	6.1
7 CONDITIONAL CORE DAMAGE PROBABILITIES .....	7.1
7.1 Risk-Informed Evaluations of Surry-1 Plant .....	7.2

7.2	Evaluations Based on PRAs for Various Plants .....	7.2
7.3	Newer Vintage Combustion Engineering Plant .....	7.5
7.4	Older Vintage Combustion Engineering Plant .....	7.5
7.5	B&W 177 Fuel Assembly Plant .....	7.6
7.6	Newer Vintage Westinghouse Plant .....	7.6
7.7	Older Vintage Westinghouse Plant .....	7.6
7.8	Newer Vintage GE Plant .....	7.7
7.9	Older Vintage GE Plant .....	7.7
7.10	Summary and Generalization of PRA Results .....	7.7
8	METHODOLOGY FOR CALCULATING CORE DAMAGE FREQUENCIES .....	8.1
9	RESULTS OF CALCULATIONS FOR SELECTED COMPONENTS .....	9.1
9.1	Analysis Procedure .....	9.1
9.2	Comparison of Probabilities with Usage Factors .....	9.3
9.3	Probabilities at 60 Years Versus 40 Years .....	9.4
9.4	Water Versus Air Environment .....	9.7
9.5	Sensitivity Calculations for Surge Line Elbow .....	9.7
10	SUMMARY AND CONCLUSIONS .....	10.1
11	REFERENCES .....	11.1
	Appendix A - Fatigue Evaluation Calculations for All Components of Selected Plants .....	A.1
	Appendix B - Core Damage Frequency Calculations .....	B.1
	Appendix C - pcPRAISE 4.2: Expanded Capabilities to Analyze Fatigue Crack Initiation .....	C.1
	Appendix D - A Review of Stress Intensity Factors for Semi-Elliptical Circumferential Interior Surface Cracks in Pipes .....	D.1
	Appendix E - Sensitivity Studies for Fracture Mechanics Calculations .....	E.1

## Figures

	Page
4.1 Example of Probabilistic S-N Curves for Low-Alloy Steel .....	4.4
6.1 Leak Probabilities Versus Time for 15.24-cm (6-in.) Diameter Pipe .....	6.4
6.2 Leak Probabilities Versus Time for 30.48-cm (12-in.) Diameter Pipe .....	6.4
6.3 Leak Probabilities Versus Time for 60.96-cm (24-in.) Diameter Pipe .....	6.5
6.4 Conditional Probabilities of Small and Large Leaks .....	6.6
9.1 Comparison of Calculated Usage Factors with Calculated Through-Wall Crack Probabilities .....	9.4
9.2 Cumulative Probability of Crack Initiation at 40 Years Versus 60 Years .....	9.5
9.3 Cumulative Probability of Through-Wall Crack at 40 Years Versus 60 Years .....	9.5
9.4 Through-Wall Cracks per Year at 40 Years Versus 60 Years .....	9.6
9.5 Core-Damage Frequency at 40 Years Versus 60 Years .....	9.6
9.6 Comparison of Probabilities of Fatigue Crack Initiation for Air Versus Water Environment and for 40-Year Life and 60-Year Life .....	9.9
9.7 Comparison of Through-Wall Crack Probabilities for Air Versus Water Environment and for 40-Year Life and 60-Year Life .....	9.9
9.8 Comparison of CDFs for Air Versus Water Environment and for 40-Year Life and 60-Year Life .....	9.10
9.9 Calculated Probabilities of Crack Initiation and Through-Wall Crack for the Surge Line Elbow of the Newer Vintage Combustion Engineering Plant .....	9.10
9.10 Calculated Probabilities of Crack Initiation and Through-Wall Crack for the Reactor Pressure Vessel (RPV) Outlet Nozzle of the Newer Vintage Combustion Engineering Plant .....	9.11
9.11 Calculated Probabilities of Through-Wall Crack for the Surge Line Elbow of the Newer Vintage Combustion Engineering Plant for Alternative Through-Wall Stress Distributions .....	9.12

## Tables

	Page
2.1 Plants Considered in the 60-Year Fatigue Study .....	2.1
2.2 Components Selected for Fatigue Analysis .....	2.1
2.3 Components for Newer Vintage Combustion Engineering Plant .....	2.2
2.4 Components for Older Vintage Combustion Engineering Plant .....	2.2
2.5 Components for Babcock and Wilcox Plant .....	2.3
2.6 Components for Newer Vintage Westinghouse Plant .....	2.3
2.7 Components for Older Vintage Westinghouse Plant .....	2.3
2.8 Components for Newer Vintage General Electric Plant .....	2.4
2.9 Components for Older Vintage General Electric Plant .....	2.4
6.1 Example Results of Calculations for Small Leaks, Large Leaks, and Pipe Breaks for Fatigue Failures Caused by Fabrication Flaws .....	6.3
6.2 Conditional Probabilities of Failure Modes Given the Occurrence of a Through-Wall Crack .....	6.6
7.1 Summary of PRAs in Terms of Plant Vendors, Plant Vintages, Break Sizes, and Leak Rates .....	7.3
7.2 Conditional Core-Damage Probabilities for PWR and BWR Plants .....	7.7
7.3 Leak/Break Categories for Generic Treatment of PRA Results for PWR and BWR Plants ..	7.8
7.4 Consequences Assigned for Generic Leak/Break Categories for PWR and BWR Plants ...	7.8
9.1 Summary of Results for All Seven Plants—Water Environment .....	9.2
9.2 Summary of Results for All Seven Plants—Air Environment .....	9.8

## Executive Summary

Some recent data indicate that the effects of light-water reactor environments could significantly reduce the fatigue resistance of materials. These data show that the American Society of Mechanical Engineers design fatigue curves may not be conservative for nuclear power plant reactor system environments. The Argonne National Laboratory has developed revised fatigue curves based on test data from small, polished specimens cycled to failure in the laboratory in water having the temperatures, pressures, and chemistries of light-water reactor operating conditions and has published these curves in NUREG/CR-6335. To assess the significance of the revised fatigue curves and to compare the expected probability of fatigue failure at a 60-year plant life versus a 40-year plant life, probabilistic fatigue calculations for a sample of components in the reactor pressure boundary have been performed at Pacific Northwest National Laboratory. Probabilities of fatigue failures and associated core-damage frequencies were estimated for RPV and piping components of five pressurized water reactor and two boiling water reactor plants. These calculations were made possible by the development of a new version of the pc-PRAISE probabilistic fracture mechanics code that has the ability to simulate the initiation of fatigue cracks in combination with a simulation of the subsequent growth of these fatigue cracks. It is recognized that there are uncertainties in the calculated failure probabilities, both in the fracture mechanics model itself and from the inputs to the model. Uncertain inputs include data for the cyclic stresses that could differ from the stresses imposed by the actual plant operating conditions and assumptions regarding strain rates and environmental variables used to predict the initiation of cracks. An appendix to this report describes sensitivity calculations that evaluate the effects of many of the uncertainties of concern.

The results of the present calculations are believed to be useful when they are applied as best estimates and in terms of relative probabilities. This report compares through-wall crack frequencies at the end of a 40-year plant life to those at the end of a 60-year plant life and component-failure probabilities for a reactor water environment with those for an air environment. The calculations of this report indicate that the critical components with the highest probabilities of failure can have through-wall crack frequencies for the water environment that are on the order of about  $5 \times 10^{-2}$  per component per year. However, these components show little or no increase in the failure frequency from 40 years to 60 years. Other components with lower failure probabilities can have their failure frequencies increased by a factor of about 10 over this same 20-year time period. In contrast, changing to a reactor water environment from an air environment increased the calculated failure probabilities by a factor of about 100.

Contributions to core damage frequencies have also been estimated for each of the vessel and piping components. These calculations were performed on a best-estimate basis using conservative inputs only when more refined calculations were not feasible. The objective was to demonstrate that none of the components are expected to make significant contributions to core damage. The maximum calculated contributions are on the order of  $10^{-6}$  per year. Calculated core-damage frequencies for the components with the highest failure frequencies show essentially no increase in core damage frequency from 40 to 60 years.

## Abbreviations

ANL	Argonne National Laboratory	LPR	low-pressure recirculation
ANSI	American National Standards Institute	LWR	light-water reactor
ASME	American Society of Mechanical Engineers	NRC	U.S. Nuclear Regulatory Commission
B&W	Babcock and Wilcox	NSSS	nuclear steam system supplier
BWR	boiling-water reactor	pc-PRAISE	probabilistic fracture mechanics code for piping reliability analysis
CCDP	conditional core damage probability	PFM	probabilistic fracture mechanics
CDF	core damage frequency	PNNL	Pacific Northwest National Laboratory
CE	Combustion Engineering	PRA	probabilistic risk assessment
CRDM	control rod drive mechanism	PWR	pressurized water reactor
CS	carbon steel	RCIC	reactor core isolation cooling
CUF	cumulative usage factor	RCS	reactor coolant systems
DO	dissolved oxygen	RHR	residual heat removal
GE	General Electric	RMS	root mean square
HPI	high-pressure injection	RPV	reactor pressure vessel
INEL	Idaho National Engineering Laboratory	S-N	strain versus life
IPE	individual plant examination	SS	stainless steel
IREP	Interim Reliability Evaluation Program	TVA	Tennessee Valley Authority
LAS	low-alloy steel	VEPCO	Virginia Power
LOCA	loss-of-coolant accident	W	Westinghouse
LPI	low-pressure injection	WOG	Westinghouse Owners Group

# 1 INTRODUCTION

Reactor pressure boundary components of many older plants were designed to codes, such as the Piping Code of the United States of America National Standards Institute ANSI B31.1, that did not require an explicit component fatigue analysis. Currently, American Society of Mechanical Engineers (ASME) Code Section III requires a fatigue evaluation of the components of the reactor-coolant pressure boundary. Aspects of the code fatigue methodology have come under review because recent test data indicate that the effects of light-water reactor (LWR) environments could significantly reduce the fatigue resistance of materials and show that the ASME design fatigue curves may not be conservative for nuclear power plant primary system environments.

Argonne National Laboratory (ANL) has developed revised fatigue curves based on laboratory test data from small, polished specimens cycled to failure in water with temperatures, pressures, and chemistries that simulate LWR conditions (NUREG/CR-6335) (Keisler et al. 1995). ANL has also developed statistical models for estimating the effects of various material, loading, and environmental conditions on the fatigue life of these materials. Fatigue strain versus life (S-N) data for carbon steel (CS), low-alloy steel (LAS), and austenitic stainless steels (SS) were published in NUREG/CR-6335. The statistical models from the ANL work can be used to estimate the probability of fatigue-crack initiation.

Using the curves developed by ANL, the Idaho National Engineering Laboratory (INEL) investigated the significance of the interim fatigue curves as published in NUREG/CR-5999 (Mujumdar et al. 1993) by performing deterministic fatigue evaluations for a sample of components in the reactor coolant pressure boundary of LWRs. Cumulative usage factors (CUFs) for each component were reported by INEL in a table format in NUREG/CR-6260. The objective of the

present study was to calculate component failure probabilities rather than fatigue usage factors. It was, however, of interest to compare trends in calculated failure probabilities with calculated fatigue usage factors. Pacific Northwest National Laboratory (PNNL) did not recalculate values of usage factors for this purpose, but based comparisons on values of usage factors from the INEL work that were based on ANL correlations (NUREG/CR-6260) (Ware et al. 1995). The INEL usage factors corresponded to the expected number of fatigue cycles (rather than the original number of fatigue cycles used for design) and, as such, were consistent with the cycles used in PNNL's probabilistic calculations.

The first evaluations of failure probabilities from fatigue of various reactor-coolant-system components were performed by U.S. Nuclear Regulatory Commission (NRC) staff under Generic Safety Issue GSI-78.<sup>(a)</sup> However, these fatigue analyses assumed a 40-year plant life and used the fatigue life data from NUREG/CR-6237. The objective of the present work by PNNL was to perform calculations necessary to determine probabilities of fatigue failure of selected LWR components and to address a 60-year plant life (versus 40-year life) using the most recent fatigue life data reported in NUREG/CR-6335 (Keisler et al. 1995) and updated by ANL.<sup>(b)</sup> PNNL and ANL research staff interacted closely to ensure that the calculations were based on the latest fatigue data and correlation equations being developed by ANL for the NRC Office of Research.

The present calculations removed many of the assumptions and approximations of the initial GSI-78 calculations. The new probabilistic

- 
- (a) Memorandum dated September 23, 1994, from E.S. Beckjord to A.C. Thadani, "Generic Issue 78, Monitoring of Fatigue Transient Limits for the Reactor Coolant System."
  - (b) Private communication with O. Chopra, "Updated Fatigue Design Curves for Austenitic Stainless Steel in LWR Environments" (1998).

fracture mechanics capabilities have permitted a number of important issues to be addressed. It is no longer necessary to assume that initiated fatigue cracks have the full service life of the plant to grow to through-wall depths. The simulations now start the growth of the cracks at whatever time the cracks may initiate. The effects of through-wall stress gradients on the growth of initiated cracks are also included in the most recent calculations with the probabilistic fracture mechanics code for piping reliability analysis (pc-PRAISE). The initial lengths of the fatigue cracks are now addressed along with a simulation of the subsequent changes in the crack lengths during the fatigue-crack-growth process. The fatigue cracks can also initiate at multiple sites around the circumference of a pipe and can subsequently link to potentially form cracking around a large fraction of the pipe circumference.

The present study is based on the cyclic stresses that the components are projected to experience during their 40-year and/or 60-year plant life. These stresses are extracted from the information presented in NUREG/CR-6260 (Ware et al. 1995), which in turn were extracted from conservatively calculated stress values given in design stress reports for the plants.

The ANL data provided the needed statistical model of the number of cycles to crack initiation. All calculations in the present report have assumed that the ANL definition of crack initiation (25 percent load drop) corresponds to a 3-mm crack in a fatigue test specimen. A crack of about 3-mm is required to increase the specimen compliance sufficiently to result in a detectable drop in load during a displacement-controlled fatigue test.

The number of cycles to crack initiation in the ANL equations is a function of the material type, water/air environment, temperature, dissolved oxygen content, sulfur content, and strain rate. In the present study, the fatigue damage caused by various stress amplitudes is calculated by Miner's rule, using fatigue SN curves that account for the statistical distribution of the cycles to crack

initiation. In the present calculations, the probability of crack initiation is equal to the probability that the calculated CUF is greater than one. It is also assumed that the initiated fatigue cracks grow based on fracture mechanics rules.

The probability that a 3-mm crack becomes a through-wall crack is computed using pc-PRAISE. Details of the pc-PRAISE code are described in NUREG/CR-5864 (Harris and Dedhia 1992). New features of the code that were developed to support the present calculations are described in Appendix C. Appendix D reviews the crack-tip stress-intensity-factor solutions used by pc-PRAISE to evaluate circumferential flaws in piping. Appendix A gives detailed inputs and results of the calculations for probabilities of crack initiation and for probabilities of through-wall cracks using the pc-PRAISE code.

A final part of the study estimated the consequences (i.e., core-damage frequencies [CDFs]) of the through-wall cracks. Conditional probabilities that a through-wall crack results in small or large leak rates were first estimated. This was followed by an evaluation based on published probabilistic risk assessment (PRA) data regarding core damage for small and large loss-of-coolant accidents (LOCAs). These risk evaluations were performed in a conservative and bounding manner. The objective was to demonstrate that the components of concern are expected to make insignificant contributions to core damage. Detailed tabulations of the calculations for CDFs are given in Appendix B.

The calculations of consequences accounted for the fact that through-wall cracks will most often cause only small leaks that have no safety consequences. Larger leak rates can cause core damage, but the conditional probabilities of core damage can still be relatively low because nuclear power plants have safety systems that are designed to mitigate the consequences of leaks and breaks. Estimates of conditional CDFs in this report were based on 1) probabilistic fracture mechanics calculations that predicted the probability that a given through-wall crack would cause

various leak rates or pipe breaks and 2) published data from PRAs that provided conditional probabilities of core damage given the occurrence of small leaks, large leaks, and pipe breaks.

Engineering Mechanics Technology Incorporated was engaged under subcontract to implement a number of PNNL-developed enhancements to the pc-PRAISE code. A parallel computational capability for predicting fatigue failures based on a Latin Hypercube method (Khaleel and Simonen 1995) was applied to benchmark the new version of pc-PRAISE. This methodology also permitted calculations of failure probabilities that were too small to address computationally by the Monte-Carlo method.

The present report includes a description of the plants and components that are addressed by the fatigue analyses. This is followed by a discussion of the fracture-mechanics methodology along with documentation of the probabilistic equations from ANL that were used to predict the number of cycles to crack initiation. Another section of the report focuses on the consequences of small and large leaks and describes how calculations were performed to estimate CDFs. The final section of the report summarizes the results in

terms of absolute and relative failure probabilities, giving particular attention to how these calculated probabilities differ for a 40-year versus 60-year plant life. Failure probabilities for water versus air environments are then compared. Appendices A and B describe actual inputs and results of the calculations. Details of the modified pc-PRAISE code are documented in Appendix C. Appendix D reviews the accuracy of crack-tip stress intensity factors calculated by pc-PRAISE. Also included in this appendix are calculations that tested the code and evaluated the sensitivity of calculated failure probabilities to modeling assumptions and input parameters. Discussions of the fracture mechanics model describe assumptions made to account for the effects of through-wall stress gradients on crack propagation and describe methods used to estimate the fractions of through-wall cracks that become small leaks and large leaks. Appendix E describes sensitivity calculations that evaluate effects of uncertainties in the fracture mechanics calculations. This appendix also describes calculations that exercise the crack linking model and shows how calculated crack lengths change when the inputs to the linking model are changed.

## 2 PLANTS AND COMPONENTS CONSIDERED

The plants considered in this study are presented in Table 2.1. As shown in Table 2.1, PNNL considered five pressurized-water reactor (PWR) plants and two boiling-water reactor (BWR) plants. The components chosen for fatigue evaluation are presented in Table 2.2. Although the fracture-mechanics calculations were based on data from stress reports for actual plants, the stress tabulations of NUREG/CR-6260 (Ware et al. 1995) did not reveal the identities of these plants. To assess the significance of a 60-year

plant life compared to a 40-year life, probabilistic fatigue evaluations of a sample of the components in the reactor-coolant pressure boundary were performed. For each plant, four to nine locations were investigated, including locations within the reactor pressure vessel. These results can be used to calculate the contribution of these components to core damage frequency and to develop recommendations for a 60-year operational period. Tables 2.3 through 2.9 give specifics of the individual components for all the plants.

<b>Table 2.1 Plants Considered in the 60-Year Fatigue Study</b>	
<b>PWRs</b>	<b>BWRs</b>
Babcock and Wilcox (B&W)	General Electric (GE) – Newer Vintage
Combustion Engineering (CE) – Newer Vintage	GE – Older Vintage
CE – Older Vintage	
Westinghouse (W) – Newer Vintage	
W – Older Vintage	

<b>Table 2.2 Components Selected for Fatigue Analysis</b>	
<b>PWRs</b>	<b>BWRs</b>
1. Reactor pressure vessel shell and lower head	1. Reactor pressure vessel shell and lower head
2. Reactor vessel inlet and outlet nozzles	2. Reactor vessel feedwater nozzle
3. Pressurizer surge line (including hot leg and pressurizer nozzles)	3. Reactor recirculation piping (including inlet and outlet nozzles)
4. Reactor coolant piping charging system nozzle	4. Core spray line reactor vessel nozzle and associated class 1 piping
5. Reactor coolant piping safety injection nozzle	5. Residual heat removal class 1 piping
6. Residual heat removal (RHR) system class 1 piping	6. Feedwater line class 1 piping

**Table 2.3 Components for Newer Vintage Combustion Engineering Plant**

Component	Location	Material
Reactor Vessel	Lower head/shell	SA-533, Grade B, Class 1 <sup>(a)</sup>
	Inlet nozzle	SA-508, Class 2 <sup>(a)</sup>
	Outlet nozzle	SA-508, Class 2 <sup>(a)</sup>
Surge Line	Elbow	SA-376, Type 316 <sup>(b)</sup>
Charging Nozzle	Nozzle	SA-182, Grade F1 <sup>(a)</sup>
	Safe end	SA-182, Type 316 <sup>(b)</sup>
Safety Injection Nozzle	Nozzle	SA-182, Grade F1 <sup>(a)</sup>
	Safe end	SA-531, Grade CF8M, Type 316 <sup>(b)</sup>
Shutdown Cooling Line	Elbow	SA-376, Type 316 <sup>(b)</sup>
(a) Carbon or low-alloy steel.		
(b) Stainless steel.		

**Table 2.4 Components for Older Vintage Combustion Engineering Plant**

Component	Location	Material
Reactor Vessel	At lower head to shell juncture	SA-533, Grade B, Class 1 <sup>(a)</sup>
	Inlet nozzle	SA-336 <sup>(a)</sup>
	Outlet nozzle	SA-336 <sup>(a)</sup>
Surge Line	Elbow	SA-376, Type 316 <sup>(b)</sup>
Charging Nozzle	Nozzle	SA-351, Type 316 <sup>(b)</sup>
Safety Injection Nozzle	Nozzle	SA-351, Type 316 <sup>(b)</sup>
Shutdown Cooling Line	Elbow	SA-376, Type 316 <sup>(b)</sup>
(a) Carbon or low-alloy steel.		
(b) Stainless steel.		

<b>Table 2.5 Components for Babcock and Wilcox Plant</b>		
<b>Component</b>	<b>Location</b>	<b>Material</b>
Reactor Vessel	Near support skirt juncture	SA-302, Grade B <sup>(a)</sup>
	Outlet nozzle	SA-508, Class 2 <sup>(a)</sup>
Makeup/HPI <sup>(b)</sup> Nozzle	Safe end	SA-376, Type 316 <sup>(c)</sup>
Decay Heat Removal Line	Reducing tee	SA-376, Type 316 <sup>(c)</sup>
(a) Carbon or low-alloy steel. (b) HPI = high-pressure injection. (c) Stainless steel.		

<b>Table 2.6 Components for Newer Vintage Westinghouse Plant</b>		
<b>Component</b>	<b>Location</b>	<b>Material</b>
Reactor Vessel	At lower head to shell juncture	SA-533, Grade B, Class 1 <sup>(a)</sup>
	Inlet nozzle	SA-508, Class 2 <sup>(a)</sup>
	Outlet nozzle	SA-508, Class 2 <sup>(a)</sup>
Charging Nozzle	Nozzle	SA-182, Type 316N <sup>(b)</sup>
Safety Injection Nozzle	Nozzle	SA-182, Type 316 <sup>(b)</sup>
Residual Heat Removal Line	Inlet transition	SA-376, Type 316 <sup>(b)</sup>
(a) Carbon or low-alloy steel. (b) Stainless steel.		

<b>Table 2.7 Components for Older Vintage Westinghouse Plant</b>		
<b>Component</b>	<b>Location</b>	<b>Material</b>
Reactor Vessel	At core support guide weld	SA-302, Grade B <sup>(a)</sup>
	Inlet nozzle inside surface	SA-302, Grade B <sup>(a)</sup>
	Inlet nozzle outside surface	SA-302, Grade B <sup>(a)</sup>
	Outlet nozzle inside surface	SA-302, Grade B <sup>(a)</sup>
	Outlet nozzle outside surface	SA-302, Grade B <sup>(a)</sup>
Charging Nozzle	Nozzle	SA-182, Type 316 <sup>(b)</sup>
Safety Injection Nozzle	Nozzle	SA-182, Type 316 <sup>(b)</sup>
Residual Heat Removal Line	Tee	SA-376, Type 316 <sup>(b)</sup>
(a) Carbon or low-alloy steel. (b) Stainless steel.		

<b>Component</b>	<b>Location</b>	<b>Material</b>
Reactor Vessel	Near CRDM penetration	SA-508, Class 2 <sup>(a)</sup>
Feedwater Nozzle	Safe end	SA-508, Class 1 <sup>(a)</sup>
Recirculation System	Tee on suction pipe	SA-358, Type 304 <sup>(b)</sup>
Core Spray Line	Safe-end extension	SA-508, Class 1 <sup>(a)</sup>
RHR Line	Straight pipe	SA-333, Grade 6 <sup>(a)</sup>
Feedwater Line	Elbow	SA-333, Grade 6 <sup>(a)</sup>
(a) Carbon or low-alloy steel.		
(b) Stainless steel.		

<b>Component</b>	<b>Location</b>	<b>Material</b>
Reactor Vessel	At lower head to shell transition	SA-302 <sup>(a)</sup>
Feedwater Nozzle	Bore	SA-508 <sup>(a)</sup>
Recirculation System	RHR return line tee	SA-358, Type 304, Class 1 <sup>(b)</sup>
Core Spray System	Nozzle	SA-302, Grade B <sup>(a)</sup>
	Safe end	SA-376, Type 316 <sup>(b)</sup>
Residual Heat Removal Line	Tapered transition	SA-358, Type 304, Class 1 <sup>(b)</sup>
Feedwater Line	RCIC tee	SA-106, Grade B <sup>(a)</sup>
(a) Carbon or low-alloy steel.		
(b) Stainless steel.		

### 3 METHODOLOGY FOR THROUGH-WALL CRACK CALCULATIONS

The calculations of this report estimate the probability that fatigue cycles will result in through-wall cracks in pressure boundary components of reactor coolant systems (RCSs) of PWR and BWR plants. Operating lives of both 40 years and 60 years are addressed. These evaluations address only the contribution of initiated fatigue cracks to failure probabilities, and exclude the contributions of pre-existing cracks. However, the scope of the calculations could be expanded to address the contributions of preexisting flaws. In such calculations the probabilities for the number and sizes of preexisting fabrication flaws would replace the calculated probabilities of crack initiation. In this regard data on occurrence rates for welding flaws in piping of 2.54- to 5.08-cm (1- to 2-in.) wall thickness would indicate occurrence rates of roughly  $10^{-2}$  flaws per inch of weld circumference for surface and near surface flaws in piping welds (WCAP-14572 Revision 1 [Westinghouse Owners Group 1997] and Chapman 1993).

The methodology of the present calculations consists of two parts. The first part calculates the probability that a fatigue crack will initiate as a function of time over the life of the plant. The second part evaluates the probability that these cracks will grow to become through-wall cracks. The following is a summary of the supporting data, the analytical models and the assumptions used in the failure probability calculations.

Stress amplitudes and the numbers of stress cycles for the selected components during a 40-year plant life were taken from NUREG/CR-6260 (Ware et al. 1995). The types of transients for the 60-year plant life were assumed to be the same as those for the 40-year plant life. The stress amplitudes were also the same as the 40-year stress amplitudes. The 60-year number of accumulated cycles was calculated by multiplying the 40-year number of cycles by a factor of 1.5.

The number of cycles to crack initiation was a function of the material type, water/air environment, temperature, dissolved oxygen content, sulfur content and strain rate. The material types were carbon steel, low-alloy steel, 304/316 austenitic stainless steel and 316NG stainless steel. The statistical models of NUREG/CR-6335 (Keisler et al. 1995) were used to calculate the number of cycles to crack initiation corresponding to given probabilities (or percentiles) of the material S-N curves. For the PWR plants, the curves for high-sulfur steel (0.015 weight percent) and a low-oxygen environment (0.01-ppm) were used. For the BWR plants, the curves for high sulfur steel and a high-oxygen environment (0.10 ppm) were used. The strain rates for both PWR and BWR components (low alloy and carbon steel) were assumed to be 0.001% (see NUREG/CR-6260) (Ware et al. 1995). For 316 stainless steel, the strain rate was 0.004%. For all components, the temperature was assumed to be 290°C. The values of elastic modulus for carbon steels, low-alloy steels, and austenitic stainless steels were 186,200, 184,200, and 175,900 Mpa ( $27.0 \times 10^6$ ,  $26.7 \times 10^6$ , and  $25.5 \times 10^6$  psi), respectively.

The interior surface of LWR reactor vessels and nozzles made of carbon/low-alloy steel are clad with stainless steel. NUREG/CR-5999 (Majumdar et al. 1993) makes no differentiation between the environmental effects caused by temperature and by contact with reactor coolant. It is expected that the temperature effect is significant, and in this sense the base metal under the cladding is not immune to environmental effects. Fatigue cracking of cladding is neglected.

The ANL statistical distributions for the number of cycles to initiate a 3-mm crack for a given cyclic stress amplitude were lognormal. The parameters of the probabilistic fatigue initiation curves were based on the ANL revised fatigue

curves published in NUREG/CR-6335 (Keisler et al. 1995). The equations for stainless steels included recent updates for fatigue life correlations provided by ANL.<sup>(a)</sup>

The CUFs as given in this report (for purposes of information only) were taken directly from the INEL work of NUREG/CR-6260 (Ware et al. 1995), which made use of the fatigue (S-N) curves of NUREG/CR-5999 (Majumdar et al. 1993). These curves accounted for environmental effects and included significant reductions in life compared to the fatigue curves of the ASME code. As such, the calculated fatigue usage factors for the sample components are generally greater than those calculated when the components were originally designed.

In the early phase of the present project, the initiated cracks were assumed for purposes of the crack-growth calculations to be present at the beginning of life. This conservative assumption was consistent with the approach used by the NRC staff in the 40-year plant life study. Concern with this assumption resulted in a major effort to expand the capabilities of the pc-PRAISE code (see Appendix C) to account for the initiation of fatigue cracks, and to simulate their growth over the time period beginning at the actual time of their initiation.

In the probabilistic fracture mechanics calculations, the crack propagation was assumed to start from a 3-mm deep initiated flaw, which can then grow to a critical size (through-wall) and result in component failure. This 3-mm size was based on the estimated crack size that can give a measurable 25 percent load drop in the testing of standard fatigue specimens. Sensitivity calculations were performed to evaluate the effect of changing this crack depth from 3 mm to 2 mm or 4 mm. The resulting changes in the calculated probabilities of through-wall cracks were about a factor of two,

and much smaller in those cases with relatively high probabilities. It was decided not to include the initial crack depth as a variable to be simulated by the probabilistic model. Furthermore, the uncertainty in the initial crack depth was considered to be indirectly captured by the statistical scatter in the fatigue life data. Further simulation of uncertainties in the crack depth could therefore introduce a double counting of the scatter in experimental data.

The cyclic stress levels from the INEL report were used to calculate both fatigue usage factors and probabilities of crack initiation. The stresses include the effects of stress concentrations in a manner prescribed by the ASME Code approach of stress indices. In many cases the stress indices may address very high local stresses (e.g. weld root stress concentrations) and have values up to 2.0. It was recognized that such surface stresses are not indicative of internal stress levels remote from the stress concentration. The present crack-growth calculations with pc-PRAISE were based on the same cyclic stresses as used for crack-initiation calculations. Adjustments were made to crack-tip stress intensity factors for deeper cracks to account for the effects of through-wall stress gradients that are characteristic of thermal type transients. However, the fracture mechanics calculations may be conservative for many locations, because the stress distributions from stress concentrations would have larger stress gradients than the stress gradients from thermal transients.

The present calculations of fatigue crack-growth rates were based on data that included the effects of environment on the growth rates. However, the growth rate correlations did not address the specific factors that enhance the crack-growth rates in the same level of detail as addressed in the Argonne correlations for crack initiation. The crack-growth calculations also assumed that the random variations in fatigue crack-growth rates were not correlated with the corresponding random variations in the cycles to crack initiation. If such correlations were to exist, the predictions for probabilities of through-wall cracks could be

---

(a) Private communication with O. Chopra, "Updated Fatigue Design Curves for Austenitic Stainless Steel in LWR Environments" (1998).

somewhat unconservative. However, this simplifying assumption greatly facilitated the calculations, and has a good technical basis because the technical literature (Wire and Li 1996) provides evidence to support the assumption of independence. In general, crack initiation and

crack growth involve independent material damage mechanisms, such that the factors of environment and loading rates affect the mechanisms for crack initiation and crack growth differently.

## 4 FATIGUE CRACK INITIATION MODEL

The present work used a crack-initiation model (NUREG/CR-6237) (Keisler et al. 1994) developed by ANL. This model estimates the probability of initiating a 3-mm deep fatigue crack based on existing fatigue (S-N) data, foreign and domestic, for carbon, low-alloy and stainless steels used in the construction of nuclear power plant components. Only data obtained on smooth specimens tested under fully reversed loading conditions were considered. A statistical distribution was fitted by ANL to S-N data to describe the scatter in the fatigue data. The ANL statistical distributions of cycles to initiate a 3-mm crack for a given cyclic stress were lognormal. The parameters of the probabilistic fatigue initiation curves were based on the ANL revised fatigue curves published in NUREG/CR-6335 (Keisler et al. 1995). The equations for stainless steels included recent updates for fatigue life correlations provided by ANL.<sup>(a)</sup>

### 4.1 Low-Alloy and Carbon Steels in Water and Air

The number of cycles ( $N_i$ ) to crack initiation in LASs and CSs for both water and air environments is expressed by (NUREG/CR-6335) (Keisler et al. 1995) as

$$\ln[N_i(x)] = (6.857 - 0.766I_w) - (0.275 - 0.382I_w)I_s + 0.52F^{-1}[x] - (1.813 + 0.219I_s)\ln\{\epsilon_a - 0.080 - 0.014I_s + 0.026F^{-1}[1-x]\} - 0.001337(1 - I_w) + 0.1097S^*T^*O^*\dot{\epsilon}^* - \ln(4)$$

where  $\epsilon_a$  = the applied strain amplitude, %  
 $I_w$  = indicator for water environment. It is 1 for water and 0 for air environment  
 $I_s$  = indicator for steel type equal to 1

for carbon steel and 0 for low-alloy steel

$T$  = the test temperature in °C. The variables  $S^*$ ,  $T^*$ ,  $O^*$ ,  $\dot{\epsilon}^*$  are transformed sulfur content, temperature, dissolved oxygen (DO), and strain rate, respectively, defined as follows:

$$S^* = \begin{cases} S & 0 < S < 0.015 \text{ wt. \%} \\ 0.015 & S > 0.015 \text{ wt. \%} \end{cases}$$

$$T^* = \begin{cases} 0 & T < 150^\circ\text{C} \\ T - 150 & T > 150^\circ\text{C} \end{cases}$$

$$O^* = \begin{cases} 0 & DO < 0.05 \text{ ppm} \\ DO & 0.05 \text{ ppm} \leq DO \leq 0.5 \text{ ppm} \\ 0.5 & DO > 0.5 \text{ ppm} \end{cases}$$

$$\dot{\epsilon}^* = \begin{cases} 0 & \dot{\epsilon} > 1\% / s \\ \ln(\dot{\epsilon}) & 0.001 \leq \dot{\epsilon} \leq 1\% / s \\ \ln(0.001) & \dot{\epsilon} > 0.001\% / s \end{cases}$$

The functions  $F^{-1}[x]$  and  $F^{-1}[1-x]$  are the inverse of the standard normal cumulative distribution function. The constant 0.1097 replaces the value of 0.554 of Equation 18 of NUREG/CR-6335 (Keisler et al. 1995) as per an eMail communication of June 25, 1996, from J. Keisler of ANL to M.A. Khaleel of PNNL.

The term  $\ln(4)$  was included by ANL in order to apply the fatigue data from small test specimens to full size components. This term applies a factor of 4.0 reduction to the cycles to failure to account for size effects, surface finish and geometry. The factor of 4.0 was selected because it gave a relatively good correlation between the small specimen fatigue data and published results of fatigue experiments performed on small (22.86-cm [9-in.] diameter) pressure vessels.

<sup>(a)</sup> Private communication with O. Chopra, "Updated Fatigue Design Curves for Austenitic Stainless Steel in LWR Environments" (1998).

## 4.2 306 and 316 Stainless Steels in Water

The fatigue life of Types 304 and 316 stainless steel in water is

$$\ln[N_f(x)] = 5.841 + 0.52 F^{-1}[x] - 2.172 \ln\{\varepsilon_a - 0.108 + 0.026 F^{-1}[1-x]\} + T^{\Delta} \dot{\varepsilon}^{\Delta} O^{\Delta} - \ln(4)$$

where  $\varepsilon_a$  = the applied strain amplitude, %  
 $T$  = the test temperature in °C. The variables  $T^{\Delta}$ ,  $\dot{\varepsilon}^{\Delta}$ ,  $O^{\Delta}$  are transformed temperature, strain rate, and DO.

The transformed variables  $T^{\Delta}$ ,  $\dot{\varepsilon}^{\Delta}$ ,  $O^{\Delta}$  are defined as follows:

$$T^{\Delta} = \begin{cases} 0 & T < 200^{\circ}\text{C} \\ 1 & T \geq 200^{\circ}\text{C} \end{cases}$$

$$\dot{\varepsilon}^{\Delta} = \begin{cases} 0 & \dot{\varepsilon} > 0.4\%/s \\ \ln(\dot{\varepsilon}/0.4) & 0.0004 \leq \dot{\varepsilon} \leq 0.4\%/s \\ \ln(0.0004/0.4) & \dot{\varepsilon} < 0.0004\%/s \end{cases}$$

$$O^{\Delta} = \begin{cases} 0.260 & \text{DO} < 0.05 \text{ ppm} \\ 0.172 & \text{DO} \geq 0.05 \text{ ppm} \end{cases}$$

The functions  $F^{-1}[x]$  and  $F^{-1}[1-x]$  are the inverse of the standard normal cumulative distribution function.

## 4.3 306 and 316 Stainless Steels in Air

The fatigue life of Types 304 and 316 stainless steel in air is

$$\ln[N_f(x)] = 6.776 + 0.52 F^{-1}[x] - 2.172 \ln\{\varepsilon_a - 0.108 + 0.026 F^{-1}[1-x]\} + T^{\Delta} \dot{\varepsilon}^{\Delta} O^{\Delta} - \ln(4)$$

where  $\varepsilon_a$  = the applied strain amplitude, %  
 $T$  = the test temperature in °C. The variables  $T^{\Delta}$  and  $\dot{\varepsilon}^{\Delta}$  are transformed

temperature and strain rate, respectively.

The transformed variables  $T^{\Delta}$  and  $\dot{\varepsilon}^{\Delta}$  are defined as follows:

$$T^{\Delta} = \begin{cases} 0 & T < 250^{\circ}\text{C} \\ ((T-250)/525)^{0.24} & T \geq 250^{\circ}\text{C} \end{cases}$$

$$\dot{\varepsilon}^{\Delta} = \begin{cases} 0 & \dot{\varepsilon} > 0.4\%/s \\ \ln(\dot{\varepsilon}/0.4) & 0.0004 \leq \dot{\varepsilon} \leq 0.4\%/s \\ \ln(0.0004/0.4) & \dot{\varepsilon} < 0.0004\%/s \end{cases}$$

The functions  $F^{-1}[x]$  and  $F^{-1}[1-x]$  are the inverse of the standard normal cumulative distribution function.

## 4.4 316NG Stainless Steel in Water

There were no available equations specific to 316NG stainless steel that expressed the variability of fatigue lives in terms of the distribution functions as given above for 304/316 stainless steel. However, ANL provided equations to PNNL that gave the median fatigue lives for both types of stainless steels, which indicated that the 316NG grade had a somewhat better fatigue life than the 304/316 materials. Coefficients in the above equation giving the statistical distribution for the 304/316 were adapted to address the 316NG material in accordance with the relative values of median fatigue lives. Only two of the 47 components addressed in the present study were of 316NG. For these components, the fatigue life of Type 316NG stainless steel was calculated from

$$\ln[N_f(x)] = 7.000 + 0.52 F^{-1}[x] - 1.788 \ln\{\varepsilon_a - 0.108 + 0.026 F^{-1}[1-x]\} + T^{\Delta} \dot{\varepsilon}^{\Delta} O^{\Delta} - \ln(4)$$

here  $\varepsilon_a$  = the applied strain amplitude, %  
 $T$  = the test temperature in °C. The variables  $T^{\Delta}$ ,  $\dot{\varepsilon}^{\Delta}$ ,  $O^{\Delta}$  are transformed temperature, strain rate, and DO, respectively.

The transformed variables  $T^d$ ,  $\dot{\epsilon}^d$ ,  $O^d$  are defined as follows:

$$T^d = \begin{cases} 0 & T < 200^\circ\text{C} \\ 1 & T \geq 200^\circ\text{C} \end{cases}$$

$$\dot{\epsilon}^d = \begin{cases} 0 & \dot{\epsilon} > 0.4\%/s \\ \ln(\dot{\epsilon}/0.4) & 0.0004 \leq \dot{\epsilon} \leq 0.4\%/s \\ \ln(0.0004/0.4) & \dot{\epsilon} < 0.0004\%/s \end{cases} \quad (4.6)$$

$$O^d = \begin{cases} 0.260 & DO < 0.05 \text{ ppm} \\ 0.172 & DO \geq 0.05 \text{ ppm} \end{cases}$$

The functions  $F^{-1}[x]$  and  $F^{-1}[1-x]$  are the inverse of the standard normal cumulative distribution function.

#### 4.5 316NG Stainless Steel in Air

There were no available equations specific to 316NG stainless steel in air that expressed the variability in fatigue lives in terms of the distribution functions as given above for 304/316 stainless steel. However, as for the case of the water environment, ANL provided equations to PNNL that gave the median fatigue lives for both types of stainless steels in air, which indicated that the 316NG grade had a somewhat better fatigue life than the 304/316 materials. Coefficients in the above equation giving the statistical distribution for the 304/316 was adapted to address the 316NG material in accordance with the relative values of median fatigue lives. Only two of the 47 components addressed in the present study were of 316NG. For these components, the fatigue life of Type 316NG stainless steel in air was calculated from

$$\ln[N_f(x)] = 7.503 + 0.52 F^{-1}[x] - 1.788 \ln\{\epsilon_a - 0.108 + 0.026 F^{-1}[1-x]\} + T^d \dot{\epsilon}^d - \ln(4)$$

where  $\epsilon_a$  = the applied strain amplitude, %  
 $T$  = the test temperature in  $^\circ\text{C}$ . The variables  $T^d$  and  $\dot{\epsilon}^d$  are transformed

temperature and strain rate, respectively.

The transformed variables  $T^d$ ,  $\dot{\epsilon}^d$  are defined as follows:

$$T^d = \begin{cases} 0 & T < 250^\circ\text{C} \\ [(T - 250)/525]^{0.24} & T \geq 250^\circ\text{C} \end{cases}$$

$$\dot{\epsilon} = \begin{cases} 0 & \dot{\epsilon} > 0.4\%/s \\ \ln(\dot{\epsilon}/0.4) & 0.0004 \leq \dot{\epsilon} \leq 0.4\%/s \\ \ln(0.0004/0.4) & \dot{\epsilon} < 0.0004\%/s \end{cases}$$

The functions  $F^{-1}[x]$  and  $F^{-1}[1-x]$  are the inverse of the standard normal cumulative distribution function.

#### 4.6 Implementation of Crack-Initiation Model

The above equations for cycles to failure were coded into a Fortran subroutine for implementation into probabilistic fracture mechanic codes such as pc-PRAISE. The calling program needs to provide values for the stress amplitude, the material type, the sulfur content (for ferritic steels), temperature, whether the environment is water or air, oxygen content of the water, and the strain rate for the stress cycle. A final parameter is a percentile value that describes the fatigue life of the simulated component relative to the median fatigue curve. Figure 4.1 was generated from data obtained from a series of calls to the subroutine. Each of the curves corresponds to the indicated percentile of data having cycles to failure less than or equal to the indicated percentile. The solid curve of Figure 4.1 is the median or 50th percentile curve for cycles to crack initiation.

When implemented into a Monte Carlo simulation, a random number (between zero and one) is sampled before the call to the subroutine to simulate the percentile S-N

curve to be used to predict fatigue-crack initiation at the particular structural location of concern. This curve is assumed to apply to all the cyclic stress transients for that location with a different curve selected on the basis of the random numbers that are generated for the other Monte-Carlo simulations.

The enhanced version of pc-PRAISE addresses crack initiation at multiple sites by subdividing the pipe circumference into a set of 5.08-cm (2-in.)-long zones. The amplitude of cyclic stresses at each site can vary in a manner specified by user input such that the fatigue cracks may initiate at some sites much sooner or later than at other sites. The model also assumes no correlation between the random scatter in crack initiation times from one site to the next. Thus, a different selection from the family of S-N

curves (as shown by the example of Figure 4.1) is sampled at random for each of the various sites around the pipe circumference. There is also an option (not used for the present calculations) that assumes that the S-N curves for all sites are perfectly correlated. This option would predict (rather unrealistically) that a fatigue crack initiates at each of the sites around the pipe circumference after precisely the same number of stress cycles.

It should also be noted that the sampled crack-growth rates from site-to-site are assumed to be independent of one another. Also, no correlation exists between the cycles to crack initiation and the subsequent crack-growth rates.

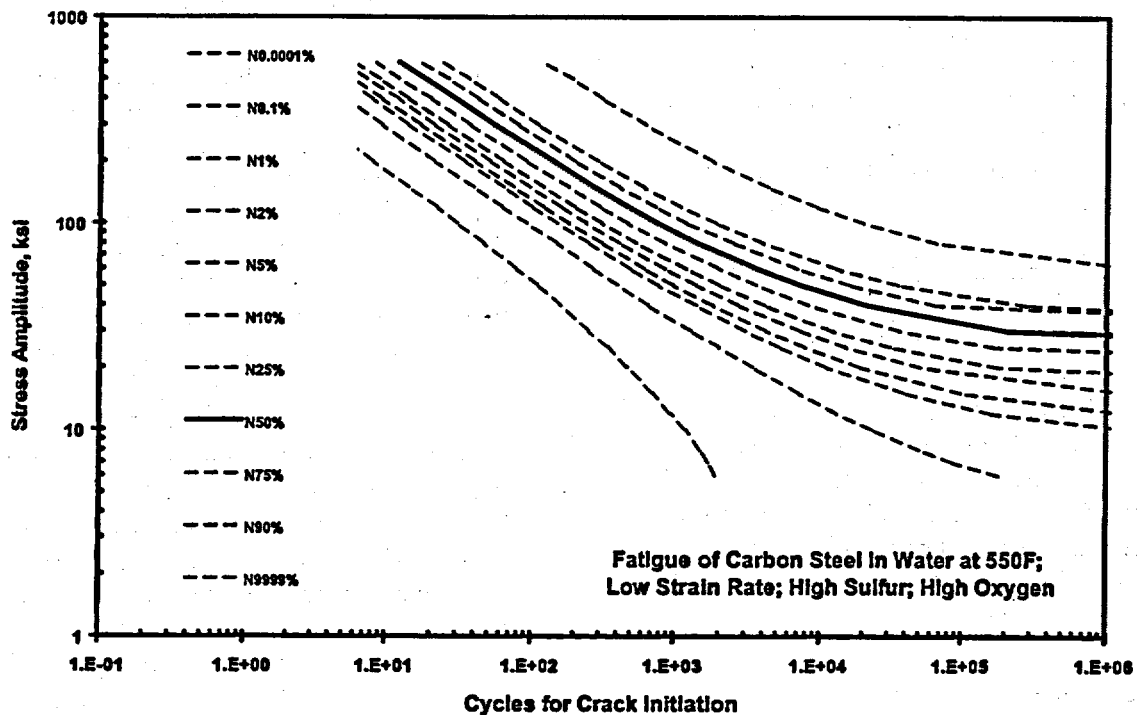


Figure 4.1 Example of Probabilistic S-N Curves for Low-Alloy Steel

Thus, cracks that initiate at less than the average number of cycles would not necessarily grow at higher than average crack-growth rates. The modified pc-PRAISE code does, however, permit the option of a perfect correlation between crack initiation and crack-growth rates, but this option was not used for the calculations of this report. Sensitivity calculations have shown that such a correlation can noticeably increase the cumulative probability of through-wall cracks for relatively reliable components (e.g., from  $10^{-4}$  to  $10^{-3}$ ), but gives relatively little increase ( $1.0 \times 10^{-1}$  to  $1.1 \times 10^{-1}$ ) in probabilities for the less reliable components of most interest to the present study.

A version of Miner's rule is used to predict the probability of fatigue crack initiation with varying cyclic stress. The method uses a generalized Miner's rule, which predicts that fatigue failure will occur when the sum

$$Q = \sum_{j=1}^j \frac{n_j}{N_j} = \sum_{j=1}^j q_j$$

becomes equal to unity, where  $n_j$  is the number of applied stress cycles  $S_j$ , and  $N_j$  is the value of cycles to failure if only  $S_j$  is applied. The above equation can be generalized by considering crack initiation to have occurred when  $Q$  exceeds unity and taking the probability of crack initiation to be equal to the probability that  $Q$  is greater than one.

#### 4.7 Treatment of Size Effects

The equations developed by ANL to predict probabilities of fatigue-crack initiation are based on a statistical treatment of data from small specimen tests. An additional term of  $\ln(4)$  is included to bring the equation into better empirical agreement with some test data on

22.86-cm (9-in.)-diameter vessels. This term is intended to account for size, geometry, and surface-finish differences between small fatigue test specimens and actual components.

The present calculations made use of the ANL equation, including the  $\ln(4)$  term, for those cases in which the model assumed only one initiation site. However, the revised pc-PRAISE model (see Appendix C) accounts for multiple initiation sites with each site covering some 5.08 cm (2 in.) of the pipe circumference. The probability of crack initiation therefore increases as the number of specified initiation sites is increased. This means that the fracture-mechanics model itself indirectly accounts for size effects, and inclusion of the  $\ln(4)$  term in the ANL equation can result in a double counting of size effects.

The  $\ln(4)$  term of the ANL equation was modified when used to address crack initiation at multiple sites. Otherwise, the model would estimate probabilities of crack initiation that were greater than those predicted by the original ANL work, which implicitly assumed only one initiation site. Following the approach used by ANL, the pc-PRAISE multiple-site model was calibrated to achieve agreement of calculated cycles to crack initiation with experimental data from the tests of the 22.86-cm (9-in.)-diameter vessels described in the ANL reports. The conclusion from this calibration effort was that the cycles to failure from the ANL equation needed to be increased by a factor of about 3.0. The net result was a factor of  $3/4$  applied to the number of cycles to failure from the small specimen data. In contrast, the ANL equation uses a factor of  $1/4$ , but bases the fatigue-life prediction on consideration of a single initiation site.

## 5 FATIGUE CRACK GROWTH MODEL

The present calculations combined probabilistic methods and fracture-mechanics models to assess the reliability of components that can have fatigue cracks initiating during the service life of the components. The pc-PRAISE code was used to calculate the probability of a through-wall crack, given that a 3-mm crack initiates at some time during the component's operating period. The fracture-mechanics model for this calculation was the same model used in prior versions of pc-PRAISE to address fatigue failures caused by pre-existing weld-fabrication defects. The main difference is that crack growth begins some time during the life of the component rather than at the beginning of life. The sizes of the initial flaws are consistent with initiated fatigue cracks rather than welding defects.

### 5.1 Fatigue-Crack-Growth Model

A two-dimensional, semi-elliptical circumferential crack at the inner surface of a component was considered. The initial depth of the crack is 3 mm, and the length of the defect was sampled from a statistical distribution. Both the lengths and depths of the cracks are allowed to grow. A leak occurs if the crack grows in a stable manner through the entire wall pipe.

In the calculations of fatigue-crack growth by pc-PRAISE, the distribution of stress through the wall thickness was based on the peak stresses used to predict the initiation of the cracks. The stress at the inner surface was identical to the cyclic stresses used for crack initiation, but the model allowed for the attenuation of high-surface stresses associated with through-wall stress gradients and/or stress concentrations.

The present methodology performed individual fracture-mechanics calculations based on the location of specific stresses. In contrast, prior calculations for through-wall cracks of the GSI-78 evaluations referenced generic studies

(NUREG/CR-5186 [Gore et al. 1988] and NUREG/CR-4483 for the reactor vessel and NUREG/CR-2189 [Harris et al. 1981], Vol. 5 for piping). The levels of cyclic stresses for the referenced calculations were in many cases significantly lower than the stresses at the high-fatigue-usage locations of concern.

### 5.2 Stress Intensity Factor

The growth of cracks in this report was governed by the crack-tip stress-intensity factor,  $K$ , which is a measure of the crack-tip singularity. The crack driving force depends on the level and distribution of stress, the crack size, and the component geometry. For example, the stress intensity factor for a complete 360-degree circumferential crack at the inside diameter of an axially loaded cylinder is given by

$$K = \sigma(\pi a)^{1/2} F\left(\frac{a}{h}, \frac{R_i}{R_o}\right)$$

where  $s$ ,  $h$ ,  $a$ ,  $R_i$ , and  $R_o$  are the stress, wall thickness, crack depth, internal radius, and external radius, respectively. The function  $F$  is obtained by the finite element or other numerical methods. The calculation of the stress-intensity factor for surface flaws is based on the individual contributions of thermal stresses, pressure stresses, and possibly cladding stresses. For cracks with a finite aspect ratio (i.e.,  $b/a$  less than 100), the stress-intensity factors become lower as the aspect ratios become smaller. Crack instability is governed by attainment of a critical value of  $K$ -applied net section stress relative to the material-flow stress. In this study, subcritical crack growth occurs before reaching the critical crack size due to cyclic loading (fatigue).

Part of the work described in this report was to compare the stress-intensity-factor solutions contained within the pc-PRAISE code with more recently published solutions from the technical

literature. The results of these comparisons are presented in Appendix D. The review of Appendix D indicates that much information on stress-intensity factors has become available since the last improvements in the influence functions for use in PRAISE were made in 1984. Of particular concern was the behavior of the pc-PRAISE solutions for very long circumferential cracks that extended a large fraction around the pipe circumference.

Appendix D concludes that the stress-intensity-factor solutions in pc-PRAISE are well behaved for very long and very deep cracks. The largest uncertainties are associated with stress-intensity factors at the surface location of the finite-length flaws. Comparisons are somewhat difficult because pc-PRAISE uses a root mean square (RMS) value based on energy release rates for stress-intensity factors, whereas most of the literature uses local values of stress-intensity factors. The surface values are important because they control the lengthwise growth of the cracks, which has a large influence on the crack lengths and calculated leak rates at the time the crack tip penetrates the outer surface of the pipe.

Another review addressed the proposed changes being made to the methodology of the ASME Section XI code for predicting the changes in the shapes of growing fatigue cracks. These code changes are based in large part on experimental results provide by Professor Iida from Japan. The Japanese experiments show that the final shape of a fatigue crack (i.e., when the crack penetrates the pipe wall) has an aspect ratio (ratio of total crack length to the crack depth) in the range of 2 to 4. These experimental values are consistent with aspect ratios predicted by pc-PRAISE. Such agreement provides indirect support to the stress-intensity-factor solutions in the code. The experimental trends do not preclude the development of very long fatigue cracks, because long fatigue cracks can also result from the linking of several individual cracks.

### 5.3 Fatigue-Crack Growth for Carbon and Low Alloy Steel Materials

Fatigue-crack growth can be described by the modified Forman relation (Forman et al. 1988), which is a general functional form for curve-fitting fatigue-crack-growth data. In addition, the well-known Paris relationship has been found by many researchers to provide a good fit for a wide variety of materials. Article A-4000 of the ASME Section XI Code (ASME 1992) relates the fatigue crack growth rate  $da/dN$  of a material to the range of applied stress intensity factor  $\Delta K$ . A probabilistic form of the ASME equations is used in the present probabilistic fracture mechanics (PFM) model for the crack-growth rates in a water environment. The fatigue crack growth rate  $da/dN$  (inches per cycle) of surface flaws is

$$\frac{da}{dN} = Z \begin{cases} 1.03 \times 10^{-12} S (\Delta K)^{5.95} & \Delta K \leq K_{I, \text{max}} \\ 1.01 \times 10^{-7} S (\Delta K)^{1.95} & \Delta K > K_{I, \text{max}} \end{cases}$$

the  $K_{I, \text{max}}$  in the above equation is

$$K_{I, \text{max}} = \begin{cases} 17.74 & R \leq 0.25 \\ 17.74 \left( \frac{3.75R + 0.06}{26.9R - 5.725} \right)^{0.25} & 0.25 < R < 0.65 \\ 12.04 & R \geq 0.65 \end{cases}$$

If  $K < K_{I, \text{max}}$  the adjustment factor  $S$  is

$$S = \begin{cases} 1.0 & R \leq 0.25 \\ 26.9R - 5.725 & 0.25 < R < 0.65 \\ 11.76 & R \geq 0.65 \end{cases}$$

while if  $K > K_{I, \text{max}}$  the factor is

$$S = \begin{cases} 1.0 & R \leq 0.25 \\ 3.75R - 0.06 & 0.25 < R < 0.65 \\ 2.5 & R \geq 0.65 \end{cases}$$

The parameter  $R$ , which accounts for mean stress effects on crack growth rates, is defined in terms of the minimum and maximum stress-intensity factors during the stress cycle as  $R = K_{\min}/K_{\max}$ . The parameter  $Z$  is added in the present model to the crack growth equation to randomize the crack-growth rates. This random variable covers all possible uncertain quantities, such as material variability, environmental variability, crack-geometry variability, crack-modeling uncertainty, and stress uncertainties. In the literature (Khaleel and Simonen 1994; Harris et al. 1981),  $Z$  is assumed to have a lognormal distribution.

#### 5.4 Fatigue-Crack Growth for Stainless Steel Materials

The fatigue crack growth rate ( $da/dN$  in inches per cycle) for austenitic stainless steel is represented by the following relation:

$$\frac{da}{dN} = C \left[ \frac{K_{\max} - K_{\min}}{\left(1 - \frac{K_{\min}}{K_{\max}}\right)^{1/2}} \right]^2$$

where  $K_{\min}$  and  $K_{\max}$  are the minimum and maximum stress intensity factors ( $\text{ksi-in}^{1/2}$ ), respectively. The scatter in the data is represented by a lognormal value of  $C$  with a median of  $9.14 \times 10^{-12}$  and standard deviation of  $2.20 \times 10^{-11}$ .

#### 5.5 Treatment of Through-Wall Stress Gradients

The cyclic stress inputs to the present fatigue calculations were the same stresses that were used in the NRC-funded research project at INEL as described in NUREG/CR-6260 (Ware et al. 1995). The data gave only peak cyclic stresses for the surface locations at which the initiation of fatigue cracks was to be evaluated and did not describe the corresponding variations of the stresses through the section thickness of the component. It was appropriate to use these peak

stresses in the present calculations for that part of the analysis that addresses the initiation aspect of fatigue cracking. However, it was judged unrealistic to assume that these peak stresses were uniformly distributed through the component wall thickness.

In earlier calculations, the stress that governs crack growth was taken to be uniformly distributed, but at a level of 50% of the peak surface stress. This simplifying assumption was not used in the present calculations because it can give unconservative predictions of fatigue crack growth. The small (3-mm deep) initiated cracks begin their growth within the region of high surface stresses, and only later is their growth governed by the reduced stress levels associated with the through-wall stress gradients. The approach that was eventually adopted was to decompose the peak stress into a component of uniform stress and a component of through-wall gradient stress. Details of the approach are described in Appendix C. A standardized (quadratic) stress gradient was developed on the basis of stress solutions related to heating and cooling ramps and step changes in surface temperatures.

Since results of detailed stress calculations were not available from the work of NUREG/CR-6260 (Ware et al. 1995), rules were developed to estimate the fraction of the peak stress to be assigned to the uniform stress category. The remaining fraction was assigned to the through-wall gradient category. In many cases, the values of peak stresses were greater than 690 MPa (100 ksi), which implied that most of the stress was due to temperature gradients caused by heating and cooling transients or were related to geometric stress concentrations. In other cases, the number of stress cycles was very large, which also suggested thermal gradient effects. Another consideration was that the ASME code stress limits do not permit membrane stresses (including secondary stresses) to be greater than three times the code design stress ( $3S_m$ ). For typical piping materials, the  $3S_m$  limit justified a

criteria that assumed that all stress ranges (or 2Sa) greater than 310 Mpa (45 ksi) should be treated as gradient stresses. The following specific rules were applied to assign stress to the uniform and gradient categories:

- Cyclic stresses associated with seismic loads were treated as 100 percent uniform stress.
- Cyclic stresses greater than 310 Mpa (45 ksi) were treated as having a uniform component of 310 Mpa (45 ksi), and the remainder were assigned to the gradient category.
- For those transients with more than 1000 cycles over a 40-year life, it was assumed that 50% of the stress was uniform stress and 50% a through-wall gradient stress. In addition, for these transients, the uniform stress component was not permitted to exceed 10 ksi.

These rules permitted calculations to be performed on a less conservative basis than assuming uniform stresses through the component cross sections. The approach ensured that shallow initiated cracks would at first be subjected to the high stresses associated with the peak surface stresses, but allowed for a reduction in crack growth rates as the cracks grew to sufficient depths to escape the full effect of the peak surface stresses. Sensitivity calculations are reported below for a high-stress component to show the effects of the assumptions used to assign stresses to the less critical gradient category.

The lower head shell for the older vintage W plant was addressed as a special case. The data on stress transients showed a high-cycle vibration that was capable of growing the 3-mm initiated fatigue crack to become a through-wall crack. Discussions with NRC staff indicated that this stress was associated with vibration of an attachment to the inner vessel wall, and it involved a large contribution from a highly localized stress concentration at an attachment

weld. Because the vibratory stress would extend only a small distance into the vessel wall, this stress was included only in the calculation of crack initiation, but excluded from the fatigue-crack-growth calculations. To account for any neglected crack growth from the peak vibrational stress, the depth of the initiated fatigue crack was increased from 3 mm to 25 mm, at which time the crack growth was driven only by the other nonvibratory stress cycles.

## 5.6 Calculation of Through-Wall Crack Frequency

Results from the pc-PRAISE code are in terms of cumulative probabilities of crack initiation and of through-wall cracking as a function of time. On the other hand, the risk calculations for CDFs required through-wall crack frequencies. Therefore, the output data from pc-PRAISE were loaded into a spreadsheet for numerical differentiation of the cumulative failure probabilities. To smooth out the numerical noise associated with the finite number of trials used in the Monte Carlo simulations, the failure rates were averaged over an 8-year time interval centered on the time of interest. Values of failure rates at 60 years were based on time increments looking backwards in time and were averaged over a 4-year interval.

In many cases, pc-PRAISE predicted cumulative probabilities for through-wall cracks that were greater than 90 percent. In these cases, the calculated failure rates would become smaller and smaller because only a very small number of the original population of components remained available to fail. A correction was made to account for the decreasing population in the following manner

$$\text{Failure Rate} = [P(t + \Delta t) - P(t)] / [\Delta t(1 - P(t))]$$

where P is the cumulative probability of the through-wall crack, t is the time value at the beginning of the interval, and  $\Delta t$  is the time increment.

The calculations of through-wall crack frequencies do not account for potential benefits of inservice inspection or maintenance programs, even though the predicted cumulative probabilities of failures for many of the components attain levels late in plant life that exceed 50 percent. On the other hand, the pc-PRAISE model does take credit for leak detection, but this only decreases the probability that initially small and inconsequential leaks will increase sufficiently over time to become much larger leaks. Leak detection has no effect on the frequencies of through-wall cracks.

The higher values of through-wall crack frequencies are based on rather conservative assumptions relative to the actual scenario that will govern the inspection and maintenance of high-fatigue locations. The model assumes that a class of

components that exhibits high failure frequencies will remain in operation until each such component eventually fails one-by-one or is retired at the end of plant life. In practice, the first failure of a group of similar components will likely cause the other members of the group to be subject to an aggressive program of corrective actions such that the probability of repeat failures is greatly reduced. Such corrective actions can include frequent inservice inspections by ultrasonics that will detect and result in repairs to fatigue cracks long before they reach significant sizes, changes to plant operational practices to reduce stress levels, or replacement of problem areas with components of improved materials and designs. The present fracture mechanics model does not address the effects of such corrective actions in reducing failure frequencies.

## 6 CONDITIONAL PROBABILITIES OF SMALL AND LARGE LEAK RATES

The fracture mechanics calculations (as described in Section 5) predict the probability that an initiated fatigue crack will become a through-wall flaw. In most cases, these penetrating flaws will begin as relatively short cracks and will result in only minor leakage, such as 3 gallons per minute (gpm), having no safety consequences. The leakage rate will tend to increase over a period of time as the crack continues to grow, which means that the leakage will eventually reach a detectable level that results in shutdown of the plant before the leak rates become sufficiently large to potentially impact plant safety. Nevertheless, some (small) fraction of the through-wall cracks can be relatively long from the onset and could therefore leak immediately at rates that are sufficiently large to be of concern to plant safety. While leak detection measures would not mitigate the effects of such cracks, safety injection systems would compensate for the losses from the RCS. Safety consequences would occur only if these normally reliable systems fail to function as intended.

The next step in the present evaluation was to estimate the probabilities that a given through-wall crack will leak at rates sufficient to cause a LOCA. Given a through-wall crack, the objective of the present calculations was to estimate the conditional probabilities that the resulting leakage would be at rates corresponding to predefined categories. These categories were selected as

1. less than 30 gpm
2. 30 gpm to 500 gpm
3. greater than 500 gpm.

These somewhat arbitrary categories were selected to correspond to the categories used in the Westinghouse Owners Group/Virginia Power

(WOG/VEPCO) pilot application of risk-informed inspection (WCAP 14572 Revision 1) (Westinghouse Owners Group 1997).

Although the pc-PRAISE fracture mechanics model can predict probabilities of both small and large leaks corresponding to the definitions for the leak rates of concern (gpm), the present study did not perform such component-specific calculations for the various locations in the seven plants. The information available to PNNL did not include sufficient load and stress data to support such calculations. In addition, many of the component geometries (e.g., nozzle configurations) did not correspond to the pc-PRAISE fracture mechanics model for circumferential cracks in piping.

Rather than performing location-specific fracture mechanics calculations, the conditional probabilities were estimated by application of trends from sensitivity calculations performed with pc-PRAISE and by reference to service experience with piping failures (small versus large leaks). Appendix C describes evaluations that address uncertainties in calculations of conditional probabilities.

Data on pipe-failure events at operating plants show that only a small fraction of through-wall flaws result in large leaks or pipe ruptures. Furthermore, the most likely failure mode depends on the particular degradation mechanism involved. For example, flow-assisted corrosion and vibrations result in relatively larger fractions of pipe breaks, whereas thermal-fatigue mechanisms and stress-corrosion cracking result in very small fractions of pipe breaks. Reviews of data from plant operating experience at nuclear power plants (Bush et al. 1996) show that the reported number of small leaks is many times greater than the number for large leaks (or ruptures). Even for

mechanisms such as vibrational fatigue and flow-assisted corrosion, the ratio can be as high as 10:1. For other mechanisms (such as stress corrosion cracking), the data indicate ratios of small leaks to large leaks in the range of 1000:1 or greater.

A number of documented cases of thermal fatigue failures at nuclear power plants have resulted in relatively long leaking cracks in piping components, which could be described as "near misses" for a large leak or pipe-rupture accidents. In this regard, the cyclic stresses addressed in the present report can be largely described as thermal-fatigue-type stresses. The observed cases of "near misses" show that long cracks capable of causing large leaks can develop. On the other hand, experience shows that even these long cracks tend to have sufficient variation in their depths along the crack front, such that one part of the crack front will usually penetrate the pipe wall and cause a detectable leak before a pipe break occurs. The pc-PRAISE was applied to gain insight into the fraction (expected to be small) of through-wall cracks that will result in significant leaks.

Probabilistic fracture mechanics models such as pc-PRAISE predict that fatigue failures will usually be in the mode of small leaks rather than as large leaks or breaks. Such calculations are sensitive to assumptions regarding the initial lengths of the flaws and to the assumptions made to predict the length-wise versus depth-wise growth. In the present work, the flaws of concern are cracks that initiate by the fatigue process. In the early phase of this project, it was assumed that initiated fatigue cracks had the same distribution of lengths as flaws originating from welding processes. These distributions predict probabilities of less than 10 percent for flaw-aspect ratios (flaw length over flaw depth), which are 10:1 or greater. Although this trend for fabrication flaws was assumed in the early work to apply also to initiated fatigue cracks, such an assumption was later judged to be unconservative for initiated fatigue cracks. Field experience with

fatigue cracks has shown that flaw-aspect ratios can be very large. Under estimation of crack lengths has a twofold effect on failure probabilities. Short cracks will have lower stress intensity factors and will therefore grow more slowly in the depth-wise direction and cause lower values of calculated probabilities for through-wall cracks. In addition, the resulting through-wall cracks will be shorter and will be less likely to cause large leaks. The pc-PRAISE code was therefore revised to better address fatigue cracks as described in Appendices C and D.

The revised pc-PRAISE model now assigns a distribution to the lengths of the 3-mm-deep initiated fatigue cracks that has a median aspect ratio of about 5:1 (ratio of total flaw length to flaw depth). The lognormal distribution of flaw lengths has a probability of  $10^{-2}$  that the length of the initiated crack will extend the full length (5.08 cm [2 in.]) of the standard initiation site, which corresponds to an aspect ratio of about 17:1. The revised pc-PRAISE model also allows for crack initiation at multiple sites around the circumference of a pipe and then simulates the possible linking of short cracks in adjacent zones to create much longer cracks. Thus, the simulation can predict the development of the very long cracks that are sometimes observed in service-degraded piping.

It should be noted that a Latin Hypercube fracture mechanics model was used to estimate failure probabilities for those components that had through-wall crack probabilities too small to be calculated with the Monte-Carlo method of pc-PRAISE. In these calculations, the aspect ratio of the initiated flaw was assumed to be 10:1, and the fracture mechanics model assumed that the fatigue crack growth process maintained this 10:1 aspect ratio. The Latin Hypercube model was benchmarked against the pc-PRAISE code in calculations for components that had higher failure probabilities. The calculated through-wall crack probabilities were in relatively good agreement. The Latin Hypercube model gave somewhat higher probabilities (factor of 2 to 10),

and this difference was attributed to more conservative stress intensity factor solutions for relatively deep cracks.

Probabilities of failure for the different leak-rate categories were estimated from results of probabilistic fracture mechanics calculations made using the pc-PRAISE code. A previous example of such calculations for fatigue failures due to fabrication flaws is documented in a recent paper (Simonen et al. 1998). Pipe diameters of 15.24 cm and 73.66 cm (6 in. and 29 in.) were addressed in these calculations giving the results of Table 6.1. These results for conditional probabilities show little effect of pipe size.

Appendix C provides other example calculations, based on the present crack-initiation model, that also address the relative fractions of failures that

are small and large leaks. The effects of circumferential variations in stress on the length-wise growth and the linking of cracks are also evaluated in Appendix E. Such stress gradients are shown to significantly reduce the likelihood of long cracks, which in turn favors small leaks versus large leaks.

Figures 6.1 to 6.3 provide results from a systematic set of calculations for probabilities of small and large leaks. These calculations expanded on the calculations described in Appendix C and covered a wider range of pipe sizes and operating pressures corresponding to both PWR and BWR plants. Results are presented only for the PWR conditions of 2250 psi. The PWR results were also applied to the BWR conditions (1200 psi pressure), a simplification that gave somewhat conservative predictions for the BWR plants.

**Table 6.1 Example Results of Calculations for Small Leaks, Large Leaks, and Pipe Breaks for Fatigue Failures Caused by Fabrication Flaws (from Simonen et al. 1998)**

Failure Mode	15.24-cm (6-in.) Pipe		73.66-cm (29-in.) Pipe	
	Cumulative Probabilities per Weld per 40 Years for the Failure Mode of Interest	Conditional Probability of Failure Mode Given a Through-Wall Crack	Cumulative Probabilities per Weld per 40 Years for the Failure Mode of Interest	Conditional Probability of Failure Mode Given a Through-Wall Crack
Through-Wall Crack < 30 gpm	1.0E-03	0.917	1.0E-05	0.986
Small Leak/Small LOCA > 30 gpm, < 500 gpm	8.0E-05	8.0E-02	1.0E-06	1.0E-01
Large Leak/Medium LOCA > 500 gpm	3.0E-06	3.0E-03	4.0E-08	4.0E-03
Pipe Break/Large LOCA > 500 gpm	3.0E-08	3.0E-05	5.0E-11	5.0E-06

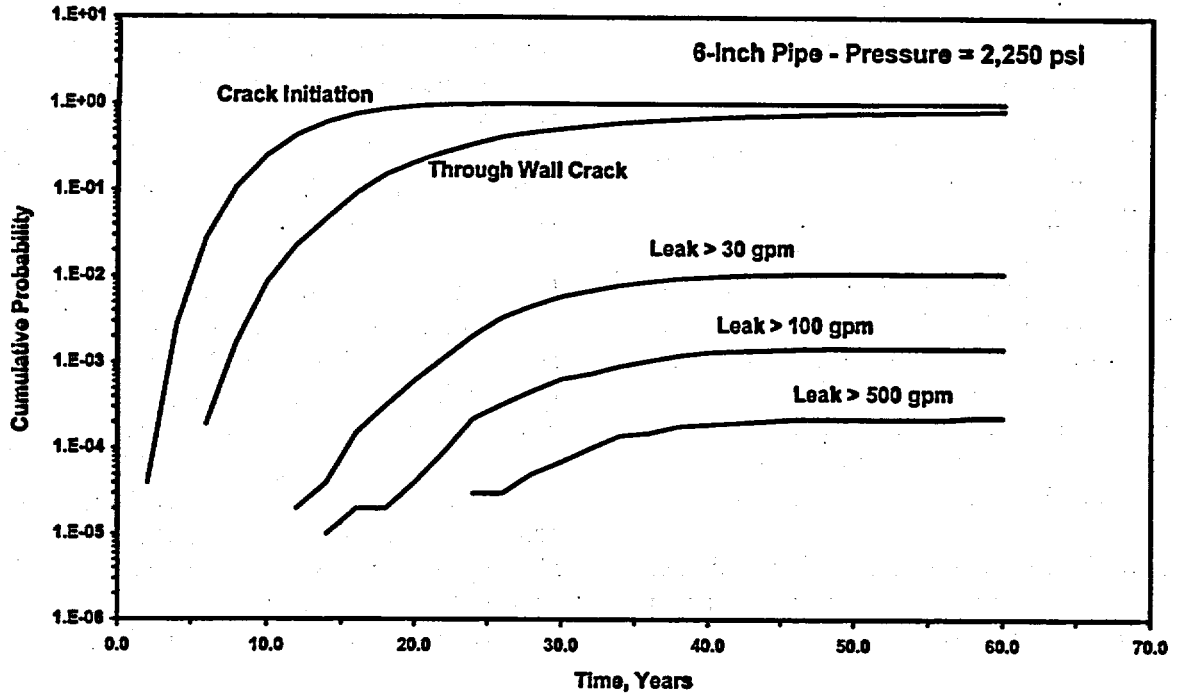


Figure 6.1 Leak Probabilities Versus Time for 15.24-cm (6-in.)-Diameter Pipe

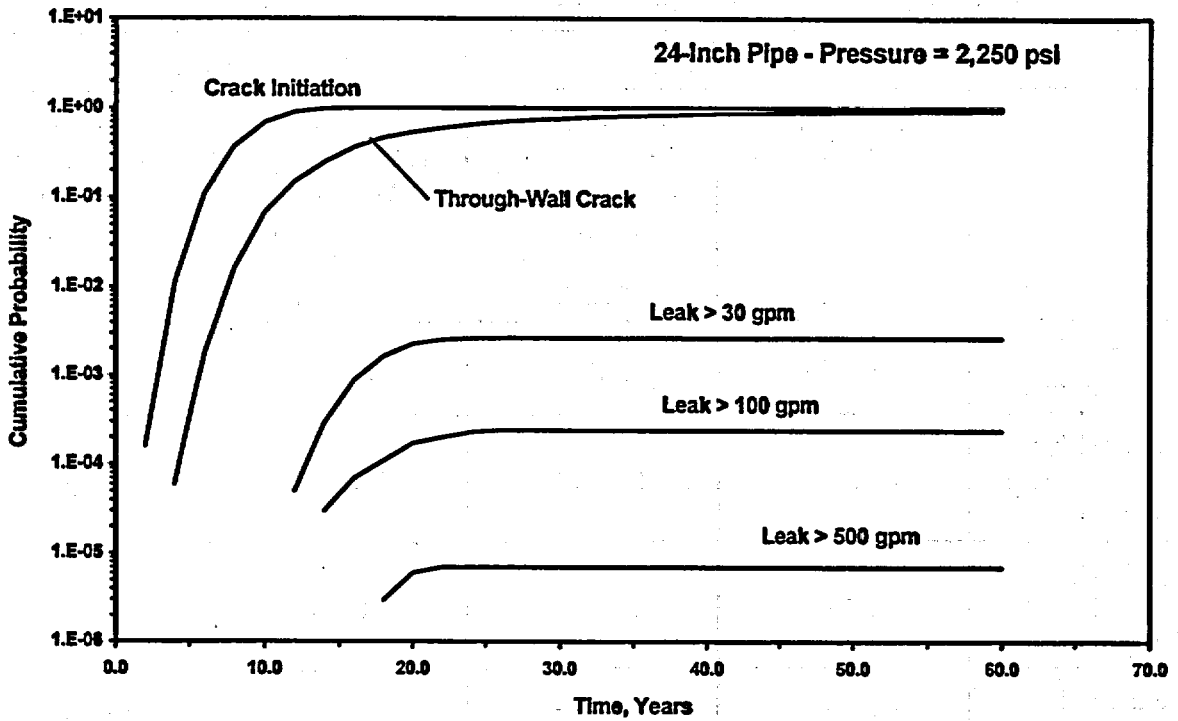


Figure 6.2 Leak Probabilities Versus Time for 30.48-cm (12-in.)-Diameter Pipe

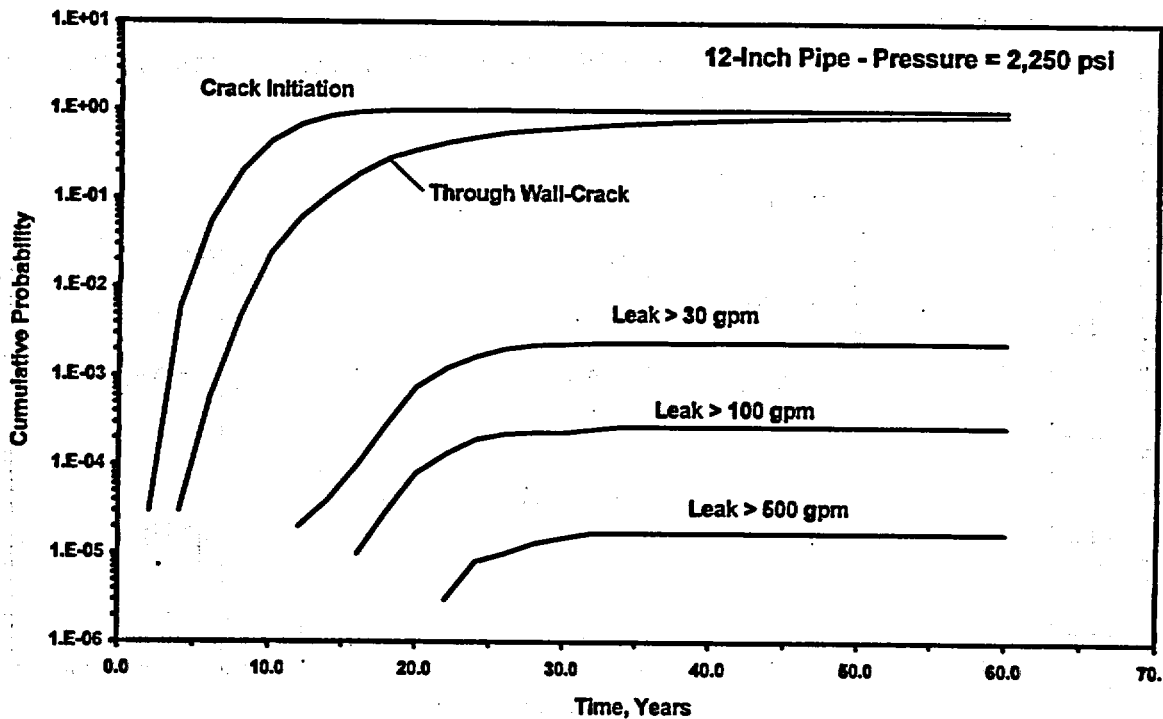


Figure 6.3 Leak Probabilities Versus Time for 60.96-cm (24-in.)-Diameter Pipe

All calculations were based on a flow stress for the piping material of 296 Mpa (43 ksi) and representative dimensions for Schedule 80 piping. This gave wall thicknesses of 1.27, 1.91, and 3.18 cm (0.5, 0.75, and 1.25 in.) for the nominal diameters of 15.24, 30.48, and 60.96 cm (6, 12, and 24 in.).

The probabilities for the leak rates of 30, 100, and 500 gpm were divided by the corresponding probabilities of through-wall cracks to derive conditional failure probabilities. Figure 6.4 summarizes the results for all pipe sizes and leak rates and shows how the conditional probabilities become smaller as the pipe diameter becomes larger. The vertical arrays of points on Figure 6.4 correspond to ratios of probabilities at different times during the 60-year plant life, with the upper points corresponding to the higher failure probabilities that are calculated for the later periods of the 60-year time span.

Table 6.2 gives the conditional probabilities of small and large leaks that were eventually used in

the calculations of this report. This table was derived by constructing curves for each of the three leak rates (30, 100, and 500 gpm) through the upper end of the scatter band of the vertical arrays of points of Figure 6.4 corresponding to each leak rate. These curves were then adjusted upwards by a factor of 10 to allow for uncertainties in the pc-PRAISE calculations. This adjustment was consistent with the intent to evaluate best-estimate CDFs, but also to use conservative approaches to address factors that were beyond the scope of the research project. Based on the sensitivity calculations of Appendix C, this factor of 10 was not applied for calculations that addressed nozzle-type locations. These nozzle locations will have relatively short through-wall cracks because of the high stress gradients in both the axial and radial directions.

The calculations for Table 6.2 did not address cracks in the thick-walled locations of reactor pressure vessels. A vessel fracture mechanics model will predict relatively long through-wall cracks because of the large wall thicknesses.

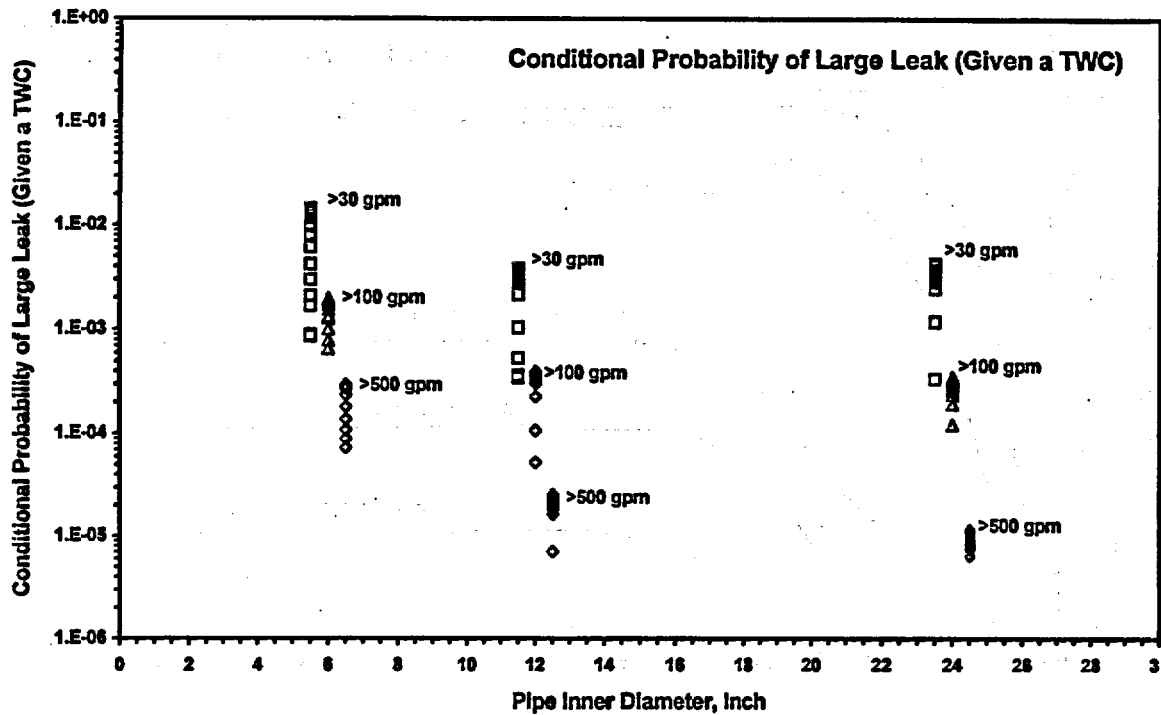


Figure 6.4 Conditional Probabilities of Small and Large Leaks

Table 6.2 Conditional Probabilities of Failure Modes Given the Occurrence of a Through-Wall Crack			
Pipe Diameter, cm (in.)	Conditional Probability of Failure Modes Given a Through-Wall Crack		
	Leak > 30 gpm	Leak > 500 gpm	Leak > 500 gpm
5.08 (2)	2E-01	8E-02	8E-02
7.62 (3)	1.5E-01	5E-02	4E-03
10.16 (4)	1E-01	4E-02	3E-03
15.24(6)	8E-02	2E-02	1E-03
20.32 (8)	6E-02	1E-02	6E-04
25.40 (10)	5E-02	7E-02	3.5E-04
> 30.48 (>12)	5E-02	5E-03	2E-04

Therefore, the conditional probabilities of Table 6.2 could be unconservative for application to vessels. It was assumed that all through-wall cracks in the vessel wall would leak at a rate greater than 30 gpm and that 10 percent of these cracks would leak at a rate greater than 500 gpm.

Refinements to the conservative assumptions used in the present estimates of conditional failure probabilities were not feasible. The limited objective of the evaluations was to show that contributions of piping and vessel failures to CDFs were small compared to contributions from other sources. Accordingly, the results were not intended to provide a basis for comparing CDF contributions from location-to-location or from plant-to-plant.

While there are uncertainties in the calculated conditional failure probabilities, trends for fatigue failures in nuclear piping systems, as indicated by databases (such as compiled by Bush et al. 1996), are consistent with the estimates of Table 6.2. The data from field experience show that the number of piping failures due to large leaks (and breaks) is significantly less than the corresponding number of failures due to small leaks.

Uncertainties in the pc-PRAISE model include the inputs for the lengths of the initiated fatigue cracks, the assumed length (5.08 cm [2 in.]) of the individual initiation sites around the pipe

circumference, the criteria used to grow and link cracks from the individual sites, and the method used by pc-PRAISE to calculate leak rates from through-wall cracks. Possible biases introduced by such uncertainties would, however, be balanced by conservative assumptions in the fracture mechanics model. This model assumes an immediate transition of part-through-wall cracks as they become through-wall cracks. The resulting cracks have lengths at the outer surface equal to the corresponding crack lengths at the inner surface. In practice, through-wall cracks are observed to begin with lengths at the outer pipe surface that are much less than their corresponding lengths at the inner surface. Therefore, the initial leak rates will be relatively small, which enables the leakage to be detected in time to allow plant shutdown before the cracks grow to become larger leaks.

In summary, the conditional leak probabilities at various rates as estimated from the pc-PRAISE calculations appear to be reasonable and consistent with data from service experience. The intent, to the extent feasible, was to perform best estimated as opposed to bounding calculations. There were, nevertheless, many uncertainties in the calculations, and this required the use of some conservative modeling assumptions and inputs to the calculations.

## 7 CONDITIONAL CORE DAMAGE PROBABILITIES

The calculations as described in Section 6 provide estimates of pipe failure frequencies for small and large leaks. This section describes how conditional core damage probabilities were estimated for these failure modes. The estimates were based on numerical parameters obtained from PRAs for some example plants that covered all seven of plant types addressed by the present fatigue evaluations. The tables of Appendix B give the conditional CDFs for all fatigue locations of the seven plant types.

Because the evaluations of CDFs were a secondary objective of the present study, it was not possible to refine the scope of calculations performed in the available PRAs. Whereas the intent was to establish best estimates of CDFs, the limitations of available PRA information required some conservative approaches to address uncertainties. Furthermore, it was not the intent to make accurate comparisons of CDFs from plant-to-plant or from location-to-location within a given plant. Meaningful comparisons of this type would require refinements to the published PRAs. The readily available PRAs covered the plant vendors and vintages of interest, but there was not a one-to-one match of the plants used for the fatigue analyses versus the plants addressed by the available PRAs. Therefore, as described below, the evaluations were performed on a generic basis using common consequences from location-to-location within each plant and differentiating from plant-to-plant only between PWR and BWR plants.

It was assumed that all fatigue locations were part of the primary-coolant-system boundary and that failures could result in a LOCA. The possible exception would be locations described as being in the RHR systems, where failures may or may not result in a LOCA during normal plant operations, depending on the alignment of isolation

values relative to the pipe-break locations. Without detailed information on the break locations, it was conservatively assumed that such pipe failures could result in a LOCA. Otherwise, an evaluation of failure consequences would have required knowledge of the plant response to RHR system failures during other modes of plant operation (e.g., shutdown risk evaluations).

Failures of the reactor pressure vessel within the shell and lower head regions were conservatively assumed to cause core damage with a 100-percent probability, based on probabilistic fracture mechanics evaluations for pressurized thermal shock (Simonen et al. 1986). While in many cases, the coolant lost from smaller leaks in the lower part of the vessel can be replaced by normal or standby systems, refinements to the evaluation were not needed to demonstrate low contributions to overall plant CDFs. Nozzle failures in the upper vessel region were assumed to be the same as failures of the reactor coolant system piping.

Conditional core damage probabilities (given a small or large leak) were established by application of PRA models. Section 7.1 presents failure consequences from a recently completed study of risk-informed inspection for the Surry-1 plant (WCAP-14572 Revision 1) (Westinghouse Owners Group 1997). These recent Surry-1 results were considered to be a state-of-the-art evaluation for the consequences of piping failures, which could serve as a benchmark for other less-recent evaluations. The other evaluations addressed various plants (e.g., the NUREG 1150<sup>(a)</sup> sample of plants) including earlier work for the Surry-1 plant. The two sets of predictions

---

(a) Second draft for peer review, Summary Report, *Severe Accident Risks: An Assessment of Five U.S. Nuclear Power Plants*, NUREG-1150, U.S. Nuclear Regulatory Commission, Washington D.C.

for core damage probabilities for Surry-1 were found to be in relatively good agreement.

Consequences of pipe failures for both PWR and BWR plants were addressed previously by PNNL in NUREG/CR-6151 (Vo et al. 1994). This study indicated that the consequences of pipe breaks are less (by an order of magnitude or more) for BWR plants than for PWR plants. An evaluation of risk-informed inspection is currently being performed by the Tennessee Valley Authority (TVA) for the Browns Ferry Unit 1 plant. Preliminary results of this study also show about an order of magnitude difference in conditional core-damage probabilities for BWR compared to PWR plants. These trends are all consistent with conditional core-damage probabilities estimated in the present study.

## 7.1 Risk-Informed Evaluations of Surry-1 Plant

Results from the pilot application for Surry-1 (WCAP-14572 Revision 1 [Westinghouse Owners Group 1997]) were used to assign conditional probabilities of core damage for each of the four categories of pipe failure. These results are applicable to older-vintage W plants. In general, the consequences of pipe failures at a PWR will be a function of the effectiveness of the low- and high-head safety injection systems in mitigating accidents. Plant-specific details, such as the number and diversity of independent trains and the capacity of pumps, are important factors. These systems are part of the nuclear steam system supplier (NSSS) portion of the plant and will tend to be similar for a given vendor and plant vintage.

Some of the locations of the present study are in the residual or decay heat removal system. The INEL report (NUREG/CR-6260 [Ware et al. 1995]) implies that these locations are in Class 1 portions of the piping, which would in turn imply that failures at these locations could result in a

LOCA in the primary coolant system. However, the exact locations are not clear, meaning that these locations would be isolated by valves from the primary coolant system during periods of normal plant operation. Pipe breaks would be a factor only if they occur during periods of shutdown cooling. The WOG/VEPCO evaluation of Surry-1 did not address shutdown risk and provides no basis to estimate the corresponding consequences of failures. Therefore, all failures of RHR piping were treated as failures of the primary coolant loop, which is believed to be a conservative assumption.

## 7.2 Evaluations Based on PRAs for Various Plants

The following sections develop first-order estimates of the conditional probability of core damage given the prior occurrence of failure of the reactor vessel, inlet nozzles, and selected RCS piping. Conditional core-damage probabilities were developed for a total of seven plant types, including old and new vintage plants supplied by CE, W, and GE, as well as a typical B&W plant.

Plant-specific PRAs were used as the basis for calculations in this report. Table 7.1 lists the plants for which PRA information was used in the present study. In some cases, the PRAs were performed as part of NRC-mandated individual plant examination (IPE) programs, and the resulting quality of the PRA may not be such to support detailed risk assessments. In the present work, the IPE information was used only in conjunction with results from other PRAs for similar plants to derive generic trends for conditional core damage probabilities. Therefore, the conclusions of the present work are not sensitive to data from any specific PRA study.

The new and old vintage CE plants were represented by the Palo Verde (Arizona Public Service Company 1992) and Calvert Cliffs (SNL 1984)

**Table 7.1 Summary of PRAs in Terms of Plant Vendors,  
Plant Vintages, Break Sizes, and Leak Rates**

LOCA Category	Plant Type						
	New-CE (Palo Verde)	OLD-CE (Calvert Cliffs)	B&W (Oconee)	NEW-W (Sequoyah)	OLD-W (Surry)	NEW-GE (Grand Gulf)	OLD-GE (Peach Bottom)
Small LOCA Diameter, cm (in.)	0.97-7.6 (0.38-3.0)	0.76-4.8 (0.3-1.9)	<10.2 (<4.0)	<5.1 (<2.0)	1.27-5.1 (0.5-2.0)	<2.79 (<1.1)	<2.3 (<0.9)
Small LOCA gpm	12-700	8-250	<1200	<300	20-300	<30	<25
Medium LOCA Diameter, cm (in.)	7.6-15.2 (3.0-6.0)	4.8-10.9 (1.9-4.3)	N/A	5.1-15.2 (2.0-6.0)	5.1-15.2 (2.0-6.0)	2.79-12.4 (1.1-4.9)	2.3-10.9 (0.9-4.3)
Medium LOCA gpm	700-2800	250-1400	N/A	300-2800	300-2800	30-750	25-550
Large LOCA Diameter, cm (in.)	>15.2 (>6.0)	>10.9 (>4.3)	>10.2 (>4.0)	>15.2 (>6.0)	>15.2 (>6.0)	>12.4 (>4.9)	>10.9 (>4.3)
Large LOCA gpm	>2800	>1400	>1200	>2800	>2800	>750	>550

PRAs. The Oconee plant (Duke Power Company 1990) was used as a representative B&W plant. New and old vintage W plants were covered by the Sequoyah and Surry-1 plants. BWR plants of GE designs were addressed by the Grand Gulf (newer vintage) and Peach Bottom (older vintage) plants. Table 7.1 also lists the break sizes (expressed as equivalent circular hole diameter) that were used in each PRA to define the LOCAs of the small, medium, and large categories. In each case, the corresponding leakage rates (for the pressure and temperature of normal plant operation) corresponded to each break diameter. These leak rates in terms of gpm were estimated from leakage calculations using the pc-PRAISE code (NUREG/CR-5186 [Gore et al. 1988]), which in turn makes use of the leak-rate model from the SQUIRT code (Paul et al. 1990).

The overall bases and assumptions of the referenced PRAs and the probability calculations are described below. Specific assumptions relative to the calculations for each plant type are described later.

- The accident sequences initiated by failure of the reactor vessel or other RCS component was modeled here as a LOCA. The break was assumed to be of sufficient size that the RCS partially or completely depressurizes, such that the plant system responds to the condition. For example, in the case of larger breaks, 1) the accumulators (or safety injection tanks) inject water immediately into the RCS to make up for the water leaking from the break, 2) low-pressure injection (LPI) systems activate to provide additional

makeup for continued core cooling, 3) low-pressure recirculation (LPR) cooling from the containment sump is established to provide long-term cooling, and 4) containment pressures and temperatures are maintained by the RHR or other safety-related system.

- Within the PRAs used for the present calculations, the ruptured RCS components were assumed to disable at least one train of the safety system designed to inject or recirculate coolant. Thus, if there is a redundant, 100% capacity train of LPI, for example, the effect of the break is to reduce the 1-out-2 LPI system to a 1-out-of-1 system. This is basically how most PRAs model large LOCAs, as most safety-injection systems inject into the RCS cold legs, resulting in the inability to inject via the affected nozzle.
- No attempt was made to model the effect of aging of the safety-system components required to respond to the ruptured RCS component.
- In general, the probabilities of unsuccessful response to the initiating events for each size of LOCA were obtained by dividing the overall CDF for LOCA sequences by the large LOCA initiator frequency.

Due to the nature of the information available from the PRAs used in the present study, it was not possible to perform detailed modeling to more precisely estimate the conditional probabilities of core damage given the specific break locations. To facilitate the approximations, the PRAs had assumed that the conditional probability of unsuccessful plant response to the initiating event was independent of break location and furthermore, that specific safety-system responses were independent of the prior initiating events and successful or unsuccessful operation of all other safety systems. The resulting conditional probabilities are therefore used in the

present study as conservative approximations of safety-system failure probabilities.

The large break was also assumed to result in rapid depressurization of the primary coolant system to below the low-pressure injection set-point such that high-pressure injection systems are not activated. Certain break locations and break sizes could result in medium or small LOCA sequences in which the RCS depressurizes to a lesser extent and more slowly. In this case, high-pressure systems would be needed to provide reactor coolant injection and recirculation.

Another area of uncertainty is that the calculations did not address the aged condition of the safety systems. Presumably, the failure rate for the aged safety system components would be higher than the plant mid-life failure rates used in most PRAs. Therefore, to properly estimate the conditional probabilities of core damage over an extended life, the effects of this aging would need to be accounted for in the conditional probabilities.

To reduce the uncertainties, a more detailed analysis would need to address these four main sources of uncertainty:

1. Effects of prior failures, such as the initiating event, on the unavailability of specific safety systems to respond to the initiator
2. Break size
3. Break location
4. Effects of aging on safety-system-component failure rates

Another case occurs in which the break or leak occurs in a safety-injection system or its transition into the RCS pipe loop. In this case, the assumption in the PRAs was that at least one train of the redundant safety-injection system has been

defeated. This would increase the unavailability of the safety-injection system to respond to the break or rupture. In general, this was treated as changing the PRA model of the safety-injection system from a 1-out-of-2 system to a 1-out-of-1 system. Assuming the two trains are independent, the unavailability of the 1-out-of-1 system can be approximated as the square root of the unavailability of the 1-out-of-2 system. Therefore, the conditional probability of core damage under these conditions at Palo Verde was estimated to be approximately  $(4E-03)^{1/2}$  or about 0.06.

Plant-specific results for conditional core-damage probabilities are described in the following subsections.

### 7.3 Newer Vintage Combustion Engineering Plant

The newer vintage CE plant used in this assessment is Palo Verde. The Palo Verde IPE was used as the basis for the calculations.

**Large LOCA.** The following two large LOCA sequences were found among the dominant sequences at Palo Verde:

1. Large LOCA followed by failure of hot-leg recirculation:  $4.6E-07/\text{yr}$
2. Large LOCA followed by failure of decay heat removal:  $4.2E-07/\text{yr}$

Thus, the total large LOCA CDF is about  $8.8E-07/\text{yr}$ . The frequency of large LOCA initiators was given to be  $2.1E-04/\text{yr}$ . Assuming that the leak or break location is in the RCS piping or at a reactor vessel nozzle, plant response would be similar to that modeled in the PRA; i.e., the unavailability of the specific safety systems defeated by the pipe or nozzle break

were already incorporated into the Palo Verde PRA models. For this case, the overall conditional probability of core damage given a large leak or break is  $8.8E-07/\text{yr} + 2.1E-04/\text{yr} = 4.19E-03$ .

**Small LOCA.** Two small LOCA sequences were found among the dominant sequences at Palo Verde. The total small LOCA CDF is about  $3.4E-06/\text{yr}$ . The frequency of small LOCA initiators was given to be  $8.0E-03/\text{yr}$ . For this case, the overall conditional probability of core damage given a small leak or break is  $3.4E-06/\text{yr} + 8.0E-03/\text{yr} = 4.25E-04$ .

### 7.4 Older Vintage Combustion Engineering Plant

The Calvert Cliffs plant was used to model older vintage CE plants. The PRA used the Calvert Cliffs Interim Reliability Evaluation Program (IREP) PRA as the basis for the calculations.

**Large LOCA.** The dominant accident sequences identified in the Calvert Cliffs IREP PRA were large LOCA sequences. The frequencies of all large LOCA sequences were less than  $1E-06/\text{yr}$ . For conservatism, this value was doubled to  $2.0E-06/\text{yr}$  to approximate the total large LOCA CDF for this plant. The large LOCA initiator frequency was given as  $2.3E-04/\text{yr}$ . Therefore, the conditional probability of core damage given a large LOCA is estimated to be  $2.0E-06/\text{yr} + 2.3E-04/\text{yr} = 8.70E-03$ .

**Small LOCA.** The estimated annual core-melt frequency resulting from small break LOCAs is about  $1.2E-05/\text{yr}$ . The small LOCA initiator frequency was given as  $2.1E-02/\text{yr}$ . Therefore, the conditional probability of core damage given a small LOCA is estimated to be  $1.2E-05/\text{yr} + 2.1E-02/\text{yr} = 5.71E-04$ .

## 7.5 B&W 177 Fuel Assembly Plant

To represent the B&W plant, the Oconee plant was selected.

**Large LOCA.** From the Oconee IPE, the calculated annual core-melt frequency resulting from large break LOCAs is about  $1.9E-06/\text{yr}$  (based on the dominant accident sequence results). The estimated large LOCA initiator frequency for the Oconee plant is  $7.0E-04$ . Therefore, the conditional core damage probability is estimated to be  $1.9E-06/\text{yr} + 7.0E-04/\text{yr} = 2.71E-03$ .

**Small LOCA.** From the Oconee IPE, the calculated annual core-melt frequency resulting from a small-break LOCAs is about  $3.7E-07/\text{yr}$  (based on the dominant accident sequence results). The estimated small LOCA initiator frequency for the Oconee plant is  $4.0E-03/\text{yr}$ . Therefore, the conditional core-damage probability is estimated to be  $3.7E-07/\text{yr} + 4.0E-03/\text{yr} = 9.25E-05$ .

## 7.6 Newer Vintage Westinghouse Plant

Sequoyah was selected to model newer vintage W Plants. The Sequoyah PRA (SNL 1990a) performed in support of the NUREG-1150<sup>(a)</sup> program was used as the basis for these calculations.

**Large LOCA.** The Sequoyah PRA stated that large LOCA sequences made up about 16% of the total CDF of  $5.72E-05/\text{yr}$ . Therefore, the total CDF due to large LOCA sequences is about  $9.36E-06/\text{yr}$ . The frequency of large LOCA initiators was given as  $5.0E-04/\text{yr}$ . As a result,

the conditional probability of core damage given a large LOCA sequence is estimated to be about  $9.36E-06/\text{yr} + 5.0E-04/\text{yr} = 1.872E-02$ .

**Small LOCA.** The total CDF due to small LOCA sequences is about  $2.7E-05/\text{yr}$ . The frequency of small LOCA initiators was given as  $1.0E-03/\text{yr}$ . As a result, the conditional probability of core damage given a small LOCA sequence is estimated from the Sequoyah PRA to be about  $2.7E-05/\text{yr} + 1.0E-03/\text{yr} = 2.7E-02$ . This small LOCA probability nearly equals that for the large LOCA and is significantly greater (by a factor of about 100) than the corresponding small LOCA probabilities for the five other PWR plants. Because the issues regarding the  $2.7E-02$  value could not be resolved, this value was replaced by the average of the small LOCA probabilities ( $4.8E-04$ ) for the other five PWR plants. The intent was to ensure that results of the present study not be biased by any uncharacteristic conservatisms in the Sequoyah PRA or by some plant-specific vulnerability unique to Sequoyah.

## 7.7 Older Vintage Westinghouse Plant

The Surry plant was selected to represent the older vintage W plant. The Surry, Unit 1 PRA NUREG/CR 4550 (SNL 1990b) was used to support the conditional core damage probability (CCDP) calculations.

**Large LOCA.** The Surry PRA estimated that the contribution from a large LOCA to total core damage frequency (/yr) is approximately 14%, which is about  $5.16E-06/\text{yr}$ . The frequency of large LOCA initiators was estimated to be  $5.0E-4/\text{yr}$ . Hence, the conditional core-damage probability is estimated to be  $5.16E-06/\text{yr} + 5.0E-04/\text{yr} = 1.03E-02$ .

**Small LOCA.** The Surry PRA estimated that the contribution from a small LOCA to total core-damage frequency is approximately 2.1%, which

---

(a) Summary Report, second draft for peer review, *Severe Accident Risks: An Assessment of Five U.S. Nuclear Power Plants*, NUREG-1150, U.S. Nuclear Regulatory Commission, Washington D.C.

is about  $8.4E-07/yr$ . The frequency of small LOCA initiators was estimated to be  $1.0E-3/yr$ . Hence, the conditional core-damage probability is estimated to be  $8.4E-07/yr + 1.0E-03/yr = 8.4E-04$ .

### 7.8 Newer Vintage GE Plant

The Grand Gulf plant was picked to represent a newer vintage GE plant. The Grand Gulf PRA addressed in NUREG/CR-4550 (SNL 1989a) was used as a basis for CCDP estimation.

**Large LOCA.** Based on the dominant-accident-sequences table, large LOCA events were estimated to contribute approximately  $1.1E-09/yr$  to the total annual core-melt frequency. The large LOCA initiator frequency was given as  $1.0E-04/yr$ . As a result, the conditional probability of core damage given a large LOCA event is estimated to be  $1.1E-09/yr + 1.0E-04/yr = 1.1E-05$ .

**Small LOCA.** Based on the dominant-accident-sequences table, small LOCA initiating events were estimated to contribute  $<1.0E-10/yr$  to the total annual core-melt frequency. The small LOCA initiator frequency was given as  $3.0E-03/yr$ . As a result, the conditional probability of core damage given a small LOCA event is estimated to be  $<1.0E-10/yr + 3.0E-03/yr < 3.3E-08$ .

### 7.9 Older Vintage GE Plant

Peach Bottom was chosen to represent an older vintage GE plant. NUREG/CR 4550 (SNL 1989b) was used as a basis for the CCDP calculation.

**Large LOCA.** The contribution to total CDF from large LOCA events is about  $5.3E-8/yr$ , based on the dominant-accident-sequences table. The large LOCA initiating-event frequency was provided as  $1.0E-04/yr$ . Finally, the conditional

probability of core damage given a large LOCA event is estimated to be about  $5.3E-08/yr + 1.0E-04/yr = 5.3E-04$ .

**Small LOCA.** The contribution to total CDF from small LOCA events is about  $4.0E-09/yr$ , based on the dominant-accident-sequences table. The small LOCA initiating-event frequency was provided as  $3.0E-03/yr$ . Finally, the conditional probability of core damage given a small LOCA event is estimated to be about  $4.0E-09/yr + 3.0E-03/yr = 1.3E-06$ .

### 7.10 Summary and Generalization of PRA Results

Table 7.2 summarizes the plant-specific PRA results for the seven plant types in terms of conditional core damage probabilities for each category of LOCA. Plant-specific definitions of

Plant Type	Conditional Core Damage Probability		
	Small LOCA	Medium LOCA	Large LOCA
New CE (Palo Verde)	4.2E-04	--	4.2E-03
Old CE (Calvert Cliffs)	5.7E-04	--	8.7E-03
B&W (Oconee)	9.2E-05	--	2.7E-03
New W (Sequoyah)	4.8E-04	--	1.9E-02
Old W (Surry-1)	8.4E-04	4.0E-03	1.0E-02
New GE (Grand Gulf)	< 3.3E-08	--	1.1E-05
Old GE (Peach Bottom)	1.6E-06	--	5.3E-04

small, medium, and large LOCAs are the same as those given in Table 7.1. In the case of the Surry-1 plant, a data point for the medium LOCA is given in Table 7.2, and the value shows a core-damage probability intermediate to the values for the small and large LOCA categories.

A review of Tables 7.1 and 7.2 shows significant differences between results for the PWR plants as a group and the BWR plants as a second group. There are similar trends both in terms of the definitions of break sizes and in the conditional CDFs within the PWR and BWR plant types. It was decided that it was not meaningful in the present evaluations to differentiate between specific PWR or BWR plants. Furthermore, the specific plants for the PRA results did not correspond (other than in terms of vendor and vintage) to the (unidentified) plants addressed in the fracture-mechanics calculations. Given that meaningful plant-specific comparisons could not be made, two "generic" categories were used with reference to Tables 7.1 and 7.2 to describe the PRA results. The pipe break or leak categories for the PWR and BWR plants were assigned as given in Table 7.3. The generic categories were selected for purposes of convenience to match the leakage rates selected in the probabilistic fracture mechanics calculations. These leakage rates were then mapped in a conservative manner to the LOCA categories of the PRAs.

The results of Table 7.2 were used to assign conditional core-damage probabilities (Table 7.4) for the PWR and BWR plants. The values listed in Table 7.4 were used to generate the numbers for core damage frequency reported in Section 9.

**Table 7.3 Leak/Break Categories for Generic Treatment of PRA Results for PWR and BWR Plants**

Plant Type	Leak with No Safety Consequences	Small LOCA	Large LOCA
PWR	<30 gpm	30-500 gpm	>500 gpm
BWR	--	>0 gpm	>30 gpm

**Table 7.4 Consequences Assigned for Generic Leak/Break Categories for PWR and BWR Plants**

Plant Type	Small LOCA	Large LOCA
PWR	5.E-04	1.E-02
BWR	1.E-06	5.E-04

## 8 METHODOLOGY FOR CALCULATING CORE DAMAGE FREQUENCIES

Through-wall cracks can cause core damage if the leakage rate through the crack exceeds the leakage rates corresponding to plant criteria for small or large LOCAs. The previous sections have described the methodologies and results for calculating frequencies of through-wall cracks, the approach used to assign through-wall cracks to the categories of small and large LOCAs, and the estimates for conditional core damage probabilities.

The following equations were used to develop the tables of Appendix B:

$$CDF = CDF_{LARGE\ LOCA} + CDF_{SMALL\ LOCA}$$

where CDF = core damage frequency contribution from through-wall cracks

$CDF_{LARGE\ LOCA}$  = core damage frequency due to large LOCAs

$CDF_{SMALL\ LOCA}$  = core damage frequency due to small LOCAs

The core damage frequency for a large LOCA is calculated as follows:

$$CDF_{LARGE\ LOCA} = F_{TWC} \times \frac{FRAC_{LARGE\ LOCA}}{COND\_CDF_{LARGE\ LOCA}} \times$$

where  $F_{TWC}$  = frequency of through-wall cracks (per year)

$FRAC_{LARGE\ LOCA}$  = fraction of through-wall cracks that result in large LOCA

$COND\_CDF_{LARGE\ LOCA}$  = conditional core damage probability given a large LOCA.

Similarly, the core-damage frequency for a small LOCA is calculated as

$$CDF_{SMALL\ LOCA} = F_{TWC} \times \frac{FRAC_{SMALL\ LOCA}}{COND\_CDF_{SMALL\ LOCA}} \times$$

where  $F_{TWC}$  = frequency of through-wall cracks (per year)

$FRAC_{SMALL\ LOCA}$  = fraction of through-wall cracks that result in small LOCA

$COND\_CDF_{SMALL\ LOCA}$  = conditional core damage probability given a small LOCA.

Both small and large LOCAs can contribute to CDFs. The consequences of large LOCAs are much greater than the consequences for small LOCAs. However, small LOCAs have much higher frequencies of occurrence, making it possible for small LOCAs to make significant contributions to core damage.

## 9 RESULTS OF CALCULATIONS FOR SELECTED COMPONENTS

Calculations were performed with the pc-PRAISE code to address the 47 selected components from the seven plants as listed in Section 2.0. These calculations predicted probabilities of crack initiation and probabilities of through-wall cracks as a function of time for plant operating periods up to 60 years. Probabilities of crack initiation were calculated using the fatigue-life correlations from the ANL research for NRC. The alternating stresses and anticipated number of cycles were the same as those used for the deterministic calculations of fatigue usage factors of NUREG/CR-6260 (Ware et al. 1995). Detailed inputs and results for the probabilistic fracture mechanics calculations are given in Appendix A. Application of these failure probability calculations to the estimation of CDFs is described by the tables of Appendix B.

Table 9.1 provides an overall summary of the final results for all the components. Results are given for both a 40-year and a 60-year operating period. Many of the components have cumulative probabilities of crack initiation and cumulative probabilities of through-wall cracks that approach unity within the 40-year to 60-year time period. Other components, often with similar values of fatigue usage factors, show much lower failure probabilities. The maximum failure rate (through-wall cracks per year) is about  $5 \times 10^{-2}$ , and the maximum core-damage frequency based on these calculated failure rates is about  $1.0 \times 10^{-6}$  per year. These maximum values correspond to components with very high cumulative failure probabilities, and the failure rates do not change significantly from 40 years to 60 years. Failure rates for other components having much lower probabilities of failure are seen to increase by as much as an order of magnitude from 40 years to 60 years, but these components make relatively small overall contributions to CDFs.

### 9.1 Analysis Procedure

The pc-PRAISE code was applied in the calculations, which implied that all the components could be approximated by the cylindrical geometry of pipe with a circumferential crack. In many cases, this geometry corresponded to the actual configuration of the component (safe ends), whereas in other cases (nozzles and elbows), the pc-PRAISE model only approximated the actual component. Crack initiation depends only on the peak local stresses, meaning that the actual component geometry was not a significant factor. In the case of the crack initiation at multiple sites, the pc-PRAISE model required an input of the number of potential 5-cm (2-in.) long initiation sites. A nominal diameter enabled the pipe circumference and the corresponding number of initiation sites to be estimated. The growth of these initiated cracks required additional definition of component geometry, and this was provided by an input for the component wall thickness. In the case of nozzle configurations, the component thickness corresponded to the smaller of the two connecting members (e.g., a pipe dimension rather than a vessel dimension).

The Monte Carlo calculations with the pc-PRAISE code were run to a maximum of  $10^6$  simulations. Because some components had very low failure probabilities, this number of simulations was sometimes inadequate to establish probabilities of through-wall cracks. Rather than reporting a probability as less than  $10^{-6}$ , additional calculations were performed with a Latin Hypercube approach developed by PNNL on a prior NRC research project (Khaleel and Simonen 1998). The italicized values in Table 9.1 were derived from these supplementary calculations. The Latin Hypercube code was benchmarked against pc-PRAISE. It was verified to predict

Table 9.1 Summary of Results for All Seven Plants—Water Environment

PLANT	COMPONENT	MAT	USEAGE@40	DET	COMCUMATIVE PFC@40YR	COMCUMATIVE PFC@40YR	COMCUMATIVE PFC@40YR	TRICYEAR @40YR	TRICYEAR @40YR	TRICYEAR @40YR	Q40YR	Q40YR	Q40YR
GE-NEW	RPV LOWER HEAD SHELL	LAS	170E-02	210E-02	70E-02	170E-02	170E-02	170E-02	170E-02	170E-02	170E-02	170E-02	170E-02
GE-NEW	RPV INLET NOZZLE	LAS	47E-01	71E-01	70E-01	70E-01	70E-01	70E-01	70E-01	70E-01	70E-01	70E-01	70E-01
GE-NEW	RPV OUTLET NOZZLE	LAS	47E-01	70E-01	70E-01	70E-01	70E-01	70E-01	70E-01	70E-01	70E-01	70E-01	70E-01
GE-NEW	RPV OUTLET ELBOW	304316	27E-01	30E-01	30E-01	30E-01	30E-01	30E-01	30E-01	30E-01	30E-01	30E-01	30E-01
GE-NEW	CHARGING NOZZLE NOZZLE	LAS	10E-01	13E-01	13E-01	13E-01	13E-01	13E-01	13E-01	13E-01	13E-01	13E-01	13E-01
GE-NEW	CHARGING NOZZLE SAFE END	304316	60E-01	73E-01	73E-01	73E-01	73E-01	73E-01	73E-01	73E-01	73E-01	73E-01	73E-01
GE-NEW	SAFETY INJECTION NOZZLE NOZZLE	LAS	43E-01	63E-01	63E-01	63E-01	63E-01	63E-01	63E-01	63E-01	63E-01	63E-01	63E-01
GE-NEW	SAFETY INJECTION NOZZLE SAFE E	304316	20E-01	23E-01	23E-01	23E-01	23E-01	23E-01	23E-01	23E-01	23E-01	23E-01	23E-01
GE-NEW	SHUTDOWN COOLING LINE ELBOW	304316	43E-01	73E-01	73E-01	73E-01	73E-01	73E-01	73E-01	73E-01	73E-01	73E-01	73E-01
GE-OLD	RPV LOWER HEAD SHELL	LAS	130E-02	130E-02	130E-02	130E-02	130E-02	130E-02	130E-02	130E-02	130E-02	130E-02	130E-02
GE-OLD	RPV INLET NOZZLE	LAS	17E-01	23E-01	23E-01	23E-01	23E-01	23E-01	23E-01	23E-01	23E-01	23E-01	23E-01
GE-OLD	RPV OUTLET NOZZLE	LAS	63E-01	63E-01	63E-01	63E-01	63E-01	63E-01	63E-01	63E-01	63E-01	63E-01	63E-01
GE-OLD	RPV OUTLET ELBOW	304316	63E-01	63E-01	63E-01	63E-01	63E-01	63E-01	63E-01	63E-01	63E-01	63E-01	63E-01
GE-OLD	CHARGING NOZZLE SAFE END	304316	63E-01	63E-01	63E-01	63E-01	63E-01	63E-01	63E-01	63E-01	63E-01	63E-01	63E-01
GE-OLD	SAFETY INJECTION NOZZLE NOZZLE	304316	17E-01	23E-01	23E-01	23E-01	23E-01	23E-01	23E-01	23E-01	23E-01	23E-01	23E-01
GE-OLD	SHUTDOWN COOLING LINE ELBOW	304316	63E-01	63E-01	63E-01	63E-01	63E-01	63E-01	63E-01	63E-01	63E-01	63E-01	63E-01
GE-NEW	RPV NEAR SUPPORT SKIRT	LAS	23E-01	23E-01	23E-01	23E-01	23E-01	23E-01	23E-01	23E-01	23E-01	23E-01	23E-01
GE-NEW	RPV OUTLET NOZZLE	LAS	43E-01	73E-01	73E-01	73E-01	73E-01	73E-01	73E-01	73E-01	73E-01	73E-01	73E-01
GE-NEW	IMAGERY NOZZLE SAFE END	304316	10E-01	13E-01	13E-01	13E-01	13E-01	13E-01	13E-01	13E-01	13E-01	13E-01	13E-01
GE-NEW	DECAY HEAT REMOVAL DUCTING T	304316	63E-01	63E-01	63E-01	63E-01	63E-01	63E-01	63E-01	63E-01	63E-01	63E-01	63E-01
GE-NEW	RPV LOWER HEAD SHELL	LAS	130E-02	130E-02	130E-02	130E-02	130E-02	130E-02	130E-02	130E-02	130E-02	130E-02	130E-02
GE-NEW	RPV INLET NOZZLE	LAS	23E-01	23E-01	23E-01	23E-01	23E-01	23E-01	23E-01	23E-01	23E-01	23E-01	23E-01
GE-NEW	RPV OUTLET NOZZLE	LAS	63E-01	63E-01	63E-01	63E-01	63E-01	63E-01	63E-01	63E-01	63E-01	63E-01	63E-01
GE-NEW	CHARGING NOZZLE NOZZLE	316NG	33E-01	33E-01	33E-01	33E-01	33E-01	33E-01	33E-01	33E-01	33E-01	33E-01	33E-01
GE-NEW	SAFETY INJECT NOZZLE NOZZLE	316NG	10E-01	13E-01	13E-01	13E-01	13E-01	13E-01	13E-01	13E-01	13E-01	13E-01	13E-01
GE-NEW	RESIDUAL HEAT INLET TRAN	304316	27E-01	30E-01	30E-01	30E-01	30E-01	30E-01	30E-01	30E-01	30E-01	30E-01	30E-01
GE-OLD	RPV LOWER HEAD SHELL	LAS	63E-01	63E-01	63E-01	63E-01	63E-01	63E-01	63E-01	63E-01	63E-01	63E-01	63E-01
GE-OLD	RPV INLET NOZZLE INNER SURFACE	LAS	30E-01	30E-01	30E-01	30E-01	30E-01	30E-01	30E-01	30E-01	30E-01	30E-01	30E-01
GE-OLD	RPV INLET NOZZLE OUTER SURFACE	LAS	43E-01	73E-01	73E-01	73E-01	73E-01	73E-01	73E-01	73E-01	73E-01	73E-01	73E-01
GE-OLD	RPV OUTLET NOZZLE INNER SURF	LAS	43E-01	73E-01	73E-01	73E-01	73E-01	73E-01	73E-01	73E-01	73E-01	73E-01	73E-01
GE-OLD	RPV OUTLET NOZZLE OUTER SURF	LAS	43E-01	73E-01	73E-01	73E-01	73E-01	73E-01	73E-01	73E-01	73E-01	73E-01	73E-01
GE-OLD	CHARGING NOZZLE NOZZLE	304316	13E-01	13E-01	13E-01	13E-01	13E-01	13E-01	13E-01	13E-01	13E-01	13E-01	13E-01
GE-OLD	SAFETY INJECTION NOZZLE NOZZLE	304316	33E-01	33E-01	33E-01	33E-01	33E-01	33E-01	33E-01	33E-01	33E-01	33E-01	33E-01
GE-OLD	RESIDUAL HEAT REMOVAL TEE	304316	20E-01	23E-01	23E-01	23E-01	23E-01	23E-01	23E-01	23E-01	23E-01	23E-01	23E-01
GE-NEW	RPV NEAR CROM PENETRATION	LAS	63E-01	63E-01	63E-01	63E-01	63E-01	63E-01	63E-01	63E-01	63E-01	63E-01	63E-01
GE-NEW	FEEDWATER NOZZLE SAFE END	LAS	130E-01	130E-01	130E-01	130E-01	130E-01	130E-01	130E-01	130E-01	130E-01	130E-01	130E-01
GE-NEW	RECIRC SYS - TEE SUCTION PIPE	304316	63E-01	63E-01	63E-01	63E-01	63E-01	63E-01	63E-01	63E-01	63E-01	63E-01	63E-01
GE-NEW	CORE SPRAY LINE SAFE END EXT	LAS	43E-01	63E-01	63E-01	63E-01	63E-01	63E-01	63E-01	63E-01	63E-01	63E-01	63E-01
GE-NEW	RR LINE STRAIGHT PIPE	LAS	130E-01	130E-01	130E-01	130E-01	130E-01	130E-01	130E-01	130E-01	130E-01	130E-01	130E-01
GE-NEW	FEEDWATER LINE ELBOW	LAS	130E-01	130E-01	130E-01	130E-01	130E-01	130E-01	130E-01	130E-01	130E-01	130E-01	130E-01
GE-OLD	RPV LOWER HEAD TO SHELL	LAS	73E-02	73E-02	73E-02	73E-02	73E-02	73E-02	73E-02	73E-02	73E-02	73E-02	73E-02
GE-OLD	RPV FEEDWATER NOZZLE BORE	LAS	130E-01	130E-01	130E-01	130E-01	130E-01	130E-01	130E-01	130E-01	130E-01	130E-01	130E-01
GE-OLD	RECIRC SYSTEM RHR RETURN LINE	304316	63E-01	63E-01	63E-01	63E-01	63E-01	63E-01	63E-01	63E-01	63E-01	63E-01	63E-01
GE-OLD	CORE SPRAY SYSTEM NOZZLE	LAS	63E-01	63E-01	63E-01	63E-01	63E-01	63E-01	63E-01	63E-01	63E-01	63E-01	63E-01
GE-OLD	CORE SPRAY SYSTEM SAFE END	304316	17E-01	23E-01	23E-01	23E-01	23E-01	23E-01	23E-01	23E-01	23E-01	23E-01	23E-01
GE-OLD	RESIDUAL HEAT TAPERED	304316	47E-01	73E-01	73E-01	73E-01	73E-01	73E-01	73E-01	73E-01	73E-01	73E-01	73E-01
GE-OLD	FEEDWATER LINE - RHC TEE	LAS	63E-01	63E-01	63E-01	63E-01	63E-01	63E-01	63E-01	63E-01	63E-01	63E-01	63E-01

identical probabilities of crack initiation and nearly the same probabilities of through-wall cracks for those cases in which the through-wall stress distribution was one of uniform tension. Due to differences in stress intensity factor solutions for deep flaws, the PNNL code gave somewhat lower probabilities for cases with large through-wall stress gradients. The supplementary calculations assumed only one initiation site, but used the unmodified ANL initiation equations, which included the  $\ln(4)$  term to account for differences in fatigue lives between test specimens and piping components. The initiated cracks were 3-mm deep and had aspect ratios of 10:1. The crack was assumed to grow with a constant aspect ratio of 10:1. The stress distributions through the wall of the component were conservatively taken to be of uniform tension. The importance sampling procedure of the Latin Hypercube code permitted calculations of through-wall crack probabilities as small as  $10^{-15}$ .

The pc-PRAISE calculations were based on a number of conservative modeling assumptions and input parameters, balanced by other unconservative assumptions and inputs. In the balance, the calculations are believed to provide realistic predictions of through-wall crack frequencies for the assumed cyclic stresses. The inputs for stress cycles as taken from the INEL report (NUREG/CR-6260 [Ware et al. 1995]) are believed in most cases to conservatively bound the stresses experienced during actual plant operation. These stresses were taken from design stress reports that assumed bounding conditions for thermal stress transients and other loads. In addition, the method used to derive load pairs from the transient descriptions assumed worst-case sequencing of loads. The method used in the present calculations to estimate through-wall stress distributions (uniform tension versus through-wall gradient) were intended to overestimate the fraction of the stress assigned to the uniform tension category. Inputs for strain rates, oxygen, and sulfur were all assigned as bounding values that are unlikely to be present simultaneously at these maximum values for any given component.

The present calculations also include some simplifications and optimistic assumptions that would balance other conservatisms. It was assumed that crack growth occurred under conditions of zero R-ratio. While this assumption will be conservative for those transients with very high stress amplitudes, crack growth rates for cases of high cycle/low stress fatigue could be underestimated. Another assumption was that random scatter in the cycles to crack initiation and the scatter in the crack growth rates were independent. Similarly, random variations in the number of cycles to crack initiation were assumed by the pc-PRAISE model that addressed multiple crack initiations to be uncorrelated from site-to-site in a given weld.

## 9.2 Comparison of Probabilities with Usage Factors

Figure 9.1 shows the degree of correlation between calculated probabilities of through-wall cracks for each of the 47 components with the fatigue usage factors reported in NUREG/CR-6260 (Ware et al. 1995). It is clear that the correlation is only approximate. This relatively poor correlation is related to the fact that the usage factors address only crack initiation, and as such do not address the specific factors for each component that determine how likely it is that an initiated crack will grow to become a through-wall crack.

The plot indicates that fatigue failures can be expected (probability of failure greater than say  $>10^{-1}$ ) even for usage factors less than one. Usage factors greater than one can sometimes result in essentially 100 percent failure probability. On the other hand, Figure 9.1 indicates that for usage factors of 0.1 or less, the probabilities of failure become relatively low ( $10^{-3}$  or less). These overall trends are consistent with the viewpoint that code usage factors were not intended to be precise predictors of cycles to fatigue failure, but rather a method to establish acceptable designs. In this regard, it should be noted that plant operating experience has shown

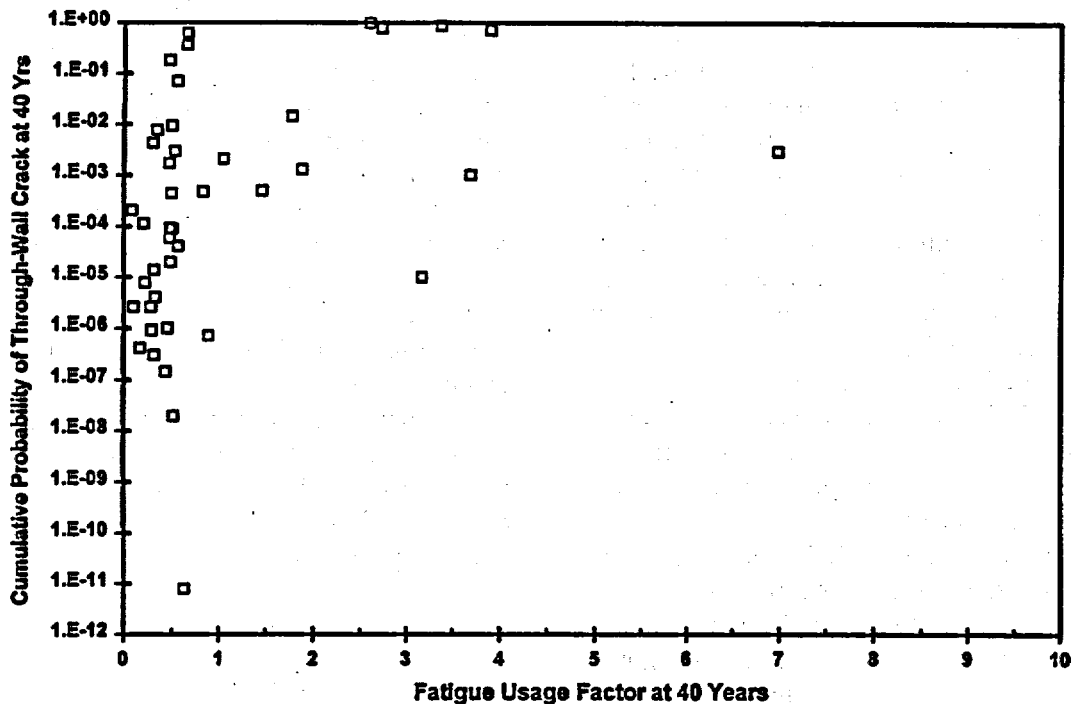


**Figure 9.1 Comparison of Calculated Usage Factors with Calculated Through-Wall Crack Probabilities**

few if any fatigue failures for the loading conditions identified in the design calculations. Instead, fatigue failures have generally been due to stresses (vibration, thermal fatigue, etc.) that were not anticipated during plant design.

### 9.3 Probabilities at 60 Years Versus 40 Years

Figures 9.2 to 9.5 show trends of the calculated results of Table 9.1. These plots display the overall range of the data and compare the probabilities and failure frequencies at the end of a 60-year plant life with the corresponding values for a 40-year plant life. The range of the through-wall crack probabilities (Figure 9.3) covers about seven orders of magnitude. When component-to-component differences in conditional probabilities of large versus small leaks and core damage are included into the comparisons, the component-to-component range for CDFs (Figure 9.5) increases to almost 12 orders of magnitude.

The probabilities and frequencies corresponding to a 60-year plant life can be a factor of 10 or greater than those for 40-year plant life. It should, however, be noted that these relative differences are greatest for those cases that have relatively small values at 40 years. In contrast, there are only small increases between 40 years to 60 years when the 40-year probabilities are already quite large. The through-wall crack frequencies (Figure 9.3) saturate at a value of about  $5 \times 10^{-2}$  (through-wall cracks per year per component), with little or no increase between 40 years and 60 years. Such components have cumulative failure probabilities that approach unity at a plant life of 40 years. In these cases, the fatigue cracks that initiate relatively early in life result in a high potential of leaking before the end of a 40-year operating period. In terms of plant operating experience and practices, it is unlikely that such high levels of fatigue damage would go unnoticed at a significant number of fatigue sites. In practice, it is likely that corrective action programs consisting of augmented inspections, repairs and replacements, along

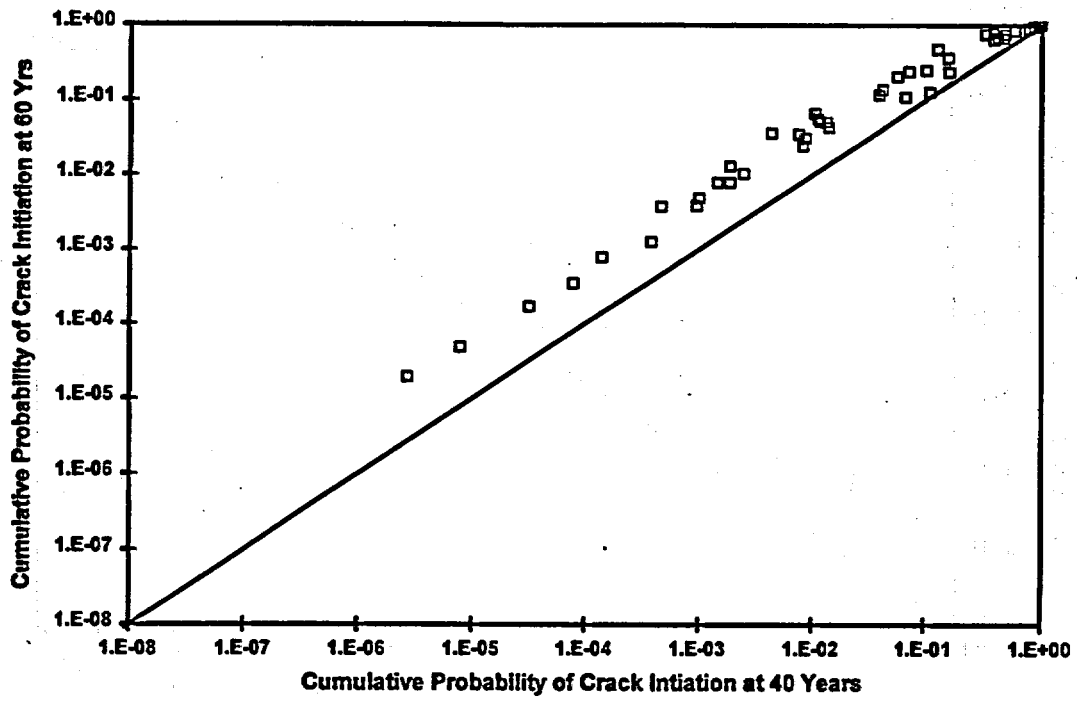


**Figure 9.2 Cumulative Probability of Crack Initiation at 40 Years Versus 60 Years**

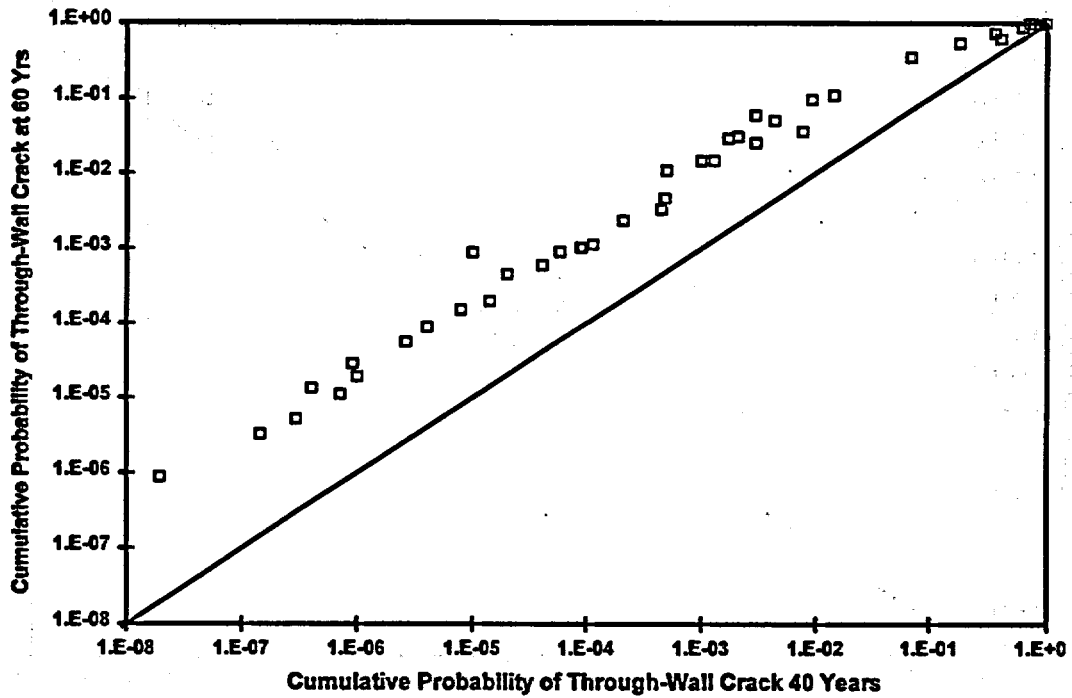


**Figure 9.3 Cumulative Probability of Through-Wall Crack at 40 Years Versus 60 Years**

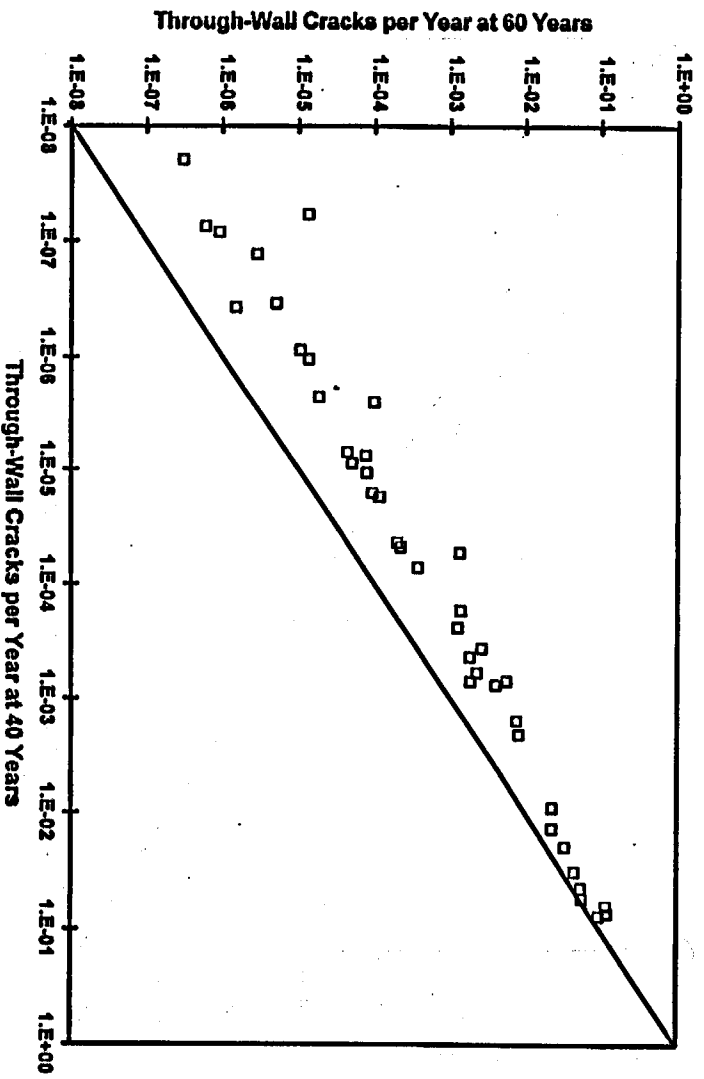


Figure 9.4 Through-Wall Cracks per Year at 40 Years Versus 60 Years

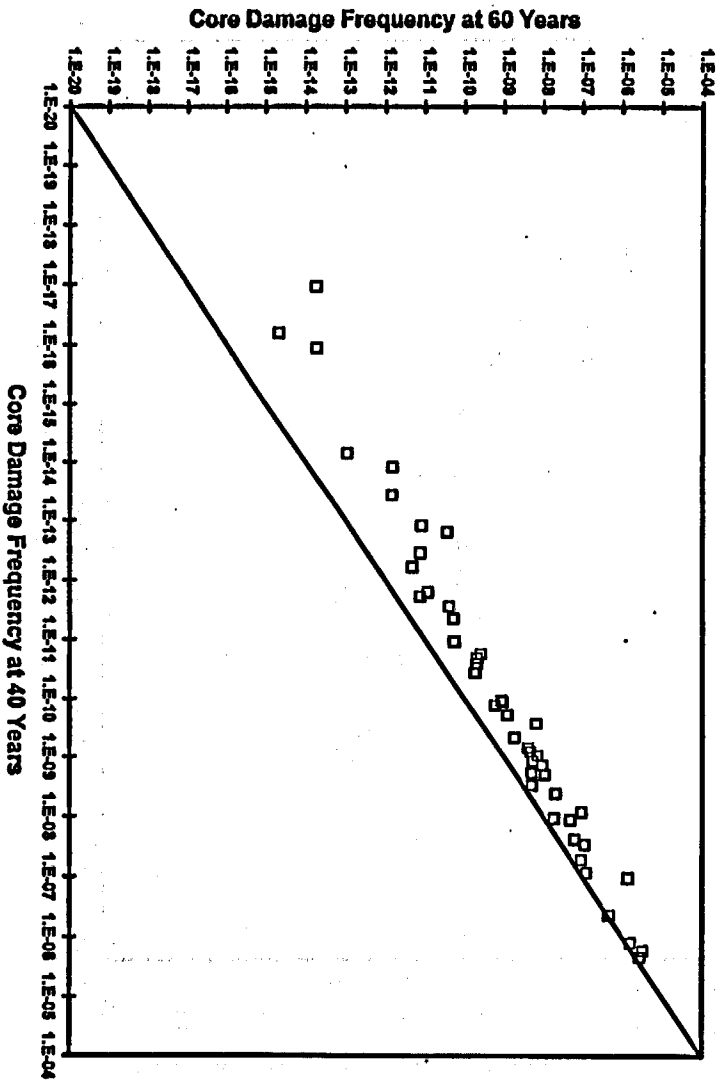


Figure 9.5 Core-Damage Frequency at 40 Years Versus 60 Years

with changes to plant operating practice would be implemented before the end of a 40-year operating period. Such programs could significantly decrease the actual failure frequencies from those calculated here. The present model neglects the significant reductions in failure frequencies from such programs.

Only three of the components in Table 9.1 have calculated CDFs that exceed  $10^{-6}$  per year. It is also noted that the CDFs for the BWR type plants are generally much lower than those for the PWR plants. This is a direct result of the lower probabilities of core damage, given the occurrence of small and large leaks. Excluding for now the B&W vessel location, the two locations of most concern (CDF >  $1.0E-06$ ) are the surge line elbow in the newer vintage CE plant and the residual heat removal system inlet transition for the newer vintage Westinghouse plant. The B&W vessel location needs further consideration to determine if the cyclic stresses have realistic values, whereas the surge line location has been subject to detailed industry stress calculations that have confirmed the high levels of the estimated stresses. Section 9.5 addresses the through-wall crack probabilities for the CE surge line location in greater detail.

#### 9.4 Water Versus Air Environment

The specific objective of the present study was to compare predicted probabilities of fatigue failures for a 60-year plant life versus a 40-year plant life with the effect of reactor coolant environments included in both evaluations. Additional calculations were performed to establish the separate effects of environment independent of the issue of 40 years versus 60 years. Table 9.2 provides results for the calculations for the air environment for comparison with the water environment data of Table 9.1.

Figures 9.6 to 9.8 use the 40-year life for the water environment as the baseline case. The data show that changing to an air environment gives lower probabilities of crack initiation and

through-wall cracks (by about a factor of 100). In contrast, changing from a 40-year life to a 60-year life increases the probabilities, but the relative increase (a factor of about 10) is not nearly as large as that associated with the environmental effects on fatigue life.

Figure 9.8 compares CDFs for air and water environments. The frequencies of through-wall cracks for the air environment had very small values. It was possible to address only about a third of the components within the computational limitations of the Monte Carlo simulation performed by the pc-PRAISE computer code. The other components were evaluated on the basis of calculations performed with the Latin hypercube approach. The results of Figure 9.8 show significant effects of the water environment and relatively less significant effects for the extended operating period from 40 years to 60 years.

#### 9.5 Sensitivity Calculations for Surge Line Elbow

This section presents some detailed pc-PRAISE results for the surge line elbow of the newer vintage CE plant and compares these results with results for another component selected from the same plant that has much lower levels of fatigue usage. A final set of results is from sensitivity calculations that made alternative assumptions regarding through-wall stress gradients. These results provide additional insights into the trends shown by Table 9.1 and by Figures 9.2 to 9.5.

Figure 9.9 presents failure probabilities predicted by pc-PRAISE for the surge line elbow in terms of probabilities of crack initiation and through-wall cracks as a function of time. It is seen that cracks initiate rather early in the plant life. There is about a 50-percent probability of initiating a fatigue crack after only 10 years of operation. Over this 10 years, about 50 percent of these initiated cracks are predicted to grow to become leaking cracks. The frequency of through-wall cracks (lower curve) increases significantly over



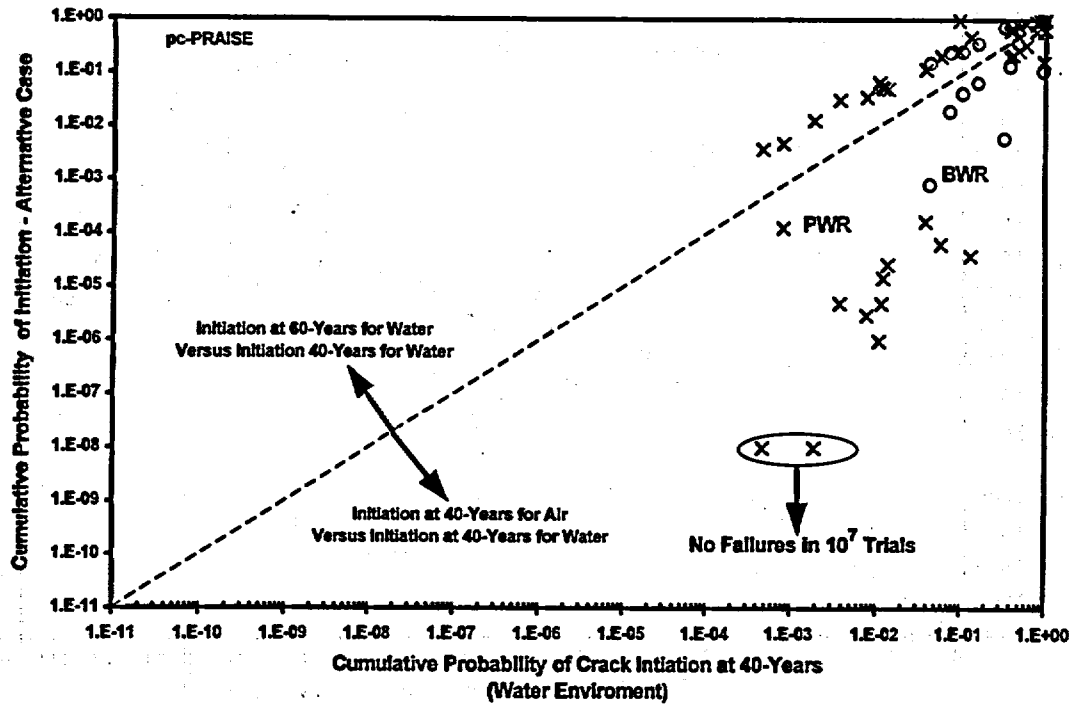


Figure 9.6 Comparison of Probabilities of Fatigue Crack Initiation for Air Versus Water Environment and for 40-Year Life and 60-Year Life

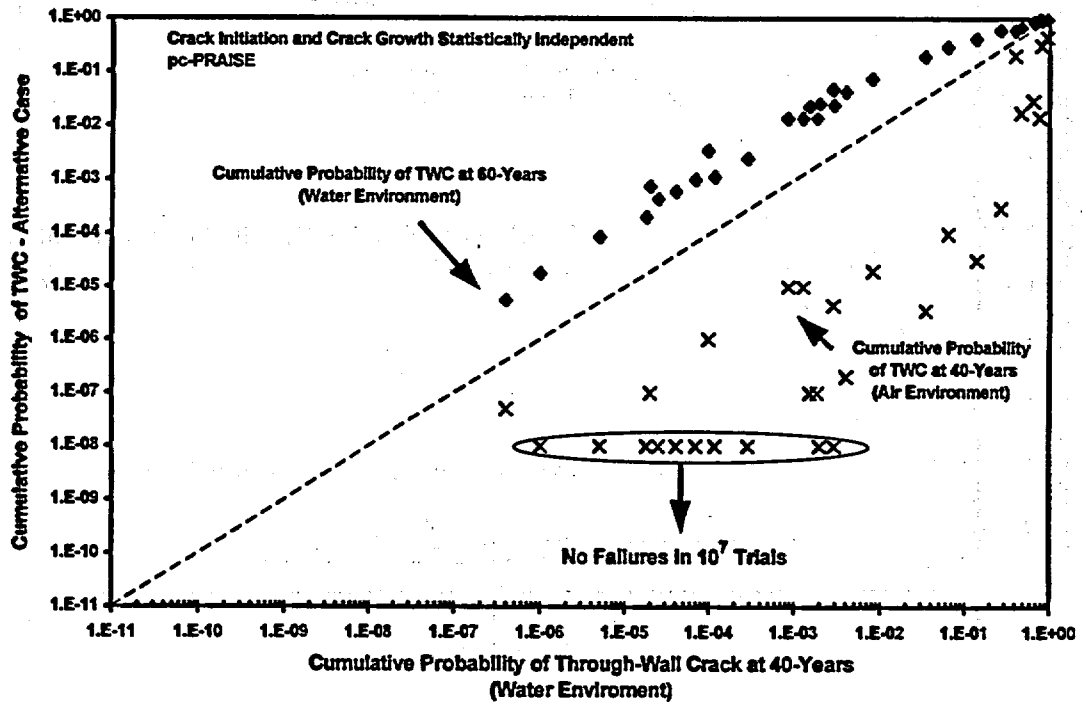


Figure 9.7 Comparison of Through-Wall Crack Probabilities for Air Versus Water Environment and for 40-Year Life and 60-Year Life

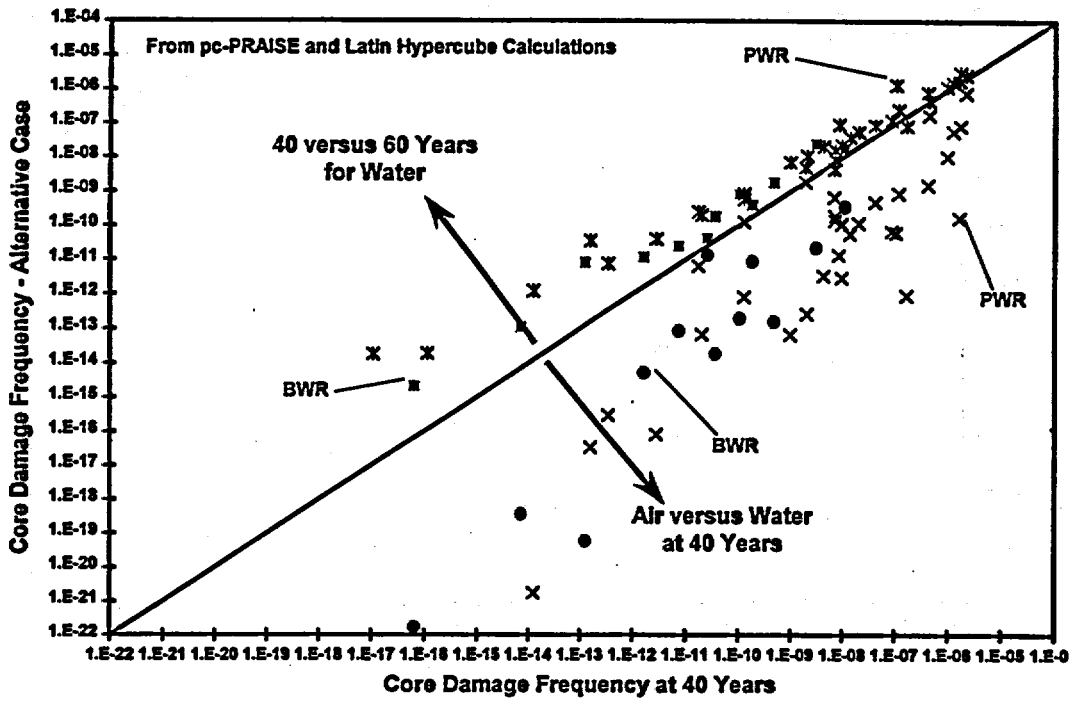


Figure 9.8 Comparison of CDFs for Air Versus Water Environment and for 40-Year Life and 60-Year Life

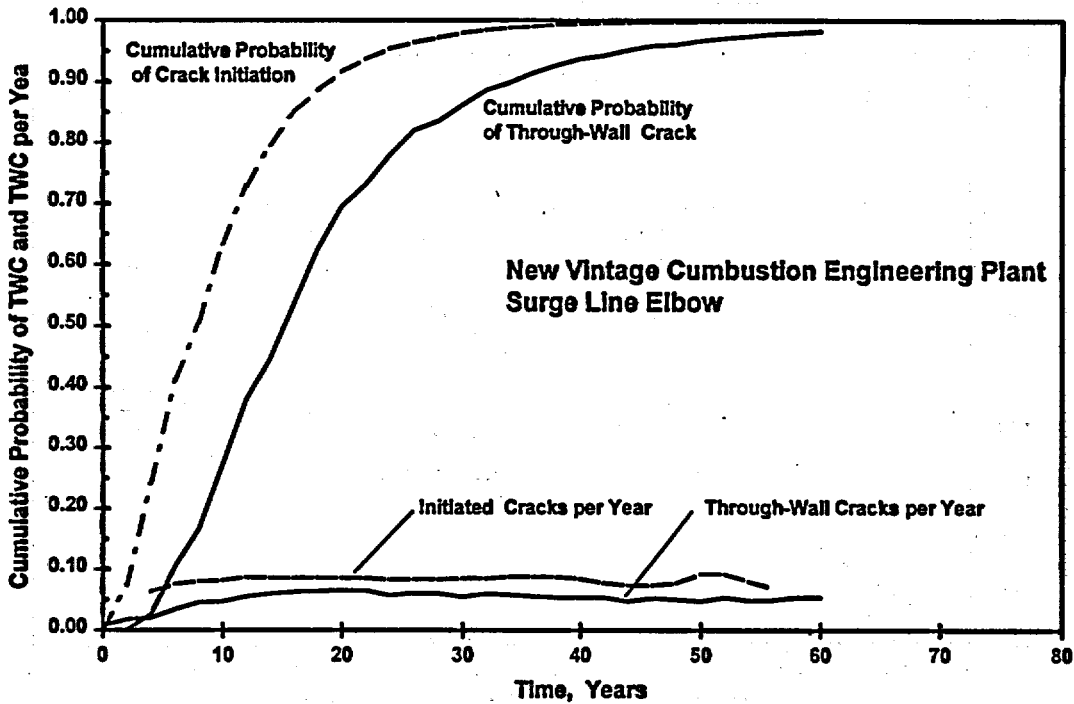


Figure 9.9 Calculated Probabilities of Crack Initiation and Through-Wall Crack for the Surge Line Elbow of the Newer Vintage CE Plant

this 10 years and then remains relatively constant over the remainder of the 60-year plant life. These results indicate a relatively constant failure rate for locations that have relatively high levels of fatigue usage.

Figure 9.10 addresses another component (reactor pressure vessel outlet nozzle for the newer vintage CE plant) that has a much lower level of fatigue usage. The failure rates for this component continue to increase significantly over the entire 60-year plant life. However, the maximum rates never approach the very high failure rates predicted for the surge line elbow. It should also be noted that the calculations for the vessel nozzle predict a much larger number of initiated cracks over the 60-year plant life compared to the number of cracks that actually grow to become through-wall cracks. This suggests that an effective inservice inspection program would have many opportunities to detect such cracks before one of these cracks results in a leak.

Figure 9.11 evaluates the effects of the critical inputs regarding stress gradients for the surge line calculations. It was recognized that the peak surface stresses, which apply strictly to the initiation of fatigue cracks, are not always representative of the stresses that grow these initiated cracks through the pipe wall. The crack growth rates and resulting probabilities of through-wall cracks will depend on the assumptions made regarding stress gradients. It should be noted that the probabilities of crack initiation are the same for all the cases of stress gradients addressed by Figure 9.11 because the cyclic surface stresses that govern crack initiation were the same for all cases.

The solid curve of Figure 9.11 shows the baseline values of through-wall crack probabilities as reported above in Table 9.2. These calculations assumed that only peak stresses greater than 310 Mpa (45 ksi) should be treated as thermal gradient stresses, whereas the most conservative assumption would be to treat the peak stress as

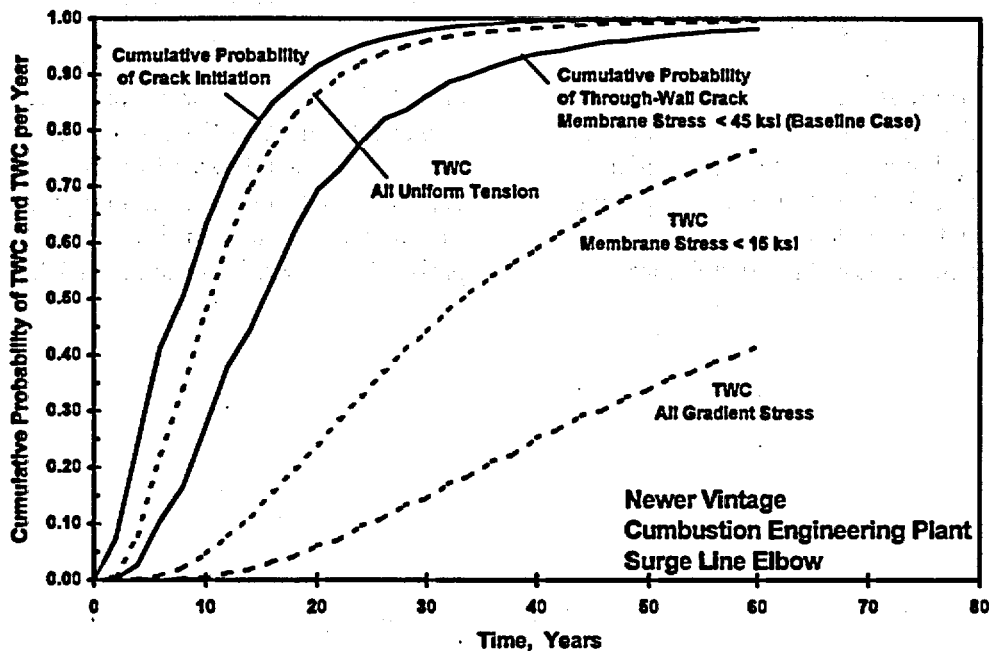
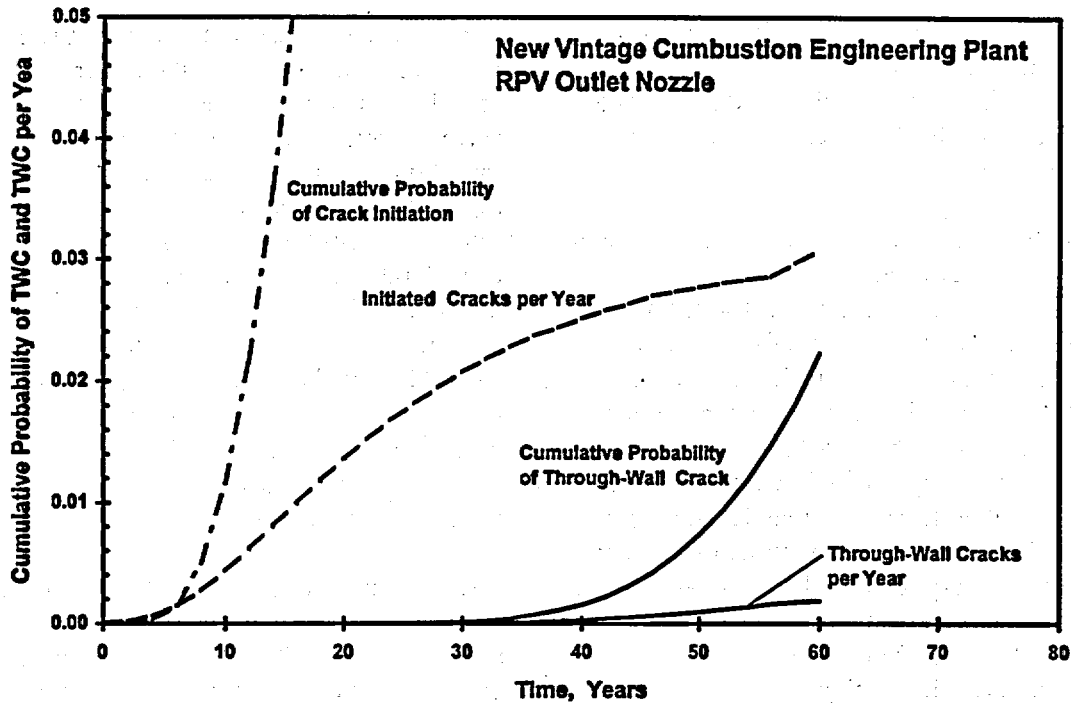


Figure 9.10 Calculated Probabilities of Crack Initiation and Through-Wall Crack for the Reactor Pressure Vessel (RPV) Outlet Nozzle of the Newer Vintage CE Plant



**Figure 9.11 Calculated Probabilities of Through-Wall Crack for the Surge Line Elbow of the Newer Vintage CE Plant for Alternative Through-Wall Stress Distributions**

entirely uniform tension stress. As indicated by Figure 9.11, the more conservative assumption increases the calculated failure probabilities by a factor of about 2.0. The other extreme assumption was to treat the peak stress as 100 percent thermal gradient. This reduces the failure

probabilities by a factor between five and ten. Perhaps the most realistic assumption shown on Figure 9.11 considered all stresses greater than say 103 Mpa (15 ksi) as thermal gradient stresses. This assumption decreases the failure probabilities by a factor of about 2.0.

## 10 SUMMARY AND CONCLUSIONS

Probabilities of fatigue failures and the associated CDFs have been estimated for RPV and piping components of five PWR and two BWR plants. These calculations were made possible by the development of a new version of the pc-PRAISE probabilistic fracture mechanics code that has the capability to simulate the initiation of fatigue cracks in combination with a simulation of the subsequent growth of these fatigue cracks. The calculations gave a wide range of failure probabilities for the selected components, with some components having end-of-life probabilities of through-wall cracks of nearly 100 percent and others with probabilities of less than  $10^{-6}$ .

It is recognized that there are uncertainties in these calculated failure probabilities and CDFs. Sources of the uncertainties come from assumptions made in the fracture mechanics and PRA models themselves and from the inputs to the models. In addressing these uncertainties, the intent was to perform best-estimate calculations. When best-estimate inputs were not available, the approach was to select conservative values. In particular, the inputs for cyclic stresses were based on design-basis data, which could differ from the stresses occurring during the actual plant operation. Other areas of uncertainty included strain rates and environmental variables used to predict fatigue-crack initiation.

The calculations of this report indicate that the components with the very high probabilities of failure can have through-wall crack frequencies

that approach about  $5 \times 10^{-2}$  per year. In contrast, other components with much lower failure probabilities can have their failure frequencies increase by factors of about 10 from 40 years to 60 years. Calculations were also performed to address the effects of reactor water environments (versus air) and to compare these effects to the effects of extended plant operation from 40 years to 60 years. The environmental effects were predicted to increase through-wall crack probabilities by as much as two orders of magnitude.

Contributions to CDFs have also been estimated for each of the vessel and piping components. The maximum calculated contributions are on the order of  $10^{-6}$  per year. This number is subject to uncertainties related to 1) conditional probabilities of larger leaks (small and large LOCAs) and 2) probabilities of core damage given the occurrence of these failure modes. Comparisons of the calculated CDFs for the most critical components with the highest frequencies of failure show essentially no increase in core-damage frequency from 40 to 60 years. On the other hand, the less critical components (with lower failure probabilities) do show significant increases in their contributions to core-damage frequency. Here again, the increases associated with the water-environment effect are a factor of 10 or more greater than the corresponding increases associated with extending the period of plant operation from 40 to 60 years.

## 11 REFERENCES

- American Society of Mechanical Engineers (ASME). 1992. *Risk-Based Inspection - Development of Guidelines: Volume 2 - Part 1 Light Water Reactor (LWR) Nuclear Power Plant Components*, CRTD-Vol. 20-2, Research Task Force on Risk-Based Inspection Guidelines, published by the Center for Research and Technology Development (also published by the U.S. Nuclear Regulatory Commission as NUREG/GR-0005, Vol. 2, Part 1, July 1993).
- Arizona Public Service Company. 1992. *Palo Verde Nuclear Generating Station Individual Plant Examination*, NRC Docket No. 05000528, Phoenix, Arizona.
- Bush, S. H., M. J. Do, A. L. Slavish, and A. D. Chockie. 1996. *Piping Failures in United States Nuclear Power Plants: 1961 - 1995*, SKI Report 96:20, prepared for Swedish Nuclear Power Inspectorate.
- Chapman, O.J.V. 1993. *Simulation of Defects in Weld Construction, Reliability and Risk in Pressure Vessels and Piping*, American Society of Mechanical Engineers, ASME PVP-Vol 251.
- Duke Power Company. 1990. *Oconee Nuclear Station, Unit 3, Probabilistic Risk Assessment, Volume 1*.
- Foreman, R. G., Y. Shivakumar, J. C. Newman, Jr., S. M. Piotrowski, and L. C. Williams. 1988. "Development of the NASA/FLAGRO Computer Program.: In: *Fracture Mechanics: Eighteenth Symposium*. ASTM STP 945, D. T. Read and R. P. Read, Eds. Philadelphia, American Society of Testing and Materials, pp. 781-803.
- Gore, B. F., T. V. Vo, A. J. Colburn, E. J. Eschbach, and M. S. Harris. 1988. *Value/Impact Analysis of Generic Issue 94 - Additional Low Temperature Overpressure Protection for Light Water Reactors*, NUREG/CR-5186, prepared by Pacific Northwest Laboratory, Richland, Washington.
- Harris, D. O., and D. Dedhia. 1992. *A Probabilistic Fracture Mechanics Code for Piping Reliability Analysis (pc-PRAISE code)*, NUREG/CR-5864, U.S. Nuclear Regulatory Commission, Washington D.C.
- Harris, D. O., E. Y. Lim, and D. D. Dedhia. 1981. *Probability of Pipe Fracture in the Primary Coolant Loop of a PWR Plant - Volume 5: Probabilistic Fracture Mechanics Analysis*, NUREG/CR-2189, Vol. 5, U.S. Nuclear Regulatory Commission, Washington D.C.
- Keisler, J., O. K. Chopra, and W. J. Shack. 1994. *Statistical Analysis of Fatigue Strain-Life Data for Carbon and Low-Alloy Steels*, NUREG/CR-6237, U.S. Nuclear Regulatory Commission, Washington D.C.
- Keisler, J., O. K. Chopra, and W. J. Shack. 1995. *Fatigue Strain-Life Behavior of Carbon and Low-Alloy Steels, Austenitic Stainless Steels, and Alloy 600 in LWR Environments*, NUREG/CR-6335, U.S. Nuclear Regulatory Commission, Washington D.C.
- Khaleel, M. A., and F. A. Simonen. 1994. *A Parametric Approach to Predicting the Effects of Fatigue on Piping Reliability, Service Experience and Reliability Improvement: Nuclear, Fossil, and Petrochemical Plants*, ASME PVP Vol. 288, pp. 117-125.

- Khaleel, M. A. and F. A. Simonen. 1995. A Model for Predicting Vessel Failure Probabilities Due to Fatigue Crack Growth, ASME PVP Vol. 304, pp. 401-416, Fatigue and Fracture Mechanics in Pressure Vessels and Piping.
- Khaleel, M.A., and F. A. Simonen. 1998. "A Probabilistic Model for Fatigue Crack Initiation and Propagation," *Fatigue, Fracture and Residual Stresses*, PVP-373, pp. 27-34, American Society of Mechanical Engineers, New York.
- Majumdar, S., O. K. Chopra, and W. J. Shack. 1993. *Interim Fatigue Curves to Selected Nuclear Power Plant Components*, NUREG/CR-5999, U.S. Nuclear Regulatory Commission, Washington D.C.
- Paul, D. D., N. Ghadiali, J. Ahmad, and G. Wilkowski. 1990. *SQUIRT: Seepage Quantification of Upsets in Reactor Tubes*, International Piping Integrity Research Group, Battelle, Columbus, Ohio.
- Sandia National Laboratories (SNL). 1984. Interim Reliability Evaluation Program: Analysis of the Calvert Cliffs Unit 1 Nuclear Power Plant, NUREG/CR-3551. Prepared by SNL, Albuquerque, New Mexico.
- Sandia National Laboratories (SNL). 1989a. Analysis of Core Damage Frequency: Grand Gulf, Unit 1, Internal Events, NUREG/CR-4550, Vol. 6, Rev. 1, prepared by SNL, Albuquerque, New Mexico.
- Sandia National Laboratories (SNL). 1989b. Analysis of Core Damage Frequency: Peach Bottom, Unit 2, Internal Events, NUREG/CR-4550, Vol. 4, Rev. 1, prepared by SNL, Albuquerque, New Mexico.
- Sandia National Laboratories (SNL). 1990a. Analysis of Core Damage Frequency: Sequoyah, Unit 1, Internal Events, NUREG/CR-4550, Vol. 5, Rev. 1, prepared by SNL, Albuquerque, New Mexico.
- Sandia National Laboratories (SNL). 1990b. Analysis of Core Damage Frequency: Surry, Unit 1, Internal Events, NUREG/CR-4550, Vol. 3, Rev. 1, prepared by SNL, Albuquerque, New Mexico.
- Simonen, F. A., D. O. Harris, and D. D. Dedhia. 1998. "Effect of Leak Detection on Piping Failure Probabilities," *Fatigue, Fracture and Residual Stresses*, PVP-373, pp. 105-113, American Society of Mechanical Engineers, New York.
- Simonen, F. A., M. R. Garnich, E. P. Simonen, S. H. Bian, K. K. Numura, W. E. Anderson, and L. T. Pedersen. 1986. *Reactor Pressure Vessel Failure Probability Following Through-Wall Cracks Due to Pressurized Thermal Shock Events*, NUREG/CR-4483, PNL-5727, U.S. Nuclear Regulatory Commission, Washington, D.C.
- Vo, T. V., B. W. Smith, F. A. Simonen, and B. W. Gore. 1994. *Feasibility of Developing Risk-Based Rankings of Pressure Boundary Systems for Inservice Inspection*, NUREG/CR-6151, prepared by Pacific Northwest National Laboratory, Richland, Washington.
- Ware, A. G., D. K. Morton, and M. E. Nitzel. 1995. *Application of NUREG/CR-5999 Interim Fatigue Curves to Selected Nuclear Power Plant Components*, NUREG/CR-6260, U.S. Nuclear Regulatory Commission, Washington D.C.
- Westinghouse Owners Group. 1997. *Westinghouse Owners Group Application of Risk-Informed Methods to Piping Inservice Inspection Topical Report*, WCAP-14572, Revision 1, October 1997.
- Wire, G. L., and Y. Y. Li. 1996. "Initiation of Environmentally-Assisted Cracking in Low Alloy Steels," *Fatigue and Fracture - Volume 1*, PVP-Vol. 323, pp. 269-289, American Society of Mechanical Engineers, New York.

## Appendix A

### Fatigue Evaluation Calculations for All Components of Selected Plants

```

NAME OF PLANT      =      CE-NEW
NAME OF COMPONENT  =      RPV LOWER HEAD/SHELL
NUM OF LOAD PAIRS  =      3
MATERIAL           =      LAS
WALL THICK (INCH) =      8.000
INNER DIAMETER    =      180.000
AIR/WATER         =      WATER
TEMPERATURE (F)   =      590.000
SULFUR (WHT%)    =      .015
DISOL O2 (PPM)   =      .010
STR RATE (%/SEC)  =      .00100
USEAGE (DETERMIN.) = .01400
P-INITIATION @40 = 7.89E-06
P-INITIATION @60 = 4.82E-05
    P-TWC @40    = 6.71E-15
    P-TWC @60    = 1.44E-12
  
```

(RESULTS FROM LATIN HYPERCUBE CALCULATION WERE USED  
AFTER 10<sup>6</sup> SIMULATIONS WITH PC-PRAISE GAVE INADEQUATE NUMBER OF FAILURES)

	LOAD PAIR	AMP (KSI)	NUM/40-YR	EDOT (%/SEC)	USEAGE
COOLDOWN/STEP LOAD INCREASE		27.110	200.0	.000000	.012000
HEATUP/COOLDOWN		16.220	300.0	.000000	.002000
LEAK TEST/HEATUP		10.130	200.0	.000000	.000000

```

NAME OF PLANT      =      CE-NEW
NAME OF COMPONENT  =      RPV INLET NOZZLE
NUM OF LOAD PAIRS  =      5
MATERIAL           =      LAS
WALL THICK (INCH) =      3.000
INNER DIAMETER    =      24.000
AIR/WATER         =      WATER
TEMPERATURE (F)   =      590.000
SULFUR (WHT%)    =      .015
DISOL O2 (PPM)   =      .010
STR RATE (%/SEC)  =      .00100
USEAGE (DETERMIN.) = .47500
P-INITIATION @40 = 1.40E-02
P-INITIATION @60 = 4.44E-02
    P-TWC @40    = 5.90E-05
    P-TWC @60    = 9.01E-04
  
```

(RESULTS FROM LATIN HYPERCUBE CALCULATION WERE USED  
AFTER 10<sup>6</sup> SIMULATIONS WITH PC-PRAISE GAVE INADEQUATE NUMBER OF FAILURES)

	LOAD PAIR	AMP (KSI)	NUM/40-YR	EDOT (%/SEC)	USEAGE
HEATUP/LEAK TEST		60.470	200.0	.000000	.230000
HEATUP/REACTOR TRIP		48.010	300.0	.000000	.156000
COOLDOWN/REACTOR TRIP		36.960	180.0	.000000	.033000
COOLDOWN/OBE		36.460	320.0	.000000	.056000
OBE/OBE		1.900	200.0	.000000	.001000

NAME OF PLANT = CE-NEW  
 NAME OF COMPONENT = RPV INLET NOZZLE  
 NUM OF LOAD PAIRS = 5  
 MATERIAL = LAS  
 WALL THICK (INCH) = 3.000  
 INNER DIAMETER = 24.000  
 AIR/WATER = WATER  
 TEMPERATURE (F) = 590.000  
 SULFUR (WHT%) = .015  
 DISOL O2 (PPM) = .010  
 STR RATE (%/SEC) = .00100  
 USAGE (DETERMIN.) = .47500  
 P-INITIATION @40 = 1.40E-02  
 P-INITIATION @60 = 4.44E-02  
 P-TWC @40 = 5.90E-05  
 P-TWC @60 = 9.01E-04

(RESULTS FROM LATIN HYPERCUBE CALCULATION WERE USED  
 AFTER 10<sup>6</sup> SIMULATIONS WITH PC-PRAISE GAVE INADEQUATE NUMBER OF FAILURES)

LOAD PAIR	AMP (KSI)	NUM/40-YR	EDOT (%/SEC)	USAGE
HEATUP/LEAK TEST	60.470	200.0	.000000	.230000
HEATUP/REACTOR TRIP	48.010	300.0	.000000	.156000
COOLDOWN/REACTOR TRIP	36.960	180.0	.000000	.033000
COOLDOWN/OBE	36.460	320.0	.000000	.056000
OBE/OBE	1.900	200.0	.000000	.001000

NAME OF PLANT = CE-NEW  
 NAME OF COMPONENT = SURGE LINE ELBOW  
 NUM OF LOAD PAIRS = 41  
 MATERIAL = 304/316  
 WALL THICK (INCH) = 1.000  
 INNER DIAMETER = 10.000  
 AIR/WATER = WATER  
 TEMPERATURE (F) = 590.000  
 SULFUR (WHT%) = .015  
 DISOL O2 (PPM) = .010  
 STR RATE (%/SEC) = .00400  
 USEAGE (DETERMIN.) = 2.59700  
 P-INITIATION @40 = 9.95E-01  
 P-INITIATION @60 = 9.99E-01  
 P-TWC @40 = 9.81E-01  
 P-TWC @60 = 9.98E-01

LOAD PAIR	AMP (KSI)	NUM/40-YR	EDOT (%/SEC)	USEAGE
HYDRO-EXTREME	190.170	6.0	.000000	.176000
8A-OBE	163.180	14.0	.000000	.280000
9B-OBE	162.060	14.0	.000000	.280000
9A-HYDRO	138.050	4.0	.000000	.053000
8E-OBE	127.940	14.0	.000000	.151000
9A-OBE	127.040	10.0	.000000	.105000
8C-OBE	64.760	68.0	.000000	.079000
9F-18	64.170	68.0	.000000	.076000
8F-18	63.390	68.0	.000000	.072000
9C-11	63.380	68.0	.000000	.072000
8D-OBE	54.020	1248.0	.000000	.614000
8G-18	52.380	23.0	.000000	.010000
8G-11	52.350	23.0	.000000	.009000
8G-17	52.350	27.0	.000000	.011000
8D-LEAK TEST	52.260	6.0	.000000	.002000
8G-LEAK TEST	52.260	109.0	.000000	.044000
9D-17	51.760	63.0	.000000	.024000
9G-UPSET 4	51.240	40.0	.000000	.015000
8H-9G	51.180	30.0	.000000	.011000
9D-12	50.960	9.0	.000000	.003000
2A-8E	40.100	90.0	.000000	.004000
8H-9G	40.090	.0	.000000	.000000
9H-10A	40.090	90.0	.000000	.004000
9E-12	39.910	81.0	.000000	.003000
9E-13	39.920	9.0	.000000	.000000
3B-13	39.030	81.0	.000000	.003000
16-SLUG2	38.940	90.0	.000000	.003000
UPSET 3-SLUG 1	38.820	30.0	.000000	.001000
3A-10A	33.100	4120.0	.000000	.061000
3B-10A	33.100	3670.0	.000000	.055000
6-10A	33.100	200.0	.000000	.003000
7-10A	33.100	4580.0	.000000	.068000
2A-SLUG 1	32.870	70.0	.000000	.001000
5-10A	29.900	9400.0	.000000	.066000
4B-10A	29.900	17040.0	.000000	.119000
4A-10A	29.900	17040.0	.000000	.119000
2A-10A	20.600	14430.0	.000000	.000000
2B-10A	20.600	15000.0	.000000	.000000
10A-UPSET 2	20.600	95.0	.000000	.000000
1B-10A	20.600	1969.0	.000000	.000000
1B-10B	20.600	87710.0	.000000	.001000

NAME OF PLANT = CE-NEW  
 NAME OF COMPONENT = CHARGING NOZZLE NOZZLE  
 NUM OF LOAD PAIRS = 5  
 MATERIAL = LAS  
 WALL THICK (INCH) = .500  
 INNER DIAMETER = 4.000  
 AIR/WATER = WATER  
 TEMPERATURE (F) = 590.000  
 SULFUR (WHT%) = .015  
 DISOL O2 (PPM) = .010  
 STR RATE (1/SEC) = .00100  
 USEAGE (DETERMIN.) = .10400  
 P-INITIATION @40 = 9.56E-04  
 P-INITIATION @60 = 3.84E-03  
     P-TWC @40 = 2.61E-06  
     P-TWC @60 = 5.50E-05

(RESULTS FROM LATIN HYPERCUBE CALCULATION WERE USED  
 AFTER 10<sup>6</sup> SIMULATIONS WITH PC-FRAISE GAVE INADEQUATE NUMBER OF FAILURES)

LOAD PAIR	AMP (KSI)	NUM/40-YR	EDOT (1/SEC)	USEAGE
LOSS OF LETDOWN/NUL	37.280	100.0	.000000	.019000
COOLDOWN/NULL	33.910	500.0	.000000	.068000
STEP DECREASE/NULL	31.280	110.0	.000000	.011000
STEP DECREASE/NULL	23.660	200.0	.000000	.006000
STEP DECREASE/LOSS OF CHARGING	10.270	100.0	.000000	.000000

NAME OF PLANT = CE-NEW  
 NAME OF COMPONENT = CHARGING NOZZLE SAFE END  
 NUM OF LOAD PAIRS = 5  
 MATERIAL = 304/316  
 WALL THICK (INCH) = .500  
 INNER DIAMETER = 4.000  
 AIR/WATER = WATER  
 TEMPERATURE (F) = 590.000  
 SULFUR (WHT%) = .015  
 DISOL O2 (PPM) = .010  
 STR RATE (%/SEC) = .00400  
 USEAGE (DETERMIN.) = .50200  
 P-INITIATION @40 = 1.06E-02  
 P-INITIATION @60 = 6.75E-02  
 P-TWC @40 = 9.00E-05  
 P-TWC @60 = 1.03E-03

	LOAD PAIR	AMP (KSI)	NUM/40-YR	EDOT (%/SEC)	USEAGE
LOSS OF LETDOWN/RECOVERY		165.200	40.0	.000000	.667000
LOSS OF CHARGING/REACTOR TRIP		125.800	12.0	.000000	.104000
REACTOR TRIP/COOLDOWN		33.900	90.0	.000000	.003000
COOLDOWN/PURIFICATION		31.900	.0	.000000	.000000
PURIFICATION/REACTOR TRIP		25.600	48.0	.000000	.000000

NAME OF PLANT = CE-NEW  
 NAME OF COMPONENT = SAFETY INJECTION NOZZLE NOZZLE  
 NUM OF LOAD PAIRS = 8  
 MATERIAL = LAS  
 WALL THICK (INCH) = .500  
 INNER DIAMETER = 6.000  
 AIR/WATER = WATER  
 TEMPERATURE (F) = 590.000  
 SULFUR (WHT%) = .015  
 DISOL O2 (PPM) = .010  
 STR RATE (%/SEC) = .00100  
 USEAGE (DETERMIN.) = .45700  
 P-INITIATION @40 = 1.01E-03  
 P-INITIATION @60 = 4.81E-03  
 P-TWC @40 = 1.00E-06  
 P-TWC @60 = 1.90E-05

	LOAD PAIR	AMP (KSI)	NUM/40-YR	EDOT (%/SEC)	USEAGE
SHUTDOWN COOLING A/TEST 15		101.570	40.0	.000000	.158000
SHUTDOWN COOLING B/TEST 14		79.810	60.0	.000000	.139000
SHUTDOWN COOLING A/OBE		54.210	50.0	.000000	.041000
SHUTDOWN COOLING/TEST 12		49.220	160.0	.000000	.092000
HEATUP/OBE		35.140	90.0	.000000	.014000
OBE/NULL		32.460	90.0	.000000	.011000
OBE/FLOW TEST		30.920	20.0	.000000	.002000
OBE/OBE		14.000	1230.0	.000000	.004000

NAME OF PLANT = CE-NEW  
 NAME OF COMPONENT = SAFETY INJECTION NOZZLE SAFE B  
 NUM OF LOAD PAIRS = 4  
 MATERIAL = 304/316  
 WALL THICK (INCH) = .500  
 INNER DIAMETER = 6.000  
 AIR/WATER = WATER  
 TEMPERATURE (F) = 590.000  
 SULFUR (WHT%) = .015  
 DISOL O2 (PPM) = .010  
 STR RATE (%/SEC) = .00400  
 USEAGE (DETERMIN.) = .28600  
 P-INITIATION @40 = 8.68E-03  
 P-INITIATION @60 = 3.16E-02  
 P-TWC @40 = 2.61E-06  
 P-TWC @60 = 5.50E-05

(RESULTS FROM LATIN HYPERCUBE CALCULATION WERE USED  
 AFTER 10<sup>6</sup> SIMULATIONS WITH PC-PRAISE GAVE INADEQUATE NUMBER OF FAILURES)

LOAD PAIR	AMP (KSI)	NUM/40-YR	EDOT (%/SEC)	USEAGE
TEST 14/TEST 15	65.860	100.0	.000000	.125000
SHUTDOWN COOLING A/B	72.080	90.0	.000000	.161000
REACTOR TRIP/FLOW TEST	23.810	20.0	.000000	.000000
HEATUP/OBE	15.820	500.0	.000000	.001000

NAME OF PLANT = CE-NEW  
 NAME OF COMPONENT = SHUTDOWN COOLING LINE ELBOW  
 NUM OF LOAD PAIRS = 9  
 MATERIAL = 304/316  
 WALL THICK (INCH) = .750  
 INNER DIAMETER = 12.000  
 AIR/WATER = WATER  
 TEMPERATURE (F) = 590.000  
 SULFUR (WHT%) = .015  
 DISOL O2 (PPM) = .010  
 STR RATE (%/SEC) = .00400  
 USEAGE (DETERMIN.) = .48700  
 P-INITIATION @40 = 1.13E-02  
 P-INITIATION @60 = 5.75E-02  
 P-TWC @40 = 2.00E-05  
 P-TWC @60 = 4.53E-04

LOAD PAIR	AMP (KSI)	NUM/40-YR	EDOT (%/SEC)	USEAGE
HEATUP/SHUTDOWN COOLING & OBE	108.710	2.0	.000000	.014000
HEATUP/SHUTDOWN COOLING 3	88.630	81.0	.000000	.297000
HEATUP/SHUTDOWN COOLING 1	87.690	7.0	.000000	.025000
SHUTDOWN COOLING 1/NULL	87.560	.0	.000000	.000000
SHUTDOWN COOLING 2/NULL	83.310	50.0	.000000	.149000
REACTOR TRIP & OBE/NULL	30.030	2.0	.000000	.001000
REACTOR TRIP/NULL	28.010	446.0	.000000	.002000
LEAK TEST/REATOR TRIP	25.080	34.0	.000000	.000000
LEAK TEST/STEP IN POWER	22.070	166.0	.000000	.000000

NAME OF PLANT = CE-OLD  
 NAME OF COMPONENT = RPV LOWER HEAD/SHELL  
 NUM OF LOAD PAIRS = 6  
 MATERIAL = LAS  
 WALL THICK (INCH) = 8.000  
 INNER DIAMETER = 180.000  
 AIR/WATER = WATER  
 TEMPERATURE (F) = 590.000  
 SULFUR (WHT%) = .015  
 DISOL O2 (PPM) = .010  
 STR RATE (t/SEC) = .00100  
 USEAGE (DETERMIN.) = .01300  
 P-INITIATION @40 = 2.68E-06  
 P-INITIATION @60 = 1.93E-05  
 P-TWC @40 = 6.36E-16  
 P-TWC @60 = 1.85E-13

(RESULTS FROM LATIN HYPERCUBE CALCULATION WERE USED  
 AFTER 10<sup>6</sup> SIMULATIONS WITH PC-PRAISE GAVE INADEQUATE NUMBER OF FAILURES)

LOAD PAIR	AMP (KSI)	NUM/40-YR	EDOT (t/SEC)	USEAGE
LOSS OF SECONDARY PRESSURE A/E	70.560	5.0	.000000	.009000
HYDROTEST/NULL	22.330	10.0	.000000	.000000
LEAK TEST/NULL	22.220	40.0	.000000	.001000
LOSS OF FLOW/NULL	18.670	40.0	.000000	.000000
REACTOR/TRIP	18.330	400.0	.000000	.013000
PLANT UNLOAD/NULL	18.000	20.0	.000000	.000000

NAME OF PLANT = CE-OLD  
 NAME OF COMPONENT = RPV INLET NOZZLE  
 NUM OF LOAD PAIRS = 4  
 MATERIAL = LAS  
 WALL THICK (INCH) = 3.000  
 INNER DIAMETER = 24.000  
 AIR/WATER = WATER  
 TEMPERATURE (F) = 590.000  
 SULFUR (WHT%) = .015  
 DISOL O2 (PPM) = .010  
 STR RATE (t/SEC) = .00100  
 USEAGE (DETERMIN.) = .17200  
 P-INITIATION @40 = 1.88E-03  
 P-INITIATION @60 = 7.89E-03  
 P-TWC @40 = 4.11E-07  
 P-TWC @60 = 1.33E-05

(RESULTS FROM LATIN HYPERCUBE CALCULATION WERE USED  
 AFTER 10<sup>6</sup> SIMULATIONS WITH PC-PRAISE GAVE INADEQUATE NUMBER OF FAILURES)

LOAD PAIR	AMP (KSI)	NUM/40-YR	EDOT (t/SEC)	USEAGE
LOSS OF SECONDARY PRESS/CD	73.470	5.0	.000000	.010000
HEATUP/COOLDOWN	39.760	495.0	.000000	.122000
LEAK TEST A/LEAK TEST B	37.360	200.0	.000000	.039000
HEATUP/HYDROTEST	27.740	100.0	.000000	.001000

NAME OF PLANT = CE-OLD  
 NAME OF COMPONENT = RPV OUTLET NOZZLE  
 NUM OF LOAD PAIRS = 8  
 MATERIAL = LAS  
 WALL THICK (INCH) = 3.000  
 INNER DIAMETER = 24.000  
 AIR/WATER = WATER  
 TEMPERATURE (F) = 590.000  
 SULFUR (WHT%) = .015  
 DISOL O2 (PPM) = .010  
 STR RATE (%/SEC) = .00100  
 USEAGE (DETERMIN.) = .55300  
 P-INITIATION @40 = 5.91E-01  
 P-INITIATION @60 = 8.46E-01  
 P-TWC @40 = 7.05E-02  
 P-TWC @60 = 3.56E-01

LOAD PAIR	AMP (KSI)	NUM/40-YR	EDOT (%/SEC)	USEAGE
LOSS OF SECONDARY PRES/HYDRO	74.460	5.0	.000000	.010000
HYDROTEST A/HYDROTEST B	38.460	5.0	.000000	.001000
HEATUP/LOSS OF LOAD	32.410	40.0	.000000	.005000
HEATUP/LOSS OF FLOW	31.730	40.0	.000000	.004000
HEATUP/COOLDOWN	31.530	420.0	.000000	.045000
COOLDOWN/PLANT LOADING	29.700	80.0	.000000	.007000
REACTOR TRIP/PLANT LOADING	25.830	400.0	.000000	.019000
REACTOR TRIP/PLANT UNLOADING	23.790	14520.0	.000000	.462000

NAME OF PLANT = CE-OLD  
 NAME OF COMPONENT = SURGE LINE ELBOW  
 NUM OF LOAD PAIRS = 15  
 MATERIAL = 304/316  
 WALL THICK (INCH) = 1.000  
 INNER DIAMETER = 10.000  
 AIR/WATER = WATER  
 TEMPERATURE (F) = 590.000  
 SULFUR (WHT%) = .015  
 DISOL O2 (PPM) = .010  
 STR RATE (%/SEC) = .00400  
 USEAGE (DETERMIN.) = .66100  
 P-INITIATION @40 = 9.39E-01  
 P-INITIATION @60 = 9.87E-01  
 P-TWC @40 = 6.27E-01  
 P-TWC @60 = 8.85E-01

LOAD PAIR	AMP (KSI)	NUM/40-YR	EDOT (%/SEC)	USEAGE
STRAT/LOSS OF FLOW WITH RT	59.560	2.0	.000000	.002000
STRAT/LOSS FLOW/LOSS LOAD	58.290	1.0	.000000	.001000
STRAT/LOSS FLOW/NO LOSS LOAD	57.010	37.0	.000000	.024000
STRAT/LOSS OF LOAD	55.450	40.0	.000000	.023000
STRATIFICATION/REACTOR TRIP	54.250	70.0	.000000	.035000
STRATIFICATION/STRATIFICATION	50.440	71.0	.000000	.023000
STRATIFICATION/REACTOR TRIP	49.190	67.0	.000000	.019000
STRATIFICATION/LOW PRESSURE	45.470	5.0	.000000	.001000
STRATIFICATION/LOW PRESSURE	44.890	202.0	.000000	.028000
STRATIFICATION/STRATIFICATION	36.990	17570.0	.000000	.498000
STRATIFICATION/LEAK TEST A	33.310	150.0	.000000	.002000
STRATIFICATION/HYDROTEST	32.660	10.0	.000000	.000000
STRATIFICATION/LEAK TEST A	29.080	200.0	.000000	.001000
STRATIFICATION/NULL	28.670	750.0	.000000	.004000
STRATIFICATION/NULL	24.570	800.0	.000000	.000000

NAME OF PLANT = CE-OLD  
 NAME OF COMPONENT = CHARGING NOZZLE SAFE END  
 NUM OF LOAD PAIRS = 6  
 MATERIAL = 304/316  
 WALL THICK (INCH) = .500  
 INNER DIAMETER = 4.000  
 AIR/WATER = WATER  
 TEMPERATURE (F) = 590.000  
 SULFUR (WHT%) = .015  
 DISOL O2 (PPM) = .010  
 STR RATE (%/SEC) = .00400  
 USEAGE (DETERMIN.) = .56200  
 P-INITIATION @40 = 1.18E-02  
 P-INITIATION @60 = 5.31E-02  
 P-TWC @40 = 4.10E-05  
 P-TWC @60 = 5.98E-04

LOAD PAIR	AMP (KSI)	NUM/40-YR	EDOT (%/SEC)	USEAGE
LOSS SECONDARY PRESS/LOSS LD B	125.930	5.0	.000000	.052000
HEAT EXCH ISOL/PLANT UNLOAD B	85.940	95.0	.000000	.315000
HEAT EXCH ISOL/PLANT UNLOAD B	63.650	115.0	.000000	.125000
LOSS OF LOAD/PLANT UNLOAD B	59.070	40.0	.000000	.031000
REACTOR TRIP/PLANT UNLOAD B	51.210	92.0	.000000	.033000
PLANT UNLOAD A/PLANT UNLOAD B	37.790	202.0	.000000	.006000

NAME OF PLANT = CE-OLD  
 NAME OF COMPONENT = SAFETY INJECTION NOZZLE SAFE E  
 NUM OF LOAD PAIRS = 4  
 MATERIAL = 304/316  
 WALL THICK (INCH) = .500  
 INNER DIAMETER = 6.000  
 AIR/WATER = WATER  
 TEMPERATURE (F) = 590.000  
 SULFUR (WHT%) = .015  
 DISOL O2 (PPM) = .010  
 STR RATE (%/SEC) = .00400  
 USEAGE (DETERMIN.) = .31700  
 P-INITIATION @40 = 7.56E-03  
 P-INITIATION @60 = 3.59E-02  
 P-TWC @40 = 1.40E-05  
 P-TWC @60 = 2.00E-04

LOAD PAIR	AMP (KSI)	NUM/40-YR	EDOT (%/SEC)	USEAGE
COOLDOWN A/NULL	72.170	101.0	.000000	.181000
COOLDOWN B/LEAK TEST	54.530	200.0	.000000	.103000
COOLDOWN B/HYDROTEST	52.330	10.0	.000000	.004000
COOLDOWN B/HEATUP	43.230	290.0	.000000	.029000

NAME OF PLANT = CE-OLD  
 NAME OF COMPONENT = SHUTDOWN COOLING LINE ELBOW  
 NUM OF LOAD PAIRS = 9  
 MATERIAL = 304/316  
 WALL THICK (INCH) = .750  
 INNER DIAMETER = 12.000  
 AIR/WATER = WATER  
 TEMPERATURE (F) = 590.000  
 SULFUR (WHT%) = .015  
 DISOL O2 (PPM) = .010  
 STR RATE (%/SEC) = .00400  
 USEAGE (DETERMIN.) = .08400  
 P-INITIATION @40 = 3.94E-02  
 P-INITIATION @60 = 1.19E-01  
 P-TWC @40 = 2.10E-04  
 P-TWC @60 = 2.36E-03

LOAD PAIR	AMP (KSI)	NUM/40-YR	EDOT (%/SEC)	USEAGE
SHUTDOWN COOLING A/RT & OBE	47.600	50.0	.000000	.011000
STEP INCREASE/EMERG INJECTION	43.480	70.0	.000000	.007000
SHUTDOWN COOLING A/LEAK TEST	43.100	200.0	.000000	.019000
STEP INCRE/SHUTDOWN COOLING A	42.780	250.0	.000000	.022000
SHUTDOWN COOLING A/REAC TRIP	35.260	400.0	.000000	.009000
STEP INCRE/SHUTDOWN COOLING B	35.260	100.0	.000000	.002000
STEP INCREASE/LEAK TEST	34.820	200.0	.000000	.004000
STEP INCREASE/NULL	34.820	500.0	.000000	.010000
STEP INCREASE/COOLDOWN	25.380	500.0	.000000	.000000

NAME OF PLANT = B&W  
 NAME OF COMPONENT = RPV NEAR SUPPORT SKIRT  
 NUM OF LOAD PAIRS = 1  
 MATERIAL = LAS  
 WALL THICK (INCH) = 8.000  
 INNER DIAMETER = 180.000  
 AIR/WATER = WATER  
 TEMPERATURE (F) = 590.000  
 SULFUR (WHT%) = .015  
 DISOL O2 (PPM) = .010  
 STR RATE (%/SEC) = .00100  
 USEAGE (DETERMIN.) = .22300  
 P-INITIATION @40 = 8.25E-03  
 P-INITIATION @60 = 2.50E-02  
 P-TWC @40 = 7.85E-06  
 P-TWC @60 = 1.52E-04

(RESULTS FROM LATIN HYPERCUBE CALCULATION WERE USED  
 AFTER 10<sup>6</sup> SIMULATIONS WITH PC-PRAISE GAVE INADEQUATE NUMBER OF FAILURES)

LOAD PAIR	AMP (KSI)	NUM/40-YR	EDOT (%/SEC)	USAGE
ALL	35.300	1440.0	.000000	.223000

NAME OF PLANT = B&W  
 NAME OF COMPONENT = RPV OUTLET NOZZLE  
 NUM OF LOAD PAIRS = 4  
 MATERIAL = LAS  
 WALL THICK (INCH) = 3.000  
 INNER DIAMETER = 24.000  
 AIR/WATER = WATER  
 TEMPERATURE (F) = 590.000  
 SULFUR (WHT%) = .015  
 DISOL O2 (PPM) = .010  
 STR RATE (%/SEC) = .00100  
 USEAGE (DETERMIN.) = .46900  
 P-INITIATION @40 = 7.74E-01  
 P-INITIATION @60 = 8.99E-01  
 P-TWC @40 = 1.83E-01  
 P-TWC @60 = 5.44E-01

LOAD PAIR	AMP (KSI)	NUM/40-YR	EDOT (%/SEC)	USAGE
HEATUP/COOLDOWN	37.960	240.0	.000000	.049000
STEP LOAD/REACTOR TRIP	22.150	480.0	.000000	.011000
PLANT LOADING/UNLOADING	17.240	48000.0	.000000	.346000
ALL OTHER	16.690	9850.0	.000000	.063000

NAME OF PLANT = B&W  
 NAME OF COMPONENT = MAKEUP/HPI NOZZLE SAFE END  
 NUM OF LOAD PAIRS = 5  
 MATERIAL = 304/316  
 WALL THICK (INCH) = .500  
 INNER DIAMETER = 6.000  
 AIR/WATER = WATER  
 TEMPERATURE (F) = 590.000  
 SULFUR (WHT%) = .015  
 DISOL O2 (PPM) = .010  
 STR RATE (%/SEC) = .00400  
 USEAGE (DETERMIN.) = 1.05100  
 P-INITIATION @40 = 1.30E-01  
 P-INITIATION @60 = 4.79E-01  
 P-TWC @40 = 2.10E-03  
 P-TWC @60 = 3.09E-02

LOAD PAIR	AMP (KSI)	NUM/40-YR	EDOT (%/SEC)	USEAGE
HPI ACTUATION A/B & OBE	225.620	.0	.000000	.000000
HPI ACTUATION A/B	221.240	33.0	.000000	.943000
RAPID DEPRESSURIZATION A/B	212.960	.0	.000000	.000000
TEST/NULL	169.310	7.0	.000000	.108000
HEATUP/COOLDOWN	11.980	200.0	.000000	.000000

NAME OF PLANT = B&W  
 NAME OF COMPONENT = DECAY HEAT REMOVAL/REDUCING T  
 NUM OF LOAD PAIRS = 10  
 MATERIAL = 304/316  
 WALL THICK (INCH) = .750  
 INNER DIAMETER = 12.000  
 AIR/WATER = WATER  
 TEMPERATURE (F) = 590.000  
 SULFUR (WHT%) = .015  
 DISOL O2 (PPM) = .010  
 STR RATE (%/SEC) = .00400  
 USEAGE (DETERMIN.) = .53000  
 P-INITIATION @40 = 5.72E-02  
 P-INITIATION @60 = 2.08E-01  
 P-TWC @40 = 3.00E-03  
 P-TWC @60 = 2.54E-02

LOAD PAIR	AMP (KSI)	NUM/40-YR	EDOT (%/SEC)	USEAGE
COOLDOWN/OBE-	94.810	30.0	.000000	.132000
COOLDOWN/OBE+	94.810	30.0	.000000	.132000
COOLDOWN/ROD WITHDRAWAL	74.130	40.0	.000000	.097000
COOLDOWN/ROD REDUCTION	70.120	47.0	.000000	.100000
COOLDOWN/UNLOADING	69.870	8.0	.000000	.017000
HYDROTEST A/HYDROTEST B	57.110	20.0	.000000	.017000
RAPID DEPRES/LEAK BACK FLOW	45.950	80.0	.000000	.019000
UNLOADING/NULL	44.350	480.0	.000000	.091000
FUNCTIONAL TEST/LEAK BACKFLOW	39.770	40.0	.000000	.004000
UNLOADING/FUNCTIONAL TEST	31.720	40.0	.000000	.001000

NAME OF PLANT = W-NEW  
 NAME OF COMPONENT = RPV LOWER HEAD/SHELL  
 NUM OF LOAD PAIRS = 9  
 MATERIAL = LAS  
 WALL THICK (INCH) = 8.000  
 INNER DIAMETER = 180.000  
 AIR/WATER = WATER  
 TEMPERATURE (F) = 590.000  
 SULFUR (WHT%) = .015  
 DISOL O2 (PPM) = .010  
 STR RATE (%/SEC) = .00100  
 USEAGE (DETERMIN.) = .01800  
 P-INITIATION @40 = 3.21E-05  
 P-INITIATION @60 = 1.71E-04  
 P-TWC @40 = 7.52E-13  
 P-TWC @60 = 9.64E-11

(RESULTS FROM LATIN HYPERCUBE CALCULATION WERE USED  
 AFTER 10<sup>6</sup> SIMULATIONS WITH PC-PRAISE GAVE INADEQUATE NUMBER OF FAILURES)

LOAD PAIR	AMP (KSI)	NUM/40-YR	EDOT (%/SEC)	USEAGE
TURBINE ROLL/INADVERTENT DEPR	25.210	20.0	.000000	.001000
REACTOR TRIP/HEATUP	24.480	200.0	.000000	.007000
REACTOR TRIP/HEATUP/HYDRO	24.350	10.0	.000000	.000000
REACTOR TRIP/LEAK TEST	24.350	190.0	.000000	.007000
INADVERTENT LOOP STARTUP/HYDRO	21.060	10.0	.000000	.000000
LEAK TEST A/LEAK TEST B	20.850	80.0	.000000	.001000
CONTROL ROD DROP/REFUELING	17.010	80.0	.000000	.001000
INADVERTENT SAFETY INJEC/COOLD	14.780	60.0	.000000	.000000
FEEDWATER CYCLING/COOLDOWN	14.600	140.0	.000000	.001000

NAME OF PLANT = W-NEW  
 NAME OF COMPONENT = RPV INLET NOZZLE  
 NUM OF LOAD PAIRS = 10  
 MATERIAL = LAS  
 WALL THICK (INCH) = 3.000  
 INNER DIAMETER = 24.000  
 AIR/WATER = WATER  
 TEMPERATURE (F) = 590.000  
 SULFUR (WHT%) = .015  
 DISOL O2 (PPM) = .010  
 STR RATE (%/SEC) = .00100  
 USEAGE (DETERMIN.) = .29000  
 P-INITIATION @40 = 2.49E-03  
 P-INITIATION @60 = 1.05E-02  
 P-TWC @40 = 9.17E-07  
 P-TWC @60 = 2.84E-05

(RESULTS FROM LATIN HYPERCUBE CALCULATION WERE USED  
 AFTER 10<sup>6</sup> SIMULATIONS WITH PC-PRAISE GAVE INADEQUATE NUMBER OF FAILURES)

LOAD PAIR	AMP (KSI)	NUM/40-YR	EDOT (%/SEC)	USEAGE
LOAD PAIR 1	55.740	200.0	.000000	.179000
LOAD PAIR 2	49.730	10.0	.000000	.006000
LOAD PAIR 3	47.110	20.0	.000000	.010000
LOAD PAIR 4	43.800	10.0	.000000	.004000
LOAD PAIR 5	43.260	250.0	.000000	.086000
LOAD PAIR 6	27.790	80.0	.000000	.005000
LOAD PAIR 7	26.610	20.0	.000000	.001000
LOAD PAIR 8	19.040	50.0	.000000	.001000
LOAD PAIR 9	17.210	30.0	.000000	.000000
LOAD PAIR 10	9.630	30.0	.000000	.000000

NAME OF PLANT = W-NEW  
NAME OF COMPONENT = RPV OUTLET NOZZLE  
NUM OF LOAD PAIRS = 26  
MATERIAL = LAS  
WALL THICK (INCH) = 3.000  
INNER DIAMETER = 24.000  
AIR/WATER = WATER  
TEMPERATURE (F) = 590.000  
SULFUR (WHT%) = .015  
DISOL O2 (PPM) = .010  
STR RATE (%/SEC) = .00100  
USEAGE (DETERMIN.) = .65800  
P-INITIATION @40 = 8.62E-01  
P-INITIATION @60 = 9.49E-01  
P-TWC @40 = 3.65E-01  
P-TWC @60 = 7.42E-01

LOAD PAIR	AMP (KSI)	NUM/40-YR	EDOT (%/SEC)	USEAGE
LOAD PAIR 1	48.680	80.0	.000000	.044000
LOAD PAIR 2	45.400	10.0	.000000	.004000
LOAD PAIR 3	44.340	20.0	.000000	.008000
LOAD PAIR 4	39.940	20.0	.000000	.005000
LOAD PAIR 5	34.390	70.0	.000000	.010000
LOAD PAIR 6	29.310	130.0	.000000	.011000
LOAD PAIR 7	28.300	150.0	.000000	.011000
LOAD PAIR 8	27.090	50.0	.000000	.003000
LOAD PAIR 9	26.990	30.0	.000000	.002000
LOAD PAIR 10	21.370	40.0	.000000	.001000
LOAD PAIR 11	20.200	1930.0	.000000	.029000
LOAD PAIR 12	20.200	2000.0	.000000	.030000
LOAD PAIR 13	20.130	9270.0	.000000	.135000
LOAD PAIR 14	18.850	60.0	.000000	.001000
LOAD PAIR 15	18.440	230.0	.000000	.002000
LOAD PAIR 16	18.350	10.0	.000000	.000000
LOAD PAIR 17	18.050	80.0	.000000	.001000
LOAD PAIR 18	17.740	160.0	.000000	.001000
LOAD PAIR 19	17.640	26400.0	.000000	.207000
LOAD PAIR 20	17.050	2000.0	.000000	.014000
LOAD PAIR 21	16.390	400.0	.000000	.002000
LOAD PAIR 22	15.990	13200.0	.000000	.073000
LOAD PAIR 23	15.370	13200.0	.000000	.064000
LOAD PAIR 24	14.900	80.0	.000000	.000000
LOAD PAIR 25	18.840	80.0	.000000	.000000
LOAD PAIR 26	14.700	70.0	.000000	.000000

NAME OF PLANT = W-NEW  
 NAME OF COMPONENT = CHARGING NOZZLE NOZZLE  
 NUM OF LOAD PAIRS = 18  
 MATERIAL = 316NG  
 WALL THICK (INCH) = .500  
 INNER DIAMETER = 4.000  
 AIR/WATER = WATER  
 TEMPERATURE (F) = 590.000  
 SULFUR (WHT%) = .015  
 DISOL O2 (PPM) = .010  
 STR RATE (%/SEC) = .00400  
 USEAGE (DETERMIN.) = 3.37300  
 P-INITIATION @40 = 9.51E-01  
 P-INITIATION @60 = 9.83E-01  
 P-TWC @40 = 8.72E-01  
 P-TWC @60 = 9.63E-01

LOAD PAIR	AMP(KSI)	NUM/40-YR	EDOT(%/SEC)	USEAGE
LOSS CHARGING-PROMPT RTN/NULL	133.440	120.0	.000000	1.818000
LOSS CHARGING-DELAY RTN/NULL	132.780	12.0	.000000	.182000
NORM CHARGING/LETDOWN SD/NULL	101.060	60.0	.000000	.330000
LOSS OF LETDOWN-DELAY RTN/NULL	56.050	8.0	.000000	.005000
REACTOR TRIP/OBE	54.230	20.0	.000000	.010000
LOSS LETDOWN-DELAY RTN/FLW INC	47.470	4.0	.000000	.001000
LOSS CHARGE-PROMPT RTN/FLW INC	46.470	120.0	.000000	.022000
STEP INC CHARGING/FLOW INC	41.740	14276.0	.000000	.977000
STEP INC CHARGE/FLOW DECREASE	40.870	124.0	.000000	.007000
LETDOWN INCREASE/FLOW DECREASE	38.490	1076.0	.000000	.037000
LETDOWN INCREASE/REACTOR TRIP	37.350	30.0	.000000	.001000
LETDOWN INCREASE/FLOW INCREASE	36.740	13294.0	.000000	.364000
COOLDOWN/FLOW INCREASE	35.480	5.0	.000000	.000000
FLOW DECREASE/FLOW DECREASE	34.880	1101.0	.000000	.023000
FLOW DECREASE/REACTOR TRIP	34.130	10.0	.000000	.000000
LETDOWN INCREASE/LETDOWN DECRE	32.330	89.0	.000000	.001000
LETDOWN INCREASE/FLOW DECREASE	31.170	14311.0	.000000	.140000
REACTOR TRIP/FLOW DECREASE	30.330	5.0	.000000	.000000

NAME OF PLANT = W-NEW  
 NAME OF COMPONENT = SAFETY INJEC NOZZLE NOZZLE  
 NUM OF LOAD PAIRS = 20  
 MATERIAL = 316NG  
 WALL THICK (INCH) = .500  
 INNER DIAMETER = 6.000  
 AIR/WATER = WATER  
 TEMPERATURE (F) = 590.000  
 SULFUR (WHT%) = .015  
 DISOL O2 (PPM) = .010  
 STR RATE (%/SEC) = .00400  
 USEAGE (DETERMIN.) = 1.46000  
 P-INITIATION @40 = 4.34E-03  
 P-INITIATION @60 = 3.69E-02  
     P-TWC @40 = 5.00E-04  
     P-TWC @60 = 1.09E-02

LOAD PAIR	AMP (KSI)	NUM/40-YR	EDOT (%/SEC)	USEAGE
SMALL LOCA B/OBE	226.910	.0	.000000	.001000
DEPRESSURIZATION B/OBE	214.500	.0	.000000	.001000
REACTOR TRIP COOLDOWN B/HEATUP	260.120	5.0	.000000	.333000
CONTINGENCY B/HEATUP GROUP	260.120	.0	.000000	.000000
INADVERTENT SI/HEATUP	259.530	25.0	.000000	1.667000
LARGE STREAM LINE BREAK/HEAT UP	252.800	.0	.000000	.000000
SMALL LOCA A	198.350	.0	.000000	.000000
DEPRESSURIZATION A/OBE	186.800	.0	.000000	.001000
REACTOR TRIP-COOLDOWN/HEATUP	230.700	.0	.000000	.000000
CONTINGENCY A/HEATUP	230.700	.0	.000000	.000000
INADVERTENT SI A/HEATUP	230.110	.0	.000000	.000000
DEPRESSURIZATION A/LOSS LOAD	153.210	.0	.000000	.000000
SMALL SLB B/HEATUP	115.090	.0	.000000	.000000
SMALL SLB A/HEATUP	94.550	.0	.000000	.000000
LARGE LOCA/LOSS OF LOAD #1	66.450	.0	.000000	.000000
LARGE LOCA/LOSS OF LOAD #2	38.120	74.0	.000000	.002000
LARGE LOCA/LOSS OF LOAD #3	38.120	42.0	.000000	.001000
LARGE LOCA/LOSS OF LOAD #4	31.120	20.0	.000000	.000000
LARGE LOCA/LOSS OF LOAD #5	28.620	148.0	.000000	.001000
LARGE LOCA/LOSS OF LOAD #6	28.420	7.0	.000000	.000000

NAME OF PLANT = W-NEW  
 NAME OF COMPONENT = RESIDUAL HEAT INLET TRAN  
 NUM OF LOAD PAIRS = 18  
 MATERIAL = 304/316  
 WALL THICK (INCH) = .750  
 INNER DIAMETER = 12.000  
 AIR/WATER = WATER  
 TEMPERATURE (F) = 590.000  
 SULFUR (WHT%) = .015  
 DISOL O2 (PPM) = .010  
 STR RATE (%/SEC) = .00400  
 USEAGE (DETERMIN.) = 2.73300  
 P-INITIATION @40 = 9.58E-01  
 P-INITIATION @60 = 9.99E-01  
     P-TWC @40 = 7.80E-01  
     P-TWC @60 = 9.80E-01

LOAD PAIR	AMP (KSI)	NUM/40-YR	EDOT (%/SEC)	USEAGE
RAPID DEPRES/STRAT 16	194.130	.0	.000000	.000000
HEATUP/STRATIFICATION 16	166.020	65.0	.000000	1.383000
OBE/STRATIFICATION 18	146.320	20.0	.000000	.308000
STRAT 16/STRAT 25	143.390	45.0	.000000	.652000
STRAT 18/STRAT 25	110.770	7.0	.000000	.050000
STRAT 18/STRAT 27	110.770	7.0	.000000	.050000
COMBINATION/STRAT 18 #1	106.520	30.0	.000000	.192000
COMBINATION/STRAT 18 #2	40.220	196.0	.000000	.008000
COMBINATION/STRAT 18 #3	39.030	140.0	.000000	.005000
COMBINATION/STRAT 18 #4	35.780	230.0	.000000	.006000
COMBINATION/STRAT 18 #5	31.930	6004.0	.000000	.070000
COMBINATION/STRAT 18 #6	31.030	80.0	.000000	.001000
COMBINATION/STRAT 18 #7	29.420	10.0	.000000	.000000
COMBINATION/STRAT 18 #8	29.280	160.0	.000000	.001000
COMBINATION/STRAT 18 #9	29.120	230.0	.000000	.001000
COMBINATION/STRAT 18 #10	28.300	90.0	.000000	.000000
COMBINATION/STRAT 18 #11	25.060	6866.0	.000000	.004000
COMBINATION/STRAT 18 #12	24.610	6534.0	.000000	.002000

NAME OF PLANT = W-OLD  
 NAME OF COMPONENT = RPV LOWER HEAD SHELL  
 NUM OF LOAD PAIRS = 2  
 MATERIAL = LAS  
 WALL THICK (INCH) = 8.000  
 INNER DIAMETER = 180.000  
 AIR/WATER = WATER  
 TEMPERATURE (F) = 590.000  
 SULFUR (WHT%) = .015  
 DISOL O2 (PPM) = .010  
 STR RATE (%/SEC) = .00100  
 USEAGE (DETERMIN.) = .89100  
 P-INITIATION @40 = 1.11E-01  
 P-INITIATION @60 = 1.28E-01  
     P-TWC @40 = 7.20E-07  
     P-TWC @60 = 1.11E-05

(LATIN HYPERCUBE CALCULATION WAS USED EVALUATE THE EFFECTS OF FRICTION  
 FORCE VIBRATION TRANSIENT. THIS TRANSIENT IS ASSOCIATED WITH HIGH LOCAL  
 STRESSES AT WELDED ATTACHMENT. FULL LEVEL OF THIS CYCLIC STRESS WAS USED TO  
 PREDICT CRACK INITIATION BUT WAS NEGLECTED FOR FATIGUE CRACK GROWTH CALCULATION.  
 THE INITIAL DEPTH OF THE INITIATED CRACK WAS HOWEVER INCREASED FROM 3-MM TO 25-MM)

	LOAD PAIR	AMP (KSI)	NUM/40-YR	EDOT (%/SEC)	USEAGE
	OBE A/OBE B	22.070	400.0	.000000	.009000
	FRICTION FORCES VIBRATION	14.980	200000.0	.000000	.882000

NAME OF PLANT = W-OLD  
 NAME OF COMPONENT = RPV INLET NOZZLE INNER SURFACE  
 NUM OF LOAD PAIRS = 3  
 MATERIAL = LAS  
 WALL THICK (INCH) = 3.000  
 INNER DIAMETER = 24.000  
 AIR/WATER = WATER  
 TEMPERATURE (F) = 590.000  
 SULFUR (WHT%) = .015  
 DISOL O2 (PPM) = .010  
 STR RATE (%/SEC) = .00100  
 USEAGE (DETERMIN.) = .30200  
 P-INITIATION @40 = 3.91E-01  
 P-INITIATION @60 = 6.44E-01  
     P-TWC @40 = 4.38E-03  
     P-TWC @60 = 5.04E-02

	LOAD PAIR	AMP (KSI)	NUM/40-YR	EDOT (%/SEC)	USEAGE
	HEATUP/COOLDOWN	15.000	350.0	.000000	.000000
	PLANT LOAD/UNLOAD	19.440	14500.0	.000000	.179000
	COMBINATION	25.560	2760.0	.000000	.123000

NAME OF PLANT = W-OLD  
 NAME OF COMPONENT = RPV INLET NOZZLE OUTER SURFACE  
 NUM OF LOAD PAIRS = 3  
 MATERIAL = LAS  
 WALL THICK (INCH) = 3.000  
 INNER DIAMETER = 24.000  
 AIR/WATER = AIR  
 TEMPERATURE (F) = 590.000  
 SULFUR (WHT%) = .015  
 DISOL O2 (PPM) = .010  
 STR RATE (%/SEC) = .00100  
 USEAGE (DETERMIN.) = .49600  
 P-INITIATION @40 = 6.81E-02  
 P-INITIATION @60 = 1.11E-01  
 P-TWC @40 = 4.48E-04  
 P-TWC @60 = 3.32E-03

(RESULTS FROM LATIN HYPERCUBE CALCULATION WERE USED BECAUSE PC-PRAISE  
 MODEL DOES NOT ADDRESS CRACK GROWTH AND INITIATION FOR AIR ENVIRONMENT)

LOAD PAIR	AMP (KSI)	NUM/40-YR	EDOT (%/SEC)	USEAGE
HEATUP/COOLDOWN	41.110	350.0	.000000	.099000
PLANT LOAD/UNLOAD	21.260	14500.0	.000000	.273000
COMBINATION	25.560	2760.0	.000000	.123000

NAME OF PLANT = W-OLD  
 NAME OF COMPONENT = RPV OUTLET NOZZLE INNER SURF  
 NUM OF LOAD PAIRS = 4  
 MATERIAL = LAS  
 WALL THICK (INCH) = 3.000  
 INNER DIAMETER = 24.000  
 AIR/WATER = WATER  
 TEMPERATURE (F) = 590.000  
 SULFUR (WHT%) = .015  
 DISOL O2 (PPM) = .010  
 STR RATE (%/SEC) = .00100  
 USEAGE (DETERMIN.) = .49900  
 P-INITIATION @40 = 4.90E-01  
 P-INITIATION @60 = 7.53E-01  
 P-TWC @40 = 9.33E-03  
 P-TWC @60 = 9.60E-02

LOAD PAIR	AMP (KSI)	NUM/40-YR	EDOT (%/SEC)	USEAGE
HEATUP/COOLDOWN	17.220	350.0	.000000	.003000
PLANT LOADING/UNLOADING	18.890	14100.0	.000000	.152000
OBE A/OBE B	20.940	400.0	.000000	.007000
COMBINATION	32.780	2760.0	.000000	.337000

NAME OF PLANT = W-OLD  
 NAME OF COMPONENT = RPV OUTLET NOZZLE OUTER SURF  
 NUM OF LOAD PAIRS = 4  
 MATERIAL = LAS  
 WALL THICK (INCH) = 3.000  
 INNER DIAMETER = 24.000  
 AIR/WATER = AIR  
 TEMPERATURE (F) = 590.000  
 SULFUR (WHT%) = .015  
 DISOL O2 (PPM) = .010  
 STR RATE (%/SEC) = .00100  
 USEAGE (DETERMIN.) = .34700  
 P-INITIATION @40 = 1.63E-01  
 P-INITIATION @60 = 2.38E-01  
     P-TWC @40 = 7.77E-03  
     P-TWC @60 = 3.60E-02

(RESULTS FROM LATIN HYPERCUBE CALCULATION WERE USED BECAUSE PC-PRAISE  
 MODEL DOES NOT ADDRESS CRACK GROWTH AND INITIATION FOR AIR ENVIRONMENT)

LOAD PAIR	AMP (KSI)	NUM/40-YR	EDOT (%/SEC)	USEAGE
HEATUP/COOLDOWN	27.780	350.0	.000000	.023000
PLANT LOADING/UNLOADING	27.220	14100.0	.000000	.845000
OBE A/OBE B	29.280	400.0	.000000	.032000
COMBINATION	30.560	2760.0	.000000	.261000

NAME OF PLANT = W-OLD  
 NAME OF COMPONENT = CHARGING NOZZLE NOZZLE  
 NUM OF LOAD PAIRS = 4  
 MATERIAL = 304/316  
 WALL THICK (INCH) = .500  
 INNER DIAMETER = 4.000  
 AIR/WATER = WATER  
 TEMPERATURE (F) = 590.000  
 SULFUR (WHT%) = .015  
 DISOL O2 (PPM) = .010  
 STR RATE (%/SEC) = .00400  
 USEAGE (DETERMIN.) = .31900  
 P-INITIATION @40 = 4.67E-04  
 P-INITIATION @60 = 3.75E-03  
     P-TWC @40 = 3.00E-07  
     P-TWC @60 = 5.20E-06

LOAD PAIR	AMP (KSI)	NUM/40-YR	EDOT (%/SEC)	USEAGE
2A/4B	84.790	20.0	.000000	.063000
2A/3B	82.860	80.0	.000000	.235000
4A/3B	46.150	20.0	.000000	.004000
3A/3B #1	46.060	100.0	.000000	.022000

NAME OF PLANT = W-OLD  
 NAME OF COMPONENT = SAFETY INJECTION NOZZLE NOZZLE  
 NUM OF LOAD PAIRS = 3  
 MATERIAL = 304/316  
 WALL THICK (INCH) = .500  
 INNER DIAMETER = 6.000  
 AIR/WATER = WATER  
 TEMPERATURE (F) = 590.000  
 SULFUR (WHT%) = .015  
 DISOL O2 (PPM) = .010  
 STR RATE (%/SEC) = .00400  
 USEAGE (DETERMIN.) = .32700  
 P-INITIATION @40 = 1.88E-03  
 P-INITIATION @60 = 1.31E-02  
 P-TWC @40 = 4.00E-06  
 P-TWC @60 = 8.80E-05

	LOAD PAIR	AMP (KSI)	NUM/40-YR	EDOT (%/SEC)	USEAGE
SAFETY INJECTION/REACTOR TRIP		102.570	70.0	.000000	.298000
INITIATION OF RHR/OBE		46.790	50.0	.000000	.010000
INITIATION OF RHR/LEAK TEST		45.490	122.0	.000000	.019000

NAME OF PLANT = W-OLD  
 NAME OF COMPONENT = RESIDUAL HEAT REMOVAL TEE  
 NUM OF LOAD PAIRS = 8  
 MATERIAL = 304/316  
 WALL THICK (INCH) = .750  
 INNER DIAMETER = 6.000  
 AIR/WATER = WATER  
 TEMPERATURE (F) = 590.000  
 SULFUR (WHT%) = .015  
 DISOL O2 (PPM) = .010  
 STR RATE (%/SEC) = .00400  
 USEAGE (DETERMIN.) = .20500  
 P-INITIATION @40 = 1.34E-02  
 P-INITIATION @60 = 5.16E-02  
 P-TWC @40 = 1.15E-04  
 P-TWC @60 = 1.14E-03

	LOAD PAIR	AMP (KSI)	NUM/40-YR	EDOT (%/SEC)	USEAGE
SHUTDOWN COOLING A/OBE		56.910	50.0	.000000	.032000
SHUTDOWN COOLING/LEAK TEST A		51.600	150.0	.000000	.057000
REACTOR TRIP/EMERGENCY INJECT		50.610	70.0	.000000	.024000
STEP POWER INC/SHUTDOWN COOL B		46.440	200.0	.000000	.037000
LEAK TEST B/REACTOR TRIP		46.280	150.0	.000000	.027000
STEP POWER INCREASE/NULL		46.260	200.0	.000000	.026000
COOLDOWN/REACTOR TRIP		32.360	180.0	.000000	.002000
STEP POWER INCREASE/COOLDOWN		32.360	20.0	.000000	.000000

NAME OF PLANT = GE-NEW  
 NAME OF COMPONENT = RPV NEAR CRDM PENETRATION  
 NUM OF LOAD PAIRS = 2  
 MATERIAL = LAS  
 WALL THICK (INCH) = 5.000  
 INNER DIAMETER = 240.000  
 AIR/WATER = WATER  
 TEMPERATURE (F) = 590.000  
 SULFUR (WHT%) = .015  
 DISOL O2 (PPM) = .100  
 STR RATE (%/SEC) = .00100  
 USEAGE (DETERMIN.) = .62800  
 P-INITIATION @40 = 7.89E-05  
 P-INITIATION @60 = 3.49E-04  
 P-TWC @40 = 7.88E-12  
 P-TWC @60 = 6.82E-10

(RESULTS FROM LATIN HYPERCUBE CALCULATION WERE USED  
 AFTER 10<sup>6</sup> SIMULATIONS WITH PC-PRAISE GAVE INADEQUATE NUMBER OF FAILURES)

	LOAD PAIR	AMP (KSI)	NUM/40-YR	EDOT (%/SEC)	USEAGE
HYDRO/OBE/LOSS FEEDWATER PUMPS		47.970	50.0	.000000	.532000
ALL OTHER		15.160	1020.0	.000000	.096000

NAME OF PLANT = GE-NEW  
 NAME OF COMPONENT = FEEDWATER NOZZLE SAFE END  
 NUM OF LOAD PAIRS = 14  
 MATERIAL = LAS  
 WALL THICK (INCH) = 1.000  
 INNER DIAMETER = 12.000  
 AIR/WATER = WATER  
 TEMPERATURE (F) = 590.000  
 SULFUR (WHT%) = .015  
 DISOL O2 (PPM) = .100  
 STR RATE (%/SEC) = .00100  
 USEAGE (DETERMIN.) = 1.88100  
 P-INITIATION @40 = 1.04E-01  
 P-INITIATION @60 = 2.53E-01  
 P-TWC @40 = 1.31E-03  
 P-TWC @60 = 1.47E-02

	LOAD PAIR	AMP (KSI)	NUM/40-YR	EDOT (%/SEC)	USEAGE
	TURBINE ROLL A/TG TRIP A	67.270	210.0	.028000	.574000
	TUBINE ROLL A/HOT STANDBY A	61.130	.0	.026000	.000000
	TURBINE ROLL A/NULL	57.790	70.0	.026000	.128000
	HOT STANDBY A/NULL	51.650	263.0	.026000	.332000
	SHUTDOWN A/NULL	35.340	1315.0	.002000	.805000
	TURBINE ROLL A/TURBINE TRIP A	29.280	.0	.001000	.000000
	TURBINE ROLL B/TG TRIP B	20.850	210.0	.001000	.018000
	TG TRIP B/NULL	19.210	.0	.001000	.000000
	TURBINE TRIP B/NULL	17.560	10.0	.001000	.002000
	OBE A/NULL	17.440	10.0	.001000	.002000
	HOT STANDBY B/NULL	13.850	222.0	.001000	.011000
	SHUTDOWN B/NULL	13.430	666.0	.001000	.005000
	STARTUP/NULL	13.330	120.0	.001000	.002000
	REVERSE OBE A/NULL	8.520	12625.0	.001000	.002000

NAME OF PLANT = GE-NEW  
 NAME OF COMPONENT = RECIRC SYS - TEE SUCTION PIPE  
 NUM OF LOAD PAIRS = 28  
 MATERIAL = 304/316  
 WALL THICK (INCH) = 1.000  
 INNER DIAMETER = 16.000  
 AIR/WATER = WATER  
 TEMPERATURE (F) = 590.000  
 SULFUR (WHT%) = .015  
 DISOL O2 (PPM) = .100  
 STR RATE (%/SEC) = .00400  
 USEAGE (DETERMIN.) = .83000  
 P-INITIATION @40 = 4.23E-02  
 P-INITIATION @60 = 1.39E-01  
     P-TWC @40 = 4.80E-04  
     P-TWC @60 = 4.67E-03

	LOAD PAIR	AMP (KSI)	NUM/40-YR	EDOT (%/SEC)	USEAGE
	COMPOSITE LOSS/NULL	98.220	10.0	.000000	.048000
	COMPOSITE LOSS/NULL	100.430	10.0	.000000	.050000
	TURBINE GENERATOR TRIP/NULL	91.870	5.0	.000000	.020000
	TURBINE GENERATOR TRIP/NULL	91.870	5.0	.000000	.020000
	COMPOSITE LOSS/NULL	91.190	10.0	.000000	.040000
	RELIEF VALVE EVENT/UNBOLT	81.320	30.0	.000000	.091000
	RELIEF VALVE EVENT/UNBOLT	81.320	93.0	.000000	.282000
	HYDRO/RELIEF VALVE EVENT #1	77.420	40.0	.000000	.108000
	HYDRO/RELIEF VALVE EVENT #2	75.040	7.0	.000000	.017000
	HYDRO/RELIEF VALVE EVENT #3	80.610	1.0	.000000	.003000
	HYDRO/RELIEF VALVE EVENT #4	62.770	9.0	.000000	.014000
	HYDRO/RELIEF VALVE EVENT #5	59.360	10.0	.000000	.011000
	HYDRO/RELIEF VALVE EVENT #6	54.760	10.0	.000000	.007000
	HYDRO/RELIEF VALVE EVENT #7	51.280	20.0	.000000	.009000
	HYDRO/RELIEF VALVE EVENT #8	50.490	111.0	.000000	.046000
	HYDRO/RELIEF VALVE EVENT #9	50.090	50.0	.000000	.020000
	HYDRO/RELIEF VALVE EVENT #10	48.540	40.0	.000000	.013000
	HYDRO/RELIEF VALVE EVENT #11	48.120	10.0	.000000	.003000
	HYDRO/RELIEF VALVE EVENT #12	48.060	10.0	.000000	.003000
	HYDRO/RELIEF VALVE EVENT #13	47.960	42.0	.000000	.013000
	HYDRO/RELIEF VALVE EVENT #14	39.700	10.0	.000000	.001000
	HYDRO/RELIEF VALVE EVENT #15	36.190	130.0	.000000	.007000
	HYDRO/RELIEF VALVE EVENT #16	33.900	111.0	.000000	.004000
	HYDRO/RELIEF VALVE EVENT #17	21.490	660.0	.000000	.000000
	HYDRO/RELIEF VALVE EVENT #18	19.700	10.0	.000000	.000000
	HYDRO/RELIEF VALVE EVENT #19	19.010	8.0	.000000	.000000
	HYDRO/RELIEF VALVE EVENT #20	18.640	10.0	.000000	.000000
	HYDRO/RELIEF VALVE EVENT #21	12.810	4800.0	.000000	.000000

NAME OF PLANT = GE-NEW  
 NAME OF COMPONENT = CORE SPRAY LINE SAFE END EXT  
 NUM OF LOAD PAIRS = 7  
 MATERIAL = LAS  
 WALL THICK (INCH) = .500  
 INNER DIAMETER = 8.000  
 AIR/WATER = WATER  
 TEMPERATURE (F) = 590.000  
 SULFUR (WHT%) = .015  
 DISOL O2 (PPM) = .100  
 STR RATE (%/SEC) = .00100  
 USAGE (DETERMIN.) = .43600  
 P-INITIATION @40 = 3.83E-04  
 P-INITIATION @60 = 1.27E-03  
     P-TWC @40 = 1.45E-07  
     P-TWC @60 = 3.25E-06

(RESULTS FROM LATIN HYPERCUBE CALCULATION WERE USED  
 AFTER 10<sup>6</sup> SIMULATIONS WITH PC-PRAISE GAVE INADEQUATE NUMBER OF FAILURES)

LOAD PAIR	AMP (KSI)	NUM/40-YR	EDOT (%/SEC)	USAGE
COOLDOWN/NULL	46.000	18.0	.000000	.038000
COOLDOWN (LOPO)/NULL	80.850	30.0	.000000	.349000
OBE/NULL	22.380	10.0	.000000	.004000
WARMUP/NULL	21.950	10.0	.000000	.001000
WARMUP (LOPO)/NULL	20.440	30.0	.000000	.002000
WARMUP/NULL	16.730	310.0	.000000	.041000
OBE/NULL	10.690	1804.0	.000000	.001000

NAME OF PLANT = GE-NEW  
 NAME OF COMPONENT = RHR LINE STRAIGHT PIPE  
 NUM OF LOAD PAIRS = 13  
 MATERIAL = LAS  
 WALL THICK (INCH) = .750  
 INNER DIAMETER = 10.000  
 AIR/WATER = WATER  
 TEMPERATURE (F) = 590.000  
 SULFUR (WHT%) = .015  
 DISOL O2 (PPM) = .100  
 STR RATE (%/SEC) = .00100  
 USAGE (DETERMIN.) = 11.26000  
 P-INITIATION @40 = 4.73E-01  
 P-INITIATION @60 = 6.71E-01  
     P-TWC @40 = 4.10E-01  
     P-TWC @60 = 6.21E-01

LOAD PAIR	AMP (KSI)	NUM/40-YR	EDOT (%/SEC)	USAGE
HIGH 4/STATIFICATION 10	46.930	5.0	.000000	.049000
HIGH 4/STATIFICATION 10	46.840	114.0	.000000	1.107000
LOW 7/STATIFICATION 10	24.730	152.0	.000000	.106000
LOW 7/STATIFICATION 10	23.780	11976.0	.000000	6.728000
HIGH 1/STATIFICATION 10	23.240	523.0	.000000	.258000
HIGH 3/STATIFICATION 10	23.140	610.0	.000000	.294000
HIGH 2/STATIFICATION 10	22.970	1620.0	.000000	.750000
HIGH 2/STATIFICATION 11	16.680	10480.0	.000000	1.385000
LOW 8/STATIFICATION 11	16.210	242.0	.000000	.029000
LOW 9/STATIFICATION 11	15.810	360.0	.000000	.039000
LOW 6/STATIFICATION 11	15.740	300.0	.000000	.032000
LOW 5/STATIFICATION 11	15.370	619.0	.000000	.061000
HIGH 1/HIGH 2	8.210	3000000.0	.000000	.422000

NAME OF PLANT - GE-NEW  
 NAME OF COMPONENT - FEEDWATER LINE ELBOW  
 NUM OF LOAD PAIRS - 28  
 MATERIAL - LAS  
 WALL THICK (INCH) - 1.000  
 INNER DIAMETER - 12.000  
 AIR/WATER - WATER  
 TEMPERATURE (F) - 590.000  
 SULFUR (WHT%) - .015  
 DISOL O2 (PPM) - .100  
 STR RATE (t/SEC) - .00100  
 USEAGE (DETERMIN.) - 3.68800  
 P-INITIATION @40 - 1.59E-01  
 P-INITIATION @60 - 3.65E-01  
 P-TWC @40 - 1.01E-03  
 P-TWC @60 - 1.46E-02

LOAD PAIR	AMP (KSI)	NUM/40-YR	EDOT (t/SEC)	USEAGE
HIGH 18/LOW 21	106.040	5.0	.117000	.025000
HIGH 18/LOW 21	103.960	5.0	.114000	.024000
HIGH 18/LOW 21	102.610	5.0	.113000	.024000
HIGH 14/LOW 17	91.590	8.0	.001000	.123000
HIGH 8/LOW 17	89.400	10.0	.095000	.037000
HIGH 3/LOW 16	88.270	5.0	.094000	.018000
HIGH 8/HIGH 7	83.760	126.0	.041000	.519000
HIGH 7/HIGH 7	81.430	10.0	.086000	.033000
HIGH 7/LOW 13	67.930	97.0	.001000	.740000
HIGH 7/LOW 13	66.710	14.0	.001000	.101000
HIGH 7/LOW 15	61.290	6.0	.001000	.035000
HIGH 7/LOW 15	61.160	64.0	.001000	.451000
HIGH 8/LOW 12	55.500	92.0	.001000	.391000
HIGH 3/LOW 12	46.630	88.0	.001000	.254000
HIGH 7/LOW 22	42.880	15.0	.001000	.029000
HIGH 3/HIGH 7	39.440	212.0	.001000	.315000
HIGH 3/HIGH 7	38.130	69.0	.001000	.104000
HIGH 3/LOW 20	36.800	11.0	.001000	.014000
HIGH 4/LOW 20	34.320	60.0	.001000	.053000
LOW 11/LOW 20	32.950	203.0	.001000	.122000
HIGH 7/LOW 11	32.530	360.0	.001000	.203000
HIGH 6/LOW 11	29.770	222.0	.025000	.035000
HIGH 2/HIGH 19	26.090	30.0	.028000	.003000
HIGH 5/HIGH 19	26.040	81.0	.028000	.007000
HIGH 5/HIGH 9	21.640	96.0	.001000	.012000
HIGH 1/HIGH 11	20.560	40.0	.001000	.003000
LOW 10/LOW 11	14.180	30.0	.001000	.001000
HIGH 5/LOW 11	11.220	11545.0	.001000	.008000

NAME OF PLANT = GE-OLD  
 NAME OF COMPONENT = RPV LOWER HEAD TO SHELL  
 NUM OF LOAD PAIRS = 2  
 MATERIAL = LAS  
 WALL THICK (INCH) = 5.000  
 INNER DIAMETER = 240.000  
 AIR/WATER = WATER  
 TEMPERATURE (F) = 590.000  
 SULFUR (WHT%) = .015  
 DISOL O2 (PPM) = .100  
 STR RATE (%/SEC) = .00100  
 USEAGE (DETERMIN.) = .07900  
 P-INITIATION @40 = 2.71E-10  
 P-INITIATION @60 = 2.76E-08  
 P-TWC @40 = 0.00E+00  
 P-TWC @60 = 0.00E+00

(RESULTS FROM LATIN HYPERCUBE CALCULATION WERE USED  
 AFTER 10<sup>6</sup> SIMULATIONS WITH PC-PRAISE GAVE INADEQUATE NUMBER OF FAILURES)

	LOAD PAIR	AMP (KSI)	NUM/40-YR	EDOT (%/SEC)	USEAGE
LOSS OF FEEDWATER PUMPS		44.440	10.0	.000000	.079000
ALL OTHER		7.780	252.0	.000000	.000000

NAME OF PLANT = GE-OLD  
 NAME OF COMPONENT = RPV FEEDWATER NOZZLE BORE  
 NUM OF LOAD PAIRS = 5  
 MATERIAL = LAS  
 WALL THICK (INCH) = 2.000  
 INNER DIAMETER = 12.000  
 AIR/WATER = WATER  
 TEMPERATURE (F) = 590.000  
 SULFUR (WHT%) = .015  
 DISOL O2 (PPM) = .100  
 STR RATE (%/SEC) = .00100  
 USEAGE (DETERMIN.) = 3.16800  
 P-INITIATION @40 = 7.27E-02  
 P-INITIATION @60 = 2.42E-01  
 P-TWC @40 = 1.00E-05  
 P-TWC @60 = 8.80E-04

	LOAD PAIR	AMP (KSI)	NUM/40-YR	EDOT (%/SEC)	USEAGE
HEATUP/COOLDOWN		45.000	170.0	.001000	1.405000
SCRAM AND OTHERS		50.560	474.0	.100000	.367000
WEEKLY POWER REDUC & OTHERS		38.330	890.0	.001400	.842000
LOSS OF FEEDWATER PUMPS		43.330	10.0	.001600	.037000
DAILY POWER REDUCTIONS		33.330	828.0	.001000	.517000

NAME OF PLANT = GE-OLD  
 NAME OF COMPONENT = RECIRC SYSTEM RHR RETURN LINE  
 NUM OF LOAD PAIRS = 23  
 MATERIAL = 304/316  
 WALL THICK (INCH) = .750  
 INNER DIAMETER = 12.000  
 AIR/WATER = WATER  
 TEMPERATURE (F) = 590.000  
 SULFUR (WHT%) = .015  
 DISOL O2 (PPM) = .100  
 STR RATE (%/SEC) = .00400  
 USEAGE (DETERMIN.) = 3.89800  
 P-INITIATION @40 = 9.43E-01  
 P-INITIATION @60 = 9.99E-01  
 P-TWC @40 = 7.12E-01  
 P-TWC @60 = 9.85E-01

LOAD PAIR	AMP (KSI)	NUM/40-YR	EDOT (%/SEC)	USEAGE
COMPOSITE LOSS E/OBE	182.760	10.0	.000000	.213000
COMPOSITE LOSS AE/RHR B	161.690	10.0	.000000	.159000
TURBINE ROLL A/RHR B	144.890	160.0	.000000	1.951000
RHR A/OBE	133.560	40.0	.000000	.400000
RHR A/TURBINE ROLL A	116.130	12.0	.000000	.086000
RHR A/COMPOSITE LOSS C	107.480	10.0	.000000	.059000
RHR A/COMPOSITE LOSS D	100.120	10.0	.000000	.050000
RHR A/COMPOSITE LOSS G	99.950	10.0	.000000	.049000
RHR A/TURBINE TRIP SCRAMS B	94.260	88.0	.000000	.379000
TURBINE TRIP B/SHUTDOWN	63.860	10.0	.000000	.017000
TURBINE TRIP A/NULL & COOLDOWN	62.870	10.0	.000000	.016000
TURBINE TRIP-SCRAMS B/SHUTDOWN	59.200	160.0	.000000	.174000
TURBINE TRIP-SCRAMS B/COOLDOWN	57.140	36.0	.000000	.032000
TURBINE ROLL B/NULL	56.850	172.0	.000000	.146000
WARMUP/COMPOSITE LOSS F	55.420	10.0	.000000	.007000
HYDROTEST DOWN/STARTUP	50.640	68.0	.000000	.029000
REDUCTION TO POWER/COOLDOWN	50.560	139.0	.000000	.058000
REDUCTION TO POWER/WARMUP	50.430	26.0	.000000	.011000
WARMUP/STARTUP #1	50.420	104.0	.000000	.043000
WARMUP/STARTUP #2	46.760	25.0	.000000	.007000
WARMUP/STARTUP #3	42.830	10.0	.000000	.002000
WARMUP/STARTUP #4	42.740	58.0	.000000	.009000
WARMUP/STARTUP #5	41.820	10.0	.000000	.001000

NAME OF PLANT = GE-OLD  
 NAME OF COMPONENT = CORE SPRAY SYSTEM NOZZLE  
 NUM OF LOAD PAIRS = 1  
 MATERIAL = LAS  
 WALL THICK (INCH) = .500  
 INNER DIAMETER = 10.000  
 AIR/WATER = WATER  
 TEMPERATURE (F) = 590.000  
 SULFUR (WHT%) = .015  
 DISOL O2 (PPM) = .100  
 STR RATE (%/SEC) = .00100  
 USEAGE (DETERMIN.) = .52000  
 P-INITIATION @40 = 1.41E-04  
 P-INITIATION @60 = 7.89E-04  
 P-TWC @40 = 1.91E-08  
 P-TWC @60 = 8.84E-07

(RESULTS FROM LATIN HYPERCUBE CALCULATION WERE USED  
 AFTER 10<sup>6</sup> SIMULATIONS WITH PC-PRAISE GAVE INADEQUATE NUMBER OF FAILURES)

LOAD PAIR	AMP (KSI)	NUM/40-YR	EDOT (%/SEC)	USEAGE
ALL	33.330	455.0	.000000	.441000

NAME OF PLANT = GE-OLD  
 NAME OF COMPONENT = CORE SPRAY SYSTEM SAFE END  
 NUM OF LOAD PAIRS = 1  
 MATERIAL = 304/316  
 WALL THICK (INCH) = .500  
 INNER DIAMETER = 10.000  
 AIR/WATER = WATER  
 TEMPERATURE (F) = 590.000  
 SULFUR (WHT%) = .015  
 DISOL O2 (PPM) = .100  
 STR RATE (%/SEC) = .00400  
 USEAGE (DETERMIN.) = 1.77200  
 P-INITIATION @40 = 3.33E-01  
 P-INITIATION @60 = 7.64E-01  
     P-TWC @40 = 1.46E-02  
     P-TWC @60 = 1.10E-01

LOAD PAIR	AMP (KSI)	NUM/40-YR	EDOT (%/SEC)	USEAGE
ALL	93.950	537.0	.000000	2.305000

NAME OF PLANT = GE-OLD  
 NAME OF COMPONENT = RESIDUAL HEAT TAPERED  
 NUM OF LOAD PAIRS = 2  
 MATERIAL = 304/316  
 WALL THICK (INCH) = .750  
 INNER DIAMETER = 12.000  
 AIR/WATER = WATER  
 TEMPERATURE (F) = 590.000  
 SULFUR (WHT%) = .015  
 DISOL O2 (PPM) = .100  
 STR RATE (%/SEC) = .00400  
 USEAGE (DETERMIN.) = .47800  
 P-INITIATION @40 = 1.47E-03  
 P-INITIATION @60 = 7.89E-03  
     P-TWC @40 = 9.21E-05  
     P-TWC @60 = 1.02E-03

(RESULTS FROM LATIN HYPERCUBE CALCULATION WERE USED  
 AFTER 10<sup>6</sup> SIMULATIONS WITH PC-PRAISE GAVE INADEQUATE NUMBER OF FAILURES)

LOAD PAIR	AMP (KSI)	NUM/40-YR	EDOT (%/SEC)	USEAGE
RHR SHUTDOWN A/B	81.780	119.0	.000000	.365000
COMPOSITE LOSS G/BLOWDOWN	37.700	8.0	.000000	.001000

NAME OF PLANT = GE-OLD  
 NAME OF COMPONENT = FEEDWATER LINE - RCIC TEE  
 NUM OF LOAD PAIRS = 27  
 MATERIAL = LAS  
 WALL THICK (INCH) = 1.000  
 INNER DIAMETER = 16.000  
 AIR/WATER = WATER  
 TEMPERATURE(F) = 590.000  
 SULFUR(WHT%) = .015  
 DISOL O2 (PPM) = .100  
 STR RATE (%/SEC) = .00100  
 USEAGE(DETERMIN.) = 6.98000  
 P-INITIATION @40 = 3.86E-01  
 P-INITIATION @60 = 7.82E-01  
 P-TWC @40 = 2.99E-03  
 P-TWC @60 = 5.92E-02

LOAD PAIR	AMP(KSI)	NUM/40-YR	EDOT(%/SEC)	USEAGE
LOW LOAD SET/RCIC INITIATIONS	121.950	10.0	.000000	.286000
LOW LOAD SET/RCIC & RWCU INIT	73.100	12.0	.000000	.110000
LOW LOAD SET/RCIC & RWCU INIT	70.780	423.0	.000000	3.555000
LOW LOAD SET/OBE	54.460	50.0	.000000	.201000
HIGH LOAD SET/RCIC & RWCU INIT	51.820	65.0	.000000	.221000
LOW LOAD SET/NULL	51.040	10.0	.000000	.032000
HIGH LOAD SET/NULL	46.880	32.0	.000000	.073000
HIGH LOAD SET/NULL	46.880	10.0	.000000	.023000
LOW LOAD SET/NULL	46.560	120.0	.000000	.267000
HIGH LOAD SET A/HIGH LOAD B	46.120	30.0	.000000	.064000
HIGH LOAD SET/LOW LOAD SET	45.890	232.0	.000000	.486000
HIGH LOAD SET/HIGH LOAD SET	45.310	22.0	.000000	.044000
HIGH LOAD SET/HIGH LOAD SET	43.600	68.0	.000000	.117000
HIGH LOAD SET/RCIC INITIATION	42.580	50.0	.000000	.078000
HIGH LOAD SET/HIGH LD SET #1	42.250	284.0	.000000	.430000
HIGH LOAD SET/HIGH LD SET #2	42.050	22.0	.000000	.033000
HIGH LOAD SET/HIGH LD SET #3	41.080	352.0	.000000	.478000
HIGH LOAD SET/HIGH LD SET #4	39.820	22.0	.000000	.026000
HIGH LOAD SET/HIGH LD SET #5	38.530	105.0	.000000	.111000
HIGH LOAD SET/HIGH LD SET #6	38.060	19.0	.000000	.019000
HIGH LOAD SET/HIGH LD SET #7	37.690	22.0	.000000	.021000
HIGH LOAD SET/HIGH LD SET #8	35.190	284.0	.000000	.211000
HIGH LOAD SET/HIGH LD SET #9	32.870	22.0	.000000	.013000
HIGH LOAD SET/HIGH LD SET #10	31.130	3.0	.000000	.001000
HIGH LOAD SET/HIGH LD SET #11	30.990	155.0	.000000	.075000
HIGH LOAD SET/HIGH LD SET #12	24.880	30.0	.000000	.001000
HIGH LOAD SET/HIGH LD SET #13	24.320	22.0	.000000	.004000

## Appendix B

### Core Damage Frequency Calculations

This appendix provides tables that detail the inputs and results for the core damage calculations for all of the components addressed in the present report.

**NEWER VINTAGE COMBUSTION ENGINEERING PLANT AT 40 YEARS**

LOCATION	MATERIAL TYPE	USAGE FACTOR AT 40 YR (INEL)	CUMULATIVE PROB. INITIATION 40 YEARS	CUMULATIVE PROB. TWC AT 40 YR	TWC PER YEAR AT 40 YR	COND. PROB. SMALL LEAK	COND. PROB. LARGE LEAK OR BREAK	COND. PROB. CORE DAMAGE GIVEN LARGE LEAK OR BREAK	CORE DAMAGE FREQUENCY PER YEAR FROM LARGE LEAKS AND BREAKS	COND. PROB. CORE DAMAGE GIVEN SMALL LEAK	CORE DAMAGE FREQUENCY PER YEAR FROM SMALL LEAKS	CORE DAMAGE FREQUENCY PER YEAR AT 40 YEAR (TOTAL)
REACTOR VESSEL SHELL/ LOWER HEAD REGION	CS	0.014	7.00E-06	6.71E-16	1.13E-16	9.00E-01	1.00E-01	1.00E+00	1.13E-16	4.23E-04	4.32E-19	1.13E-16
REACTOR VESSEL INLET NOZZLE	CS	0.475	1.40E-02	5.90E-06	7.50E-06	5.00E-03	2.00E-05	1.00E-02	1.50E-12	5.00E-04	1.88E-11	2.03E-11
REACTOR VESSEL OUTLET NOZZLE	CS	0.472	4.22E-01	1.74E-03	3.59E-04	5.00E-03	2.00E-05	1.00E-02	7.15E-11	5.00E-04	8.04E-10	9.55E-10
PRESSURIZER SURGE LINE (ELBOW)	SS	2.597	9.95E-01	9.81E-01	7.40E-02	5.00E-02	3.50E-04	1.00E-02	2.66E-07	5.00E-04	1.90E-06	2.17E-06
CHARGING SYSTEM NOZZLE FORGING	CS	0.104	9.56E-04	2.61E-06	3.46E-07	1.00E-02	3.00E-04	1.00E-02	1.04E-12	5.00E-04	1.73E-12	2.77E-12
CHARGING SYSTEM NOZZLE SAFE END	SS	0.502	1.04E-02	9.00E-05	1.75E-06	1.00E-01	3.00E-03	1.00E-02	5.25E-10	5.00E-04	8.75E-10	1.40E-09
SAFETY INJECTION SYSTEM NOZZLE FORGING	CS	0.457	1.01E-03	1.00E-06	3.75E-07	5.00E-03	1.00E-04	1.00E-02	3.75E-13	5.00E-04	1.50E-12	1.88E-12
SAFETY INJECTION NOZZLE SAFE END	SS	0.286	8.68E-03	2.61E-06	3.46E-07	5.00E-02	1.00E-03	1.00E-02	3.46E-12	5.00E-04	1.38E-11	1.73E-11
SHUTDOWN COOLING LINE (ELBOW)	SS	0.487	1.13E-02	2.00E-06	7.00E-06	5.00E-02	2.00E-04	1.00E-02	1.40E-11	5.00E-04	1.75E-10	1.88E-10

NEWER VINTAGE COMBUSTION ENGINEERING PLANT AT 60 YEARS

LOCATION	MATERIAL TYPE	USAGE FACTOR AT 60 YR (WEL)	CUMULATIVE PROB. INITIATION 60 YEARS	CUMULATIVE PROB. TWC AT 60 YR	TWC PER YEAR AT 60 YR	COND. PROB. SMALL LEAK	COND. PROB. LARGE LEAK OR BREAK	COND. PROB. CORE DAMAGE GIVEN LARGE LEAK OR BREAK	COND. PROB. CORE DAMAGE GIVEN SMALL LEAK	CORE DAMAGE FREQUENCY PER YEAR FROM LARGE BREAKS AND BREAKS	CORE DAMAGE FREQUENCY PER YEAR FROM SMALL LEAKS	CORE DAMAGE FREQUENCY PER YEAR AT 60 YEAR (TOTAL)
REACTOR VESSEL SHELL/LOWER HEAD REGION	CS	0.020	4.82E-05	1.41E-12	1.90E-13	8.00E-01	1.00E-01	1.00E-00	4.33E-04	1.80E-14	7.27E-17	1.91E-14
REACTOR VESSEL INLET NOZZLE	CS	0.712	4.41E-02	9.01E-04	7.59E-05	8.00E-03	2.00E-05	1.00E-02	8.00E-04	1.82E-11	1.90E-10	2.09E-10
REACTOR VESSEL OUTLET NOZZLE	CS	0.708	8.87E-01	2.90E-02	2.87E-03	8.00E-03	2.00E-05	1.00E-02	8.00E-04	5.15E-10	6.42E-09	6.93E-09
PRESSURIZER SURGE LINE (ELBOW)	SS	3.897	8.09E-01	9.88E-01	8.38E-02	8.00E-02	3.80E-04	1.00E-02	8.00E-04	3.28E-07	2.34E-06	2.87E-06
CHARGING SYSTEM NOZZLE FORGING	CS	0.156	3.84E-03	5.90E-05	5.08E-06	1.00E-02	3.00E-04	1.00E-02	5.00E-04	1.82E-11	2.53E-11	4.05E-11
CHARGING SYSTEM NOZZLE SAFE END	SS	0.783	6.79E-02	1.83E-03	1.19E-04	1.00E-01	3.00E-03	1.00E-02	5.00E-04	3.45E-09	5.78E-09	9.21E-09
SAFETY INJECTION SYSTEM NOZZLE FORGING	CS	0.892	4.81E-03	1.90E-06	1.99E-06	8.00E-03	1.00E-04	1.00E-02	5.00E-04	1.99E-12	6.00E-12	7.50E-12
SAFETY INJECTION NOZZLE SAFE END	SS	0.429	3.10E-02	5.90E-05	8.00E-06	8.00E-02	1.00E-03	1.00E-02	5.00E-04	8.00E-11	2.02E-10	2.53E-10
SHUTDOWN COOLING LINE (ELBOW)	SS	0.731	5.79E-02	4.83E-04	4.40E-05	8.00E-02	2.00E-04	1.00E-02	8.00E-04	8.00E-11	1.10E-09	1.19E-09

**OLDER VINTAGE COMBUSTION ENGINEERING PLANT AT 40 YEARS**

LOCATION	MATERIAL TYPE	USAGE FACTOR AT 40 YR (INEL)	CUMULATIVE PROB. INITIATION 40 YEARS	CUMULATIVE PROB. TWC AT 40 YR	TWC PER YEAR AT 40 YR	COND. PROB. SMALL LEAK	COND. PROB. LARGE LEAK OR BREAK	COND. PROB. CORE DAMAGE GIVEN LARGE LEAK OR BREAK	CORE DAMAGE FREQUENCY AT 40 YEAR FROM LARGE LEAKS AND BREAKS	COND. PROB. CORE DAMAGE GIVEN SMALL LEAK	CORE DAMAGE FREQUENCY AT 40 YEAR FROM SMALL LEAKS	CORE DAMAGE FREQUENCY PER YEAR AT 40 YEAR (TOTAL)
REACTOR VESSEL SHELL LOWER HEAD REGION	CS	0.013	2.88E-06	6.36E-16	1.07E-16	9.00E-01	1.00E-01	1.00E+00	1.07E-17	5.71E-04	5.50E-20	1.08E-17
REACTOR VESSEL INLET NOZZLE	CS	0.172	1.88E-03	4.11E-07	5.87E-06	5.00E-03	2.00E-06	1.00E-02	1.17E-14	5.00E-04	1.47E-13	1.58E-13
REACTOR VESSEL OUTLET NOZZLE	CS	0.553	5.91E-01	7.08E-02	8.98E-03	5.00E-03	2.00E-05	1.00E-02	1.80E-09	5.00E-04	2.25E-08	2.42E-08
PRESSURIZER SURGE LINE ELBOW	SS	0.541	9.38E-01	6.27E-01	4.36E-02	5.00E-02	3.50E-04	1.00E-02	1.53E-07	5.00E-04	1.00E-06	1.24E-06
CHARGING SYSTEM NOZZLE SAFE END	SS	0.582	1.18E-02	4.10E-05	8.76E-06	1.00E-01	3.00E-03	1.00E-02	2.83E-10	5.00E-04	4.38E-10	7.00E-10
SAFETY INJECTION SAFE END	SS	0.317	7.56E-03	1.40E-05	2.25E-06	8.00E-02	1.00E-03	1.00E-02	2.25E-11	5.00E-04	9.00E-11	1.13E-10
SHUTDOWN COOLING SYSTEM PIPING	SS	0.084	3.94E-02	2.10E-04	4.38E-05	5.00E-02	2.00E-04	1.00E-02	8.75E-11	5.00E-04	1.00E-09	1.18E-09

**OLDER VINTAGE COMBUSTION ENGINEERING PLANT AT 60 YEARS**

LOCATION	MATERIAL TYPE	USAGE FACTOR AT 60 YR (NEL)	CUMULATIVE PROB. INITIATION 60 YEARS	CUMULATIVE PROB. TWC AT 60 YR	TWC PER YEAR AT 60 YR	COND. PROB. SMALL LEAK	COND. PROB. LARGE LEAK OR BREAK	COND. PROB. CORE DAMAGE GIVEN LARGE LEAK OR BREAK	CORE DAMAGE FREQUENCY PER YEAR AT 60 YEAR FROM LARGE LEAKS AND BREAKS	COND. PROB. CORE DAMAGE GIVEN SMALL LEAK	CORE DAMAGE FREQUENCY PER YEAR AT 60 YEAR FROM SMALL LEAKS	CORE DAMAGE FREQUENCY PER YEAR AT 60 YEAR (TOTAL)
REACTOR VESSEL SHELL LOWER HEAD REGION	CS	0.020	1.93E-05	1.85E-13	1.85E-13	9.00E-01	1.00E-01	1.00E+00	1.95E-14	5.71E-04	9.91E-17	1.86E-14
REACTOR VESSEL INLET NOZZLE	CS	0.298	7.89E-03	1.33E-05	1.33E-05	5.00E-03	2.00E-03	1.00E-02	2.60E-12	5.06E-04	3.33E-11	3.59E-11
REACTOR VESSEL OUTLET NOZZLE	CS	0.520	5.46E-01	3.53E-01	2.27E-02	5.00E-03	2.00E-05	1.00E-02	4.54E-09	5.00E-04	5.60E-08	6.13E-08
PRESSURIZER SURGE LINE ELBOW	SS	0.992	9.87E-01	8.89E-01	5.49E-02	5.00E-02	3.50E-04	1.00E-02	1.92E-07	5.00E-04	1.37E-06	1.56E-06
CHARGING SYSTEM NOZZLE SAFE END	SS	0.843	5.31E-02	5.98E-04	5.05E-05	1.00E-01	3.00E-03	1.00E-02	1.52E-09	5.00E-04	2.53E-09	4.04E-09
SAFETY INJECTION SAFE END	SS	0.475	3.99E-02	2.00E-04	1.85E-03	5.00E-02	1.00E-03	1.00E-02	1.85E-10	5.00E-04	7.40E-10	9.25E-10
SHUTDOWN COOLING SYSTEM PIPING	SS	0.126	1.19E-01	2.36E-03	1.96E-04	5.00E-02	2.00E-04	1.00E-02	3.96E-10	5.00E-04	4.95E-09	5.35E-09

B.S.

**B&W 177 FUEL ASSEMBLY PLANT AT 40 YEARS**

LOCATION	MATERIAL TYPE	USAGE FACTOR AT 40 YR (HELI)	CUMULATIVE PROB. INITIATION 40 YEARS	CUMULATIVE PROB. TWC AT 40 YR	TWC PER YEAR AT 40 YR	COND. PROB. SMALL LEAK	COND. PROB. LARGE LEAK OR BREAK	COND. PROB. CORE DAMAGE GIVEN LARGE LEAK OR BREAK	CORE DAMAGE FREQUENCY PER YEAR AT 40 YEARS FROM LARGE LEAKS AND BREAKS	COND. PROB. CORE DAMAGE GIVEN SMALL LEAK	CORE DAMAGE FREQUENCY PER YEAR AT 40 YEARS FROM SMALL LEAKS	CORE DAMAGE FREQUENCY PER YEAR AT 40 YEARS (TOTAL)
REACTOR VESSEL LOWER HEAD	CS	0.223	8.23E-03	7.86E-06	1.04E-06	9.00E-01	1.00E-01	1.00E+00	1.04E-07	9.25E-05	8.66E-11	1.04E-07
REACTOR VESSEL OUTLET NOZZLE	CS	0.448	7.74E-01	1.88E-01	1.24E-02	6.00E-03	2.00E-06	1.00E-02	3.89E-09	6.00E-04	4.88E-08	6.28E-08
WAKEUP / HPI NOZZLE SAFE END	SS	1.961	1.20E-01	2.10E-03	6.88E-04	6.00E-02	1.00E-03	1.00E-02	6.88E-09	6.00E-04	2.38E-08	2.84E-08
DECAY HEAT REMOVAL SYSTEM PIPING (REDUCING TEE)	SS	0.630	6.72E-02	3.00E-03	4.38E-04	6.00E-02	2.00E-04	1.00E-02	8.62E-10	6.00E-04	1.08E-08	1.16E-08

**B&W 177 FUEL ASSEMBLY PLANT AT 60 YEARS**

LOCATION	MATERIAL TYPE	USAGE FACTOR AT 60 YR (NEU)	CUMULATIVE PROB. INITIATION 60 YEARS	CUMULATIVE PROB. TWC AT 60 YR	TWC PER YEAR AT 60 YR	COND. PROB. SMALL LEAK	COND. PROB. LARGE LEAK OR BREAK	COND. PROB. CORE DAMAGE GIVEN LARGE LEAK OR BREAK	CORE DAMAGE FREQUENCY PER YEAR AT 60 YEAR FROM LARGE LEAKS AND BREAKS	COND. PROB. CORE DAMAGE GIVEN SMALL LEAK	CORE DAMAGE FREQUENCY PER YEAR AT 60 YEAR FROM SMALL LEAKS	CORE DAMAGE FREQUENCY PER YEAR AT 60 YEAR (TOTAL)
REACTOR VESSEL LOWER HEAD	C8	0.335	2.80E-02	1.52E-04	1.38E-05	0.00E-01	1.00E-01	1.00E+00	1.38E-06	0.23E-05	1.13E-09	1.38E-06
REACTOR VESSEL OUTLET NOZZLE	C9	0.704	8.09E-01	8.44E-01	3.39E-02	8.00E-03	2.00E-03	1.00E-02	6.09E-09	8.00E-04	8.37E-08	8.09E-08
MAKEUP / HPI NOZZLE SAFE END	S8	1.880	4.79E-01	3.08E-02	2.22E-03	8.00E-02	1.00E-03	1.00E-02	2.22E-09	8.00E-04	8.09E-08	1.11E-07
DECAY HEAT REMOVAL SYSTEM PIPING (REDUCING TEES)	S9	0.795	2.08E-01	2.44E-02	1.79E-03	8.00E-02	2.00E-04	1.00E-02	3.57E-09	5.00E-04	4.49E-08	4.87E-08

**NEWER VINTAGE WESTINGHOUSE PLANT AT 40 YEARS**

LOCATION	MATERIAL TYPE	USAGE FACTOR AT 40 YR (INEL)	CUMULATIVE PROB. INITIATION 40 YEARS	CUMULATIVE PROB. TWC AT 40 YR	TWC PER YEAR AT 40 YR	COND. PROB. SMALL LEAK	COND. PROB. LARGE LEAK OR BREAK	COND. PROB. CORE DAMAGE GIVEN LARGE LEAK OR BREAK	CORE DAMAGE FREQUENCY PER YEAR AT 40 YEAR FROM LARGE LEAKS AND BREAKS	COND. PROB. CORE DAMAGE GIVEN SMALL LEAK	CORE DAMAGE FREQUENCY PER YEAR AT 40 YEAR FROM SMALL LEAKS	CORE DAMAGE FREQUENCY PER YEAR AT 40 YEAR (TOTAL)
REACTOR VESSEL LOWER HEAD	CS	0.018	3.21E-05	7.52E-13	1.23E-13	9.00E-01	1.00E-01	1.00E+00	1.23E-14	4.80E-04	6.31E-17	1.24E-14
REACTOR VESSEL INLET NOZZLE	CS	0.290	2.48E-03	9.17E-07	1.30E-07	5.00E-03	2.00E-05	1.00E-02	2.80E-14	5.00E-04	3.25E-13	3.51E-13
REACTOR VESSEL OUTLET NOZZLE	CS	0.658	8.62E-01	3.85E-01	3.17E-02	5.00E-03	2.00E-05	1.00E-02	6.35E-09	5.00E-04	7.94E-08	8.57E-08
CHARGING NOZZLE NOZZLE	SS	3.373	9.51E-01	8.72E-01	5.38E-02	1.00E-02	3.00E-04	1.00E-02	1.81E-07	5.00E-04	2.69E-07	4.31E-07
SAFETY INJECTION NOZZLE NOZZLE	SS	1.460	4.34E-03	5.00E-04	5.33E-05	8.00E-03	1.00E-04	1.00E-02	5.33E-11	5.00E-04	2.13E-10	2.67E-10
RESIDUAL HEAT REMOVAL PIPING (INLET TRANSITION)	SS	2.733	9.58E-01	7.80E-01	6.25E-02	5.00E-02	2.00E-04	1.00E-02	1.25E-07	5.00E-04	1.58E-08	1.60E-08

NEWER VINTAGE WESTINGHOUSE PLANT AT 60 YEARS

LOCATION	MATERIAL TYPE	USAGE FACTOR AT 60 YR (INEL)	CUMULATIVE PROB. INITIATION 60 YEARS	CUMULATIVE PROB. TWC AT 60 YR	TWC PER YEAR AT 60 YR	COND. PROB. SMALL LEAK	COND. PROB. LARGE LEAK OR BREAK	COND. PROB. CORE DAMAGE GIVEN LARGE LEAK OR BREAK	CORE DAMAGE FREQUENCY PER YEAR AT 60 YEAR FROM LARGE LEAKS AND BREAKS	COND. PROB. CORE DAMAGE GIVEN SMALL LEAK	CORE DAMAGE FREQUENCY PER YEAR AT 60 YEAR FROM SMALL LEAKS	CORE DAMAGE FREQUENCY PER YEAR (TOTAL)
REACTOR VESSEL LOWER HEAD	CS	0.027	1.71E-04	9.64E-11	1.21E-11	9.00E-01	1.00E-01	1.00E+00	1.21E-12	2.70E-02	2.94E-13	1.50E-12
REACTOR VESSEL INLET NOZZLE	CS	0.435	1.03E-02	2.94E-05	2.03E-05	5.00E-03	2.00E-03	1.00E-02	5.00E-13	8.00E-04	7.00E-12	7.64E-12
REACTOR VESSEL OUTLET NOZZLE	CS	0.897	9.49E-01	7.42E-01	4.50E-02	5.00E-03	2.00E-05	1.00E-02	9.00E-09	5.00E-04	1.13E-07	1.22E-07
CHARGING NOZZLE NOZZLE	SS	5.039	9.83E-01	9.83E-01	5.00E-02	1.00E-02	3.00E-04	1.00E-02	1.70E-07	5.00E-04	2.83E-07	4.93E-07
SAFETY INJECTION NOZZLE NOZZLE	SS	2.190	3.09E-02	1.99E-02	1.30E-03	8.00E-03	1.00E-04	1.00E-02	1.30E-09	8.00E-04	5.20E-09	6.50E-09
RESIDUAL HEAT REMOVAL PIPING (INLET TRANSITION)	SS	4.039	9.89E-01	9.80E-01	1.16E-01	5.00E-02	2.00E-04	1.00E-02	2.39E-07	5.00E-04	2.94E-08	3.17E-08

OLDER VINTAGE WESTINGHOUSE PLANT AT 40 YEARS												
LOCATION	MATERIAL TYPE	USAGE FACTOR AT 40 YR (NET)	CUMULATIVE PROB. INITIATION 40 YEARS	CUMULATIVE PROB. TWC AT 40 YR	TWC PER YEAR AT 40 YR	COND. PROB. SMALL LEAK	COND. PROB. LARGE LEAK OR BREAK	COND. PROB. CORE DAMAGE GIVEN FROM LARGE OR BREAK	COND. PROB. CORE DAMAGE PER YEAR FROM LARGE BREAKS	COND. PROB. CORE DAMAGE PER YEAR FROM SMALL LEAKS	FREQUENCY DAMAGE PER YEAR AT 40 YR	FREQUENCY DAMAGE PER YEAR (TOTAL)
REACTOR VESSEL LOWER HEAD AND SHELL	CS	0.801	1.11E-01	7.20E-07	8.12E-08	1.00E-01	1.00E-01	1.00E+00	8.12E-08	8.40E-04	8.34E-11	8.44E-09
REACTOR VESSEL WLET NOZZLE (INSIDE SURFACE)	CS	0.302	1.91E-01	4.32E-03	7.51E-04	5.00E-03	2.00E-03	1.00E-02	1.51E-10	5.00E-04	1.88E-09	2.01E-09
REACTOR VESSEL WLET NOZZLE (OUTSIDE SURFACE)	CS	0.498	6.81E-02	4.48E-04	4.75E-05	5.00E-03	2.00E-03	1.00E-02	9.50E-12	5.00E-04	1.18E-10	1.28E-10
REACTOR VESSEL OUTLET NOZZLE (INSIDE SURFACE)	CS	0.469	4.90E-01	8.13E-03	1.58E-03	5.00E-03	2.00E-03	1.00E-02	1.12E-10	5.00E-04	3.90E-09	4.21E-09
REACTOR VESSEL OUTLET NOZZLE (OUTSIDE SURFACE)	CS	0.347	1.61E-01	7.71E-03	8.89E-04	5.00E-03	2.00E-03	1.00E-02	1.40E-10	5.00E-04	1.75E-09	1.89E-09
CHARGING NOZZLE	SS	0.318	4.87E-04	3.00E-07	7.50E-08	1.00E-02	3.00E-04	1.00E-02	2.25E-13	5.00E-04	3.75E-13	8.80E-13
SAFETY INJECTION NOZZLE	SS	0.327	1.88E-03	4.00E-06	8.75E-07	8.00E-03	1.00E-04	1.00E-02	8.75E-13	5.00E-04	3.50E-12	4.31E-12
RESIDUAL HEAT REMOVAL PIPING	SS	0.206	1.24E-02	1.15E-04	1.81E-06	8.00E-02	1.00E-03	1.00E-02	1.81E-10	5.00E-04	8.50E-10	8.13E-10

**OLDER VINTAGE WESTINGHOUSE PLANT AT 60 YEARS**

LOCATION	MATERIAL TYPE	USAGE FACTOR AT 60 YR (INEL)	CUMULATIVE PROB. INITIATION 60 YEARS	CUMULATIVE PROB. TWC AT 60 YR	TWC PER YEAR AT 60 YR	COND. PROB. SMALL LEAK	COND. PROB. LARGE LEAK OR BREAK	COND. PROB. CORE DAMAGE GIVEN LARGE LEAK OR BREAK	CORE DAMAGE FREQUENCY PER YEAR FROM LARGE LEAKS AND BREAKS	COND. PROB. CORE DAMAGE GIVEN SMALL LEAK	CORE DAMAGE FREQUENCY PER YEAR AT 60 YEAR FROM SMALL LEAKS	CORE DAMAGE FREQUENCY PER YEAR AT 60 YEAR (TOTAL)
REACTOR VESSEL LOWER HEAD AND SHELL	CS	1.336	1.26E-01	1.11E-05	9.09E-07	9.00E-01	1.00E-01	1.00E+00	9.00E-06	8.40E-04	6.88E-10	9.19E-06
REACTOR VESSEL INLET NOZZLE (INSIDE SURFACE)	CS	0.458	6.44E-01	5.04E-02	3.86E-03	5.00E-03	2.00E-05	1.00E-02	7.92E-10	5.00E-04	9.90E-09	1.07E-06
REACTOR VESSEL INLET NOZZLE (OUTSIDE SURFACE)	CS	0.743	1.11E-01	3.32E-03	2.16E-04	5.00E-03	2.00E-05	1.00E-02	4.38E-11	5.00E-04	5.45E-10	5.89E-10
REACTOR VESSEL OUTLET NOZZLE (INSIDE SURFACE)	CS	0.749	7.53E-01	9.60E-02	7.54E-03	5.00E-03	2.00E-05	1.00E-02	1.51E-09	5.00E-04	1.89E-06	2.04E-06
REACTOR VESSEL OUTLET NOZZLE (OUTSIDE SURFACE)	CS	0.520	2.38E-01	3.60E-02	1.83E-03	5.00E-03	2.00E-05	1.00E-02	3.66E-10	5.00E-04	4.58E-09	4.94E-09
CHARGING NOZZLE	SS	0.479	3.78E-03	5.20E-06	6.00E-07	1.00E-02	3.00E-04	1.00E-02	1.80E-12	5.00E-04	3.00E-12	4.80E-12
SAFETY INJECTION NOZZLE	SS	0.490	1.31E-02	8.80E-05	1.05E-05	5.00E-03	1.00E-04	1.00E-02	1.05E-11	5.00E-04	4.20E-11	5.25E-11
RESIDUAL HEAT REMOVAL PIPING	SS	0.306	5.16E-02	1.14E-03	9.26E-05	5.00E-02	1.00E-03	1.00E-02	9.26E-10	5.00E-04	3.70E-09	4.63E-09

NEWER VINTAGE GENERAL ELECTRIC PLANT AT 40 YEARS

LOCATION	MATERIAL TYPE	USAGE FACTOR AT 40 YR (MEL)	CUMULATIVE PROB. INITIATION 40 YEARS	CUMULATIVE PROB. TWC AT 40 YR	TWC PER YEAR AT 40 YR	COND. PROB. SMALL LEAK	COND. PROB. LARGE LEAK OR BREAK	COND. PROB. CORE DAMAGE GIVEN LARGE LEAK OR BREAK	CORE DAMAGE FREQUENCY PER YEAR AT 40 YEAR FROM LARGE LEAKS AND BREAKS	COND. PROB. CORE DAMAGE GIVEN SMALL LEAK	CORE DAMAGE FREQUENCY PER YEAR AT 40 YEAR FROM SMALL LEAKS	CORE DAMAGE FREQUENCY PER YEAR AT 40 YEAR (TOTAL)
REACTOR VESSEL LOWER HEAD CRUMI PENETRATION WELDS	CS	0.029	7.28E-05	7.28E-12	1.25E-12	9.00E-01	1.00E-01	1.00E+00	1.25E-13	1.00E-06	1.13E-16	1.25E-13
REACTOR VESSEL FEEDWATER NOZZLE SAFE END	CS	1.881	1.04E-01	1.31E-03	2.39E-04	5.00E-02	2.00E-04	5.00E-04	2.39E-11	1.00E-06	1.19E-11	2.57E-11
RECHIRCULATION SYSTEM PIPING (TEE)	SS	0.830	4.23E-02	4.89E-04	7.13E-05	5.00E-02	2.00E-04	5.00E-04	7.13E-12	1.00E-06	3.56E-12	1.07E-11
CORE SPRAY NOZZLE SAFE END EXTENSION	Ni-Cr-Fe	0.438	3.83E-04	1.45E-07	1.97E-06	5.00E-02	5.00E-04	5.00E-04	5.91E-15	1.00E-06	1.18E-15	7.09E-15
FEEDWATER LINE PIPING (ELBOW)	CS	3.088	1.59E-01	1.01E-03	1.69E-04	5.00E-02	2.00E-04	5.00E-04	1.69E-11	1.00E-06	8.45E-12	2.54E-11
RESIDUAL HEAT REMOVAL SUCTION PIPING (STRAIGHT PIPE)	CS	11.250	4.73E-01	4.10E-01	1.55E-02	5.00E-02	3.50E-04	5.00E-04	2.35E-09	1.00E-06	6.75E-10	3.04E-09

**NEWER VINTAGE GENERAL ELECTRIC PLANT AT 60 YEARS**

LOCATION	MATERIAL TYPE	USAGE FACTOR AT 60 YR (INEL)	CUMULATIVE PROB. INITIATION 60 YEARS	CUMULATIVE PROB. TWC AT 60 YR	TWC PER YEAR AT 60 YR	COND. PROB. SMALL LEAK	COND. PROB. LARGE LEAK OR BREAK	COND. PROB. CORE DAMAGE GIVEN LARGE LEAK OR BREAK	CORE DAMAGE FREQUENCY PER YEAR AT 60 YEAR FROM LARGE LEAKS AND BREAKS	COND. PROB. CORE DAMAGE GIVEN SMALL LEAK	CORE DAMAGE FREQUENCY PER YEAR AT 60 YEAR FROM SMALL LEAKS	CORE DAMAGE FREQUENCY PER YEAR AT 60 YEAR (TOTAL)
REACTOR VESSEL LOWER HEAD CRDM PENETRATION WELDS	CS	0.943	3.49E-04	6.02E-10	6.20E-11	9.00E-01	1.00E-01	1.00E+00	8.26E-12	1.00E-06	7.43E-17	8.26E-12
REACTOR VESSEL FEEDWATER NOZZLE SAFE END	CS	2.817	2.83E-01	1.47E-02	1.23E-03	5.00E-02	2.00E-04	5.00E-04	1.23E-10	1.00E-06	6.14E-11	1.94E-10
RECIRCULATION SYSTEM PIPING (TEE)	SS	1.254	1.39E-01	4.07E-03	3.66E-04	5.00E-02	2.00E-04	5.00E-04	3.66E-11	1.00E-06	1.83E-11	5.49E-11
CORE SPRAY NOZZLE SAFE END EXTENSION	Ni-Cr-Fe	0.858	1.27E-03	3.25E-06	3.04E-07	5.00E-02	5.00E-04	5.00E-04	9.12E-14	1.00E-06	1.92E-14	1.09E-13
FEEDWATER LINE PIPING (ELBOW)	CS	5.540	3.85E-01	1.40E-02	1.35E-03	5.00E-02	2.00E-04	5.00E-04	1.35E-10	1.00E-06	6.76E-11	2.03E-10
RESIDUAL HEAT REMOVAL SUCTION PIPING (STRAIGHT PIPE)	CS	16.896	6.71E-01	6.21E-01	2.25E-02	5.00E-02	3.50E-04	5.00E-04	3.94E-09	1.00E-06	1.13E-09	5.06E-09

B.13

**OLDER VINTAGE GENERAL ELECTRIC PLANT AT 40 YEARS**

LOCATION	MATERIAL TYPE	USAGE FACTOR AT 40 YR (INEL)	CUMULATIVE PROB. INITIATION 40 YEARS	CUMULATIVE PROB. TWC AT 40 YR	TWC PER YEAR AT 40 YR	COND. PROB. SMALL LEAK	COND. PROB. LARGE LEAK OR BREAK	COND. PROB. CORE DAMAGE GIVEN LARGE LEAK OR BREAK	CORE DAMAGE FREQUENCY PER YEAR AT 40 YEAR FROM LARGE LEAKS AND BREAKS	COND. PROB. CORE DAMAGE GIVEN SMALL LEAK	CORE DAMAGE FREQUENCY PER YEAR AT 40 YEAR FROM SMALL LEAKS	CORE DAMAGE FREQUENCY PER YEAR AT 40 YEAR (TOTAL)
REACTOR VESSEL SHELL AND LOWER H	CS	0.070	2.71E-10	0.00E+00	0.00E+00	0.00E-01	1.00E-01	1.00E+00	0.00E+00	1.00E-00	0.00E+00	0.00E+00
REACTOR VESSEL FEEDWATER NOZZLE (BORE)	CS	3.160	7.27E-02	1.00E-05	2.50E-04	5.00E-03	2.00E-03	5.00E-04	2.50E-14	1.00E-00	1.25E-14	3.75E-14
RECIRCULATION SYSTEM PIPING (RHR RETURN TEE)	SS	3.000	0.43E-01	7.12E-01	7.20E-02	5.00E-02	2.00E-04	5.00E-04	7.20E-09	1.00E-00	3.60E-09	1.00E-00
CORE SPRAY NOZZLE	CS	0.520	1.41E-04	1.01E-04	2.85E-00	5.00E-03	3.50E-05	5.00E-04	4.90E-17	1.00E-00	1.43E-17	6.41E-17
CORE SPRAY NOZZLE SAFE END	SS	1.772	3.33E-01	1.44E-02	2.08E-03	5.00E-02	3.50E-04	5.00E-04	3.84E-10	1.00E-00	1.04E-10	4.88E-10
RESIDUAL HEAT REMOVAL SYSTEM PIPING (TAPER TRANSITION)	SS	0.470	1.47E-03	0.21E-05	1.07E-05	5.00E-02	2.00E-04	5.00E-04	1.07E-12	1.00E-00	5.35E-13	1.01E-12
FEEDWATER LINE PIPING (TEE)	CS	0.900	3.84E-01	2.90E-03	0.94E-04	5.00E-02	2.00E-04	5.00E-04	6.94E-11	1.00E-00	3.44E-11	1.04E-10

B.14

**OLDER VINTAGE GENERAL ELECTRIC PLANT AT 60 YEARS**

LOCATION	MATERIAL TYPE	USAGE FACTOR AT 60 YR (MEL)	CUMULATIVE PROB. INITIATION 60 YEARS	CUMULATIVE PROB. TWC AT 60 YR	TWC PER YEAR AT 60 YR	COND. PROB. SMALL LEAK	COND. PROB. LARGE LEAK OR BREAK	COND. PROB. CORE DAMAGE GIVEN LARGE LEAK OR BREAK	CORE DAMAGE FREQUENCY AT 60 YEAR FROM LARGE LEAKS AND BREAKS	COND. PROB. CORE DAMAGE GIVEN SMALL LEAK	CORE DAMAGE FREQUENCY AT 60 YEAR FROM SMALL LEAKS	CORE DAMAGE FREQUENCY PER YEAR AT 60 YEAR (TOTAL)
REACTOR VESSEL SHELL AND LOWER H	CS	0.116	2.79E-09	0.00E+00	0.00E+00	0.00E-01	1.00E-01	1.00E+00	0.00E+00	1.00E-06	0.00E+00	0.00E+00
REACTOR VESSEL FEEDWATER NOZZLE (BORE)	CS	4.780	2.42E-01	8.89E-04	9.78E-06	6.00E-03	2.00E-05	6.00E-04	9.78E-13	1.00E-06	4.88E-13	1.48E-12
RECIRCULATION SYSTEM PIPING (RHR RETURN TEE)	SS	5.843	9.89E-01	9.88E-01	1.23E-01	6.00E-02	2.00E-04	6.00E-04	1.23E-06	1.00E-06	6.13E-09	1.84E-08
CORE SPRAY NOZZLE	CS	0.780	7.89E-04	8.84E-07	9.51E-06	6.00E-03	3.50E-06	6.00E-04	1.66E-16	1.00E-06	4.78E-16	2.14E-15
CORE SPRAY NOZZLE SAFE END	SS	2.838	7.84E-01	1.19E-01	8.04E-03	6.00E-02	3.80E-04	6.00E-04	1.41E-09	1.00E-06	4.02E-10	1.81E-09
RESIDUAL HEAT REMOVAL SYSTEM PIPING (TAPER TRANSITION)	SS	0.717	7.89E-03	1.82E-03	7.82E-05	6.00E-02	2.00E-04	6.00E-04	7.82E-12	1.00E-06	3.91E-12	1.17E-11
FEEDWATER LINE PIPING (TEE)	CS	10.475	7.82E-01	6.82E-02	6.54E-03	6.00E-02	2.00E-04	6.00E-04	6.54E-10	1.00E-06	2.77E-10	8.30E-10

## Appendix C

### pcPRAISE 4.2: Expanded Capabilities to Analyze Fatigue Crack Initiation

#### C.1 Introduction

This appendix describes modifications to pcPRAISE to provide capabilities for probabilistic analysis of fatigue-crack initiation and growth. This expanded version of the software is referred to as Version 4.2. The PRAISE code was originally developed to provide a probabilistic treatment of the growth of crack-like weld defects in piping due to cyclic loading (Harris et al. 1981; Lim 1981). This treatment of fatigue-crack growth was later expanded to include the initiation and growth of stress corrosion cracks (Harris et al. 1986). The software was then made to run on a personal computer for ease and economy of use (Harris et al. 1992). The purpose of the efforts reported herein is to expand the capabilities of PRAISE to include a probabilistic treatment of fatigue-crack initiation. The current capabilities for analyzing fatigue-crack growth are then used to continue the calculations to crack penetration of the pipe wall.

The expanded capabilities are based to a large extent on the results of data analyses performed by Argonne National Laboratory (ANL) personnel on the results of fatigue tests of pressure boundary materials in light-water reactor (LWR) environments (Keisler et al. 1995; Keisler and Chopra 1995; Keisler et al. 1996). They provide relations giving the probability of crack initiation as a function of the number of cycles for a given cyclic stress. The influence of the strain rate, sulfur content, oxygen content of the reactor water, and the temperature are considered. Some adjustments to the ANL relations were made by Pacific Northwest National Laboratory (PNNL) personnel based on discussions with ANL. A FORTRAN subroutine was provided to Engineering Mechanics Technology, Inc. (EMT) by PNNL that defines the strain life curve for a given probability of crack initiation and for a given temperature, strain rate, oxygen content, and sulfur content. This subroutine was used by EMT as a starting point in the current efforts.

#### C.2 Crack Initiation Correlations

The ANL crack initiation correlations were for cycles for the tensile load to drop by 25%. This corresponds to a crack of approximately 3 mm depth (0.12 in.) (Keisler et al. 1995; Keisler et al. 1996). The specimen size was assumed to be about 2-in. (51.76-mm) gauge length. The fatigue tests were performed under fully reversed loading (i.e., a mean load of zero). The subroutine provided by PNNL already had size-effect and surface-finish adjustments, but a single factor was considered to account for size regardless of size. The subroutine provides cycles to initiation for a given probability of initiation and set of conditions (material, cyclic stress, strain rate, oxygen level, and sulfur content). The relations

“should not be extrapolated beyond a probability of 0.02%” (Keisler et al. 1995; Keisler et al. 1996); hence, they are not suitable for initiation probabilities below about  $2 \times 10^{-4}$ .

### C.3 PRAISE Modifications to Consider Fatigue-Crack Initiation

Modifications were made to pcPRAISE to consider the initiation of cracks and their subsequent growth to become through-wall. For initiation, the PNNL subroutine for initiation was used in conjunction with Monte Carlo simulation to estimate the probability of initiation as a function of time. The subroutine provides results for a constant stress amplitude, whereas the stress histories to be considered, have cyclic stresses of different amplitudes. The Miner’s rule was used to account for these more complex stress histories. The stress history is typically defined in terms shown in Table C.1.

The cycles per year (third column) is equal to the cycles per 40-year life divided by 40; that is, the cycling rate is considered to be constant. A description of each transient is usually provided. The fatigue damage as a function of time is expressed as

$$D(t) = \sum_{j=1}^M \frac{n_j t}{N_1(\sigma_{a,j})} = t \sum_{j=1}^M \frac{n_j}{N_1(\sigma_{a,j})} = t \dot{D} \quad (C.1)$$

where  $N_1(\sigma_{a,j})$  is the cycles to initiation for the cyclic stress,  $\sigma_{a,j}$ , and is a random variable. The time to initiation,  $t_i$ , is the time for  $D$  to reach the value of unity. Hence,  $t_i$  is equal to  $1/\dot{D}$ . The Monte Carlo simulation consists of

1. sampling from a uniform unit variate,
2. calculating the cycles to initiation for this quantile for each cyclic stress (from the PNNL subroutine)
3. calculating  $t_i = 1/\dot{D}$ .

This provides a histogram of  $t_i$ , from which the probability of crack initiation as a function of time follows.

ID	Stress Amplitude	Cycles Per 40-Year Life	Cycles Per Year
1	$\sigma_{a,1}$	$n_1$	$\dot{n}_1$
2	$\sigma_{a,2}$	$n_2$	$\dot{n}_2$
--	--	--	
M	$\sigma_{a,M}$	$n_M$	$\dot{n}_M$

This procedure provides the initiation probability for a single "specimen." In order to account for different sizes of components, as well as for stress variations along the surface for a given component, the component is divided into "specimens" of a given unit length. This length was selected to be 2 in. (50.76 mm), but this is under the control of the user. pcPRAISE considers circumferential cracks in pipes. The pipe thickness and inside radius are specified, which defines the inside circumference. The user specifies the number of initiation sites, and the software takes the length of the "specimens" to be the inner circumference divided by the number of specimens. When analyzing cracks in components other than girth welds in pipes, the length of the component to be considered is  $2\pi R_i$ , and the appropriate length is obtained by using the corresponding  $R_i$  and the number of initiation sites ("specimens"). (Care must be taken that the specified  $R_i$  and pressure do not lead to inappropriate pressure stresses.)

Since multiple initiation sites are employed, some adjustment should be made to the size/surface finish compensations made by ANL. A portion of the size/surface finish effect introduced by ANL is removed by multiplying each sampled initiation time by a constant between 1 (using the ANL size/surface finish factor) and 4 (using the ANL laboratory specimen correlations). The value of this adjustment factor is discussed in Section C.6. The distribution of initiation time is determined for each of the specimens in a component. The initiation times in each specimen can either be independent or dependent. If dependent and no stress gradient, then each specimen will initiate a crack at the same time. This results in initiated cracks being as long as the component, such as completely around the circumference for a girth weld in a pipe. This leads to all leaks being double-ended pipe breaks. Hence, independent initiation is believed to be the most realistic.

## C.4 PRAISE Modifications for Crack Growth

Once a crack initiates, pcPRAISE calculates its subsequent growth.

### C.4.1 Initiated Crack Size

As discussed above, an initiated crack is considered to be 3 mm (0.12 in.) deep. It is still necessary to specify the surface length,  $2b_o$ , of the initiated crack. Although cracks that grow from a small defect will tend to be nearly semi-circular ( $b_o/a_o \sim 1$ ), the median length of an initiated crack is taken to be 7.6 mm (0.3 in.). This is believed to be conservative. The initial length is taken to be a random variable. The value of  $b_o$  itself could be the random variable, and this is one alternative that was considered.

Taking  $b_o$  to be lognormal with a median value of 7.6 mm (0.30 in.), it is then only necessary to define the shape parameter,  $\mu$ , in order to define the complete distribution. A couple of items of interest in the distribution of  $b_o$  are (1) the probability that  $b/a$  at initiation is less than 1, which is physically unrealistic because the crack would then be tunneling into the specimen. The other item of interest is (2) the probability that  $2b_o$  would be greater than the "specimen" size of 50.76 mm (2 in.). Table C.2 summarizes these items of interest as a function of  $\mu$ .

$\mu$	$P(b_o > 1 \text{ in.})(25.38 \text{ mm})$	$P(b_o > 2a_o)$	$P(b_o < a_o)$	cov
1	0.114	0.59	0.18	1.31
0.518	$10^{-2}$	0.67	0.038	0.555
0.500	$8 \times 10^{-3}$	0.67	0.033	0.533
0.390	$10^{-3}$	0.72	0.009	0.405
0.324	$10^{-4}$	0.75	0.002	0.333

When  $\mu=1$ , the probability of having  $b_o < a_o$  is quite high, and the probability of having a crack longer than the specimen length is also high. Hence, a value of  $\mu$  of 1 does not look realistic. As  $\mu$  is decreased, both of these probabilities decrease. When one crack in 100 has a  $2b_o > 2$ , the probability that  $b_o < a_o$  decreases to 0.038—which seems to be a reasonable value. The problem remains, however, that it is not possible to control both  $P(b_o > 1 \text{ in. } [25.38 \text{ mm}])$  and  $P(b_o < a_o)$  with only  $\mu$  to vary.

Another way to treat the problem is to take  $(b_o - a_o)$  to be lognormally distributed. This would guarantee that  $b_o$  is greater than  $a_o$ .  $P(b_o > 1)$  can then be any number desired, depending on the value of  $m$ . Fixing the median  $b_o$  at 0.3 in. (7.6 mm), Table C.3 summarizes the influence of  $m$  on some characteristics of the distribution of  $b_o$ .

It appears that either of the above approaches is reasonable. If  $b_o$  is considered with  $P(b_o > 1) = 0.01$ , then  $\mu = 0.518$ . If  $(b_o - a_o)$  is used with  $P(b_o > 1) = 0.01$ , then  $\mu = 0.682$ . The selection of the random variable is discussed along with an example problem in Section C6.1.

#### C.4.2 Linking of Multiple Cracks

Multiple cracks can initiate in a component and then grow to perhaps eventually coalesce. The criteria for linking of multiple cracks are already in pcPRAISE to account for multiple initiations of stress corrosion cracks (Harris et al. 1986; Harris et al. 1992). The criteria are based on procedures in the

$\mu$	$P(b_o > 1 \text{ in.})(25.38 \text{ mm})$	$P(b_o > 2a_o)$	cov
1	$5.6 \times 10^{-2}$	0.657	1.31
0.682	$10^{-2}$	0.724	0.77
0.514	$10^{-3}$	0.785	0.55

American Society of Mechanical Engineers (ASME) Boiler and Pressure Vessel Code in use at the time that Reference 3 NUREG/CR-4792, Vol. 3 (Harris et al. 1986) was prepared. Section 3.3 of NUREG/CR-5684 (Harris et al. 1992) discusses the linking procedures.

### C.4.3 Correlations Between Initiation and Growth Properties

It is conceivable that there is a correlation between the initiation and growth properties of the material. That is, if the crack-initiation characteristics are poor, then the growth characteristics are also poor. pcPRAISE provides for treating these properties as either independent or correlated. If they are correlated, then the one minus the sampled random number used for the initiation simulations is used for the growth relation. (The "one minus" is used because a low quantile is poor for initiation, but good for growth). Physically, there does not seem to be a reason for the properties to be correlated, and all examples in this report take them to be independent.

### C.4.4 Modification of Fatigue Crack Growth Relations for Ferritic Material

The fatigue-crack-growth characteristics for ferritic steels that are built into pcPRAISE are for LWR environments. They are discussed in Section 4.2.2 of Reference 4 NUREG/CR-5684 (Harris et al. 1992). At very high values of  $\Delta K$ , the crack growth relation falls below the air line for this material, which is physically unrealistic. For median properties, this occurs at a  $\Delta K$  of about 100 ksi-in.<sup>1/2</sup> and a  $da/dN$  of about  $10^{-3}$  in. per cycle. For ferritic steel in air, the crack growth rate is given by

$$\frac{da}{dN} = CAK^{3.726} \quad (C.2)$$

The exponent 3.726 comes from the ASME Boiler and Pressure Vessel Code. No effect of R is considered for growth in air. C for the ASME air line is  $2.67 \times 10^{-11}$ , which is an upper-bound value. Consider C to be lognormally distributed with the ASME value being at the 95<sup>th</sup> percentile. The scatter in air will be less than in water. Therefore, the shape parameter, m, will be less than for values for water. Taking  $\mu$  to be the smallest value used in the treatment in pcPRAISE for water provides a value of 0.542. Once  $\mu$  is fixed, the median value of C can be evaluated, which leads to  $C_{50} = 1.10 \times 10^{-11}$ .

To analyze fatigue crack growth in ferritic materials in water, a sample is drawn for the fatigue crack growth rate in water. The same random number is used to sample the fatigue crack growth rate in air. The crack growth rate is then taken to be the largest of the two. The water value will be the largest until  $\Delta K$  exceeds about 100 ksi-in.<sup>1/2</sup>

### C.5 Definition of Stresses

Information on the stress histories is often in the form summarized in Table C.1, which is simply the stresses at the high-stress point, which is generally on the surface. This is sufficient for the calculations of crack initiation, but much more information is required for the crack growth calculations. There can be strong stress gradients through the component thickness as well as along the surface. The stresses,

such as summarized in Table C.1, could be assumed to be uniform everywhere, which would be overly conservative and would lead to unrealistic results. Hence, it is desired to account for stress gradients in the crack-growth analysis.

### C.5.1 Through-Wall Stress Gradients

The stresses, such as summarized in Table C.1, include contributions from many factors, including pressure, deadweight, restraint of thermal expansion, seismic events, and thermal transients, as well as geometric stress concentrations such as can occur near nozzles. In the absence of geometric stress concentrations, none of the stress contributors will have through-wall gradients, except for the thermal transients. The ASME Boiler and Pressure Vessel Code prescribes limits on the stresses, except for thermal transient stresses (which are often referred to as radial gradient stresses). In the absence of geometric stress concentrations, large stresses in the cyclic stress history will always be of the radial gradient type. Such large stresses are often present in the stress histories of the components and are major contributors to fatigue crack initiation. Hence, some generic radial gradient of stresses is of use in definition of stresses to be used in the fatigue crack growth analysis.

A general radial stress gradient can be developed from the example problem of a pipe with an inside wall temperature that is linearly varying with time at the rate  $\dot{T}$ . The outside surface of the pipe is taken to be insulated. The pipe is treated as a slab of thickness  $h$ . For a pipe initially at a uniform temperature, with the ramp temperature change starting at  $t=0$ , the temperature after a short transient is given by the following expression (see for instance, Carslaw and Jaeger 1959).

$$T(\xi, t) = \dot{T}t - \frac{\dot{T}h^2}{\kappa} \left[ \xi \left( 1 - \frac{\xi}{2} \right) \right] \quad (C.3)$$

where  $\xi=x/h$ ,  $h$  is the wall thickness, and  $\kappa$  is the thermal diffusivity. The radial gradient thermal stresses can be obtained from the temperature field by integration using expressions in Timoshenko and Goodier (1951). Taking  $h \ll R$ , the axial stress is obtained as

$$\sigma(\xi) = \sigma_G \left( 1 - 3\xi + \frac{3}{2}\xi^2 \right) \quad (C.4)$$

The term  $\sigma_G$  is the maximum radial gradient thermal stress, which occurs at the inside surface. The term  $\sigma(\xi)$  in Equation C.4 is self-equilibrating through the wall thickness.

The stress gradient in Equation C.4 can also be obtained as the only second-order polynomial that is self-equilibrating through the thickness and meets the requirements for an insulated outside surface. This gradient also provides a close approximation to the stress intensity factors obtained by the use of TIFFANY (Dedhia et al. 1982) for a step change in temperature, when the value of  $\sigma_G$  is obtained from TIFFANY itself. Hence, the gradient of Equation C.4 provides very accurate results for a linear temperature variation and a good approximation for a step temperature change of the coolant. The value of  $\sigma_G$  comes from the specified stresses.

The pcPRAISE code was modified so that the cyclic stresses, such as obtained from Table C.1, can be decomposed into a uniform, linear and general gradient [Eq. 4]. If other gradients are desired, it is necessary for the user to supply a table of stress-intensity factors as a function of crack size. This can be accomplished by using TIFFANY.

### C.5.2 Surface-Stress Gradients

Gradients along the surface can be present in addition to the through-thickness gradient discussed above. This can be especially important near geometric discontinuities such as nozzles. Even if only pressure is present, through-thickness gradients can be significant. Cohen (1977) provides some information on stress gradients near nozzles in a BWR pressure vessel. This information is used here to estimate through-wall gradients. Table C.4, which is a portion of Table 1 of Cohen 1977 provides the pressure-induced stress in the nozzle region at the location of peak stress at the surface.

The thickness (h) of 9.22 in. (234 mm) is the distance along a diagonal line originating at the high-stress point and going from the inside surface to the outside surface. Since it is along a diagonal, it is greater than the conventional measure of the thickness. For a given point on the surface (a given y), these results are plotted as a function of the dimensionless distance into the thickness, x/h, in Figure C.1. The smooth solid line is a fit to the results that is a combination of uniform tension and the generalized radial gradient for thermal stresses given in Equation C.4. The smooth solid line is a plot of

$$\frac{\sigma(\xi)}{\sigma(0)} = \frac{2}{3} + \frac{1}{3} \left( 1 - 3\xi + \frac{3}{2}\xi^2 \right) \quad (C.5)$$

which is 2/3 tension and 1/3 general gradient. This is seen to provide a good fit the data of Table C.4, except for one case. This case is for y=10.3, which are the lowest stresses in the table. For the higher stresses, the fit is good. The 2/3 tension and 1/3 gradient fit to the nozzle stresses is convenient because it uses stress variations that have already been included in the initiation version of pcPRAISE.

Distance Along Surface, y, in.	Distance into Thickness, x, in.					
	0.0	0.46	1.28	2.98	4.44	9.22
0.00	55.0	51.2	45.4	35.0	30.7	25.8
1.04	48.1	47.9	44.5	33.7	29.7	25.5
1.70	45.2	45.5	43.2	32.6	28.5	24.0
2.98	41.8	40.8	36.7	27.9	23.8	21.6
4.44	36.3	35.2	30.9	21.8	20.4	18.7
10.3	14.4	14.0	12.0	6.28	1.76	3.63

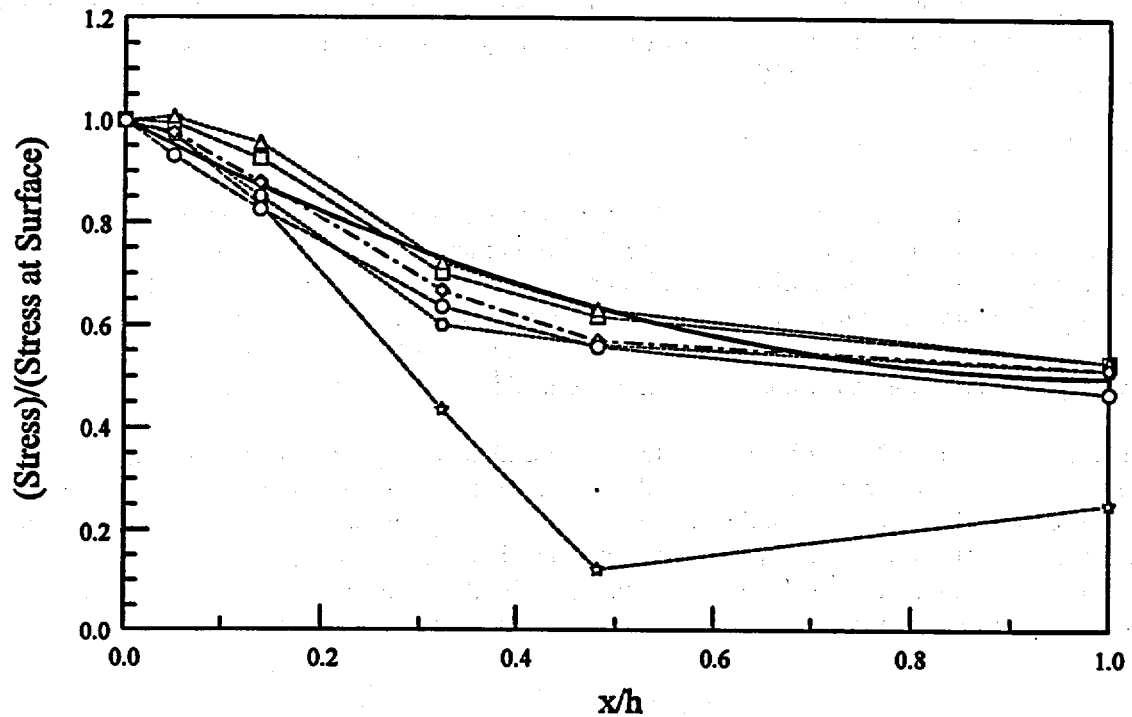


**Figure C.1 Normalized Stresses Near a Nozzle Versus Dimensionless Distance Through the Thickness**

The other question is the variation of stress along the surface away from the high-stress point. Figure C.2 provides such results and shows that the high stresses are localized. They drop to about 1/3 the peak in one thickness. The decrease in stress is approximately linear.

### C.5.3 Definition of Stresses in pcPRAISE

The inputs to a crack initiation and growth analysis by using pcPRAISE are usually in the form as summarized in Table C.1. At a given location in the component (usually the point of highest stress), through-wall gradients must be defined in terms of a uniform tension (T), through-wall bending (B), general gradient (G), or user-defined (UD). These all add up to two times the specified stress amplitude. (pcPRAISE uses stress range, max-min, rather than stress amplitude). The surface stress gradient is then defined by specifying a multiplier on the stresses for each "specimen."

The results of Table C.1 will then look like those indicated by the format of Table C.5. In each line of this table,  $T+B+G+UD=\Delta\sigma$ . The variation along the surface is specified by defining a multiplier for each specimen. For a component of length 2M inches, such as the circumference of a pipe, a set of M multipliers is specified. Note that all of the stresses (T,B,G,UD) are scaled by this multiplier.

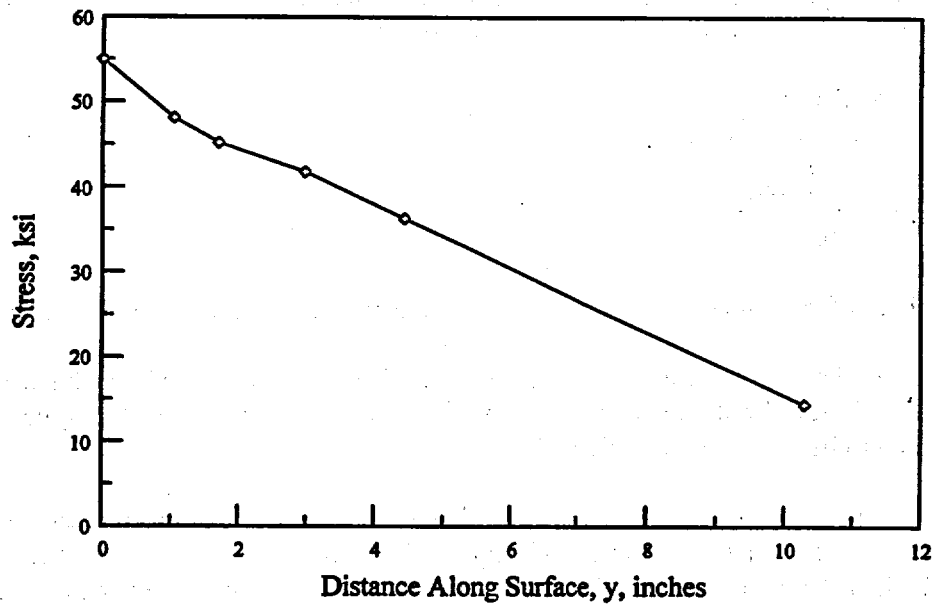


Figure C.2 Variation of Stresses Along the Surface as a Function of Distance from the Point of Maximum Stress

**Table C.5 Format of Table for Typical Definition of Stress History for Fatigue-Crack-Growth Analysis**

ID	Stress Amplitude	Stress Range, $\Delta\sigma$	Cycles Per Year	Tension, T	Bending, B	General Gradient, G	User Defined, UD
1	$\sigma_{a,1}$	$2 \sigma_{a,1}$	$\dot{n}_1$	--	--	--	--
2	$\sigma_{a,2}$	$2 \sigma_{a,2}$	$\dot{n}_2$	--	--	--	--
--	--	--	--	--	--	--	--
M	$\sigma_{a,M}$	$2 \sigma_{a,M}$	$\dot{n}_M$	--	--	--	--

## C.6 Example Problems

Example problems were run as the pcPRAISE developments were underway to provide guidance in the developments.

### C.6.1 Preliminary Examples

A series of example runs were made to study the influence of various factors on the predicted leak and double-ended pipe break (DEPB) probabilities. A representative example problem was selected from a

set of components provided to EMT by PNNL. The example is based on the makeup/HPI nozzle safe end for a B&W plant. The following information was provided:

thickness = 0.75 in.  
 sulfur content = 0.015 wt%  
 oxygen level = 0  
 strain rate = 0.004%/sec  
 304 stainless steel

The stress history for the makeup/HPI nozzle was taken to be representative and is given by Table C.6.

The heat up/cool down stress is explicitly given. There is no seismic stress in the history. All of the stress above the heat up/cool down is therefore taken to be of the thermal gradient type. The cyclic stress history is taken to be as shown in Table C.7.

To define the number of initiation sites, the pipe diameter is needed. For this representative example problem, the outside diameter was taken to be 9 in. (22.86 cm). The pressure was taken to be 2250 psi, which results in a pressure stress of 5.11 ksi. The deadweight stress was taken to be zero, so the pressure provided the only primary stress. A detectable leak was taken to be 5 gpm, and a big leak was taken to be 100 gpm. The half-lengths of through-wall cracks that result in these leak rates with the specified stresses was computed with pcPRAISE to be 1.49 in. (3.78 cm) and 3.78 in. (9.6 cm), respectively. These were used as inputs to pcPRAISE.

$\sigma_s$ , ksi	Cycles/40 Years	Name of Transient
221.24	33	HPI actuation, A/B
169.31	7	test/null
11.98	200	heat up/cool down

$\Delta\sigma$ , ksi	Cycles/40 Years	Tension, T, ksi	Gradient, G, ksi
442.48	33	23.96	418.52
338.62	7	23.96	314.66
23.96	200	23.96	0

Seven separate cases were considered, as summarized in Table C.8. The Case 2a was run outside pcPRAISE using Monte Carlo with the initiation probability subroutine supplied by PNNL in conjunction with a deterministic SmartCrack run. SmartCrack is a deterministic fracture mechanics software developed by EMT that gives the same deterministic fatigue lifetime as pcPRAISE for the same problem. One deterministic SmartCrack run was made using the median value of C for austenitic stainless steel. The statistical distribution of the growth part of the lifetime is then approximately lognormally distributed with a median value as obtained from the SmartCrack run and the same m as for austenitic stainless steel because C is the dominant random variable for the growth part of the analysis.

The initiation and growth probabilities were then combined to give the probability of a through-wall crack by convolution integration in MATHCAD. The good agreement between Cases 2 and 2a provides a good check on pcPRAISE. All runs were made with a median half-crack length at an initiation of 0.30 in. (0.76 cm). All of the pcPRAISE runs in Table C.8 were made with 107 trials. The critical net section stress failure criterion was used for the double-ended pipe break computations. The flow stress was taken to be normally distributed with a mean of 43 ksi and a standard deviation of 4.2 ksi. The initiation and growth characteristics were taken to be independent, except for Case 5).

The base case is Case 2. Case 1 is the same as 2, but with a uniform stress. A comparison of Cases 1 and 2 shows the large conservatism associated with the assumption of uniform stress. Case 3 considers a random value of  $b_0$  (half-crack length at initiation). A comparison of Case 3 with 2 shows that considering  $b_0$  to be random does not strongly influence the leak probabilities, but does have a large effect on the big leak and DEPB probabilities. Hence, the distribution of  $b_0$  is important in leak-before-break considerations.

Case 4 has multiple independent initiation sites (12) to account for components larger than specimens. The multiple initiation sites greatly increase all of the probabilities. A comparison with Case 3 shows that the initiation and leak results for 1 site and 12 sites are approximately related by the equation  $P_{12} = 1 - (1 - P_1)^{12}$ . (For small probabilities, this is approximately  $P_{12} \sim 12P_1$ .) The influence of multiple initiation sites on the big leak and DEPB results is stronger than this; the ratio of the DEPB results at 60 years is 155, which is much larger than 12.

Case 5 is the same as Case 4, but with the initiations all correlated. This means that all sites initiate cracks at the same time (See Section 4.3). Hence, the initiation probabilities are nearly the same as for one initiation site (Cases 1-3), but the big leak and DEPB probabilities are much higher than for one initiation site. The leak, big leak, and DEPB probabilities are all very nearly equal. This is because all cracks initiate at the same time, so once one initiates, there are cracks all the way around the pipe. With no circumferential variation, this means that, once these cracks link, any leak is also a DEPB. This is not reasonable; the DEPB probabilities are way too high. Correlated initiation times are therefore not recommended for use.

In Case 6, all the sampled initiation times are multiplied by 4 to remove the factor introduced by ANL to account for component size, or 2 (Case 6a) to partially account for size effects. Component size is considered here by use of multiple initiation sites. Comparison with Case 4 shows that this greatly reduces all of the failure probabilities, with the multiplier of 4 having a larger effect than 2. A comparison of Case 6a with 3 shows that 12 initiation sites with a multiplier of 2 provides nearly the same results as one initiation site with the ANL correlation. Hence, a multiplier of 2 is suggested for future use.

Table C.8 Example Problem Runs

							Cumulative Probabilities at 40 Years				Cumulative Probabilities at 60 Years			
#	Init. Sites	$\mu$	$t_i$	$t_i$ ind. or corr.	Stress	Circ. Var.	Initiation	Through Wall	Big Leak	DEPB	Initiation	Through Wall	Big Leak	DEPB
1	1	0	1	--	all T	--	$3.30 \times 10^{-1}$	$2.23 \times 10^{-1}$	$<10^{-7}$	$<10^{-7}$	$5.95 \times 10^{-1}$	$4.85 \times 10^{-1}$	$<10^{-7}$	$<10^{-7}$
2	1	0	1	--	T,G	--	$3.30 \times 10^{-1}$	$8.98 \times 10^{-2}$	$<10^{-7}$	$<10^{-7}$	$5.95 \times 10^{-1}$	$4.94 \times 10^{-2}$	$2 \times 10^{-7}$	$<10^{-7}$
2a	1	0	1	--	T,G	--	$3.49 \times 10^{-1}$	$1.01 \times 10^{-2}$	--	--	$6.04 \times 10^{-1}$	$5.32 \times 10^{-2}$	--	--
3	1	1	1	--	T,G	--	$3.30 \times 10^{-1}$	$1.29 \times 10^{-2}$	$8.12 \times 10^{-4}$	$4.55 \times 10^{-5}$	$5.95 \times 10^{-1}$	$6.19 \times 10^{-2}$	$2.52 \times 10^{-3}$	$1.32 \times 10^{-4}$
4	12	1	1	ind.	T,G	none	$9.92 \times 10^{-1}$	$2.32 \times 10^{-1}$	$7.45 \times 10^{-3}$	$2.07 \times 10^{-3}$	$1.00 \times 10^{-6}$	$7.80 \times 10^{-1}$	$3.77 \times 10^{-1}$	$2.05 \times 10^{-2}$
5	12	1	1	corr.	T,G	none	$3.30 \times 10^{-1}$	$1.18 \times 10^{-1}$	$1.18 \times 10^{-1}$	$1.15 \times 10^{-1}$	$5.95 \times 10^{-1}$	$3.24 \times 10^{-1}$	$3.24 \times 10^{-1}$	$3.17 \times 10^{-1}$
6	12	1	4	ind.	T,G	none	$3.23 \times 10^{-2}$	$4.36 \times 10^{-4}$	$3.80 \times 10^{-5}$	$2.30 \times 10^{-6}$	$1.98 \times 10^{-1}$	$7.97 \times 10^{-3}$	$5.75 \times 10^{-4}$	$2.82 \times 10^{-5}$
6a	12	1	2	ind.	T,G	none	$4.87 \times 10^{-1}$	$1.55 \times 10^{-2}$	$1.73 \times 10^{-3}$	$8.05 \times 10^{-5}$	$9.05 \times 10^{-1}$	$1.51 \times 10^{-1}$	$2.46 \times 10^{-2}$	$6.09 \times 10^{-4}$
6b	12	*	4	ind.	T,G	none	$3.24 \times 10^{-2}$	$2.90 \times 10^{-4}$	$1.00 \times 10^{-7}$	$<10^{-7}$	$1.98 \times 10^{-1}$	$6.09 \times 10^{-3}$	$1.06 \times 10^{-5}$	$<10^{-7}$
7	12	1	4	ind.	T,G	1/2 cos	$7.74 \times 10^{-3}$	$8.12 \times 10^{-5}$	$7.20 \times 10^{-6}$	$3.00 \times 10^{-7}$	$5.53 \times 10^{-2}$	$1.56 \times 10^{-3}$	$1.09 \times 10^{-4}$	$6.00 \times 10^{-6}$
7a	12	1	4	ind.	T,G	3/4 cos	$1.10 \times 10^{-2}$	$1.08 \times 10^{-4}$	$9.90 \times 10^{-4}$	$2.00 \times 10^{-7}$	$7.90 \times 10^{-2}$	$2.17 \times 10^{-3}$	$1.58 \times 10^{-4}$	$6.90 \times 10^{-6}$
7b	12	1	4	ind.	T,G	9/10 cos	$1.91 \times 10^{-2}$	$2.00 \times 10^{-4}$	$1.94 \times 10^{-5}$	$1.00 \times 10^{-6}$	$1.31 \times 10^{-1}$	$3.86 \times 10^{-3}$	$2.82 \times 10^{-4}$	$1.59 \times 10^{-5}$

\* $\mu=0.541$  for run 6b  
 $b_{50}=0.30$  in. (0.76 cm),  $\mu$  is second parameter of lognormal b.  
The length of an initiation site is 2 in. (5.08 cm).  
Growth and initiation independent.  
10 million trials.

b for detectable leak (5 gpm) = 1.49 in. (3.78 cm).  
b for big leak (100 gpm) = 3.78 in. (9.6 cm).

A comparison of Cases 6 and 6b shows that the value of  $m$  for  $b_o$  has an appreciable influence on the big leak and DEPB probabilities.

Case 7 is the same as Case 6, but with a circumferential variation of stress. The maximum stresses are as given above. The stresses  $180^\circ$  from the maximum stress are  $\frac{1}{2}$ ,  $\frac{3}{4}$ , or  $\frac{9}{10}$  the maximum (Cases 7, 7a, 7b), with a cosine variation in between. This provides a factor of 4 to 10 on the results. This is not a huge effect.

To further study the influence of the distribution of  $b_o$ , a series of runs was made based on Case 6 of Table C.8. Various values of  $\mu$  were considered with  $b_o$  as the random variable. Runs were also made with  $(b_o - a_o)$  as the random variable with  $\mu$  of 0.682. Table C.9 summarizes the results. All of these runs are for 12 initiation sites and a multiplier on initiation time of 4. As discussed in Section 4.1, the value of  $\mu$  of 1 with  $b_o$  as the independent variable gives too high a probability of  $b_o < a_o$  and  $b_o > 1$ . The two left columns provide comparable results. It is suggested that  $(b_o - a_o)$  be used as the independent variable with  $\mu = 0.682$ .

In summary, the value of  $\mu$  in the distribution of the surface length of initiated cracks has a large effect on the big leak and DEPB results. Hence, additional attention was focused on this parameter. Based on results in Section 4.1 and immediately above, it was decided to treat  $(b_o - a_o)$  as a lognormal random variable. Example results with this assumption are included in the next section. It appears that the size/surface finish effect is best handled by using the ANL correlations, but using a multiplier of less

Table C.9 Results for Case 6 with Various Treatments of the Length of Initiated Cracks				
	Ind. Var.	$b_o$	$b_o$	$b_o - a_o$
	$\mu$	1	0.518	0.682
	$P(b_o < a_o)$	0.18	0.038	0
	$P(b_o > 1)$	0.114	$10^{-2}$	$10^{-2}$
Cum. at 40 Years	$P_I$	$3.23 \times 10^{-2}$	$3.23 \times 10^{-2}$	$3.23 \times 10^{-2}$
	$P_{leak}$	$4.36 \times 10^{-4}$	$2.89 \times 10^{-4}$	$2.88 \times 10^{-4}$
	$P_{big\ leak}$	$3.80 \times 10^{-5}$	$1.00 \times 10^{-7}$	$2.00 \times 10^{-7}$
	$P_{DEPB}$	$2.30 \times 10^{-6}$	$<10^{-7}$	$<10^{-7}$
Cum. at 60 Years	$P_I$	$1.98 \times 10^{-1}$	$1.98 \times 10^{-1}$	$1.98 \times 10^{-1}$
	$P_{leak}$	$7.97 \times 10^{-3}$	$6.04 \times 10^{-3}$	$6.08 \times 10^{-3}$
	$P_{leak}$	$5.75 \times 10^{-4}$	$1.01 \times 10^{-5}$	$1.10 \times 10^{-5}$
	$P_{DEPB}$	$2.82 \times 10^{-5}$	$<10^{-7}$	$<10^{-7}$
12 initiation sites, $t_i$ multiplier = 4, $10^7$ trials				

than 4 in conjunction with multiple initiation sites. This provides a size effect that does depend on size and also allows for consideration of surface stress gradients. The preliminary results in Table C.8 suggest that a multiplier of 2 be used, which is employed in the example in the next section.

### C.6.2 Refined Example

The example problem of the previous section was analyzed using 12 initiation sites with a multiplier on  $t_i$  of 2 and using  $(b_o - a_o)$  as the random variable describing the size of the initiated cracks. In accordance with the discussion in Section C4.1, the median value of  $(b_o - a_o)$  was taken to be 0.18 in. (0.46 cm), with a shape parameter,  $m$ , of 0.682. The median of  $(b_o - a_o)$  corresponds to a median initiated surface length,  $2b_o$ , of 0.60 in. (1.52 cm), which gives a median  $b_o/a_o$  of 2.5. This is believed to be conservative because initiated cracks would be expected to be nearly semi-circular in shape. The value of  $m$  of 0.682 along with the median value of  $b_o$  results in 1 crack in 100 having an initiated length greater than the unit length of 2 in. (5.08 cm).

In addition to the probability results, the crack-linking procedures were reviewed, and selected crack-size results were printed out in pcPRAISE. The probability results are included in Section C6.2.1, and linking results are discussed in Section C6.2.2.

#### C.6.2.1 Probability Results

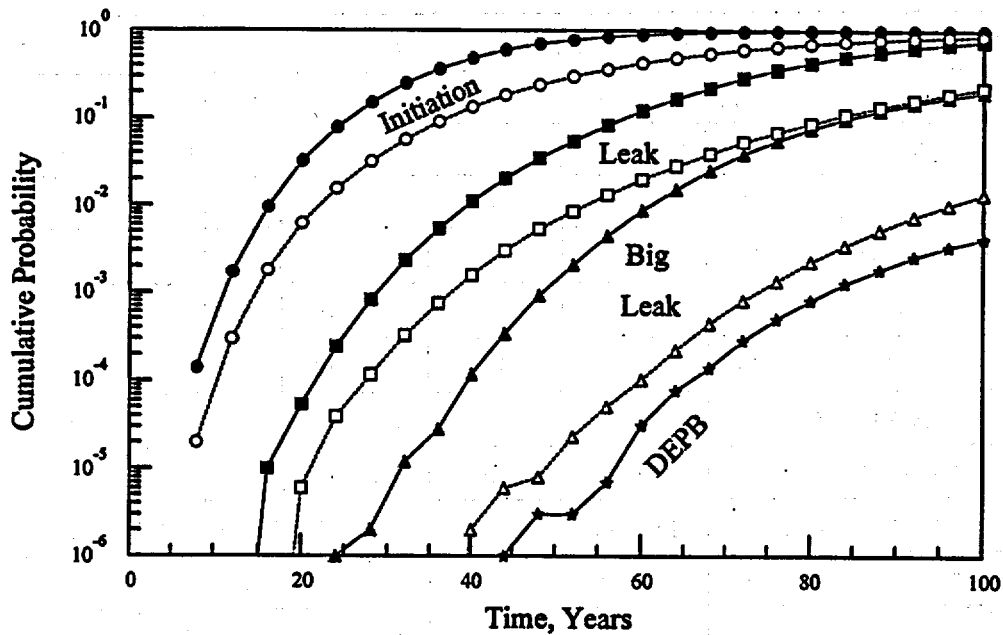
In addition to probability of crack initiation, the probability of a leak (through-wall crack), large leak and DEPB were evaluated. Analyses were performed for no circumferential variation of the stresses and for a strong circumferential variation. The results provide information on the relative leak-to-break probability for situations with and without variations of stress on the surface. Such information is useful in leak-before-break assessments.

For the case of no circumferential stress variation, the stresses in Table C.7 were taken to be axisymmetric. In components such as nozzles, the peak stress can be very localized, with significant gradients along the surface. To estimate the influence of such surface gradients, calculations were performed with a strong variation from one initiation site to another. The minimum stresses at the ID were taken to be  $1/4$  of the maximum as defined in Table C.7 and to be located  $180^\circ$  from the high-stress point. A cosine variation of ID stress with position around the circumference was assumed. The pcPRAISE calculations in this section were performed with 106 trials. The results for both cases are provided in Table C.10. Note that the results are for times extending to 100 years.

Figure C.3 provides a plot of these results, with the solid line being for the case of no circumferential stress variation and the dashed line being for a variation. No results are plotted for the DEPB probability with stress variation because no such failures occurred in the 106 trials performed. A comparison of the results in Table C.10 shows that the presence of the surface-stress gradient has a substantial influence in this example. The influence of the gradient becomes progressively less for big leaks, leaks, and initiation, as can be seen in Figure C.3. The influence is larger than observed in the earlier example in Table C.8. This is because the stress variation is larger, but could also be due to the distribution of initiated surface crack lengths being different.

**Table C.10 Summary of Cumulative Probability Results for Refined Example Problem**

Time Years	No Surface Gradient				With Surface Gradient			
	Initiation	Leak	Big Leak	DEPB	Initiation	Leak	Big Leak	DEPB
4	<10 <sup>-6</sup>	<10 <sup>-6</sup>						
8	1.14 × 10 <sup>-4</sup>	<10 <sup>-6</sup>	<10 <sup>-6</sup>	<10 <sup>-6</sup>	2.00 × 10 <sup>-5</sup>	<10 <sup>-6</sup>	<10 <sup>-6</sup>	<10 <sup>-6</sup>
12	1.72 × 10 <sup>-3</sup>	<10 <sup>-6</sup>	<10 <sup>-6</sup>	<10 <sup>-6</sup>	2.98 × 10 <sup>-4</sup>	<10 <sup>-6</sup>	<10 <sup>-6</sup>	<10 <sup>-6</sup>
16	9.58 × 10 <sup>-3</sup>	1.00 × 10 <sup>-5</sup>	<10 <sup>-6</sup>	<10 <sup>-6</sup>	1.80 × 10 <sup>-3</sup>	<10 <sup>-6</sup>	<10 <sup>-6</sup>	<10 <sup>-6</sup>
20	3.26 × 10 <sup>-2</sup>	5.40 × 10 <sup>-5</sup>	<10 <sup>-6</sup>	<10 <sup>-6</sup>	6.20 × 10 <sup>-3</sup>	6.00 × 10 <sup>-6</sup>	<10 <sup>-6</sup>	<10 <sup>-6</sup>
24	7.88 × 10 <sup>-2</sup>	2.42 × 10 <sup>-4</sup>	1.00 × 10 <sup>-6</sup>	<10 <sup>-6</sup>	1.56 × 10 <sup>-2</sup>	3.90 × 10 <sup>-5</sup>	<10 <sup>-6</sup>	<10 <sup>-6</sup>
28	1.52 × 10 <sup>-1</sup>	8.22 × 10 <sup>-4</sup>	2.00 × 10 <sup>-6</sup>	<10 <sup>-6</sup>	3.21 × 10 <sup>-2</sup>	1.16 × 10 <sup>-4</sup>	<10 <sup>-6</sup>	<10 <sup>-6</sup>
32	2.51 × 10 <sup>-1</sup>	2.32 × 10 <sup>-3</sup>	1.20 × 10 <sup>-5</sup>	<10 <sup>-6</sup>	5.75 × 10 <sup>-2</sup>	3.26 × 10 <sup>-4</sup>	<10 <sup>-6</sup>	<10 <sup>-6</sup>
36	3.66 × 10 <sup>-1</sup>	5.38 × 10 <sup>-3</sup>	2.80 × 10 <sup>-5</sup>	<10 <sup>-6</sup>	9.20 × 10 <sup>-2</sup>	7.50 × 10 <sup>-4</sup>	<10 <sup>-6</sup>	<10 <sup>-6</sup>
40	4.88 × 10 <sup>-1</sup>	1.11 × 10 <sup>-2</sup>	1.19 × 10 <sup>-4</sup>	<10 <sup>-6</sup>	1.35 × 10 <sup>-1</sup>	1.59 × 10 <sup>-3</sup>	2.00 × 10 <sup>-6</sup>	<10 <sup>-6</sup>
44	6.04 × 10 <sup>-1</sup>	2.05 × 10 <sup>-2</sup>	3.41 × 10 <sup>-4</sup>	1.00 × 10 <sup>-6</sup>	1.86 × 10 <sup>-1</sup>	3.00 × 10 <sup>-3</sup>	6.00 × 10 <sup>-6</sup>	<10 <sup>-6</sup>
48	7.07 × 10 <sup>-1</sup>	3.53 × 10 <sup>-2</sup>	9.25 × 10 <sup>-4</sup>	3.00 × 10 <sup>-6</sup>	2.42 × 10 <sup>-1</sup>	5.38 × 10 <sup>-3</sup>	8.00 × 10 <sup>-6</sup>	<10 <sup>-6</sup>
52	7.91 × 10 <sup>-1</sup>	5.56 × 10 <sup>-2</sup>	2.09 × 10 <sup>-3</sup>	3.00 × 10 <sup>-6</sup>	3.03 × 10 <sup>-1</sup>	8.59 × 10 <sup>-3</sup>	2.30 × 10 <sup>-5</sup>	<10 <sup>-6</sup>
56	8.57 × 10 <sup>-1</sup>	8.48 × 10 <sup>-2</sup>	4.51 × 10 <sup>-3</sup>	7.00 × 10 <sup>-6</sup>	3.66 × 10 <sup>-1</sup>	1.33 × 10 <sup>-2</sup>	5.10 × 10 <sup>-5</sup>	<10 <sup>-6</sup>
60	9.05 × 10 <sup>-1</sup>	1.23 × 10 <sup>-1</sup>	8.78 × 10 <sup>-3</sup>	3.10 × 10 <sup>-5</sup>	4.30 × 10 <sup>-1</sup>	2.00 × 10 <sup>-2</sup>	1.03 × 10 <sup>-4</sup>	<10 <sup>-6</sup>
64	9.39 × 10 <sup>-1</sup>	1.69 × 10 <sup>-1</sup>	1.54 × 10 <sup>-2</sup>	7.70 × 10 <sup>-5</sup>	4.92 × 10 <sup>-1</sup>	2.85 × 10 <sup>-2</sup>	2.21 × 10 <sup>-4</sup>	<10 <sup>-6</sup>
68	9.62 × 10 <sup>-1</sup>	2.25 × 10 <sup>-1</sup>	2.54 × 10 <sup>-2</sup>	1.40 × 10 <sup>-4</sup>	5.52 × 10 <sup>-1</sup>	3.96 × 10 <sup>-2</sup>	4.44 × 10 <sup>-4</sup>	<10 <sup>-6</sup>
72	9.77 × 10 <sup>-1</sup>	2.90 × 10 <sup>-1</sup>	3.92 × 10 <sup>-2</sup>	2.84 × 10 <sup>-4</sup>	6.08 × 10 <sup>-1</sup>	5.37 × 10 <sup>-2</sup>	8.05 × 10 <sup>-4</sup>	<10 <sup>-6</sup>
76	9.86 × 10 <sup>-1</sup>	3.58 × 10 <sup>-1</sup>	5.60 × 10 <sup>-2</sup>	4.97 × 10 <sup>-4</sup>	6.60 × 10 <sup>-1</sup>	6.96 × 10 <sup>-2</sup>	1.35 × 10 <sup>-3</sup>	<10 <sup>-6</sup>
80	9.92 × 10 <sup>-1</sup>	4.31 × 10 <sup>-1</sup>	7.74 × 10 <sup>-2</sup>	8.08 × 10 <sup>-4</sup>	7.08 × 10 <sup>-1</sup>	8.85 × 10 <sup>-2</sup>	2.25 × 10 <sup>-3</sup>	<10 <sup>-6</sup>
84	9.95 × 10 <sup>-1</sup>	5.04 × 10 <sup>-1</sup>	1.00 × 10 <sup>-1</sup>	1.27 × 10 <sup>-3</sup>	7.50 × 10 <sup>-1</sup>	1.1 × 10 <sup>-1</sup>	3.45 × 10 <sup>-3</sup>	<10 <sup>-6</sup>
88	9.97 × 10 <sup>-1</sup>	5.75 × 10 <sup>-1</sup>	1.25 × 10 <sup>-1</sup>	1.82 × 10 <sup>-3</sup>	7.88 × 10 <sup>-1</sup>	1.36 × 10 <sup>-1</sup>	5.18 × 10 <sup>-3</sup>	<10 <sup>-6</sup>
92	9.98 × 10 <sup>-1</sup>	6.45 × 10 <sup>-1</sup>	1.52 × 10 <sup>-1</sup>	2.56 × 10 <sup>-3</sup>	8.22 × 10 <sup>-1</sup>	1.63 × 10 <sup>-1</sup>	7.46 × 10 <sup>-3</sup>	<10 <sup>-6</sup>
96	9.99 × 10 <sup>-1</sup>	7.06 × 10 <sup>-1</sup>	1.77 × 10 <sup>-1</sup>	3.33 × 10 <sup>-3</sup>	8.50 × 10 <sup>-1</sup>	1.93 × 10 <sup>-1</sup>	1.01 × 10 <sup>-2</sup>	<10 <sup>-6</sup>
100	9.99 × 10 <sup>-1</sup>	7.61 × 10 <sup>-1</sup>	2.01 × 10 <sup>-1</sup>	4.17 × 10 <sup>-3</sup>	8.75 × 10 <sup>-1</sup>	2.25 × 10 <sup>-1</sup>	1.35 × 10 <sup>-2</sup>	<10 <sup>-6</sup>



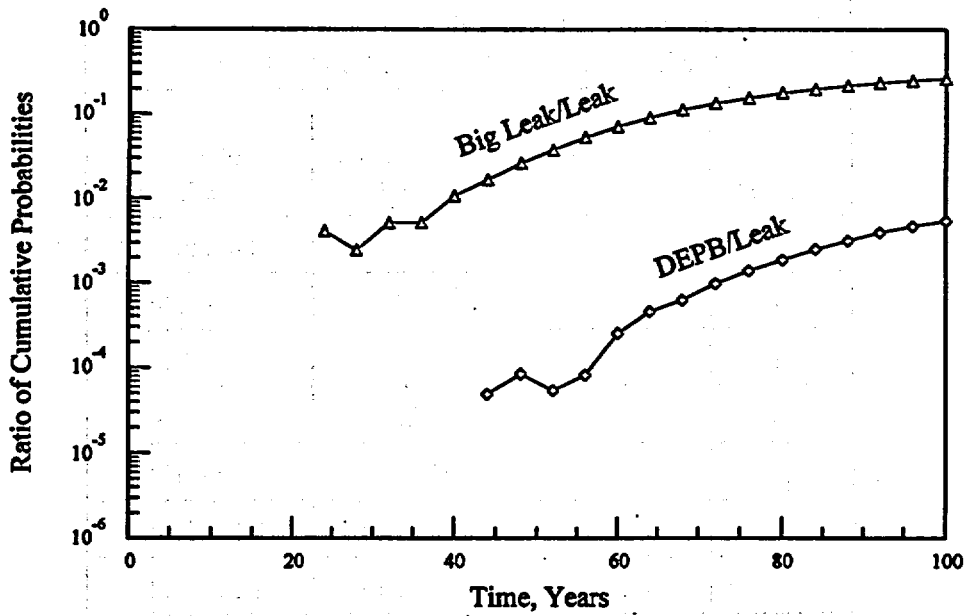
**Figure C.3 Cumulative Failure Probabilities as Functions of Time for Example Problem. (Solid lines are for no circumferential stress variation, and dashed lines are for variation)**

Table C.10 shows that when the gradient was present, no double-ended pipe breaks occurred in one million trials out to 100 years, as compared to over 4000 when no surface gradient was included ( $4.17 \times 10^{-3}$  at 100 years). Thus, the gradient reduced the DEP probability by over 3 orders of magnitude.

The ratios of big leak and DEP probabilities to the leak probability are of particular interest in leak-before-break assessments. These ratios for no surface stress variation are included in Figure C.4 as functions of time. Note that the relative DEP to leak probability is less than  $10^{-5}$  for times less than 40 years and less than  $10^{-2}$  after 100 years. The big leak-to-leak probability remains below 0.26 for times out to 100 years. Figure C.5 presents the ratio of the big leak to leak for the case of circumferential stress variation. A comparison of these figures shows that the percentage of leaks that are large is considerably lower for the case of a stress variation.

### C.6.2.2 Crack Linking

Provisions were added to the pcPRAISE output to summarize the linking of cracks, which is described here. The results for the example problem of Section C6.2.1 with no stress gradient are considered. (The corresponding results with the circumferential gradient are not as informative because the strong gradient results in less crack linking.) Table C.11 provides an example of the information in pcPRAISE on crack initiations.



**Figure C.4 Ratios of Big Leak and DEPB Probabilities to Leak Probability - No Surface Stress Variation**

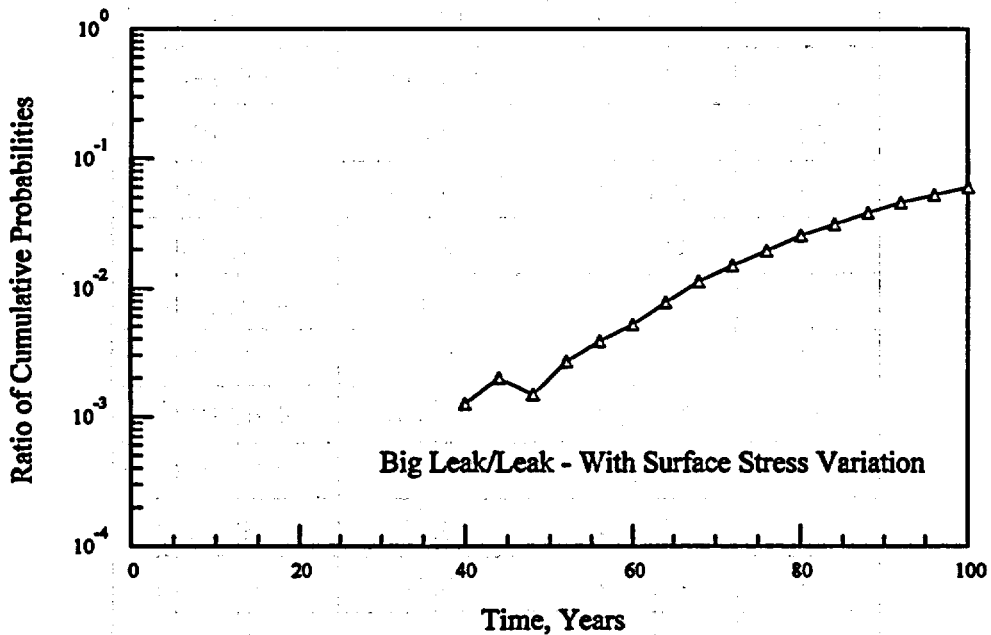


**Figure C.5 Ratio of Big Leak to Leak Probability - with Surface Stress Variation**

**Table C.11 Crack Initiation Information from pcPRAISE  
for Example Problem with No Gradient**

<b>Time (Years)</b>	<b>Total Initiated Cracks</b>	<b>First Number of Cracks</b>	<b>Initiated Probability</b>
4	0	0	0.0000E+00
8	114	114	1.1400E-04
12	1,612	1,611	1.7250E-03
16	7,913	7,857	9.5820E-03
20	23,457	23,017	3.2599E-02
24	48,702	46,249	7.8848E-02
28	82,386	73,540	1.5239E-01
32	121,465	98,644	2.5103E-01
36	162,020	114,905	3.6594E-01
40	203,474	122,012	4.8795E-01
44	239,637	115,705	6.0365E-01
48	275,533	103,015	7.0667E-01
52	300,787	83,899	7.9057E-01
56	325,264	65,664	8.5623E-01
60	344,107	48,290	9.0452E-01
64	357,684	34,116	9.3864E-01
68	364,293	22,878	9.6152E-01
72	368,039	15,016	9.7653E-01
76	367,522	9,390	9.8592E-01
80	365,334	5,862	9.9178E-01
84	361,883	3,517	9.9530E-01
88	354,896	1,963	9.9726E-01
92	348,266	1,257	9.9852E-01
96	332,408	660	9.9918E-01
100	324,492	334	9.9951E-01

In this table, the second column is the number of cracks that initiated within the time increment, and the third column is the number of cracks that initiated within the time increment that were the very first initiations during that trial. The fourth column is the cumulative probability of crack initiation, which is the running sum of the third column divided by the number of trials.

Table C.12 is a summary of crack initiation and linking. Such results are printed out for each evaluation time that is a multiple of 10. The evaluation times for the example problem are the times included in Table C.11. Hence, the crack-linking information is printed out for 20, 40, 60, 80, and 100 years. Table C.12 includes the crack-linking information at 40 years.

The results in Table C.12 are summarized on a crack-by-crack basis, so information is lost regarding cracks on a weld-by-weld (trial-by-trial) basis. The sum of all cracks in Table C.13 must be less than the number of initiation sites times the number of trials. The table provides a snapshot of the cracks that were present at the given time and gives the depth (as a fraction of the wall thickness), the surface length (as a fraction of the inner pipe circumference), and the number of initiated cracks that linked to form that crack. For instance, for cracks with  $a/h$  between 0.80 and 0.95, there were 2637 cracks with surface lengths in the range of 20-40% of the circumference. Of these cracks, 1657 of them were formed by a single initiating crack, 794 were formed by the linking of two initiating cracks, 180 were formed by the linking of 3 cracks, and 6 were formed by the linking of 4 cracks. None were formed by the linking of 5 or more cracks.

Cracks in the depth range of  $0.95 < a/h < 1.0$  are mostly through-wall cracks, which are of particular interest. Table entries for this range of depths provide information on the length distribution of through-wall cracks and how many cracks linked to form them. Any cracks that grew to become leaks before 40 years also appear in the table.

Table C.13 summarizes results on a weld-by-weld (trial-by-trial) basis. This table shows up in the pcPRAISE output directly along with the data of Table C.14. The number of individual cracks involved is not given, but only the sum of the surface lengths.

The number of cracks at 40 years that exceed a given value of  $a/h$  and fall within a range of surface length to circumference is given. The sum of the second column ( $a/h > 0$ ) gives the number of cracked welds regardless of the circumferential extent of cracking. When these are divided by the number of trials, the result is nearly equal to the crack initiation probability. The entries for cracks of greater depths can best be described by visualizing the extent of cracking that would be seen if material were removed from the inside diameter of the pipe. For instance, if the inner 60% of the material was removed, out of 106 welds, 47,539 would have cracks whose surface length (after material removal) was in the range 0-20% of the circumference. Similarly, there would be 2 welds with a total crack-surface length of 60-80% of the circumference. There could be many cracks adding up to this length, or simply one long crack. The columns in Table C.13 are the histogram of the circumferential extent of cracking at the surface (after material removal). When normalized by the sum of entries in the column, the entries are the probability of seeing a given range of circumferential cracking given that a crack is observed (after material removal). It is apparent that the numbers do not need to decrease monotonically as one proceeds down a column. It is not so apparent that the numbers do not need to decrease monotonically as one proceeds from right to left in a row. Although this is the case in Table C.13, it is not the case for the same problem at 80 years, as seen in Table C.14.

**Table C.12 Example of Crack-Linking Information Printed Out in pcPRAISE 4.0  
at Time 40.00 Years**

.00 < a/h <= .30

% circumf.	[ ALL ]	[ 1 ]	[ 2 ]	[ 3 ]	[ 4 ]	[ 5 ]	[ 6-10 ]	[ 11-15 ]	[ 16-20 ]	[ 21-30 ]	[ 31-40 ]	[ >41 ]
.0- 20.0	380858	380801	57	0	0	0	0	0	0	0	0	0
20.0- 40.0	20	17	2	1	0	0	0	0	0	0	0	0
40.0- 60.0	0	0	0	0	0	0	0	0	0	0	0	0
60.0- 80.0	0	0	0	0	0	0	0	0	0	0	0	0
80.0-100.0	0	0	0	0	0	0	0	0	0	0	0	0

.30 < a/h <= .60

% circumf.	[ ALL ]	[ 1 ]	[ 2 ]	[ 3 ]	[ 4 ]	[ 5 ]	[ 6-10 ]	[ 11-15 ]	[ 16-20 ]	[ 21-30 ]	[ 31-40 ]	[ >41 ]
.0- 20.0	193277	191770	1497	10	0	0	0	0	0	0	0	0
20.0- 40.0	38	18	4	16	0	0	0	0	0	0	0	0
40.0- 60.0	0	0	0	0	0	0	0	0	0	0	0	0
60.0- 80.0	0	0	0	0	0	0	0	0	0	0	0	0
80.0-100.0	0	0	0	0	0	0	0	0	0	0	0	0

.60 < a/h <= .80

% circumf.	[ ALL ]	[ 1 ]	[ 2 ]	[ 3 ]	[ 4 ]	[ 5 ]	[ 6-10 ]	[ 11-15 ]	[ 16-20 ]	[ 21-30 ]	[ 31-40 ]	[ >41 ]
.0- 20.0	36720	33818	2890	12	0	0	0	0	0	0	0	0
20.0- 40.0	134	13	22	97	2	0	0	0	0	0	0	0
40.0- 60.0	0	0	0	0	0	0	0	0	0	0	0	0
60.0- 80.0	0	0	0	0	0	0	0	0	0	0	0	0
80.0-100.0	0	0	0	0	0	0	0	0	0	0	0	0

.80 < a/h <= .95

% circumf.	[ ALL ]	[ 1 ]	[ 2 ]	[ 3 ]	[ 4 ]	[ 5 ]	[ 6-10 ]	[ 11-15 ]	[ 16-20 ]	[ 21-30 ]	[ 31-40 ]	[ >41 ]
.0- 20.0	11493	9817	1676	0	0	0	0	0	0	0	0	0
20.0- 40.0	2637	1657	794	180	6	0	0	0	0	0	0	0
40.0- 60.0	5	0	2	1	2	0	0	0	0	0	0	0
60.0- 80.0	0	0	0	0	0	0	0	0	0	0	0	0
80.0-100.0	0	0	0	0	0	0	0	0	0	0	0	0

.95 < a/h <= 99.00

% circumf.	[ ALL ]	[ 1 ]	[ 2 ]	[ 3 ]	[ 4 ]	[ 5 ]	[ 6-10 ]	[ 11-15 ]	[ 16-20 ]	[ 21-30 ]	[ 31-40 ]	[ >41 ]
.0- 20.0	978	662	313	3	0	0	0	0	0	0	0	0
20.0- 40.0	12292	9580	2448	247	17	0	0	0	0	0	0	0
40.0- 60.0	30	0	10	11	9	0	0	0	0	0	0	0
60.0- 80.0	2	0	0	1	1	0	0	0	0	0	0	0
80.0-100.0	0	0	0	0	0	0	0	0	0	0	0	0

<b>Table C.13 Crack-Size Data Sorted on a Weld-by-Weld Basis (40 Years)</b>					
	<b>&gt;0</b>	<b>&gt;0.3 h</b>	<b>&gt;0.6 h</b>	<b>&gt;0.8 h</b>	<b>&gt;.95 h</b>
<b>0-20%</b>	468,138	215,792	47,539	12,337	978
<b>20-40%</b>	19,993	17,511	15,602	14,923	12,292
<b>40-60%</b>	118	99	85	63	30
<b>60-80%</b>	3	3	2	2	2
<b>&gt;80%</b>	0	0	0	0	0

<b>Table C.14 Crack-Size Data Sorted on a Weld-by-Weld Basis (80 Years)</b>					
	<b>&gt;0</b>	<b>&gt;0.3 h</b>	<b>&gt;0.6 h</b>	<b>&gt;0.8 h</b>	<b>&gt;.95 h</b>
<b>0-20%</b>	278,364	297,066	185,559	81,448	9,364
<b>20-40%</b>	557,410	527,960	473,116	450,358	413,425
<b>40-60%</b>	143,227	118,659	83,609	59,823	33,299
<b>60-80%</b>	11,553	10,256	8,025	6,030	3,537
<b>&gt;80%</b>	1,243	1,237	1,226	1,192	1,147

## **C.7 Detailed Formats for Input Data**

The modifications to pcPRAISE to incorporate the capabilities for analyzing crack initiation necessitated the addition and alteration of many of the input data, such as are described in Section 8.3 of the pcPRAISE manual (Harris et al. 1992). Hence, it was necessary to update the description of the input deck. The updates are included in the following pages of this Appendix.

CARD TITLE CARD  
READ Always

ID

0A

VARIABLE	COLUMNS	FORMAT	DESCRIPTION
TITLE	1-80	20A4	Problem description

CARD PROBLEM CONTROL VARIABLES  
READ Always

ID

0B

VARIABLE	COLUMNS	FORMAT	DESCRIPTION
INCIAT	1-5	I5	0: Run for pre-existing cracks only. 1: SCC initiated cracks only. 2: Pre-existing & initiated cracks only. 3: Fatigue-initiated cracks only.
IFAILC	6-10	I5	Failure criteria to be used: 0: Net section failure. 1: $J_{Isc}$ dJ/da exceedance. 2: Both.
ICRACKS	11-15	I5	Stress corrosion crack/fatigue crack initiation sites (used only if INCIAT $\geq$ 1).
IREPLS	16-20	I5	Number of replications for crack initiation problem (not used for INCIAT = 0 or = 2.). If IREPLS < 0, then IREPLS = 10 <sup>-IREPLS</sup> .
IPRAIS	21-25	I5	Not used.
IREPAR	26-30	I5	= 0: Welds with cracks that leak and are detected and replaced with perfect welds. = 1: Cracks that leak and are detected and removed. At the time of repair, all leakers are repaired. If INCIAT = 0, then IREPAR is set to 1.
BNDRY	31-40	F10.3	Boundary in terms of a/h, above which initiated cracks are not included. For example, 1.1: Initiated cracks will always be included. -0.1: Initiated cracks will never be included. Used only in INCIAT = 2.
ISF	41-45	I5	Material type (for fatigue properties) 0: Austenitic or other. 1: Ferritic. (Not used for INCIAT=3. Use MTTYPE)
MTTYPE	51-55	I5	Material Type for SCC: =1 for 304 =2 for 316NG for INCIAT=3: =11 for low alloy steel =12 for carbon steel =13 for 304/316 =14 for 316NG
ISEED	56-62	I7	Seed for random number generator
ISEEDR	63-70	I7	Seed for random number generator
IREMED	71-75	I5	Number of future remedial actions (change in water chemistry, IHSI, etc.). (IRMED $\leq$ 4)
ITBLMX	76-80	I5	Number of crack sizes for which exceedance probabilities are tabulated. (0 $\leq$ ITBLMX $\leq$ 5)

CARD PROBLEM SPECIFICATION  
 READ Always

ID

1B

VARIABLE	COLUMNS	FORMAT	DESCRIPTION
NTRIES	1-5	I-5	Option for number of replications to be drawn from each cell. When NTRIES<0: Then ABS (NTRIES) replications will be taken from each and every cell. If NTRIES=0: Not used. If NTRIES>0: The user inputs a number for each cell. This number is then multiplied by NTRIES to obtain the number of samples for each cell.
ISQARE	6-10	I5	Cell definition option. ISQARE = 0: User inputs coordinates for each cell in the state space. ISQARE = 1: pc-PRAISE internally sets up a regular grid of rectangular cells. ISQARE = 2: If INCIAT = 1 or 3.
KTYPES	11-15	I5	Number of transient types experienced by plant.
KRKDIS	16-20	I5	Initial crack size distributions. KRKDIS = 1: Crack depth is lognormal. Aspect ratio is lognormal. KRKDIS = 2: Crack depth is lognormal. Aspect ratio is exponential. KRKDIS = 3: Crack depth is exponential. Aspect ratio is lognormal. KRKDIS = 4: Crack depth is exponential. Aspect ratio is exponential.
NEVAL	21-25	I5	Option for times during plant lifetime when the reliability is to be evaluated. NEVAL<0: Evaluation is performed for every ABS (NEVAL) year. NEVAL>0: Number of user supplied times that an evaluation is performed.
NINSPT	26-30	I5	Number of user specified in-service inspection times.
NQUAKE	31-35	I5	Seismic evaluation option. NQUAKE = 0: No earthquakes are modeled. NQUAKE = 1: Earthquakes at each evaluation time.
IDDEBUG	36-40	I5	Debugging output option. IDDEBUG=0: Normal output is printed. IDDEBUG=1: Additional debugging output will be printed.
KONPRP	41-45	I5	Flag for distribution of fatigue crack growth. KONPRP=0: C is lognormally distributed if ISF=0, or built-in distribution for ferritic if ISF=1 KONPRP=1: C is constant if ISF=0, or the median crack growth is used if ISF=1.
NEQUINT	46-50	I5	Number of seismic intensity classes to be simulated. If NQUAKE=0, set NEQUINT=0. pcPRAISE as currently dimensioned can handle up to 10 classes.

**CARD PROBLEM SPECIFICATION (cont.)**  
**READ Always**

ID

1B

VARIABLE	COLUMNS	FORMAT	DESCRIPTION
MCELLS	51-55	I5	Number of cells in the calculational grid. IF ISQARE=1, the value of MCELLS is ignored.
KNSFLO	56-60	I5	Option for flow stress definition. KNSFLO=0, flow stress is normally distributed. KNSFLO=1, flow stress is constant.
NSKIP	61-65	I5	Parameter to specify the number of evaluation times that are skipped in the printout of the indicator functions. Subroutine OUTS prints every NSKIP-th evaluation time. If NSKIP $\geq$ 0, the indicator functions are not printed.
NPSI	66-70	I5	Option for pre-service inspection. NPSI=0 for no pre-service inspection. NPSI=1 for a pre-service inspection.
ISCC	71-75	I5	Option for modeling stress corrosion cracking (SCC). ISCC=1: Stress corrosion cracking only. ISCC=2: Fatigue only (no SCC). ISCC=3: Both fatigue and SCC.  If INCIAT $>$ 0, ISCC should be either 1 or -1.
ISIGRS	76-80	I5	Option for modeling contribution of residual stresses. ISIGRS=0: Residual stresses are not modeled. ISIGRS=1: Residual stresses are modeled (coefficients to be entered by the user). ISIGRS=2: Contribution of residual stresses is modeled. Built in residual stresses for large lines (20-30 inch OD) are used. ISIGRS=3: Contribution of residual stresses is modeled. Built in residual stresses for intermediate lines (10-20 inch OD) are used. ISIGRS=4: Contribution of residual stresses is modeled. Built in residual stresses for small lines (<10 inch OD) are used. ISIGRS=5: Contribution of IHSI or MSIP residual stresses is modeled. User to input the mean and standard deviation of stress at the ID.

**CARD FATIGUE INITIATION INPUTS**  
 READ IF INCIAT=3.

ID 1B0

VARIABLE	COLUMNS	FORMAT	DESCRIPTION
NSTRDIS	1-10	I10	Distribution of stress around the circumference. 0: Uniform 1: User-specified. Specify using AngMults( ) variable (Card 6E2).
SULFUR	11-20	E10.0	Sulfur (wt percent).
DOXY	21-30	E10.0	Dissolved oxygen (ppm).
ANFIXED	31-40	E10.0	Depth of the initiated crack (in.).
BMEDIAN	41-50	E10.0	Median length minus depth (b-a) of the initiated crack (in.).
BSD	51-60	E10.0	Standard deviation of ln(b-a) of the initiated crack.
IICORR	61-65	I5	Flag indicating whether the specimens around the circumference are correlated. 0: independent (a random sample is taken for each specimen). 1: dependent (only one random sample is taken per weld).
IGCORR	65-70	I5	Flag indicating whether growth is correlated to initiation. 0: not correlated (growth constant sampled independently). 1: correlated (percentile sampled for initiation used for growth).
TIMEX	71-80	E10.0	Multiplier for initiation times. (should be >=0).

**CARD CRACK SIZE EXCEEDANCE**  
 READ Only if ITBLMX>0 on Card 0B

ID 1B1

VARIABLE	COLUMNS	FORMAT	DESCRIPTION
AOHTBL(1)	1-8	F8.4	Crack size for generating crack size exceedance probabilities. A maximum of five crack sizes can be specified. Each crack size is defined by AOHTBL( ) and BOCTBL( ).  AOHTBL( )=fractional crack depth a/h.  BOCTBL( )=fractional crack length (total crack length to inside pipe circumference ratio).
BOCTBL(1)	9-16	F8.4	
AOHTBL(2)	17-24	F8.4	
BOCTBL(2)	25-32	F8.4	
AOHTBL(3)	33-40	F8.4	
BOCTBL(3)	41-48	F8.4	
AOHTBL(4)	49-56	F8.4	
BOCTBL(4)	57-64	F8.4	
AOHTBL(5)	65-72	F8.4	
BOCTBL(5)	73-80	F8.4	

**CARD IHSI and MSIP RESIDUAL STRESS DISTRIBUTION**  
**READ Only if ISIGRS = 5 or 6 on Card 1B**

ID

1C0

VARIABLE	COLUMNS	FORMAT	DESCRIPTION
RSIN	1-10	E10.3	Residual stress on the inside surface of a pipe (ksi). (for ISIGRS=5)
RSOUT	11-20	E10.3	Residual stress on the outside surface of a pipe (ksi). (for ISIGRS=5)
RSINM	1-10	E10.3	Mean of the IHSI or MSIP residual stress on the ID (ksi). (for ISIGRS=6)
RSIND	1-10	E10.3	Standard deviation of the IHSI or MSIP residual stress on the ID (ksi). (for ISIGRS=6)

**CARD RESIDUAL STRESS MODEL DEFINITION**  
**READ Only if ISIGRS = 1 on Card 1B**

ID

1C

VARIABLE	COLUMNS	FORMAT	DESCRIPTION
KKA	1-5	I5	The number of (a/b) terms in the polynomial that defines the contribution of residual stress to the "RMS-averaged" stress-intensity factor in the depth direction.
LLA	6-10	I5	The number of (a/h) terms in the polynomial that defines the contribution of residual stress to the "RMS-averaged" stress-intensity factor in the depth direction.
KKB	11-15	I5	The number of (a/b) terms in the polynomial that defines the contribution of residual stress to the "RMS-averaged" stress-intensity factor in the length direction.
LLB	16-20	I5	The number of (a/h) terms in the polynomial that defines the contribution of residual stress to the "RMS-averaged" stress-intensity factor in the length direction.

**CARD TIME PARAMETERS, NDE PARAMETERS**  
**READ Always**

ID

ID

VARIABLE	COLUMNS	FORMAT	DESCRIPTION
THRIZN	1-10	E10.3	Maximum plant lifetime for the simulation (years).
DTSCC	11-20	E10.3	Time step to be used in calculating SCC growth (years). Used only if ISCC=1 or -1 on Card 1B.
ICTYPE	21-25	I5	Crack orientation flag. =0: circumferential crack =1: longitudinal crack (disabled in pcPRAISE)

The following inputs are not required if NPSI=0 and NIPST=0.

IRTYPE	26-30	I5	Default values of NDE parameters EPST, ASTAR, and ANNU for various pipe types. =0: thick-walled austenitic pipe. =1: thick-walled ferritic pipe. =2: thin-walled austenitic pipe.  For these conditions, the default values are  <table style="margin-left: auto; margin-right: auto;"> <thead> <tr> <th>IRTYPE</th> <th>EPST</th> <th>ASTAR</th> <th>ANNU</th> </tr> </thead> <tbody> <tr> <td>0</td> <td>0</td> <td>0.5*THICK</td> <td>1.6</td> </tr> <tr> <td>1</td> <td>0.005</td> <td>0.25</td> <td>3.0</td> </tr> <tr> <td>2</td> <td>0.005</td> <td>0.25</td> <td>1.33</td> </tr> </tbody> </table>	IRTYPE	EPST	ASTAR	ANNU	0	0	0.5*THICK	1.6	1	0.005	0.25	3.0	2	0.005	0.25	1.33
IRTYPE	EPST	ASTAR	ANNU																
0	0	0.5*THICK	1.6																
1	0.005	0.25	3.0																
2	0.005	0.25	1.33																
EPST	31-40	E10.0	User-specified value of $\epsilon$ parameter; overrides default value. Leave blank to use default.																
ASTAR	41-50	E10.0	User-specified depth of crack with 50% probability of detection (inches); overrides default value. Leave blank to use default.																
TRANSD	51-60	E10.0	Transducer diameter (inches); default = 1 in.																
ANUU	61-70	E10.0	User-specified value of $\nu$ parameter; overrides default value. Leave blank to use default.																
INDPRB	71-75	I5	Flag for selecting independent (=0) of dependent (=1) inspections.																
NDE TWO	76-80	I5	Flag for the ISI & PSI NDE parameters. =0: ISI parameters same as PSI. =1: ISI parameters different than PSI.																

**CARD NDE PARAMETERS FOR ISI**  
 READ If NDE TWO ≠ 0

ID

1E

VARIABLE	COLUMNS	FORMAT	DESCRIPTION
IPTYPE2	1-5	I5	See definition for prior input record
EPST2	6-15	E10.0	See definition for prior input record
ASTAR2	16-25	E10.0	See definition for prior input record
TRANSD2	26-35	E10.0	See definition for prior input record
ANUU2	36-45	E10.0	See definition for prior input record

**CARD PIPE DIMENSIONS**  
 READ Always

ID

2A

VARIABLE	COLUMNS	FORMAT	DESCRIPTION
THICK	1-10	E10.3	Wall thickness of the pipe (in.).
RIN	11-20	E10.3	Inside radius of pipe (in.).
ELOVRR	21-30	E10.3	L/R ratio.

**CARD FATIGUE CRACK GROWTH CHARACTERISTICS**  
 READ Always

ID

2B

VARIABLE	COLUMNS	FORMAT	DESCRIPTION
THRHL	1-10	E10.3	Threshold value in the crack-growth relation (ksi-in <sup>1/2</sup> ).
EMEXP	11-20	E10.3	Exponent in the crack-growth relation.
CONSMU	21-30	E10.3	Parameter for the constant in the crack-growth relation. If KONPRP = 1: CONSMU is the constant. If KONPRP = 0: CONSMU is the median of the lognormal distribution that describes the "constant."
CONS90	31-34	E10.3	Parameter for the constant in the crack-growth relation. If KONPRP = 0: CONS90 is ignored. If KONPRP = 1: CONS90 is the 90 <sup>th</sup> percentile of the lognormal distribution.

**CARD SCC VARIABLE**  
 READ If ISCC ≠ 0 or INCIAT ≠ 0 and INCIAT ≠ 3

ID

2B-1

VARIABLE	COLUMNS	FORMAT	DESCRIPTION
OSTART	1-10	F10.5	Oxygen concentration at start-up (ppm).
OSTEDY	11-20	F10.5	Oxygen concentration at steady state (ppm).
TFSTDY	21-30	F10.5	Steady-state temperature (°F).
DURATN	31-40	F10.5	Duration of heat-up transient (hr).
CONDC	41-50	F10.5	Coolant conductivity (ms/cm).

**CARD FLOW STRESS**  
 READ Always

ID

2C0

VARIABLE	COLUMNS	FORMAT	DESCRIPTION
SFLOMU	1-10	E10.4	The mean value of the flow stress (ksi).
SFLOSD	11-20	E10.4	Standard deviation of the flow stress (ksi). (Read if KNSFLO = 0)
XJIC	21-30	E10.4	$J_{Ic}$ (in-kips/in <sup>2</sup> ) Required only if IFAILC ≠ 0.
DJDAMT	31-40	E10.4	dJ/da (ksi) Required only if IFAILC ≠ 0.
SIGO	41-50	E10.4	Yield strength (ksi).
DEE	51-60	E10.4	Constant D (ksi) in the power law $e = (\sigma/D)^n$ .
YOUNGS	61-70	E10.4	Young's modulus (ksi).
XN	71-80	E10.4	Exponent n in the power law $e = (\sigma/D)^n$ .

**CARD ULTIMATE STRESS DEFINITION**  
 READ Always

ID

2D

VARIABLE	COLUMNS	FORMAT	DESCRIPTION
SULTMU	1-10	E10.0	Mean value of the ultimate stress.
SULTSD	11-20	E10.0	>0: standard deviation of the ultimate stress (ksi). <0: constant ultimate stress.
IULT	21-25	I5	Indicator for interpolation of pipe-break probability; ABS(IULT) = number of interpolated points. >0: linear interpolation. <0: logarithmic interpolation.

**CARD INITIAL CRACK DEPTH DISTRIBUTION**  
 READ Only if INCIAT = 0 or 2

ID

3A

VARIABLE	COLUMNS	FORMAT	DESCRIPTION
AMEDIN	1-10	E10.3	Median of the lognormal distribution of crack depth. (Read if KRKDIS = 1 or 2)
ASIGMA	11-20	E10.3	Shape factor [= standard deviation of ln(a)] of the lognormal distribution of crack depth. (Read if KRKDIS = 1 or 2)
ALAMDA	1-10	E10.3	Rate parameter (in. <sup>-1</sup> ) of exponential distribution of crack depth. (Read if KRKDIS = 3 or 4)

**CARD INITIAL CRACK ASPECT RATIO DISTRIBUTION**  
 READ Only if INCIAT = 0 or 2

ID

3B

VARIABLE	COLUMNS	FORMAT	DESCRIPTION
BOAMED	1-10	E10.3	Parameter analogous to the median in the truncated lognormal distribution of initial crack aspect ratio. (Read if KRKDIS = 1 or 3)
BAOSIG	11-20	E10.3	Parameter analogous to the shape factor in the truncated lognormal distribution of initial aspect ratio. (Read if KRKDIS = 1 or 3)
BAOLDA	1-10	E10.3	Rate parameter for shifted exponential distribution of initial crack aspect ratio. (Read if KRKDIS = 2 or 4).

**CARD EARTHQUAKE EVALUATION TIMES**  
 READ Only if NEVAL > 0

ID

4A

VARIABLE	COLUMNS	FORMAT	DESCRIPTION
TEVAL	1-80	8E10.3	Earthquake evaluation times (years)

**CARD IN-SERVICE INSPECTION TIMES**  
 READ Only if NINSPT > 0

ID

4B

VARIABLE	COLUMNS	FORMAT	DESCRIPTION
TINSPT	1-80	8E10.3	In-service inspection times (years)

**CARD LEAK RATE AND DETECTION DEFINITIONS**  
 READ Always

ID

4C

VARIABLE	COLUMNS	FORMAT	DESCRIPTION
FNDLK	1-10	E10.3	Threshold for detectable leak rates.
ALKBIG	11-20	E10.3	Threshold for discriminating between leaks and big leaks.
EVLEAK	21-30	E10.3	Pathway loss coefficient (velocity heads per mm of wall thickness), use 3 for SCC crack and 6 for fatigue crack. Default is 3.
FKLEAK	31-40	E10.3	Surface roughness. Use 0.0002441 in. for SCC crack and 0.00015748 in. for fatigue crack. Default is SCC crack (0.0002441 in.)

**CARD STRATIFIED SAMPLE SPACE**  
 READ Only if ISQARE ≠ 0

ID

5A

VARIABLE	COLUMNS	FORMAT	DESCRIPTION
NAOH	1-5	I5	Number of divisions of the a/h coordinate in the sample space definition. The a/h coordinate is limited to the region $AOHLOW \leq a/h \leq AOHUP$ .
NAOB	6-10	I5	Number of divisions of the a/b coordinate in the sample space definition. The a/b coordinate is limited to the region $AOBLFT \leq a/b \leq AOBRTG$ .
AOHLOW	11-20	E10.3	Lower limit on the a/h coordinate.
AOHUP	21-30	E10.3	Upper limit on the a/h coordinate.
AOBLFT	31-40	E10.3	Lower limit on the a/b coordinate.
AOHRGT	41-50	E10.3	Upper limit on the a/b coordinate.

**CARD STRATIFIED SAMPLE SPACE [cont.]**  
 READ Only if ISQARE = 0

ID

5A

VARIABLE	COLUMNS	FORMAT	DESCRIPTION
AOHSIZ(M,1)	1-10	E10.4	Lower boundary of the a/h coordinate in the definition of the M-th stratification cell.
AOHSIZ(M,2)	11-20	E10.4	Upper boundary of the a/h coordinate in the definition of the M-th stratification cell.
AOBSIZ(M,1)	21-30	E10.4	Left boundary of the a/b coordinate in the definition of the M-th stratification cell.
AOBSIZ(M,2)	31-40	E10.4	Right boundary of the a/b coordinate in the definition of the M-th stratification cell.
NUMTRY	41-50	I10	Number of trials to be taken from the M-th cell.

**CARD STRATIFIED SAMPLE SPACE [cont.]**  
 READ Only if ISQARE ≠ 0 and NTRIES > 0

ID

5A

VARIABLE	COLUMNS	FORMAT	DESCRIPTION
NUMTRY(M)	1-50	S110	Number of trials to be taken from the M-th cell.

**CARD STRESS VALUES**  
 READ Always

ID

6A

VARIABLE	COLUMNS	FORMAT	DESCRIPTION
SIGCLD	1-10	E10.3	Deadweight stress (ksi). This is the load-controlled stress in the cold shutdown condition.
SGDWTE	11-20	E10.3	Deadweight and restraint of thermal expansion components of stress in the hot normal operating condition.
OPPRES	21-30	E10.3	Normal operating pressure of the system (ksi).
PRFPRS	31-40	E10.3	Hydrostatic proof pressure (ksi). If no proof test is to be included, set this value to any arbitrary negative number.
SIGVIB	41-50	E10.3	Peak-to-peak value of the high-cycle vibratory stresses (ksi). If SIGVIB<0, no vibratory stresses are included.
VBTHLD	51-60	E10.3	Threshold value of the load ratio [ $R^*$ in Equation 4-4 and Section 3.9 of NUREG-2301], which is used in the vibratory stress model.

**CARD SPECIFICATIONS FOR THE TABLE OF  $g_{min}$   
 AND  $g_{max}$  FUNCTIONS**  
 READ Only if KTYPES > 1

ID

6B

VARIABLE	COLUMNS	FORMAT	DESCRIPTION
NX	1-5	I5	Number of entries in the a/b coordinate for the input of the $g^*_{min}$ and $g^*_{max}$ functions. In the current version, NX should always be 6.
NY	6-10	I5	Number of entries in the a/h coordinate for the input of the $g^*_{min}$ and $g^*_{max}$ functions. In the current version, NY should always be 9.
IX	11-15	I5	Number of entries in the a/b coordinate for the internal tables of $g_{min}$ and $g_{max}$ .
IY	16-20	I5	Number of entries in the a/h coordinate for the internal tables of $g_{min}$ and $g_{max}$ . Optimum values for IX and IY are 20.

**CARD A/H COORDINATES FOR TABULAR INPUT OF  
 CONTRIBUTION OF RADIAL GRADIENT THERMAL  
 STRESSES TO STRESS INTENSITY FACTORS**  
 READ Only if KTYPES > 1

ID

6C

VARIABLE	COLUMNS	FORMAT	DESCRIPTION
AAOH(I)	1-80	8F10.3	Values of the a/h coordinate in the tabulated input for the contribution of radial gradient thermal stress to the stress intensity factor ( $I=1, \dots, NY$ )

**CARD B/A COORDINATES FOR TABULAR INPUT OF CONTRIBUTION OF RADIAL GRADIENT THERMAL STRESSES TO STRESS INTENSITY FACTORS**

ID

6D

READ Only if KTYPES > 1

VARIABLE	COLUMNS	FORMAT	DESCRIPTION
ABOA(I)	1-80	8F10.3	Values of the b/a coordinate in the tabulated input for the contribution of radial gradient thermal stress to the stress intensity factor (I=1,...,NX).

**CARD FREQUENCY OF HEAT UP/COOL DOWN AND TRANSIENTS**

ID

6E

READ Always

VARIABLE	COLUMNS	FORMAT	DESCRIPTION
NCYBLK	1-5	I5	Number of cycles in the equivalent event.
BLAMDA(K)	6-15	E10.0	Arrival time for transients.  If BLAMDA(K)>0.0: the k-th transient arrives at uniformly spaced intervals of BLAMDA(K) years.  If BLAMDA(K)<0.0: the k-th transient is treated as a Poisson process with ABS(BLAMDA[K]) as the average number of arrivals per year.  If stress corrosion crack initiation is included, then BLAMDA(K) should always be greater than 0.0 (the arrival times uniformly spaced).
TEMP(K)	16-20	F5.1	Coolant temperature (°F) for K=1. Temperature excursion during the transient for K>1.
TITLE(K)	21-80	6A10	Description for the k-th transient.

**CARD FATIGUE CRACK INITIATION INPUTS FACTORS**

ID

6E1

READ If INCIAT=3. This card should follow immediately after 6E. The data are for each transient, K. Components of stresses are in terms of cyclic stress =  $\sigma_{max} - \sigma_{min}$  rather than stress amplitude =  $\frac{1}{2}(\sigma_{max} - \sigma_{min})$  as used in ASME Section III fatigue evaluations

VARIABLE	COLUMNS	FORMAT	DESCRIPTION
EDOTF(K)	1-10	E10.0	Strain rate (% per second).
NTRNTYPE(K)	11-20	I10	Transient type: 1: specify tension, bending, thermal gradients (on this card) 2: provide a TIFFANY file (Card 6F).
STRUNIF(K)	21-30	E10.0	Tension components (ksi) (if NTRNTYPE[k]=1) Not used if K=1.
STRBEND(K)	31-40	E10.0	Bending components (ksi) (if NTRNTYPE[k]=1). Not used if K=1.
STRGRAD(K)	41-50	E10.0	Thermal gradient components (ksi). (if NTRNTYPE(k)=1) Not used if K=1.

**CARD ANGULAR VARIATION OF STRESS**  
 READ if INCIAT=3 AND NstrDis=1  
 For each transient, k. This card should follow 6E1

ID

6E2

VARIABLE	COLUMNS	FORMAT	DESCRIPTION
ANGMULTS (K,I)	1-10	8E10.0	Multipliers on the stress and computed stress-intensity factors for the initiated cracks. (I=1,ICRACKS)

**CARD TABULATED FUNCTIONS FOR  $g^*_{min}$  AND  $g^*_{max}$**   
 READ if K>1 and INCIAT ≠ 3.  
 If INCIAT = 3, then read if K>1 and NTRNTYPE(K) = 2.

ID

6F

VARIABLE	COLUMNS	FORMAT	DESCRIPTION
GDAMIN(I,J,K)	1-72	9F8.5	$g^*_{min,a}(J=1,..., NY)$
GDAMAX(I,J,K)	1-72	9F8.5	$g^*_{max,a}(J=1,..., NY)$
GDAMIN(I,J,K)	1-72	9F8.5	$g^*_{min,b}(J=1,..., NY)$
GDAMAX(I,J,K)	1-72	9F8.5	$g^*_{max,b}(J=1,..., NY)$

**CARD COEFFICIENTS FOR THE POLYNOMIAL THAT DEFINES  
 THE CONTRIBUTION OF WELDING RESIDUAL STRESSES  
 TO THE STRESS INTENSITY FACTOR IN THE DEPTH  
 DIRECTION**

ID

6G

READ Only if ISIGRS=1 on Card 1B

VARIABLE	COLUMNS	FORMAT	DESCRIPTION
B(L,K)	1-80	8E10.3	B(L,K), L=1,..., LLA  A separate card is used for each value of K (K = 1,..., KKA).  LLA corresponds to L in Equation 5-5; KKA corresponds to K in Equation 5-5.

**CARD COEFFICIENTS FOR THE POLYNOMIAL THAT DEFINES  
THE CONTRIBUTION OF WELDING RESIDUAL STRESSES  
TO THE STRESS INTENSITY FACTOR IN THE LENGTH  
DIRECTION**

ID

6H

READ Only if ISIGRS=1 on Card 1B

VARIABLE	COLUMNS	FORMAT	DESCRIPTION
B(L,K)	1-80	8E10.3	B(L,K), L=1,..., LLB  A separate card is used for each value of K (K = 1,..., KKB).  LLB corresponds to L in Equation 5-5; KKA corresponds to K in Equation 5-5.

**CARD EARTHQUAKES PER MAGNITUDE CATEGORY**

ID

7A

READ Only if NQUAKE =1 on Card 1B

VARIABLE	COLUMNS	FORMAT	DESCRIPTION
NEQCLS(N)	1-80	16I5	Number of earthquakes in the n-th magnitude category. A maximum of ten earthquakes can be modeled in each category.

**CARD SEISMIC CRACK GROWTH PARAMETERS**

ID

7B

READ Only if NQUAKE =1 on Card 1B

VARIABLE	COLUMNS	FORMAT	DESCRIPTION
----------	---------	--------	-------------

The following card is repeated for each earthquake that is modeled. They are grouped by earthquake category, while LEQ is the index on earthquakes within an intensity category.

NYNCEQ (N,LEQ)	1-10	I10	Number of equivalent constant amplitude cycles used to represent the crack growth.
SIGEQ (N, LEQ)	11-20	F10.3	Stress amplitude (ksi)
SGEQMX (N, LEQ)	21-30	F10.3	Maximum stress during the event (ksi) (used in the failure criteria).
TITLE (N, LEQ)	31-80	5A10	Description of this particular earthquake.

**CARD INPUTS FOR MID-LIFE CHANGES IN OPERATING STRESSES, CHEMISTRY, OR RESIDUAL STRESS**

ID

8A

READ Only if IREMEDI > 0

VARIABLE	COLUMNS	FORMAT	DESCRIPTION
RTIMES(I)	1-10	E10.4	Time (years) at which one or more of the following variables are changed.
THICKS(I)	11-20	E10.4	Wall thickness of pipe (inches).
OSTARS(I)	21-30	E10.4	Oxygen concentration in coolant at start-up (ppm).
OSTDYS(I)	31-40	E10.4	Oxygen concentration in coolant at steady-state (ppm).
CONDUS(I)	41-50	E10.4	Coolant conductivity (ms/cm).
SIGCLDS(I)	51-60	E10.4	Deadweight stress (ksi).
SDWTES(I)	61-70	E10.4	Deadweight and restraint of thermal expansion components of stress in the hot normal operating condition (ksi).
SGVIBS(I)	71-80	E10.4	Peak-to-peak value of the high-cycle vibratory stresses (ksi). If SIGVIB < 0, no vibratory stresses are modeled.

**CARD INPUTS FOR MID-LIFE CHANGES IN OPERATING STRESSES, CHEMISTRY, OR RESIDUAL STRESS [continued]**

ID

8B

READ Only if IREMEDI > 0

VARIABLE	COLUMNS	FORMAT	DESCRIPTION
ISIGRX(I)	1-10	I10	IHSI or MSIP residual stress flag (6 or 7). A value of 7 indicates no change from the previous state.
RSINMS(I)	11-20	E10.4	Mean value of the stress at the ID (ksi). (MSIP or IHSI stress). Not required if ISIGRX(I) is 7.
RSISDS(I)	21-30	E10.4	Standard deviation value of the stress at the ID (ksi). (MSIP or IHSI stress). Not required if ISIGRX(I) is 7.

## C.8 References

Carslaw, H.S., and J. C. Jaeger. 1959. *Conduction of Heat in Solids*, second edition, Clarendon Press, Oxford.

Cohen, L. M., J. L. McLean, G. Moy, and P. M. Besuner. 1977. *Improved Evaluation of Nozzle Corner Cracking*, EPRI NP-399, Electric Power Research Institute, Palo Alto, California.

Dedhia, D. D., D. O. Harris, and V. E. Denny. 1982. *TIFFANY: A Computer Code for Thermal Stress Intensity Factors for Surface Cracks in Clad Piping*, SAI-331-82-PA, Science Applications, Inc., Palo Alto, California, November 1982 (LLNL Contract No. 8679501, Task 2).

Harris, D. O., D. D. Dedhia, E. D. Eason, and S. P. Patterson. 1986. *Probability of Failure in BWR Reactor Coolant Piping*, NUREG/CR-4792, Vol. 3, U.S. Nuclear Regulatory Commission, Washington, D.C.

Harris, D. O., D. Dedhia, and S. C. Lu. 1992. *Theoretical and User's Manual for pc-PRAISE*, NUREG/CR-5864, U.S. Nuclear Regulatory Commission, Washington, D.C.

Harris, D. O., E. Y. Lim, and D. D. Dedhia. 1981. *Probability of Pipe Fracture in the Primary Coolant Loop of a PWR Plant, Vol. 5: Probabilistic Fracture Mechanics Analysis*, NUREG/CR-2189, Vol. 5, U.S. Nuclear Regulatory Commission, Washington, D.C.

Keisler, J. M., and O. K. Chopra. 1995. "Statistical Analysis of Fatigue Strain-Life Data for Carbon and Low-Alloy Steels," *Risk and Safety Assessment: Where is the Balance?*, ASME PVP-Vol. 296/SERA-Vol. 3, pp. 355-366.

Keisler, J. M., O. K. Chopra, and W. J. Shack. 1995. *Fatigue Strain-Life Behavior of Carbon and Low-Alloy Steels, Austenitic Stainless Steels, and Alloy 600 in LWR Environments*, NUREG/CR-6335, U.S. Nuclear Regulatory Commission, Washington, D.C.

Keisler, J. M., O. K. Chopra, and W. J. Shack. 1996. "Statistical Models for Estimating Fatigue Strain-Life Behavior of Pressure Boundary Materials in Light Water Reactor Environments," *Nuclear Engineering and Design*, Vol. 167, pp. 129-154.

Lim, E. Y. 1981. *Probability of Pipe Fracture in the Primary Coolant Loop, of a PWR Plant, Vol. 9: PRAISE Computer Code User's Manual*, NUREG/CR-2189, Vol. 9, U.S. Nuclear Regulatory Commission, Washington, D.C.

Timoshenko, S., and J. N. Goodier. 1951. *Theory of Elasticity*, Second Edition, McGraw Hill Book Co., New York.

## Appendix D

### A Review of Stress Intensity Factors for Semi-Elliptical Circumferential Interior Surface Cracks in Pipes

#### D.1 Introduction

Circumferential interior surface cracks in pipes are considered in the PRAISE software, which was originally developed in 1981 (Harris et al. 1981). Figure D.1 shows the crack configuration considered. Influence functions were developed at that time, which allowed the evaluation of stress intensity factors for complex radial variations of stress, such as occur in pipes during rapid coolant temperature excursions. These influence functions were incorporated into the TIFFANY software (Dedhia et al. 1982), which is used to develop stress-intensity factors because of radial gradient thermal stresses for use in PRAISE analyses. The influence functions were updated in 1984 (Dedhia and Harris 1984) to improve their accuracy, but not much has been done to them since. The improved influence functions have been incorporated into TIFFANY.

A great deal of work has been performed on computation of stress-intensity factors in cracked pipes since the original development of the influence functions as part of the PRAISE code development. The purpose of this document is to review the more recent work and assess the accuracy of the existing influence functions.

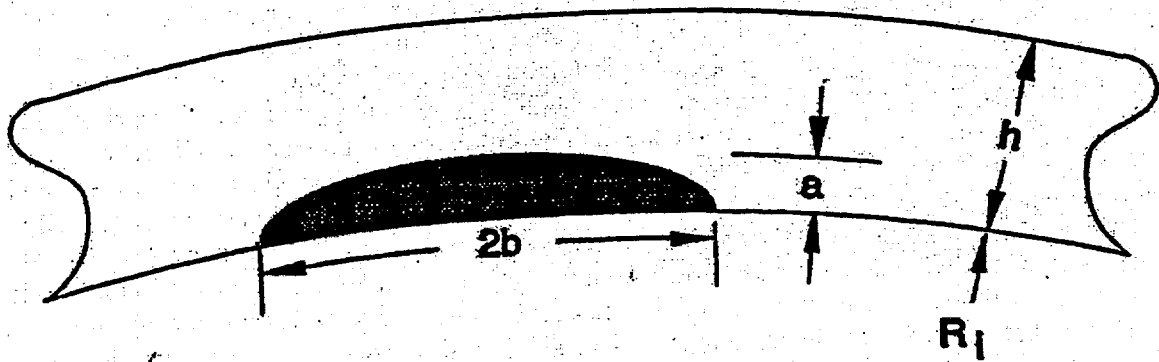


Figure D.1 Semi-Elliptical Circumferential Crack at the Inner Surface of a Pipe

#### D.2 Review of Original PRAISE Computations

As reported in Appendix B of Harris et al. (1981), numerical calculations of the stresses and crack surface displacements were made by the use of boundary integral equation techniques. At that time, the existing stress intensity solutions for semi-elliptical surface cracks in pipes were very limited, and information that included stress gradients was even sparser. Appendix B of Harris et al. (1981) reports the results and compares them to information existing at that time. These results are also reviewed in Lim et al. (1983).

One of the main outcomes from the original set of results was the remarkable similarity of stress intensity factors in flat plates, axial cracks in pipes, and circumferential cracks in pipes. The three different crack configurations were indistinguishable within the range of crack sizes considered at that time, which was  $a/h$  from 0 to 0.8,  $a/b$  from 1 to 1/6, and  $RI/h$  of 5, 10, and infinity (flat plate). The similarity of the results for the different crack orientations is mentioned in Harris et al. (1981) and Lim et al. (1983). The influence functions in TIFFANY were developed for circumferential cracks, but are equally applicable for flat plates and axial cracks with a degree of accuracy comparable to the accuracy of the results themselves. The similarity of the results came as something of a surprise to many in the fracture mechanics community, including the authors. Extensive computations have been made on axial and circumferential cracks in the intervening years, and the similarity has been observed by many more recent investigators. One example is the quote from Chen et al. (1991), who states in his abstract that "According to these results, the stress intensity factors for a semi-elliptical surface crack in a hollow cylinder can be approximated by those for a semi-elliptical surface crack in a plate within about 3% in the case when  $RI/h > 2.5$ ,  $b/a$  from 1 to 2 and  $b/h < 0.6$ ." Similarly, Keeney and Bryson (1995) found that "...there are essentially no differences between calculated SIFs for circumferential and axial inner-surface flaws having  $a/h$  less than 0.3. Small differences (~5%) can be observed for flaw geometries having an  $a/h$  of 0.5 and  $2b/a=10$ ." Numerous additional such conclusions can be found in the literature. The similarities of results for different crack configurations will be further shown later in some comparisons, and the small influence of  $RI/h$  will be shown in the review of the most recent and comprehensive set of results for circumferential cracks provided by Chapuliot et al. (1998).

One important aspect of the subcritical crack growth analysis in PRAISE is the use of the (square) root (of the) mean square (RMS)-averaged stress-intensity factors, rather than just the local values. All stress intensity factors used in PRAISE and calculated by TIFFANY are RMS values. Hence, all values reported here are RMS values, unless explicitly stated otherwise. Many investigators report only the value of the stress intensity factor at the point of maximum crack depth,  $a$ , and the surface point,  $b$  (or close to the surface point, since the local value of  $K$  at the surface is zero). They handle stress gradients by considering polynomial curve fits to the stress variation with distance from the cracked surface (usually of third order). The author believes that the RMS-averaged values are more appropriate. They are related to the energy release rate as the crack extends in either the surface or depth direction while being constrained to remain an ellipse. They were especially useful in earlier years because they can be determined from the crack surface displacements for a single stress system on the crack face (usually uniform pressure), which eliminates the need to perform calculations for a variety of stresses, such as are necessary when considering polynomials. The need for additional calculations is not such a disadvantage now that computer time and memory is so much more economical. Figure D.2 schematically shows an elliptical crack that is fixed in the length direction ( $b$ ) and allowed to grow in the depth direction ( $a$ ).

The energy release rates for cracks growing in the  $a$  and  $b$  directions are related to the local values of  $K$  by the following relations:

$$\frac{EG_a}{1-\nu^2} = \bar{K}_a^2 = \frac{1}{\Delta A_a} \int_{-\pi/2}^{\pi/2} K^2(\phi) d[\Delta A_a(\phi)]$$

$$\frac{EG_b}{1-\nu^2} = \bar{K}_b^2 = \frac{1}{\Delta A_b} \int_{-\pi/2}^{\pi/2} K^2(\phi) d[\Delta A_b(\phi)] \quad (D.1)$$



Equations D.1 and D.2 allow the RMS values of K to be evaluated from the local values.

Improved influence functions were reported in Dedhia and Harris (1984) and were incorporated into TIFFANY. Comparisons of results generated by use of the improved influence functions were made with the results for axial cracks in a cylinder with  $R_1/h = 10$  reported by Raju and Newman (1982). Raju and Newman reported results for stresses on the crack face that varied as  $(x/a)^n$ , with n equal to 0, 1, 2, and 3 (x is the radial distance from the inner surface of the pipe). They reported values as a function of position on the crack front, so RMS values could be calculated. If the stresses are expressed as

$$\sigma(u) = \sigma_0 + \sigma_1 u + \sigma_2 u^2 + \sigma_3 u^3 \quad (D.3)$$

where  $u = x/h$ , then the stress intensity factors can be expressed as

$$K = (\sigma_0 i_0 + \sigma_1 i_1 \alpha + \sigma_2 i_2 \alpha^2 + \sigma_3 i_3 \alpha^3) \sqrt{\pi a} \quad (D.4)$$

Table D.1 provides the local and RMS results of Raju and Newman (1982) in terms of the dimensionless parameters  $i_n$ . The values of  $a/h$  and  $a/b$  are the ones that are included in Raju and Newman (1982).

Figures D.3 to D.5 present comparisons of the Raju and Newman (1982) RMS values with the corresponding results obtained by use of the influence functions in TIFFANY. The four lines and four sets of data points in Figures D.3 to D.5 (and subsequent figures in this appendix) correspond to the values for the exponent n from zero to three. The top line is for  $n = 0$ , with n increasing monotonically for successively lower lines. The lines are for the influence functions and the data points are as tabulated from other investigators. The plot on the right is for the depth direction ( $K_z$ ), and the plot on the left is for the surface direction ( $K_s$ ).

Figures D.3 to D.5 are included in Dedhia and Harris (1984). They show fairly good agreement between Raju and Newman's RMS values and the corresponding values from the influence function within the limited range of  $a/b$  for which information is available.

Many investigators report only the local values of K at the deepest point and at the surface. Table D.1 provides a direct comparison of these two types of values as generated by Raju and Newman (1982). The table shows the similarity, but the comparison is better seen by repeating Figures D.3 to D.5, but now with the local values, as shown in Figures D.6 to D.8.

Figures D.6 to D.8 show a much poorer agreement between the influence function results and the local values than was observed for the RMS values in Figures D.3 to D.5. The local a values are consistently higher than the influence function results, and the local b values are consistently lower. The disagreement is especially pronounced for the b direction and larger values of the exponent n.

At this point, it appears that stress intensity factors for flat plates and axial and circumferential cracks in cylinders are very similar and that the TIFFANY influence function provides results that are in good agreement with the RMS values generated from the local values reported by Raju and Newman (Raju and Newman 1982). The agreement is not so good for the local values, especially in the b direction with the larger exponents.

Exponent	a/h		a/b = 1		a/b = 1/2.5		a/b = 1/5	
			Depth	Surface	Depth	Surface	Depth	Surface
0	0.2	RMS	0.653	0.681	0.877	0.738	0.982	0.770
		local	0.646	0.726	0.932	0.676	1.062	0.578
	0.5	RMS	0.678	0.718	0.990	0.861	1.248	0.954
		local	0.669	0.777	1.058	0.814	1.359	0.753
	0.8	RMS	0.702	0.764	1.155	1.046	1.656	1.255
		local	0.694	0.858	1.211	1.060	1.783	1.123
1	0.2	RMS	0.403	0.264	0.494	0.283	0.535	0.287
		local	0.455	0.125	0.584	0.109	0.641	0.075
	0.5	RMS	0.412	0.274	0.536	0.320	0.627	0.350
		local	0.464	0.141	0.629	0.153	0.746	0.132
	0.8	RMS	0.425	0.284	0.597	0.372	0.786	0.451
		local	0.484	0.162	0.701	0.225	0.914	0.241
2	0.2	RMS	0.305	0.154	0.358	0.163	0.381	0.165
		local	0.375	0.047	0.455	0.037	0.490	0.022
	0.5	RMS	0.309	0.158	0.378	0.179	0.426	0.194
		local	0.380	0.054	0.477	0.060	0.544	0.050
	0.8	RMS	0.318	0.161	0.412	0.202	—	0.198
		local	0.394	0.063	0.523	0.092	0.639	0.099
3	0.2	RMS	0.249	0.105	0.284	0.110	0.288	0.108
		local	0.326	0.024	0.383	0.018	0.417	0.010
	0.5	RMS	0.251	0.107	0.297	0.119	0.327	0.128
		local	0.328	0.028	0.397	0.031	0.440	0.026
	0.8	RMS	0.258	0.109	0.319	0.131	0.374	0.152
		local	0.339	0.032	0.429	0.049	0.504	0.053

All values are in terms of  $i_n$  in Equation D.4, with n being the "exponent."

### D.3 Comparisons with Recent Results

The earlier comparisons, as summarized in the above section, showed that the TIFFANY influence functions agree well with the results of others for the range of crack sizes for which results were available. Considerable additional work has been performed on surface cracks in pipes since the review summarized above, which does not contain any results newer than 1984. Typical runs made by use of pcPRAISE (Harris et al. 1981; Harris et al. 1992) may involve crack sizes outside the range considered in the original development of the influence functions. It is therefore desirable to use the influence functions to generate results for a wider range of crack sizes and compare them with recent results.

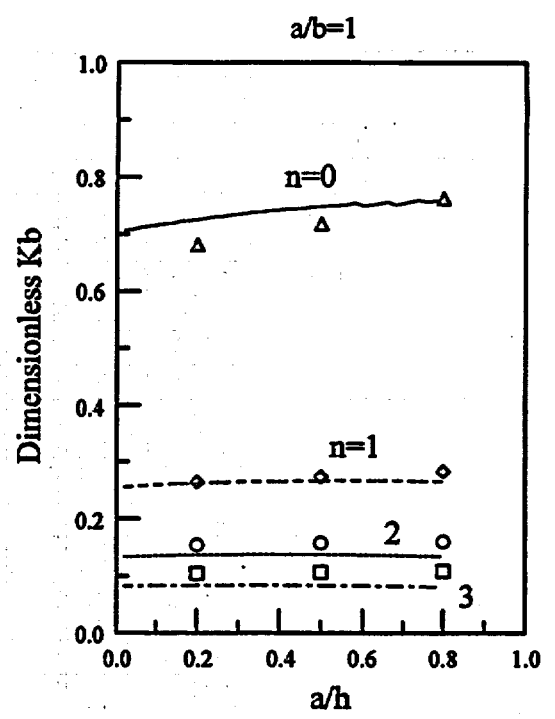
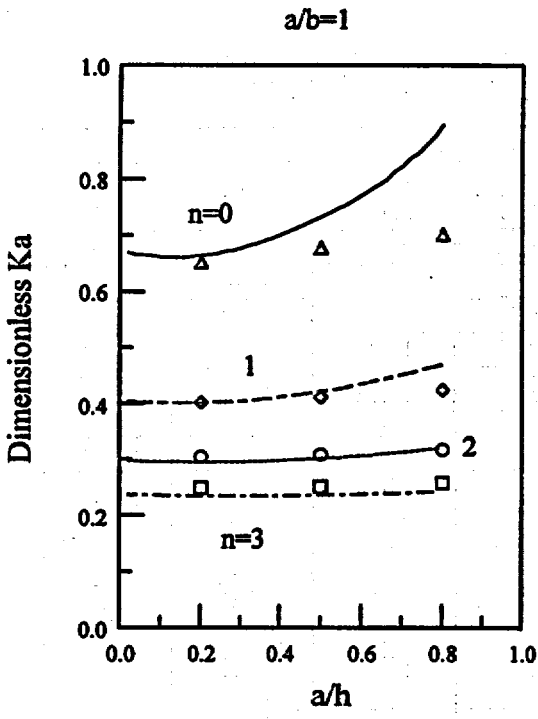


Figure D.3 Comparison of Raju-Newman RMS Values of  $i_n$  with RMS Results from TIFFANY,  $a/b=1$

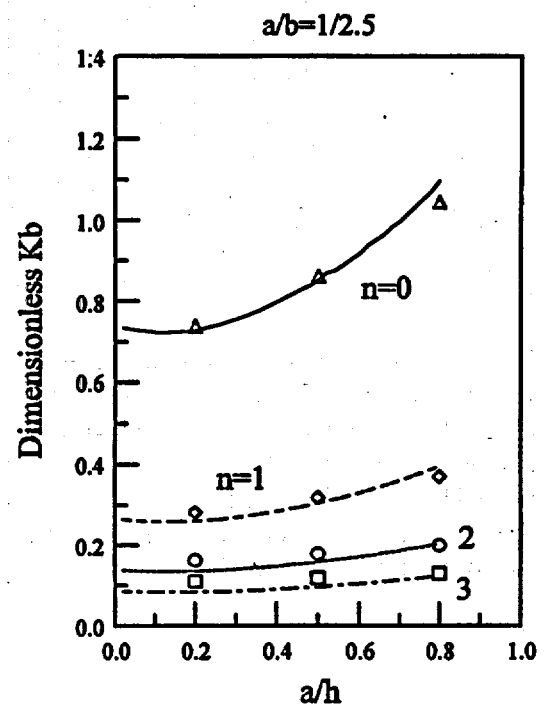
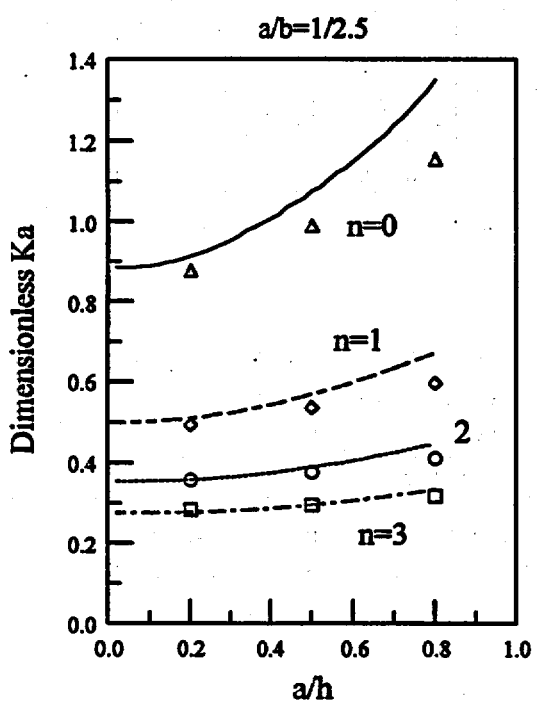


Figure D.4 Comparison of Raju-Newman RMS Values with RMS Results from TIFFANY,  $a/b=1/2.5$

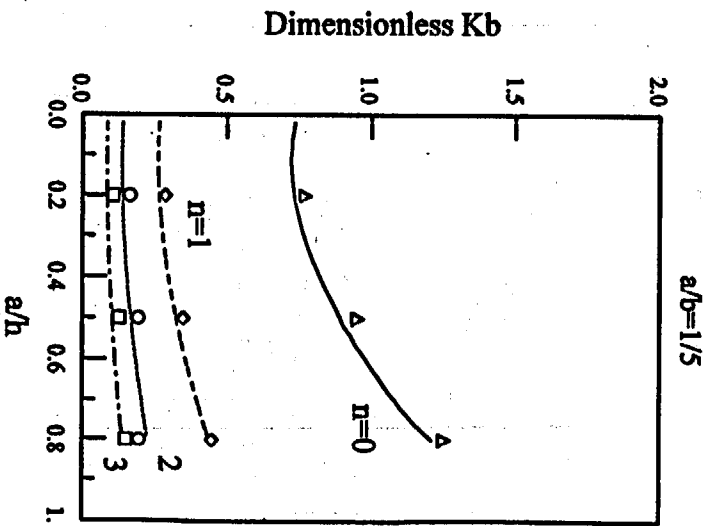
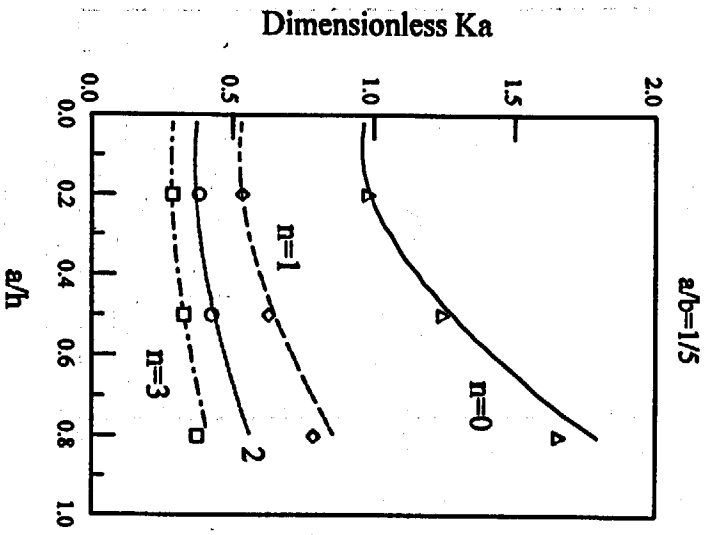


Figure D.5 Comparison of Raju-Newman RMS Values with RMS Results from TIEFANY,  $a/b=1/5$

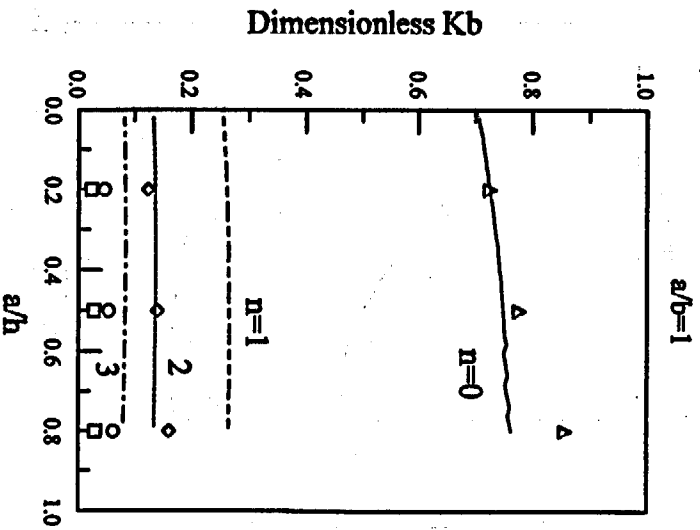
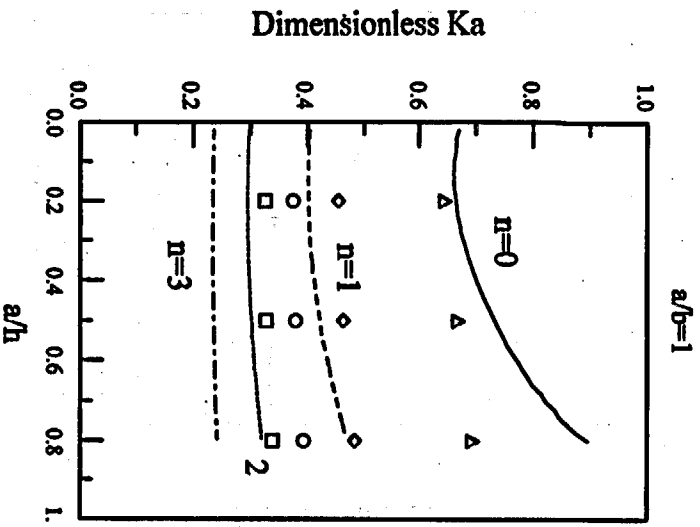


Figure D.6 Comparison of Raju-Newman Local Values with RMS Results from TIEFANY,  $a/b=1$

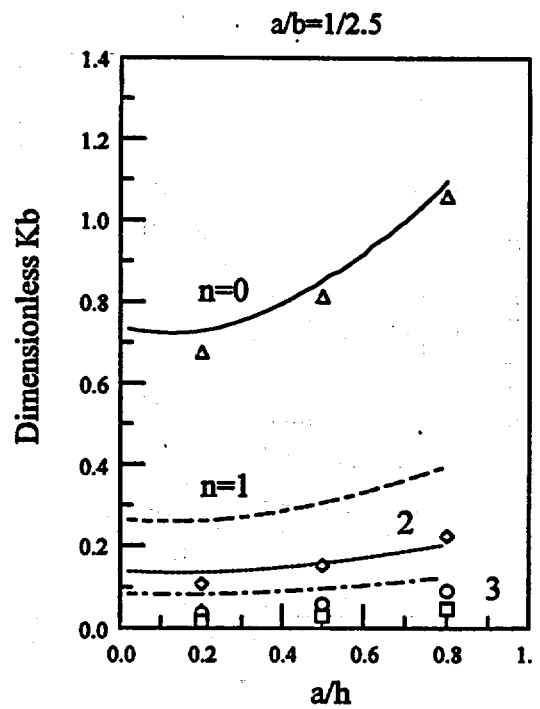
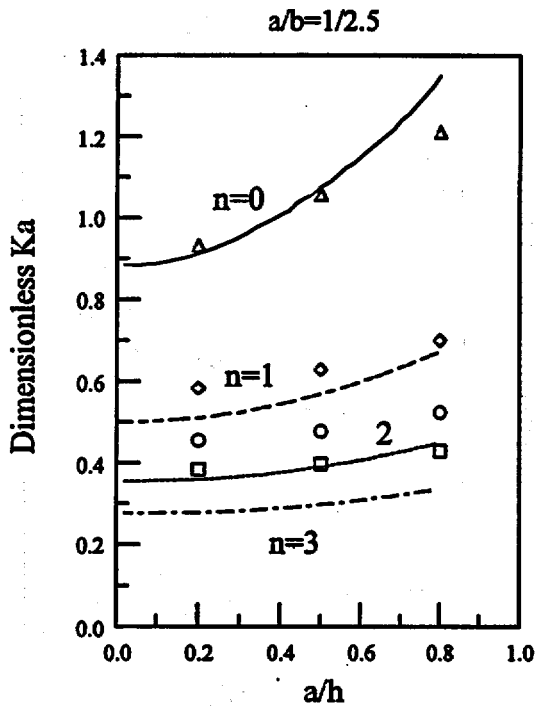


Figure D.7 Comparison of Raju-Newman Local Values with RMS Results from TIFFANY,  $a/b=1/2.5$

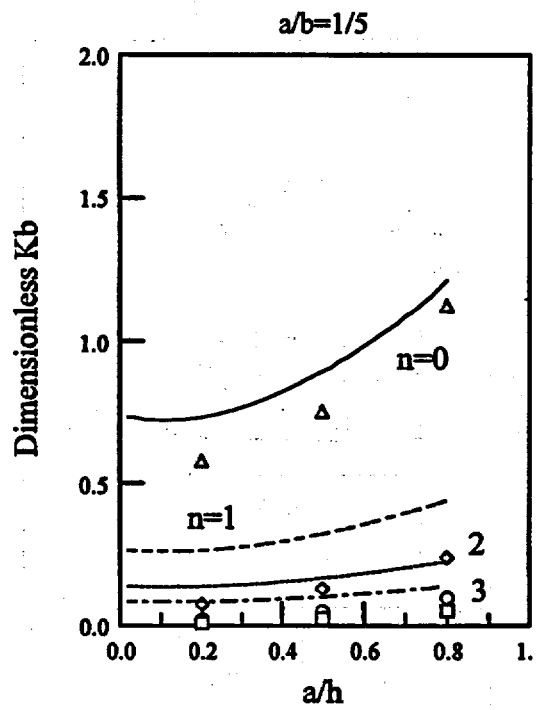
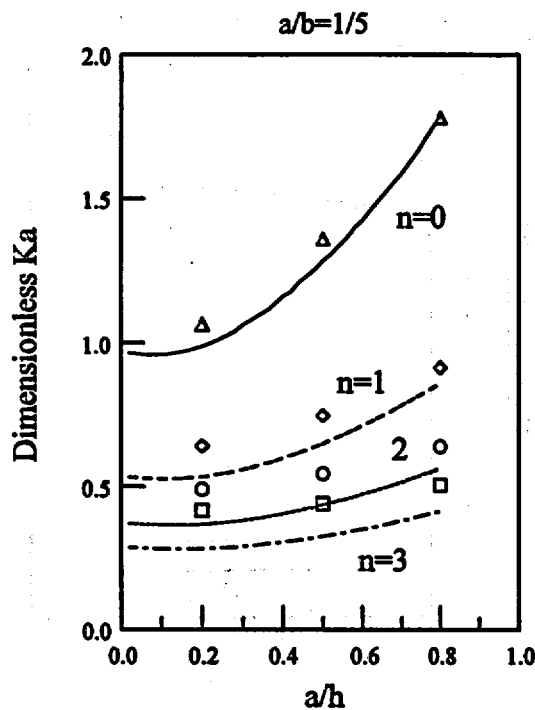


Figure D.8 Comparison of Raju-Newman Local Values with RMS Results from TIFFANY,  $a/b=1/5$

A computerized literature search was performed on cracks in cylinders. The initial search identified 146 pages of citations. These were trimmed to about 55 references for which abstracts were obtained. This process showed that there were sufficient literature sources on circumferential cracks, so that axial cracks were not considered further. Some six references were identified as being particularly relevant, but this review concentrates on the work of Chapuliot et al. (1998) because it is the most recent and contains by far the widest range of crack sizes and values of  $R_1/h$ . Chapuliot et al. (1998) provide comparisons with other publications that were identified, such as Bergman (1995), and they claim excellent agreement. Poette and Albaladejo (1991) is another useful publication. Chapuliot et al. (1998), provide only the local values at the deepest point and the surface. They provide results for  $a/b$  from 0 to 1,  $a/h$  from 0 to 0.8, and  $h/R_1$  from 0 (flat plate) to 1. Figures D.9 and D.10 provide comparisons of results generated by the TIFFANY influence functions with corresponding local results from Chapuliot et al. (1998). Results are included out to  $a/b$  of 1/16, which the smallest value considered by Chapuliot et al., other than complete circumferential cracks, which they consider as  $a/b=0$ . Once again, the results are for  $n=0-3$ , with  $n$  increasing down the figure. Figure D.9 provides results for the depth direction and Figure D.10 for the surface direction.

Figures D.9 and D.10 show fairly good agreement, but there are some considerable differences. However, the differences are similar to those observed in Figures D.6 to D.8 and can be attributed to the fact that local values are being compared to RMS values generated by the influence functions. The comparison in Figures D.9 and D.10 are similar to the comparison in Figures D.6 to D.8 in that the local  $a$  values are consistently above the RMS values (especially for  $n>0$ ), and the  $b$  values are consistently lower. The main conclusion to be drawn from Figures D.9 and D.10 is that the influence function results are well behaved for cracks much longer than were included in the original computations; results are provided out for  $a/b$  as small as 1/16. There is not good agreement in the  $b$  results shown in Figure D.10, and the agreement is poorer as  $a/b$  decreases and  $n$  increases. The final frame in Figure D.10 shows some large discrepancies, but these may largely be due to comparisons between local and RMS values.

Another factor in discrepancies for the  $b$  direction is complications at the free surface. Chapuliot notes a disagreement with Raju and Newman at the surface and states that "this discrepancy can be explained by the difficulty encountered in modeling the crack front in the area near the surface point for a long semi-elliptical defect." Table D.2 provides a comparison between Chapuliot et al. (1998), and Raju and Newman (1982).

Results for the depth direction agree very well, with the differences perhaps due to differences between circumferential and axial cracks. There is generally good agreement in the surface direction, but there are also some large differences especially for longer and deeper cracks with larger  $n$ . The lack of agreement shown in the surface direction suggests that there is some inaccuracy in the results in Table D.2. The results would not be so sensitive to the finite element modeling at the surface if the RMS values were employed because the RMS results do not depend solely on the surface value.

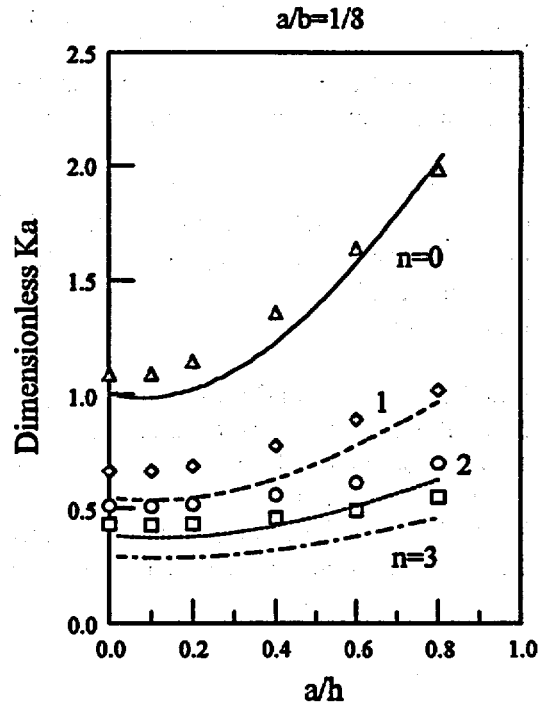
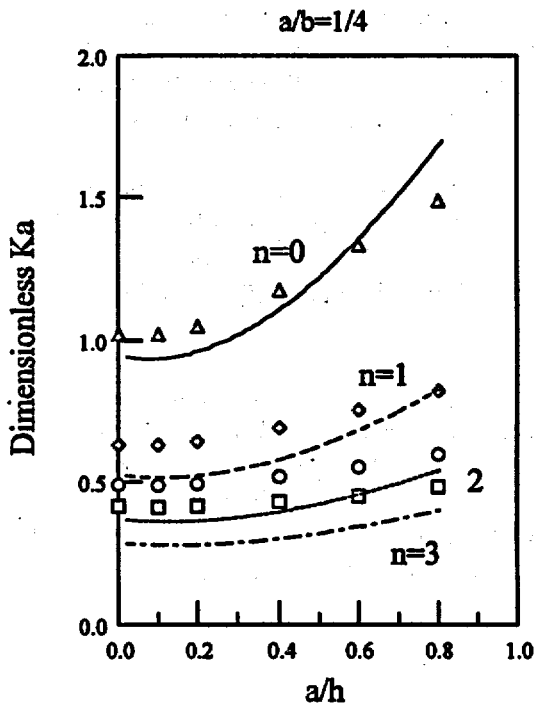
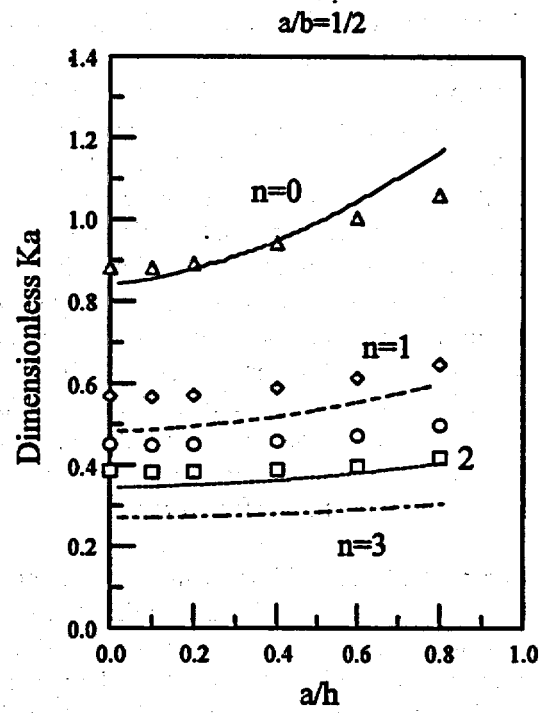
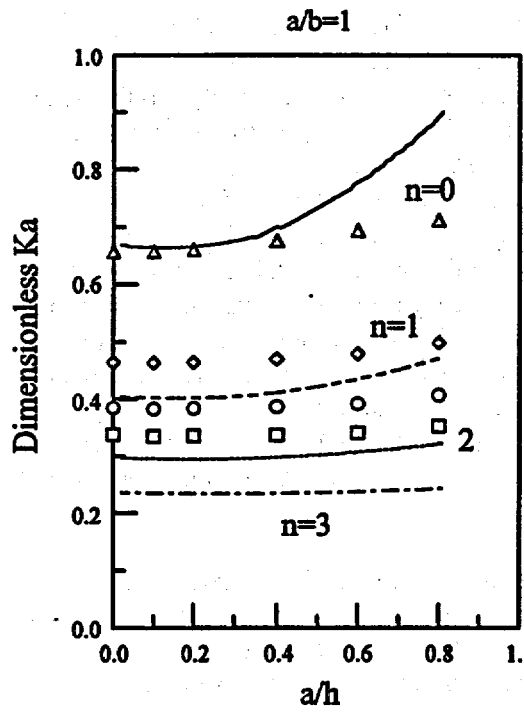


**Figure D.9 Dimensionless Stress Intensity Factors for Growth in the Depth Direction Showing Comparison of RMS TIFFANY Influence Function Results (lines) with Chapuliot et al. (1998) Local Results (points)**

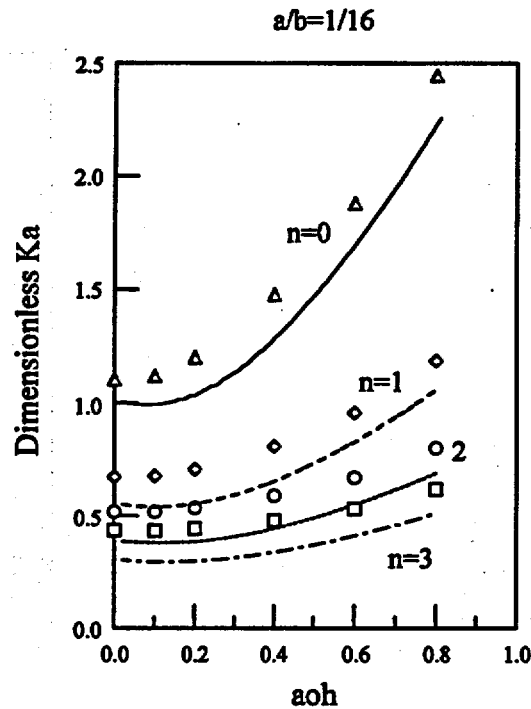


Figure D.9 (Continued)

#### D.4 Comparisons for Very Long Cracks

The above results are for  $a/b$  less than  $1/16$ . In some instances, PRAISE calculations may involve even longer cracks. Chapuliot et al. provide results for such cracks, and Table D.3 provides a comparison with the influence-function results.

Table D.3 shows the same behavior as observed earlier in that the local values of  $K$  are higher in the depth direction and lower in the surface direction than the RMS values. The RMS influence-function values do not become erratic at these very long cracks. The influence function curve fit is based on computations with  $2b/a$  less than 10, and the above table contains values of  $2b/a$  of up to 128. However, the RMS values for the surface length direction often increase as the crack gets longer, which is contrary to physical expectations and the results of Chapuliot. This behavior is not expected to cause problems in PRAISE calculations.

#### D.5 Comparisons for Very Deep Cracks

The above comparisons are all for cracks with  $a/h \leq 0.8$ . PRAISE calculations may involve cracks deeper than this. Murakami (1992) presents results for semi-elliptical cracks in plates that are close to or actually penetrating the back surface of the plate. He provides local results for tension and bending as a function of position along the crack front, from which RMS values can be obtained by use of Equations D.1 and D.2. Two sets of comparable results for tension and bending are used in PRAISE: 1) uniform or linearly varying stress from the influence function and 2) the polynomial curve fit for stress-intensity factors for uniform stress or bending. The polynomial fits for tension and bending are

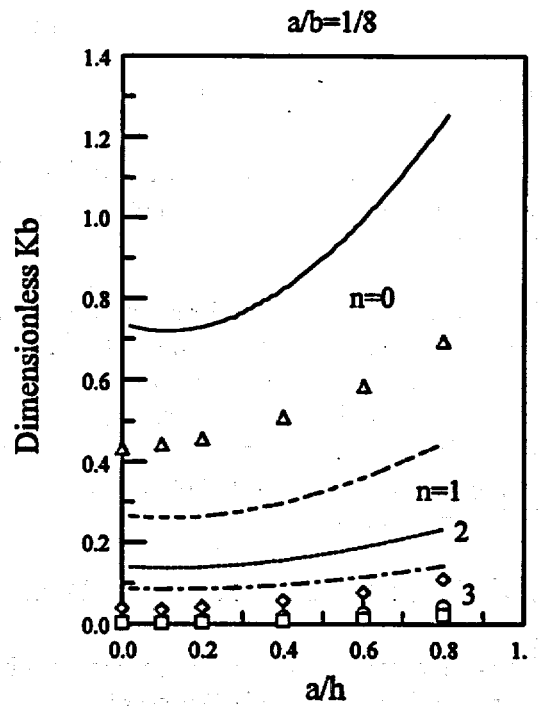
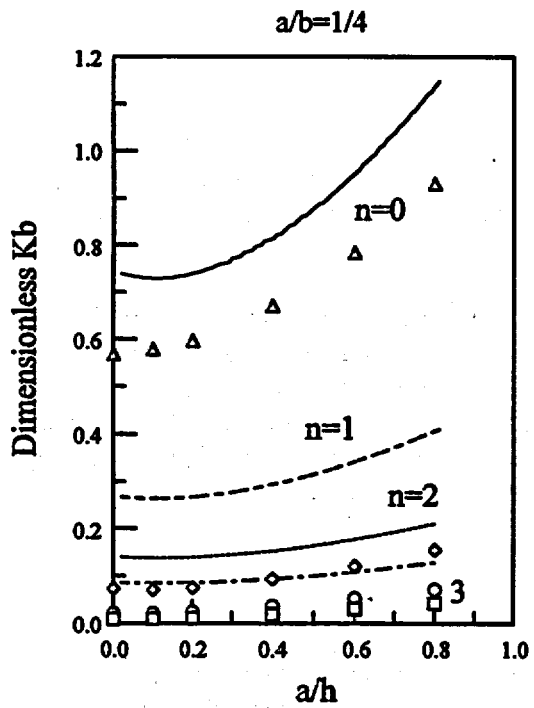
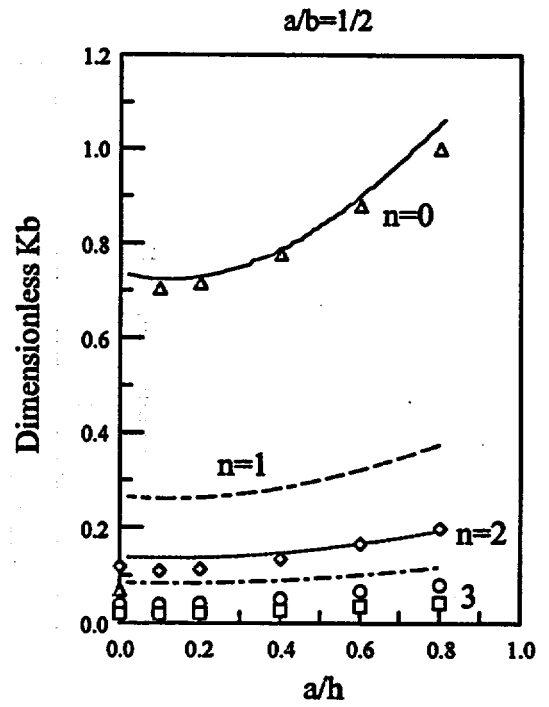
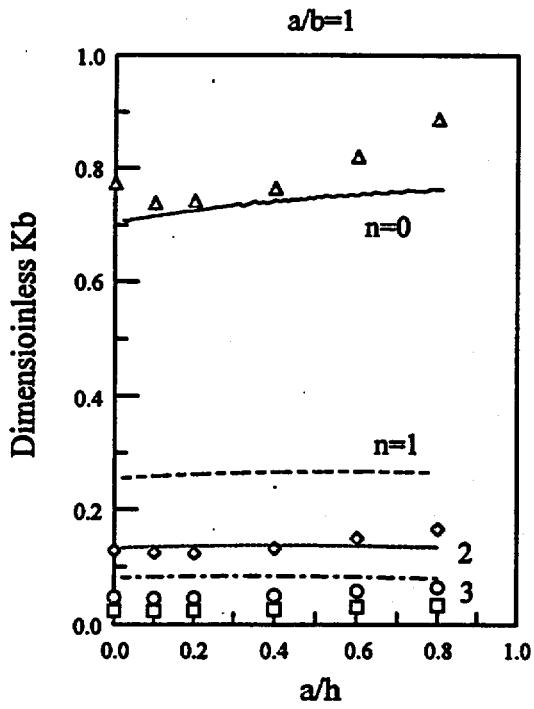


**Figure D.10 Dimensionless Stress Intensity Factors for Growth in the Surface Direction Showing Comparison of TIFFANY Influence Function RMS Results (lines) with Chapuliot et al. (1998) Local Results (points)**

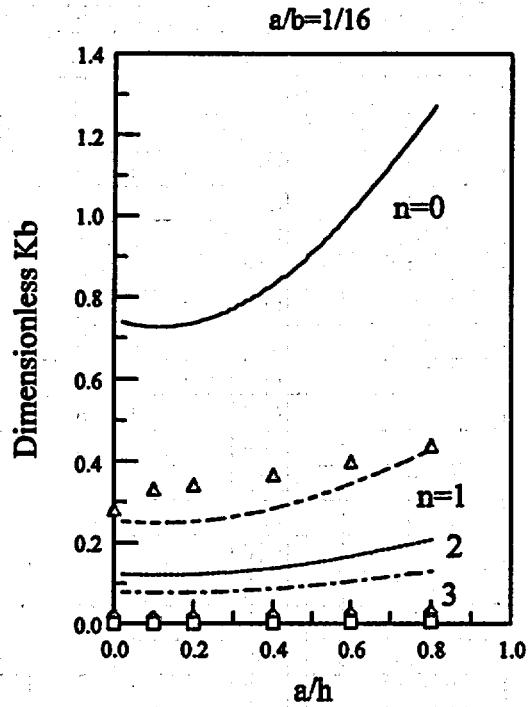


Figure D.10 (Continued)

Table D.2 Comparison of Local Dimensionless K from Raju-Newman (axial) with Chapuliot (circumferential), $R_r/h=10$								
		$a/b=1$		$a/b=1/2.5$		$a/b=1/5$		
Exponent	$a/h$		Depth	Surface	Depth	Surface	Depth	Surface
0	0.2	Chap	0.661	0.742	0.952	0.686	1.088	0.549
		R-N	0.646	0.726	0.932	0.676	1.062	0.578
	0.8	Chap	0.712	0.888	1.173	1.012	1.656	0.857
		R-N	0.694	0.858	1.211	1.060	1.783	1.123
1	0.2	Chap	0.465	0.124	0.594	0.103	0.651	0.064
		R-N	0.455	0.125	0.584	0.109	0.641	0.075
	0.8	Chap	0.498	0.166	0.694	0.200	0.884	0.155
		R-N	0.484	0.162	0.701	0.225	0.914	0.241
2	0.2	Chap	0.383	0.047	0.466	0.036	0.503	0.020
		R-N	0.375	0.047	0.455	0.037	0.490	0.022
	0.8	Chap	0.403	0.065	0.527	0.071	0.633	0.065
		R-N	0.394	0.063	0.523	0.092	0.639	0.099
3	0.2	Chap	0.335	0.024	0.395	0.018	0.421	0.009
		R-N	0.326	0.024	0.383	0.018	0.417	0.010
	0.8	Chap	0.350	0.034	0.438	0.044	0.508	0.034
		R-N	0.339	0.032	0.429	0.049	0.504	0.053

Note: The Chapuliot values for  $a/b$  equal to  $1/2.5$  and  $1/5$  were obtained by cubic spline interpolation with parabolic end conditions.

			a/b = 1/16		a/b = 1/32		a/b = 1/64	
Exponent	a/h		Depth	Surface	Depth	Surface	Depth	Surface
0	0.2	Chap	1.202	0.342	1.178	0.171	1.167	0.086
		RMS	1.035	0.737	1.062	0.798	1.178	0.539
	0.8	Chap	2.446	0.439	2.573	0.220	2.636	0.110
		RMS	2.256	1.258	2.38	1.365	2.583	0.932
1	0.2	Chap	0.708	0.0194	0.722	0.0097	0.728	0.0048
		RMS	0.385	0.252	0.540	0.342	0.678	0.343
	0.8	Chap	1.188	0.0439	1.248	0.022	1.277	0.011
		RMS	1.073	0.430	1.098	0.580	1.377	0.585
2	0.2	Chap	0.535	0.0414	0.544	0.0207	0.549	0.0104
		RMS	0.387	0.123	0.016	0.157	0.444	0.227
	0.8	Chap	0.802	0.0139	0.841	0.007	0.860	0.003
		RMS	0.696	0.208	0.669	0.265	0.857	0.381
3	0.2	Chap	0.444	0.0018	0.452	0.0009	0.455	0.0004
		RMS	0.299	0.078	0.270	0.079	0.317	0.152
	0.8	Chap	0.619	0.0067	0.648	0.0033	0.662	0.0017
		RMS	0.518	0.132	0.481	0.132	0.585	0.254

used in PRAISE to streamline the calculations because the vast majority of stresses considered in PRAISE are either uniform or vary linearly through the thickness. The polynomial fits are based on influence function results for  $a/h \leq 0.8$  and provide good fits within this range. Hence, the results reviewed earlier did not consider the fits. However, the fits may be poor for deeper cracks, so the curve fit results are included below along with the results obtained by integration of the influence functions. The polynomial fits are given in Section 2.1.1 of Harris et al. (1992). Table D.4 provides the three sets of results for uniform tension.

Table D.5 summarizes the three sets of results for a linear stress gradient. Some of the values of K are negative for the case of through-wall bending. Therefore a stress system that varies linearly from a value of  $s$  at the crack surface to 0 at the opposite surface is considered in Table D.5

The results of Tables D.4 and D.5 show that neither the polynomial curve fits nor the influence function behaves erratically for very deep cracks. The infinite values at  $a/h=1$  for the polynomial curve fit is built into the assumed functional form. This singularity does not have a large effect even at cracks as deep as 95% of the wall thickness.

## D.6 Concluding Remarks

A great deal of information on stress intensity factors for circumferential cracks in pipes has become available since the last improvements in the influence functions for use with PRAISE in 1984. The work of Chapuliot et al. (1998) is very comprehensive and provides a good basis for comparing the PRAISE stress intensity factors with recent results. Such comparisons have been presented, and the largest source of disagreement appears to be due to the reporting of only local values of K at the depth and surface by Chapuliot and the use of RMS-averaged stress intensity factors by PRAISE. Hence, accurate direct comparisons cannot be made. In instances where direct comparisons can be made, such as with the work

of Raju and Newman (1982), the agreement is much better. Use of the influence functions for cracks that are much longer than included in the original computations reveals that the resulting stress intensity factors do not behave erratically, but do not show the expected behavior of decreasing K for the surface

Table D.4 Comparison of RMS Values of Dimensionless K for Very Deep Cracks with Uniform Tension					
a/h		a/b=1		a/b=1/5	
		Depth	Surface	Depth	Surface
0.80	Murakami	0.745	0.843	1.660	1.355
	IF	0.892	0.763	1.775	1.231
	Polynomial	0.896	0.762	1.793	1.209
0.85	Murakami	0.756	0.857	1.690	1.396
	IF	0.926	0.766	1.874	1.298
	Polynomial	0.956	0.779	1.930	1.298
0.90	Murakami	0.773	0.875	1.730	1.450
	IF	0.959	0.765	1.972	1.367
	Polynomial	1.056	0.828	2.140	1.442
0.95	Murakami	0.802	0.890	1.797	1.505
	IF	0.999	0.765	2.079	1.367
	Polynomial	1.314	0.950	2.636	1.780
1.0	Murakami	0.933	0.908	2.071	1.591
	IF	--	--	--	--
	Polynomial	∞	∞	∞	∞

Table D.5 Comparison of RMS Values of Dimensionless K/s√πa for Very Deep Cracks with Bending					
a/h		a/b=1		a/b=1/5	
		Depth	Surface	Depth	Surface
0.80	Murakami	0.408	0.624	1.404	1.486
	IF	0.513	0.549	1.084	0.879
	Polynomial	0.517	0.553	1.097	0.861
0.85	Murakami	0.389	0.622	1.570	1.539
	IF	0.515	0.541	1.103	0.900
	Polynomial	0.545	0.554	1.151	0.909
0.90	Murakami	0.374	0.622	1.676	1.555
	IF	0.517	0.530	1.123	0.925
	Polynomial	0.614	0.580	1.278	1.009
0.95	Murakami	0.356	0.618	1.717	1.497
	IF	0.520	0.516	1.134	0.950
	Polynomial	0.835	0.700	1.682	1.302
1.0	Murakami	0.362	0.611	1.781	1.487
	IF	--	--	--	--
	Polynomial	∞	∞	∞	∞

Stress = s at cracked surface, zero at other surface.

direction with increasing crack length. Comparisons of the influence functions for very deep cracks with the results of other investigators, and the associated polynomial curve fit for uniform and linearly varying stresses, shows that the PRAISE results do not behave erratically for crack depths approaching the wall thickness. In fact, the agreements are quite good, considering that the PRAISE results are based on computations with  $a/h \leq 0.8$ . Overall, the influence functions could be improved, but not with available information (because Chapuliot reports only surface and depth values).

A closely related question is the use of RMS versus local values of K for analysis of subcritical crack growth. It appears to the author that the RMS values are more physically appealing because the growth of elliptical cracks should be controlled by K along the crack front rather than just the local value. The fact that the RMS values are related to the strain-energy release rates adds credence to the use of RMS values. The fracture mechanics literature is divided-some use the local values, and some use the RMS values. However, the great majority use the local values, such as in the National Aeronautics and Space Administration (NASA) fracture control programs and in the NASGRO software developed for these programs. This question could be sorted out on the basis of experimental observations of fatigue crack growth of semi-elliptical cracks. These observations must be on specimens with complex stress gradients; otherwise, the local and RMS values are too close to one another, and the answer is lost in the scatter. To the author's knowledge, the definitive experiments related to this question remain to be performed.

If local values of K were to be used in PRAISE and TIFFANY, then the influence functions could be improved, based on the tabulations in Chapuliot et al. (1998). If information on values of K at some intermediate positions on the crack front could be obtained from Chapuliot, then the PRAISE influence functions could be economically updated and the use of RMS values retained.

## D.7 References

Bergman, M. 1995. "Stress Intensity Factors for Circumferential Surface Cracks in Pipes," *Fatigue and Fracture in Engineering Materials and Structures*, Vol. 18, No. 10, pp. 1155-1172.

Chapuliot, S., M. H. Lacroix, and P. LeDellou. 1998. "Stress Intensity Factors for Internal Circumferential Cracks in Tubes Over a Wide Range of Radius Over Thickness Ratios," *Fatigue, Fracture, and High Temperature Design Methods in Pressure Vessels and Piping - 98*, ASME PVP-Vol. 365, pp. 95-106.

Chen D., H. Nisitani, and K. Mori. 1991. "Tension or Bending of Cylindrical Vessels with a Surface Crack," *Trans. Japanese Society of Mechanical Engineers, Part A*. Vol. 57, No. 540, pp. 1710-1714.

Dedhia, D., D. O. Harris, and V. E. Denny. 1982. *TIFFANY: A Computer Code for Thermal Stress Intensity Factors for Surface Cracks in Clad Piping*, Report SAI-331-82-PA, Science Applications, Inc., Palo Alto, California (LLNL Contract No. 8679501, Task 2).

Dedhia, D., and D. O. Harris. 1984. "Improved Influence Functions for Part-Circumferential Cracks in Pipes," *Circumferential Cracks in Pressure Vessels and Piping - Vol. II*, ASME PVP - Vol. 95, pp. 35-48.

Harris, D. O., E. Y. Lim, and D. Dedhia. 1981. *Probability of Pipe Fracture in the Primary Coolant Loop of a PWR Plant, Volume 5: Probabilistic Fracture Mechanics Analysis*, Report NUREG/CR-2189, Vol. 5, U.S. Nuclear Regulatory Commission, Washington, D.C.

Harris, D.O., D. Dedhia, and S. C. Lu. 1992. *Theoretical and User's Manual for pc-PRAISE*, Report NUREG/CR-5864, U.S. Nuclear Regulatory Commission, Washington, D.C.

Keeney, J. A., and J. W. Bryson. 1995. "Stress-Intensity Factor Influence Coefficients for Semielliptical Inner-Surface Flaws in Clad Pressure Vessels," *Fracture Mechanics: 26th Volume*, ASTM STP 1256, pp. 430-443.

Lim, E. Y., D. Dedhia, and D. O. Harris. 1983. "Approximate Influence Functions for Part-Circumferential Interior Surface Cracks in Pipes," *Fracture Mechanics: Fourteenth Symposium - Vol. 1: Theory and Analysis*, ASTM STP 791, pp. I-281-I-296.

Murakami, Y. (Ed.). 1992. *Stress Intensity Factors Handbook*, Volume 3, Pergamon Press, New York.

Poette, C., and S. Albaladejo. 1991. "Stress Intensity Factors and Influence Functions for Circumferential Surface Cracks in Pipes," *Engineering Fracture Mechanics*, Vol. 39, No. 4, pp. 641-650.

Raju, I. S., and J. C. Newman, Jr. 1982. "Stress-Intensity Factor Influence Coefficients for Internal and External Surface Cracks in Cylindrical Vessels," *Aspects of Fracture Mechanics in Pressure Vessels and Piping*, ASME PVP - Vol. 58, pp. 37-48.

## Appendix E

### Sensitivity Studies for Fracture Mechanics Calculations

#### E.1 Introduction

This appendix presents results from two sets of sensitivity calculations. The first calculations were performed early during the research project and used the Latin hypercube cube methodology. These early calculations guided modifications to the pc-PRAISE code. The second set of sensitivity calculations was performed at the end of the research project with the modified version of pc-PRAISE. The objective of these calculations was to demonstrate the capabilities of the new crack-linking model. The results of the calculations showed the extent of crack linking and showed how the linking is dependent on input parameters to the probabilistic model.

#### E.2 Baseline Calculations

Before the modified version of pc-PRAISE was developed, sensitivity calculations were performed before the detailed evaluations of the components. These calculations applied the software described in an American Society of Mechanical Engineers (ASME) paper (Simonen and Khaleel 1998). The Latin hypercube approach featured in the methodology permitted rapid calculations of very small values of component failure probabilities. Application of the alternative Latin hypercube approach provided the following benefits:

1. The code served as an early test bed for the subroutine developed for simulating probabilities of cracking initiation as based on the equations from Argonne National Laboratory.
2. The code was an independent basis for validating the calculated probabilities of crack initiation and through-wall cracking provided by the new version of the pc-PRAISE code.
3. The code provided a method for calculating the very low values of through-wall crack probabilities that applied to some of the components. These probabilities could not be evaluated with the less efficient Monte Carlo methodology used by the pc-PRAISE code.
4. The code facilitated the sensitivity studies described here. A single input file could be used to address all the components of interest, and the calculations for all the components, including those with very small failure probabilities, could be calculated within a few minutes on a personal computer.

The discussion below describes the inputs and results of the sensitivity calculations. Inputs for the baseline cases of the sensitivity calculations were essentially the same as the inputs later used for the final pc-PRAISE runs of this report and as described in detail for each component in Appendix A.

**Wall Thickness** - The baseline wall thicknesses for the components were the same values listed in Appendix A. Sensitivity calculations studied systematic effects of wall thickness on through-wall crack probabilities by arbitrarily assigning the wall thickness of all components to either a small value (2.54 cm [1.0 in.]) or large value (20.32 cm [8.0 in.]).

**Stress Gradient** - The baseline was that of a zero through-wall stress gradient, meaning that the peak stress governing crack initiation at the inner surface remained uniform through the wall thickness and governed the growth ( $da/dN$ ) of the initiated crack. Several alternative assumptions regarding through-wall stress gradients were addressed by the sensitivity calculations.

**Initial Flaw Depth** - The baseline depth of the initiated crack was assigned a deterministic value of 3 mm. Variations from this initial flaw depth were considered in the sensitivity calculations.

**Flaw Length** - The baseline calculations assumed a flaw-aspect ratio of 10:1 corresponding to a semi-elliptical surface flaw of length  $10 \times 3 \text{ mm} = 30 \text{ mm}$ . For the baseline calculations, the flaw was assumed to grow with a constant aspect ratio. Alternative assumptions regarding the initial flaw length and changes in flaw-aspect ratios were considered by the sensitivity calculations.

**Multiple Crack-Initiation Sites** - The Latin hypercube calculations addressed only the initiation and growth of a single flaw and did not simulate the initiation and linking of multiple flaws as was possible with the later calculations performed with the pc-PRAISE code. As such, the calculations are relevant only to probabilities of through-wall cracks and were not intended to address probabilities of large leaks and pipe breaks.

**Correlations Between Crack Initiation and Crack Growth** - The baseline case assumed that the random variations in crack-growth rates ( $da/dN$ ) were independent of random variations in the number of cycles to crack initiation. This assumption was used for all the later calculations with the pc-PRAISE code. Sensitivity calculations addressed the effect of a perfect correlation between crack initiation and crack growth by using the same random number to sample from the distributions for crack initiation and crack growth.

**Start of Fatigue Crack Growth** - The baseline assumption was that fatigue-crack growth began with a crack depth of 3 mm and started at the time corresponding to the number of stress cycles needed to initiate the crack. Sensitivity calculations were performed to study the effect of a conservative assumption used in past calculations, whereby it was arbitrarily assumed that cracks that initiated any time during the life of the component were present (3-mm deep) and began to grow by fatigue at time = 0.0.

**Oxygen Content of Reactor Water** - The baseline cases used a reactor-water oxygen content of 0.010 ppm (10 ppb) for pressurized-water reactor (PWR) plants and 0.100 ppm (100 ppb) for boiling-water reactor (BWR) plants. These values were considered to realistic levels, but somewhat higher than expected for typical plant operating conditions. Sensitivity calculations considered somewhat lower and more typical values for water chemistries.

**Sulfur Content** - The baseline value of sulfur content was 0.015 weight percent for low-alloy steels. For stainless steels, the sulfur content does not appear in the equations for fatigue-crack initiation.

**Sensitivity calculations** considered the effects of somewhat lower and more typical values of sulfur than the bounding value of 0.015 percent.

**Strain Rate** - Lower strain rates result in fewer cycles to crack initiation and is a critical input parameter to the probabilistic fracture mechanics calculations. The baseline cases assumed a common strain rate of 0.001 percent per second for all components and all transients. Somewhat lower values were used for sensitivity calculations.

### E.3 Initial Flaw Depth (Figure E.1)

The Argonne National Laboratory (ANL) fracture mechanics model defines crack initiation as a surface flaw with a depth of about 3 mm. This depth was based on consideration of the 25 percent load drop method used to detect the presence of a crack in the fatigue testing procedure. In a given test, the actual depth of the crack could be somewhat less than 3 mm or greater than 3 mm. To address uncertainties regarding the initial crack depth, calculations were performed for flaw depths of 2 mm and 4 mm. As shown by Figure E.1, the calculated probabilities of through-wall crack increases somewhat for the 4-mm crack and decreases somewhat for the 2-mm crack. The increases or decreases are on the order of a factor of 2 and become insignificant for those components having relatively high failure probabilities.

Consideration was given to simulated simulating the initial flaw depth as an additional variable in the probabilistic model. This approach was not adopted because 1) the calculated failure probabilities were relatively insensitive to the assumed value of flaw depth and 2) uncertainties in the actual flaw depth corresponding to data on cycles to crack initiation are adequately included in the variability in cycles to crack initiation.

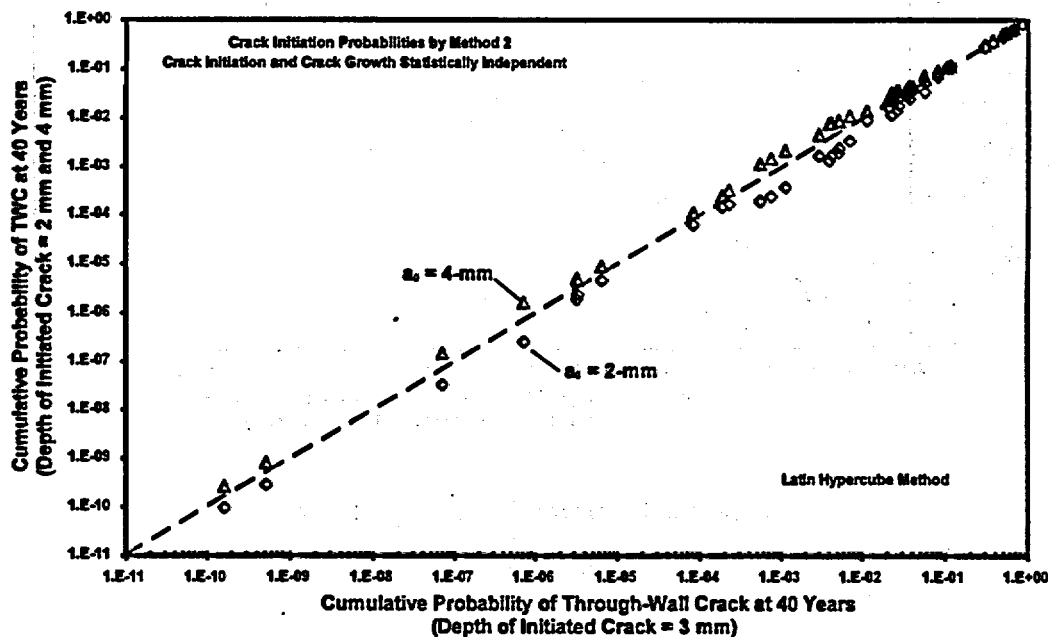


Figure E.1 Effects of Initial Crack Depth

## E.4 Flaw Length or Aspect Ratio (Figures E.2 and E.3)

The baseline fracture mechanics model used with the Latin hypercube method assumed that initiated cracks have aspect ratios of 10:1 (a length of 30 mm for the flaw depth of 3 mm). It was furthermore assumed that the aspect ratios of growing fatigue cracks remain at 10:1 as the cracks increase in depth.

Figure E.2 shows the effect of replacing the 10:1 aspect ratio with a value of 3:1. The smaller value of 3:1 was selected as bounding and somewhat less than typically observed for aspect ratios of growing fatigue cracks. The calculated probabilities of through-wall cracks decrease by a factor as great as 10, with the difference being greatest for low-failure probabilities and becoming relatively small for cases with relatively high failure probabilities. The results indicate (for purposes of predicting probabilities of through-wall cracks, but not for probabilities of large leaks and breaks) that precise inputs for modeling of flaw lengths is not critical to the calculations, provided that assumed values of aspect ratio are taken at relatively large values.

Figure E.3 shows the effect of a modification to the assumption that flaws grow with constant aspect ratio. Based on trends noted from the pc-PRAISE calculations, it was assumed that the increase in crack length was two times the corresponding increase in flaw depth. The resulting calculated failure probabilities are only slightly less than those obtained by assuming that a 10:1 aspect ratio is maintained as the fatigue cracks grow to through-wall depth.

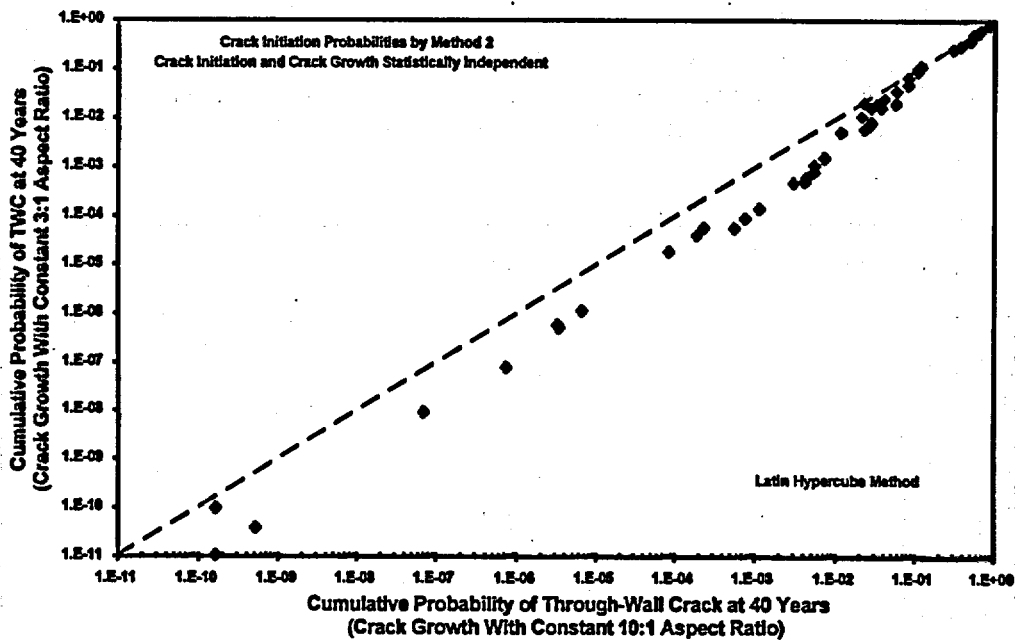


Figure E.2 Effect of Flaw-Aspect Ratio

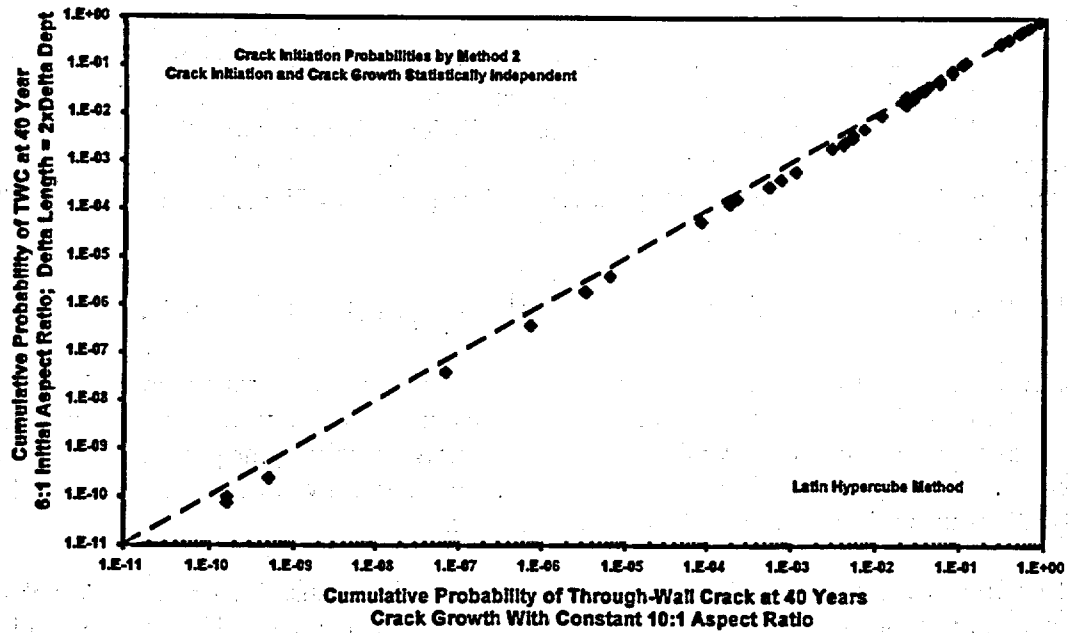


Figure E.3 Effect of Changing Aspect Ratio During Flaw Growth

### E.5 Effect of Wall Thickness (Figure E.4)

The results of Figure E.4 were generated by arbitrarily changing the wall thickness of each component to first 2.54 cm (1.0 in.) and then to 20.32 cm (8.0-in.). Whereas the probabilities of initiating a fatigue

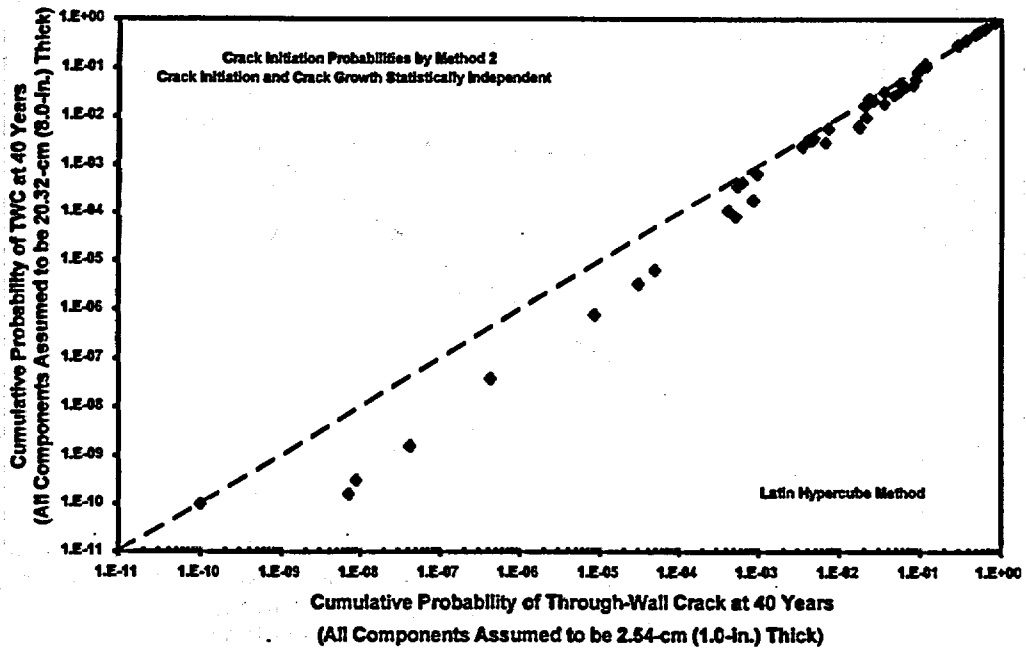


Figure E.4 Effect of Wall Thickness

crack do not change (there were no changes in the cyclic stress), the thicker component should have a greater fatigue life because more stress cycles are needed to grow the crack through the thicker metal path. The calculated results of Figure E.4 are consistent with this expectation, where the difference in failure probabilities are about a factor of 10 for relatively low failure probabilities, but become insignificant when the failure probabilities are relatively large. The results of Figure E.4 are based on a uniform through-thickness distribution of cyclic stress. The presence of large stress gradients will tend to offset the wall thickness effect seen in Figure E.4.

### E.6 Effect of Through-Wall Stress Gradients (Figures E.5 to E.9)

The baseline case conservatively assumes a uniform distribution of stress through the wall thickness, which means that the peak surface stress that governs crack initiation also is available to grow the small initiated crack to become a through-wall crack. For most stress transients, the peak surface stress is associated with stress gradients. Figures E.5 to E.9 show the sensitivity of calculated probabilities of through-wall cracks to the magnitude of these stress gradients.

Figure E.5 assumes a relatively modest gradient consisting of a linear distribution of stress such that the stress at the outer surface is 50 percent of the peak stress at the inner surface. This modest gradient has only a small effect (factor of 2 or less) in terms of decreasing the calculated probabilities of through-wall cracks.

Figure E.6 increases the magnitude of the linear stress gradient such that the outer surface stress becomes zero. In this case, the calculated probabilities of through-wall cracks decrease by as much as a factor of 10 relative to the baseline case.

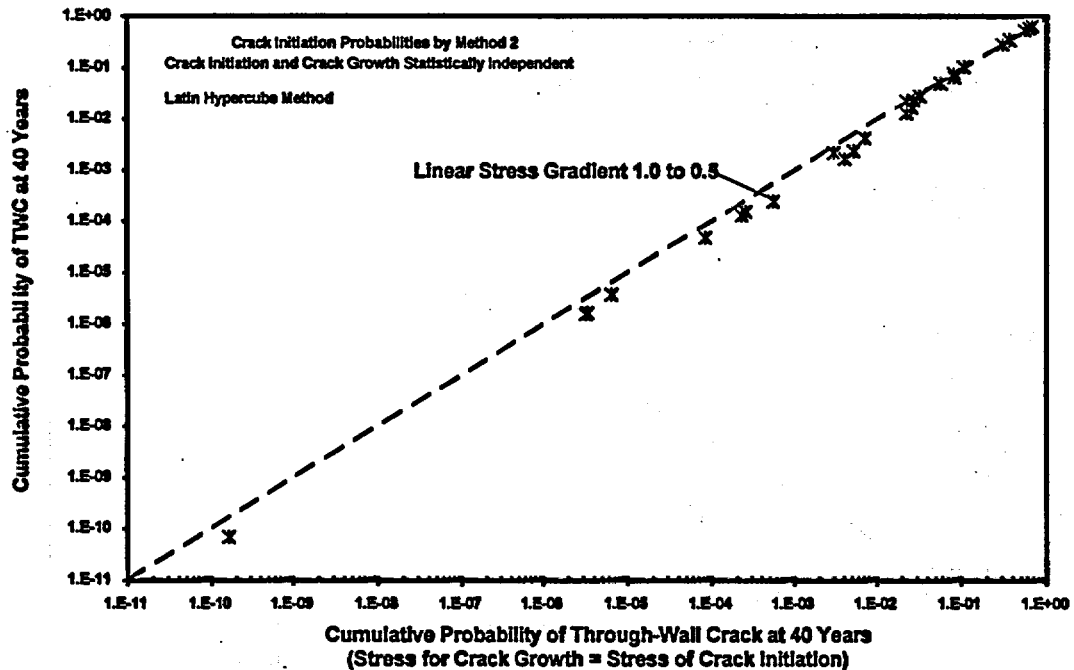


Figure E.5 Effect of Small Linear Stress Gradient

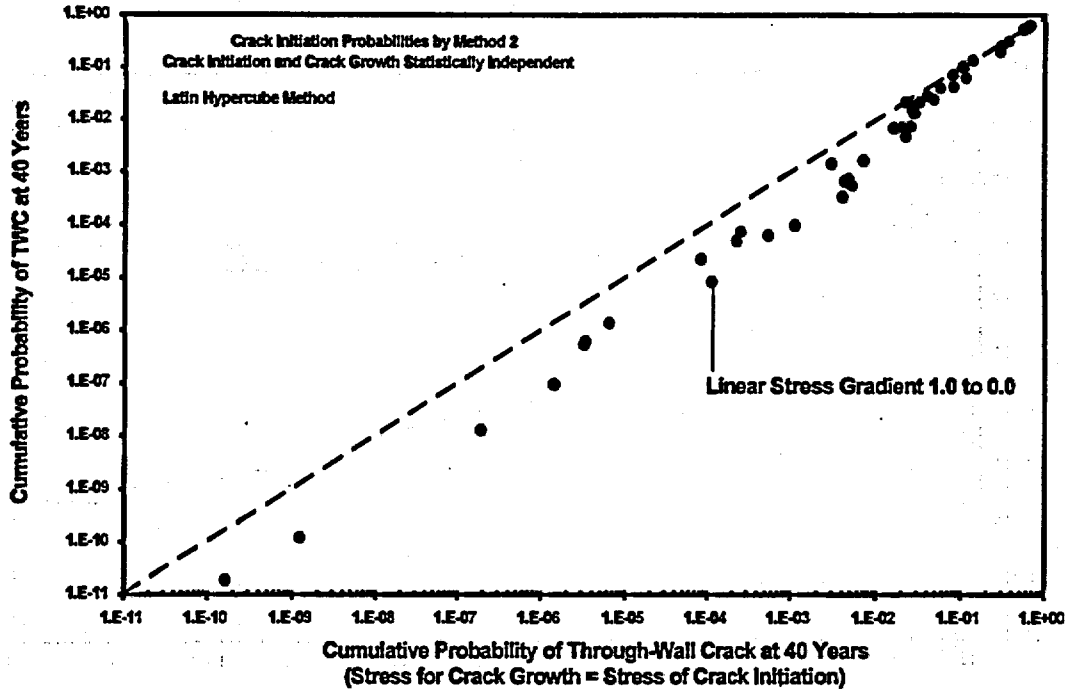


Figure E.6 Effect of Larger Linear Stress Gradient

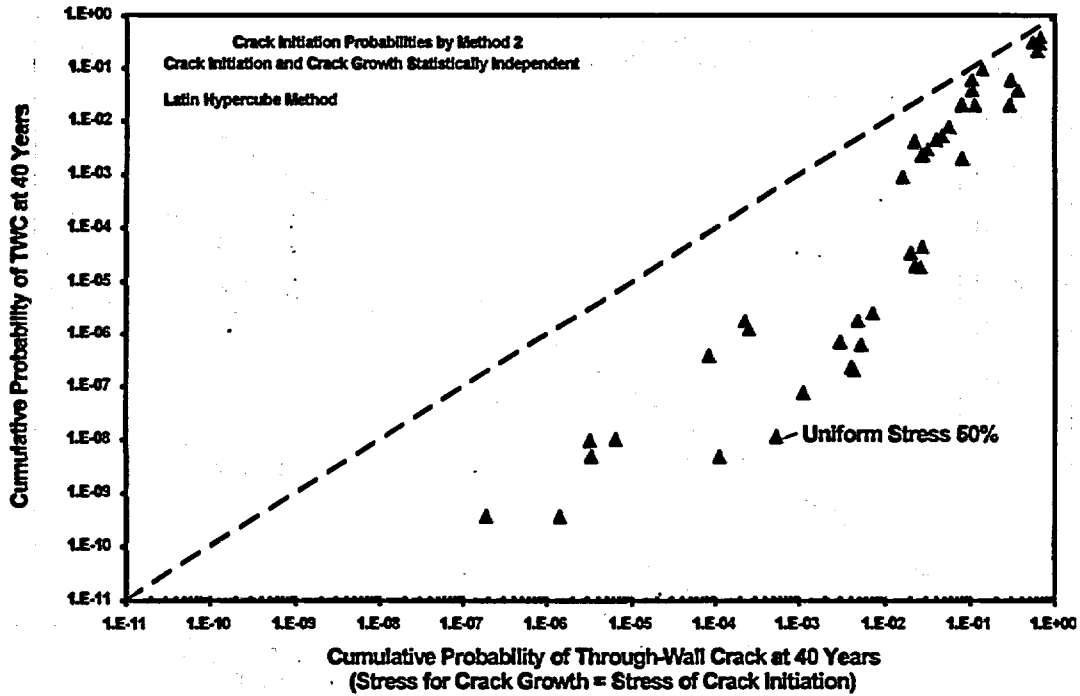


Figure E.7 Effect of Reduced Stress for Growth of Fatigue Crack

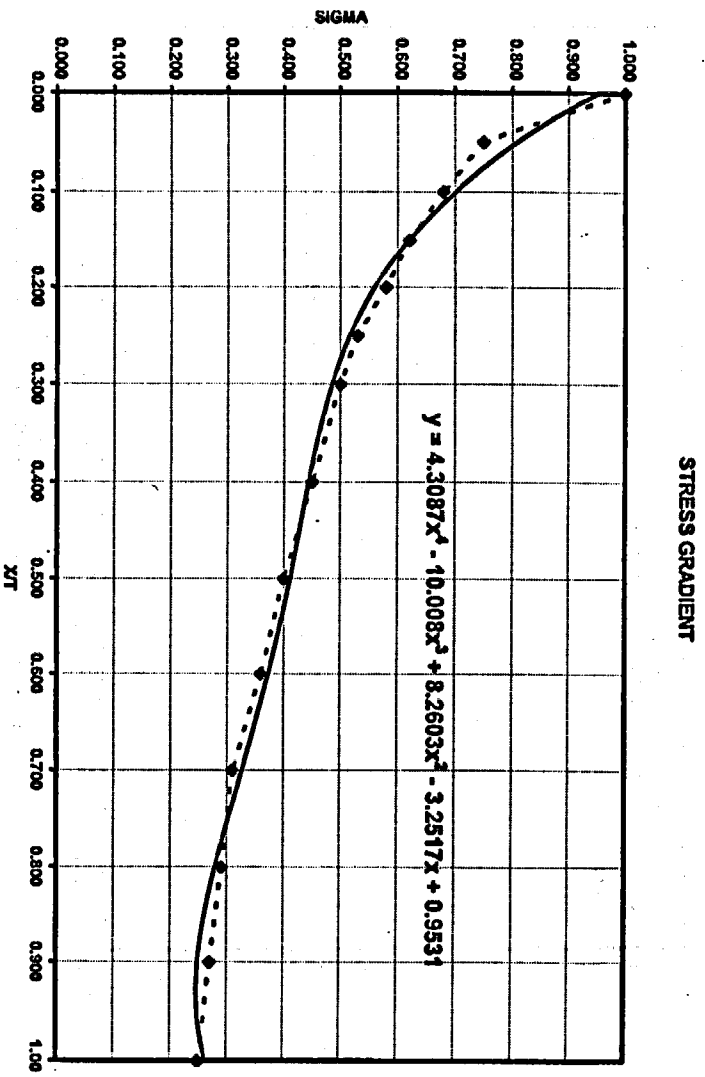


Figure E.8 Nonlinear Stress Gradient

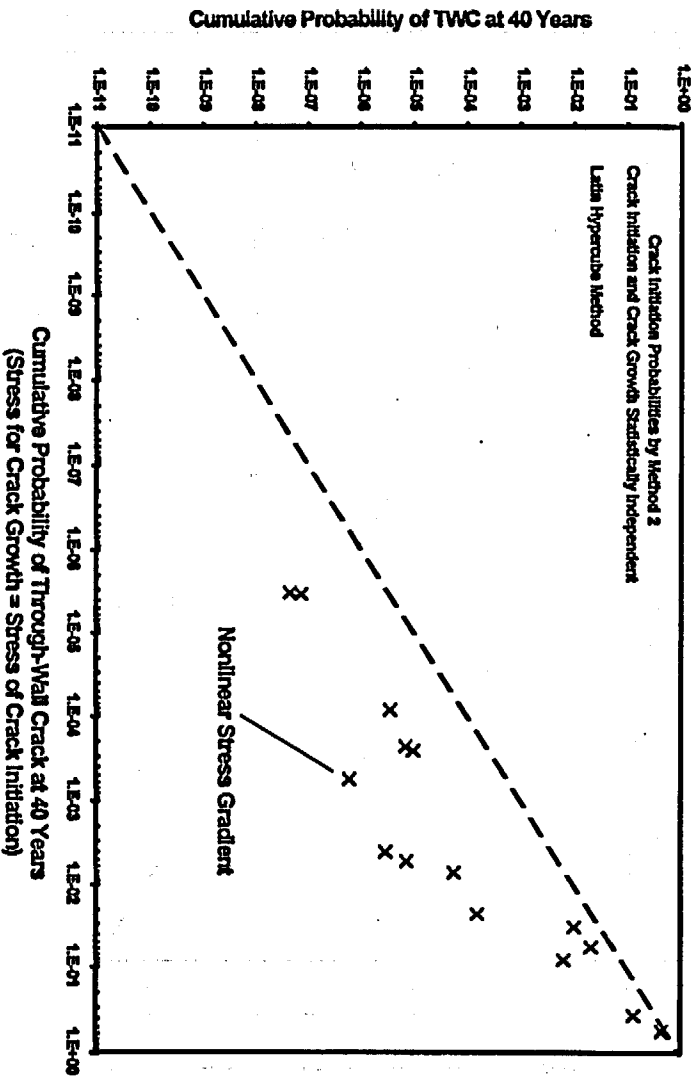


Figure E.9 Effect of Nonlinear Stress Gradient

Figure E.7 is based on a rather extreme assumption whereby the stress used for calculating crack-growth rates was assumed to be uniformly distributed through the wall thickness, but this stress was reduced to 50% of the peak surface stress used for the initiation of the crack. Such an assumption could approximate the situation where crack initiation is from very localized stress concentration. The resulting effect on through-wall crack probabilities is substantial and amounts to 3-4 orders of magnitude for cases of lower failure probabilities. The effect is much smaller for components with the higher failure probabilities, but is still a factor of about 10.

The results of Figures E.8 and E.9 are based on an assumed stress gradient that is more realistic or typical of a stress gradient produced by a transient thermal stress. The stress decreases (Figure E.8) most rapidly near the critical inner surface and eventually decreases at the outer surface to a level of 25% of the peak surface stress. Figure E.9 shows an effect of stress gradient that is about two orders of magnitude for lower failure-probability components and about one order of magnitude for components with higher failure probabilities.

It was concluded that realistic predictions of through-wall crack probabilities require modeling of through-wall stress gradients.

### E.7 Monte-Carlo Versus Latin Hypercube (Figure E.10)

Figure E.10 shows good agreement in calculated through-wall crack probabilities when failure probabilities are calculated using the Latin hypercube as opposed to the more conventional Monte Carlo approach. The comparison is limited to failure probabilities greater than about  $1.0E-04$  due to the larger

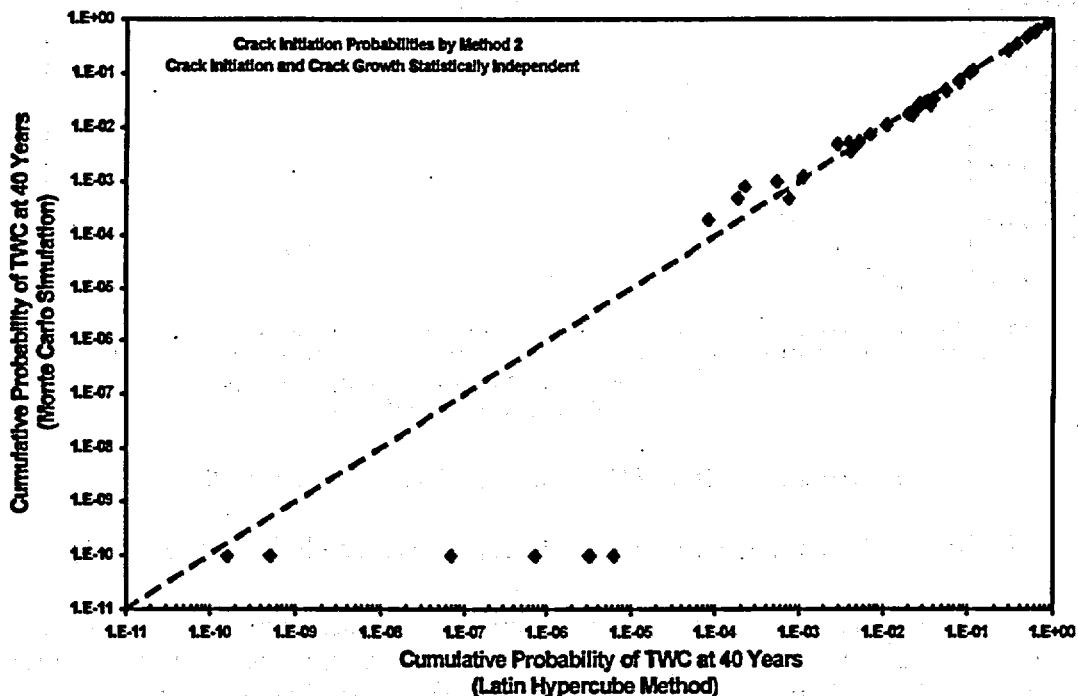


Figure E.10 Comparison of Monte Carlo and Latin Hypercube Predictions

computational effort associated with the Monte Carlo method. All calculations for Figure E.10 were performed with the special code that was developed by PNNL and that did not involve any application of the pc-PRAISE code.

### E.8 Crack Growth Starting at Time = 0.0 (Figure E.11)

Figure E.11 shows that the simplifying assumption used in prior calculations by PNNL can result in a significant overestimation of probabilities of through-wall cracks. The baseline calculation assumed that the crack-growth process begins only after the crack initiates. The simplified analysis first predicts if a crack initiates at any time over the evaluation period of interest. If a crack does initiate within this time period, the crack-growth process is assumed to occur over the entire time period. This approach will overestimate the maximum crack depth and will provide conservative predictions of through-wall crack probabilities. Figure E.11 indicates that failure probabilities can be overestimated by a factor of two orders of magnitude, although the differences become relatively small for components with the higher values of calculated failure probabilities.

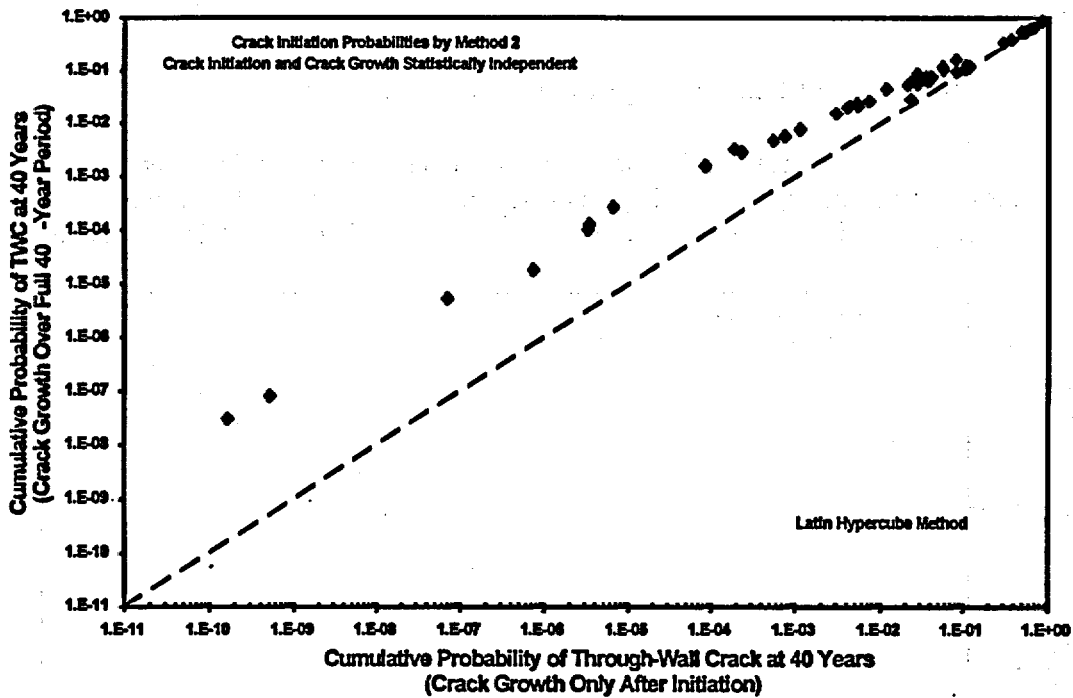


Figure E.11 Effect of Growing Cracks from Time = 0.0

### E.9 Correlation of Crack Initiation and Crack Growth (Figure E.12)

It was possible to modify the source code used for the Monte Carlo simulation (but not the Latin hypercube method) to assume perfect correlation between the random variations in crack initiation with the corresponding variations in the crack-growth rates. Such correlations were expected to increase the probability for that a crack that which initiates at a small number of stress cycles will subsequently grow at a faster than average crack-growth rate. The data points of Figure E.12 confirm this expectation. The

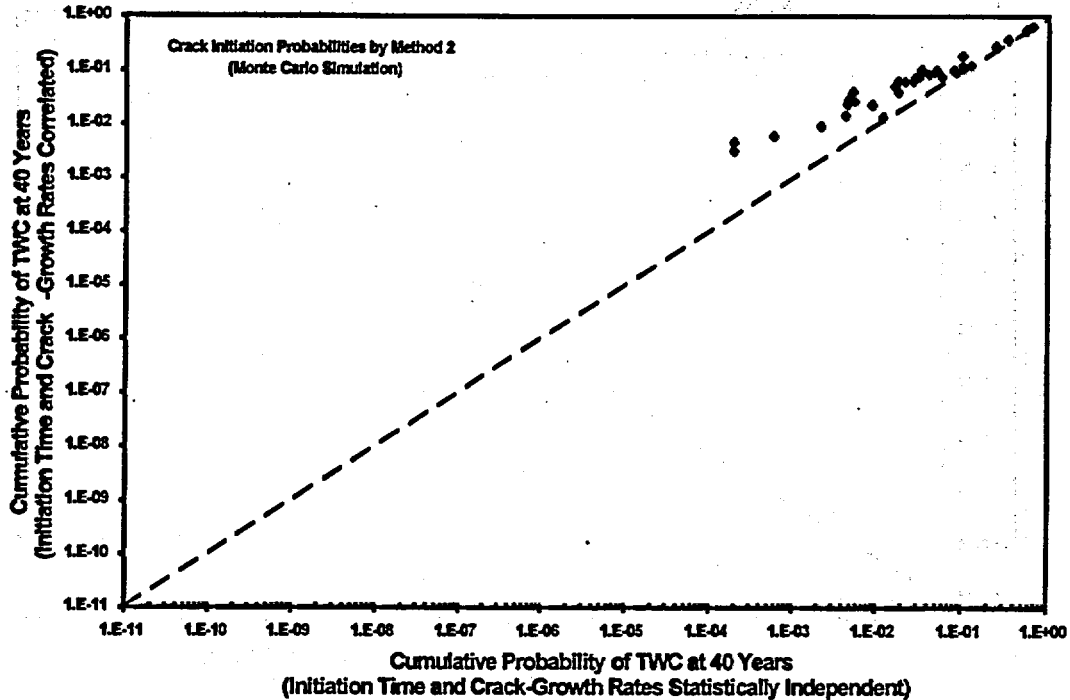


Figure E.12 Effect of Correlation Between Crack Initiation and Crack Growth

correlation increases the calculated failure probabilities by up to an order of magnitude, with the effect being larger when the failure probabilities are smaller. At failure probabilities greater than 1.0E-01, the effect appears to be negligible.

## E.10 Environmental and Material Characteristics (Figures E.13 to E.18)

A number of uncertain inputs for environmental parameters must be defined for application of the ANL equations for fatigue-crack initiation. The calculations of Figures E.13 to E.18 address the effects of these uncertainties on the calculated probabilities of through-wall cracks. The inputs of interest are the oxygen content of the reactor water, the sulfur content of the steel, and the strain rate associated with the cyclic stresses.

Figure E.13 addresses the effect of oxygen content with the baseline case for these calculations being a relatively low oxygen level of 0.01 ppm that is typical of PWR conditions. The sensitivity calculations increased this level to 0.10 ppm (BWR conditions). It should be noted that these sensitivity calculations arbitrarily assigned the same oxygen level to all components without regard to whether they corresponded to a PWR or BWR plant. It is seen in Figure E.13 that increasing the oxygen level over the selected range of uncertainty has at most an order of magnitude effect on calculated probabilities of through-wall cracks. In some cases, the probabilities increase (ferritic steel components), and in other cases, there is a decrease in the calculated probabilities (stainless steel components) decrease.

Figures E.14 and E.15 show the sensitivity of calculated failure probabilities to strain rates and indicate that low strain rates can result in higher values of calculated failure probabilities. The default strain rate used in the baseline calculations was 0.001. Figure E.14 shows the effect of using a value of 0.01, which

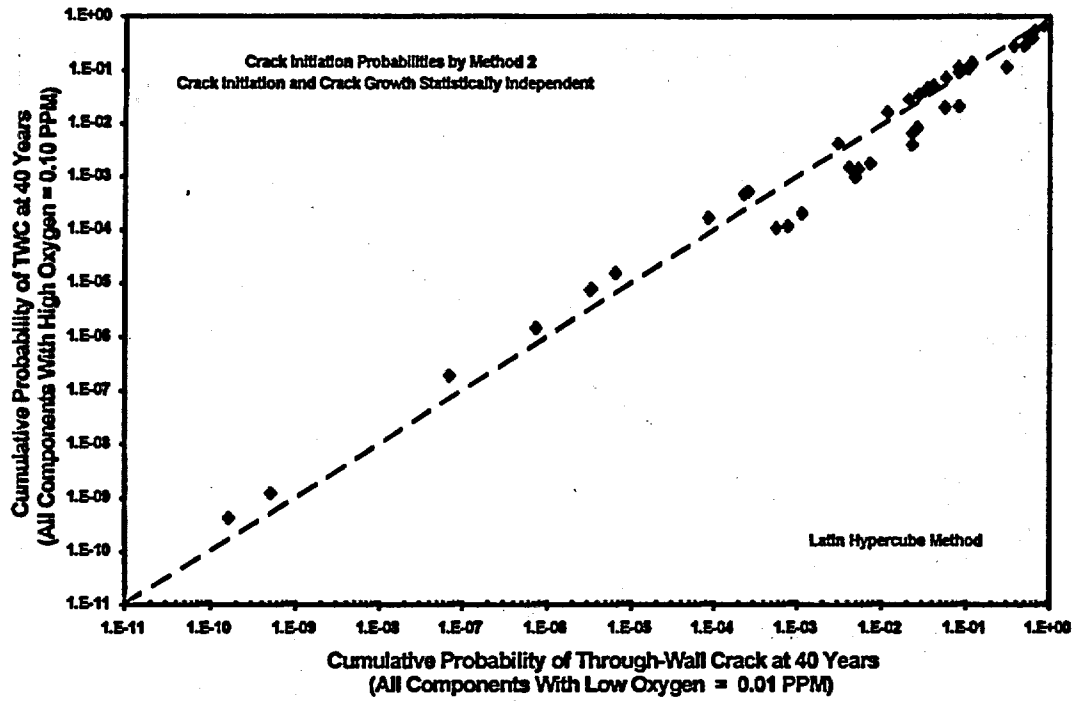


Figure E.13 Effect of Increased Oxygen Content

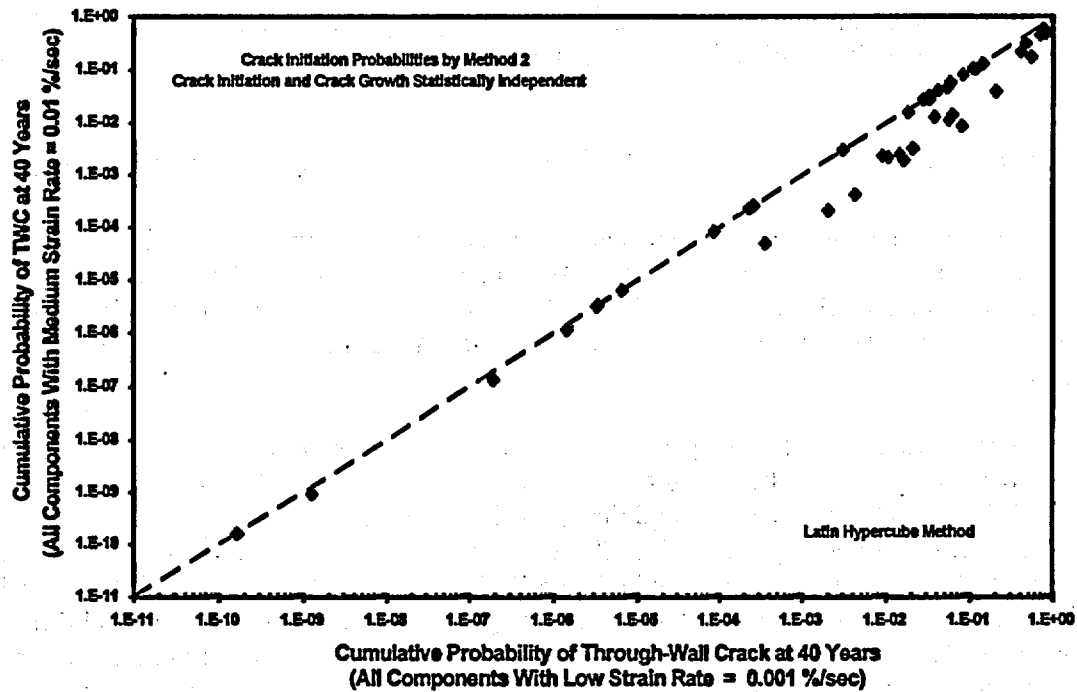


Figure E.14 Effect of Small Increase in Strain Rate

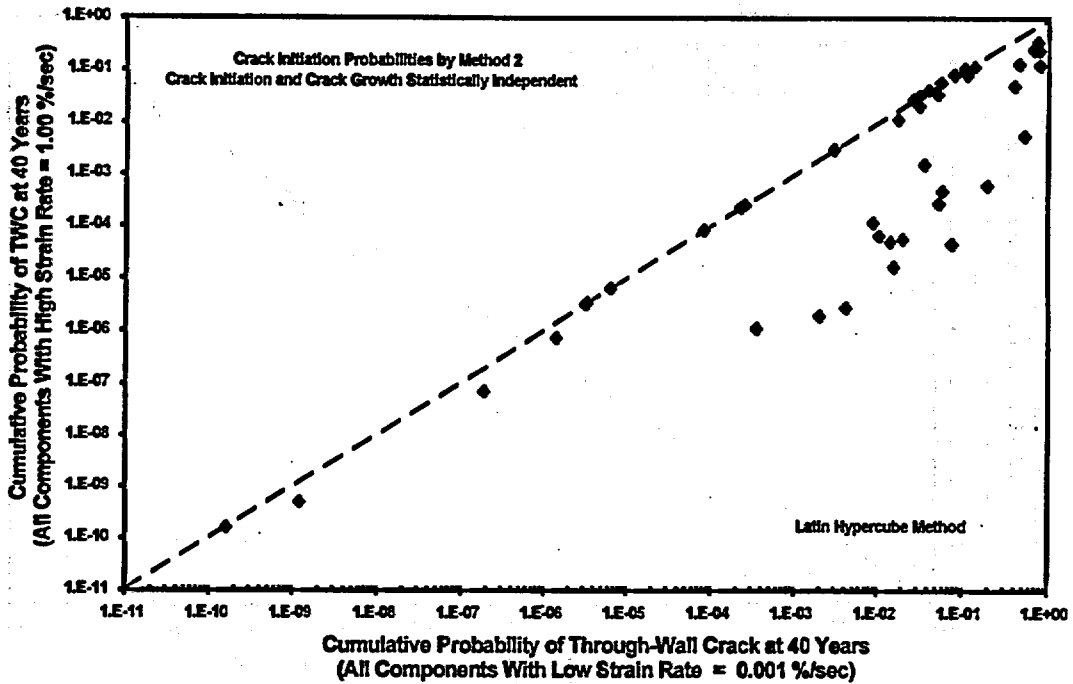


Figure E.15 Effect of Large Increase in Strain Rate

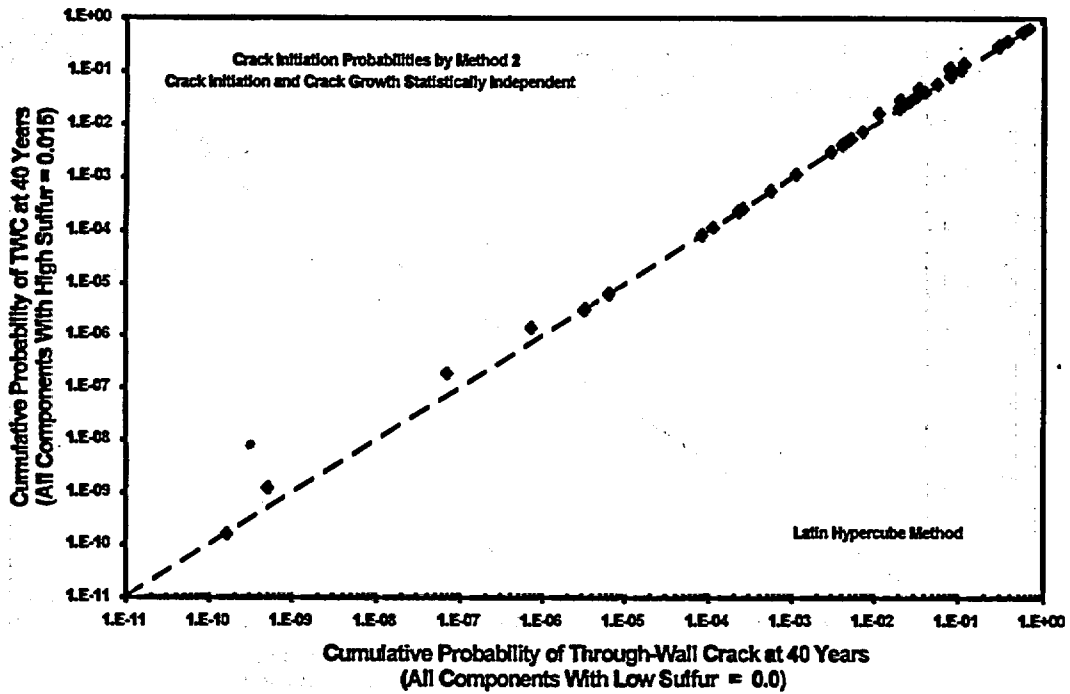


Figure E.16 Effect of Reduced Sulfur Content

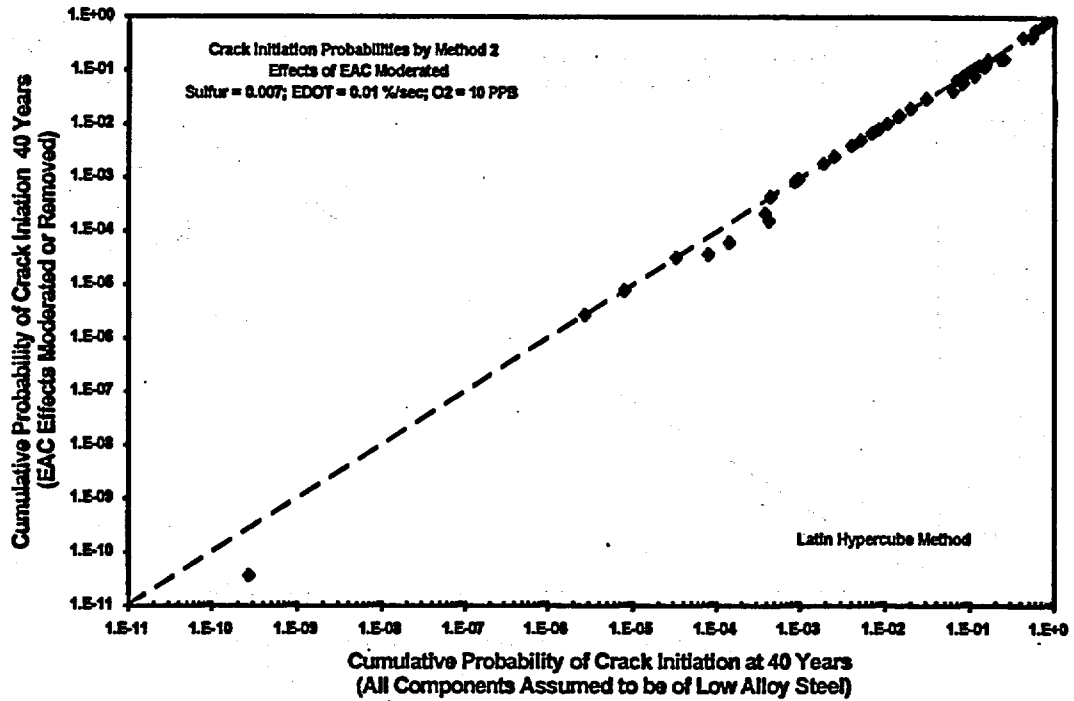


Figure E.17 Effect of Reduced EAC for Low-Alloy Steel

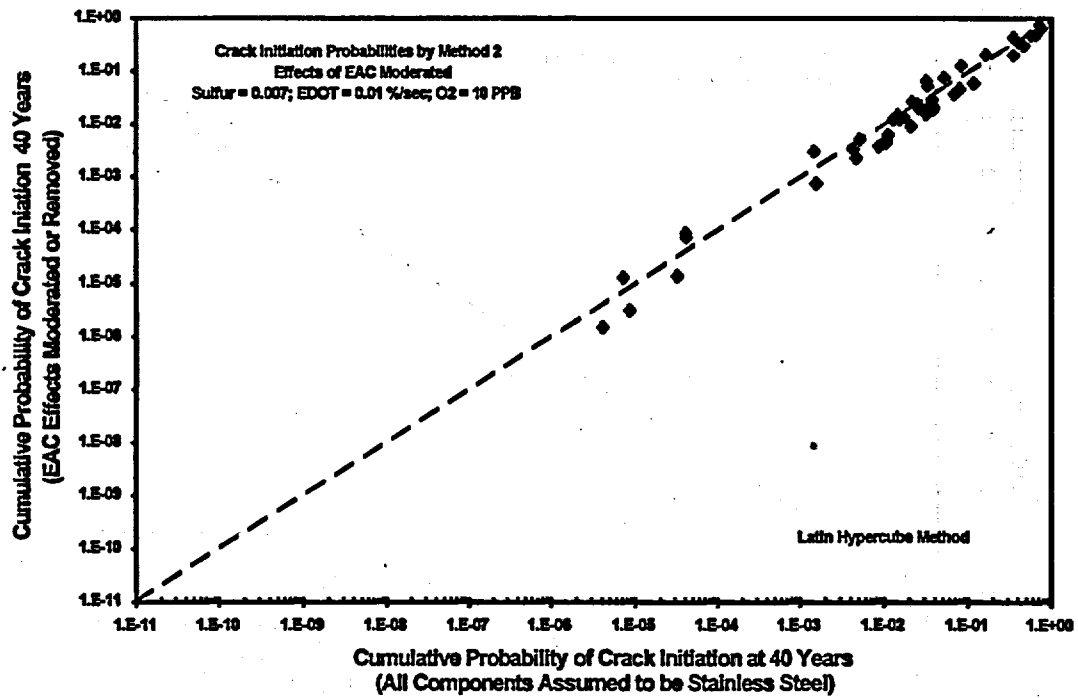


Figure E.18 Effect of Reduced EAC for Stainless Steel

could correspond to an actual transient with a relatively rapid loading rate. With the faster loading rates, it is seen in Figure E.14 that some of the calculated failure probabilities decrease by as much as a factor of 10. Failure probabilities for another grouping of components (ferritic steel) show little if any change. Figure E.15 increases the strain rate by a factor of 1000, and these results show more substantial decreases in calculated failure probabilities for the higher strain rate.

Figure E.16 shows the effect of increasing the sulfur content of the steel from 0.0 percent to 0.015 percent. Some failure probabilities show no increase (stainless steel) whereas other components show only a modest increase (less than a factor of 2.0).

Figure E.17 (low-alloy steel) and Figure E.18 (stainless steel) show the effect of changing the inputs from bounding values that govern environmentally assisted fatigue to more moderate values that may be more typical of actual plant operation. Each figure has baseline inputs of strain rates of 0.001%/min, oxygen of 100 ppb, and sulfur of 0.015 percent. In constructing these figures, the material type for all components was arbitrarily set to either low-alloy steel (Figure E.17) or stainless steel (Figure E.18) for purposes of addressing effects of environmental factors. Within the relatively small range of uncertainty (as considered here) the changes in calculated failure probabilities were relatively small (factor of 2 or less). The assumption in these calculations was that the exclusion of environmental effects could not be justified for any of the components. Other sensitivity calculations (not reported in this appendix) compare calculated through-wall crack probabilities for air environment versus probabilities for water environment.

## **E.11 A Study of Crack Lengths and Linking as Predicted by pc-PRAISE**

The pc-PRAISE model for fatigue crack initiation was applied to simulate the initiation, growth, and linking of thermal fatigue cracks for a small-diameter pipe. The objective was to demonstrate the ability of pc-PRAISE to predict realistic lengths of circumferential cracks. A second objective was to perform sensitivity calculations to evaluate the effects of modeling assumptions and alternative inputs to the model. The calculated crack lengths were then compared to the size and shape of the cracking reported for a small-diameter pipe of the high-pressure injection system at the Oconee 2 plant.

The calculations address a stainless steel pipe with an inner diameter of 7.37 cm (2.9 in.) and a wall thickness of .76 cm (0.3 in.). The baseline case of the calculation was intended to correspond to inputs and assumptions used for the selected components of the recent PNNL calculations. The following describes the baseline case:

- 100% of the cyclic stress assigned to the thermal-gradient category
- no circumferential variation of cyclic stress
- cycles to crack initiation sampled independently at each circumferential site
- five sites for crack initiation around circumference of the pipe
- 1-percent probability that the length of the initiated fatigue crack will exceed the length of the initiation site.

Table E.1 lists the calculations for five variations of the input parameters from those of the baseline case.

The magnitudes and numbers of the cyclic stresses were selected to give calculated probabilities of through-wall cracks that approached 100 percent. The objective was not to predict failure probabilities per se, but to predict the circumferential extent of cracking that develops late in the life of a highly stressed component.

It was not possible to make a direct comparison of the probabilistic calculations with the single observed case of Oconee-2 pipe failure (see Figure E.19). The present comparisons were therefore based on calculated distributions of cracks corresponding to the time at which the probability of through-wall cracking attained a value of 50 percent.

A further complication was that the pc-PRAISE model assumes that initiated fatigue cracks start immediately with a depth of 3 mm. For the small 7.62-cm (3-in.) diameter pipe, this 3-mm crack is about 40 percent of the pipe wall. Much of the cracking in the Oconee-2 event was of depths less than 30 percent of the pipe wall. The pc-PRAISE model does not currently address the growth of the very shallow cracks. The output of the computer code fails to define the depths of these small cracks before such time that the crack attains the threshold depth of 3-mm. Therefore, that portion of the Oconee cracking with depths less than 3-mm should be treated as uncracked in the context of the approach taken by the fracture mechanics model.

The cracked Oconee pipe of interest is shown by Figure E.19. The crack length at the outer surface had become 21 percent of the pipe circumference when the leak rate caused the plant operators to bring the plant into a shutdown mode. In addition to the through-wall portion of the crack, the pipe had part-through cracking around the remaining circumference. About 47 percent of the pipe circumference had cracking that exceeded the 3-mm threshold of the pc-PRAISE model.

Table E.2 shows a typical output table produced by pc-PRAISE. This table provided data on the simulated crack lengths and the extent of crack linking.

The columns of Table E.1 further summarize trends from the detailed output tables such as Table E.2. Several global measures of the extent of circumferential cracking are used to describe the circumferential cracking as indicated by the column headings.

The baseline case of Table E.1 predicts that 40 to 60 percent of the pipe circumference will be cracked (at a probability of about 50 percent), depending on the particular measure selected to describe the circumferential cracking. The percentage range is generally consistent with an interpretation of the cracking of the Oconee pipe. The higher numbers (60%) of the final two columns of Table E.1 are based on a weld-by-weld summary of the simulated data. These tabulations characterize only the total amount of circumferential cracking and do not consider whether this cracking is from one big crack or from the sum of several smaller unconnected cracks.

The second calculation assumes that part of the cyclic stress is uniform tension (i.e., 20%) rather than a pure through-wall thermal-gradient stress. The predicted probability for long cracks decreases markedly. This suggests that the cracking pattern of the Oconee failure is characteristic of a pure thermal-gradient stress.

<b>Table E.1 Comparison of Alternative pc-PRAISE Calculations with Oconee-2 Event</b>				
<b>Measure of the Circumferential Extent of Cracking</b>				
	<b>Percent of Deep Cracks (A/t &gt;80%) that are the Result of Two or More Linking of Cracks from Adjacent Sites (Q1)</b>	<b>Percent of Deep Cracks (A/t &gt;80%) That are Longer than 40% of the Circumference (Q4)</b>	<b>Percent of Cracked Welds That have Cracking over More than 60% of the Inner Circumference (Q2)</b>	<b>Percent of the Welds that have Deep Cracking (A/t &gt;80%) that Extends the Deep Cracking over More than 60% of the Circumference (Q3)</b>
<b>Oconee-2</b>	<b>(%)</b>	<b>100%</b>	<b>0% If Cracking &lt;3-mm is Neglected 100% If Crack &lt;3-mm is Included (%)</b>	<b>0%</b>
Baseline Calculation	78.0	73.4	51.8	52.6
Calculation with 80% thermal-gradient stress and 20% uniform-tension stress	31.1	3.4	0.2	0.0
Calculation with 5 circumferential sites for crack initiation increased to 10 sites	19.8	24.4	64.0	59.3
Calculation with length of initiated crack increased from 1% probability for 5.08-cm (2-in.) crack to 10% probability	78.9	81.5	59.0	58.1
Cycles for crack initiation 100% correlated from site-to-site (but no circumferential variation in cyclic stress)	100.0	98.8	84.2	92.8
Cycles for crack initiation 100% correlated from site-to-site (with a 20% circumferential variation in cyclic stress)	89.4	92.8	71.1	77.4

**Table E.2 Output from pc-PRAISE for Baseline Calculation Showing Extent of Crack Linking**

At time (yrs) 20.00

.00< a/h <= .30

% circumf.	[ ALL ]	[ 1 ]	[ 2 ]	[ 3 ]	[ 4 ]	[ 5 ]	[6-10 ]	[11-15]	[16-20]	[21-30]	[31-40]	[ >41 ]
.0- 20.0	01	0	0	0	0	0	0	0	0	0	0	0
20.0- 40.0	01	0	0	0	0	0	0	0	0	0	0	0
40.0- 60.0	01	0	0	0	0	0	0	0	0	0	0	0
60.0- 80.0	01	0	0	0	0	0	0	0	0	0	0	0
80.0-100.0	01	0	0	0	0	0	0	0	0	0	0	0

.30< a/h <= .60

% circumf.	[ ALL ]	[ 1 ]	[ 2 ]	[ 3 ]	[ 4 ]	[ 5 ]	[6-10 ]	[11-15]	[16-20]	[21-30]	[31-40]	[ >41 ]
.0- 20.0	4221	422	0	0	0	0	0	0	0	0	0	0
20.0- 40.0	01	0	0	0	0	0	0	0	0	0	0	0
40.0- 60.0	01	0	0	0	0	0	0	0	0	0	0	0
60.0- 80.0	01	0	0	0	0	0	0	0	0	0	0	0
80.0-100.0	01	0	0	0	0	0	0	0	0	0	0	0

.60< a/h <= .80

% circumf.	[ ALL ]	[ 1 ]	[ 2 ]	[ 3 ]	[ 4 ]	[ 5 ]	[6-10 ]	[11-15]	[16-20]	[21-30]	[31-40]	[ >41 ]
.0- 20.0	4171	417	0	0	0	0	0	0	0	0	0	0
20.0- 40.0	71	3	4	0	0	0	0	0	0	0	0	0
40.0- 60.0	11	0	0	1	0	0	0	0	0	0	0	0
60.0- 80.0	01	0	0	0	0	0	0	0	0	0	0	0
80.0-100.0	01	0	0	0	0	0	0	0	0	0	0	0

.80< a/h <= .95

% circumf.	[ ALL ]	[ 1 ]	[ 2 ]	[ 3 ]	[ 4 ]	[ 5 ]	[6-10 ]	[11-15]	[16-20]	[21-30]	[31-40]	[ >41 ]
.0- 20.0	451	45	0	0	0	0	0	0	0	0	0	0
20.0- 40.0	1901	108	82	0	0	0	0	0	0	0	0	0
40.0- 60.0	1101	0	53	57	0	0	0	0	0	0	0	0
60.0- 80.0	261	0	0	19	7	0	0	0	0	0	0	0
80.0-100.0	31	0	0	0	0	3	0	0	0	0	0	0

.95< a/h <= 99.00

% circumf.	[ ALL ]	[ 1 ]	[ 2 ]	[ 3 ]	[ 4 ]	[ 5 ]	[6-10 ]	[11-15]	[16-20]	[21-30]	[31-40]	[ >41 ]
.0- 20.0	01	0	0	0	0	0	0	0	0	0	0	0
20.0- 40.0	71	7	0	0	0	0	0	0	0	0	0	0
40.0- 60.0	1341	35	92	7	0	0	0	0	0	0	0	0
60.0- 80.0	3071	0	4	120	183	0	0	0	0	0	0	0
80.0-100.0	631	0	0	13	41	9	0	0	0	0	0	0

	>0	>0.3h	>0.6h	>0.8h	>.95h
0 - 20%	44	44	84	18	0
20-40%	158	158	152	131	7
40-60%	278	278	259	241	134
60-80%	417	417	396	364	307
>80%	98	98	83	69	63

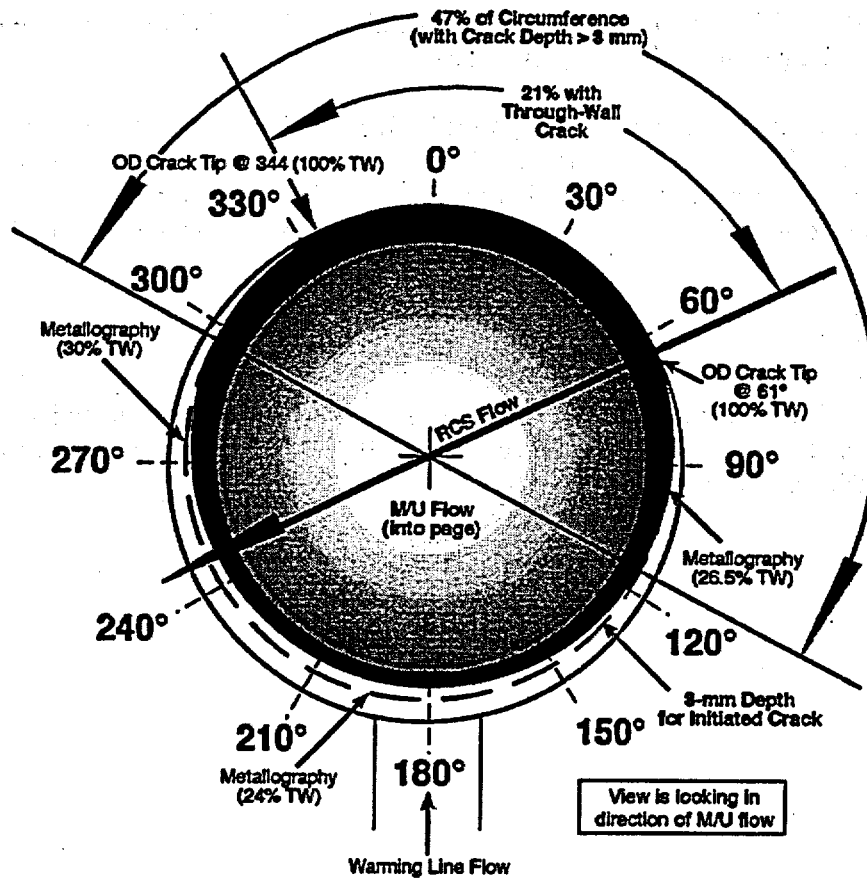


**Figure E.19 Small-Diameter Pipe with Cracking Caused by Thermal-Fatigue Stresses (LER No. 270/97-001)**

The third calculation of Table E.1 increases the number of crack initiation sites from 5 to 10. The length of the sites decreased from about 5.08 cm (2 in.) to about 2.54 cm (1 in.). There is little change in the overall amount of circumferential cracking changes little, but the lengths of the individual cracks tend to decrease. This means that there are more cracks, but the average length of the cracks becomes shorter:

The fourth calculation of Table E.1 keeps the number of initiation sites at five, but increases the probability that a long crack will span the entire 5.08-cm (2-in.) length of the initiation site. The median length of the initiated crack was not changed from the baseline value of 1.52 cm (0.6 in.). Table E.1 shows little change in the calculated probabilities for larger amounts of circumferential cracking.

The fifth calculation of Table E.1 assumes a perfect correlation between the cycles to crack initiation from site-to-site in a given weld. That is, if one of the five sites becomes cracked, the assumption is that all of the other sites will also crack at the same time. This assumption ignores the characteristic scatter in fatigue data. The predictions of Table E.1 show very high probabilities for cracking a large fraction of the pipe circumference.

The final calculation of Table E.1 expands on the previous calculation. The site-to-site randomness of fatigue lives is again taken to be zero, but there is a 20% circumferential variation in the cyclic stress

level. The circumferential variation gives a modest reduction in the probability for large fractions of circumferential cracking compared to the previous case.

The discussion here is an interpretation of the pc-PRAISE predictions compared to the cracking observed at Oconee. It appears that the predicted cracking is generally consistent with the observed cracking. The service failure had deep cracking over 20 to 50 percent of the pipe circumference, whereas the pc-PRAISE baseline calculation predicted deep cracking over some 40 to 60 percent of the pipe circumference.

## **E.12 Reference**

Simonen, F. A., and M. A. Khaleel. 1998. "A Probabilistic Fracture Mechanics Model for Fatigue Crack Initiation in Piping," PVP-373, pp. 27-34, Proceedings of 1998 ASME Pressure Vessel and Piping Conference, San Diego, California.

### BIBLIOGRAPHIC DATA SHEET

(See instructions on the reverse)

1. REPORT NUMBER  
(Assigned by NRC, Add Vol., Supp., Rev.,  
and Addendum Numbers, if any.)

NUREG/CR-6674

PNNL-13227

2. TITLE AND SUBTITLE

Fatigue Analysis of Components for 60-Year Plant Life

3. DATE REPORT PUBLISHED

MONTH	YEAR
June	2000

4. FIN OR GRANT NUMBER

W6671

5. AUTHOR(S)

M.A. Khaleel, F.A. Simonen/PNNL  
D.O. Harris, D. Dedhia/EMT

6. TYPE OF REPORT

Technical

7. PERIOD COVERED (Inclusive Dates)

8. PERFORMING ORGANIZATION - NAME AND ADDRESS (If NRC, provide Division, Office or Region, U.S. Nuclear Regulatory Commission, and mailing address; if contractor, provide name and mailing address.)

Pacific Northwest National Laboratory  
Richland, WA 99352

Subcontractor:  
Engineering Mechanics Technology, Inc.  
San Jose, CA 95129

9. SPONSORING ORGANIZATION - NAME AND ADDRESS (If NRC, type "Same as above"; if contractor, provide NRC Division, Office or Region, U.S. Nuclear Regulatory Commission, and mailing address.)

Division of Engineering Technology  
Office of Nuclear Regulatory Research  
U.S. Nuclear Regulatory Commission  
Washington, DC 20555-0001

10. SUPPLEMENTARY NOTES

Syed K. Shaukat, NRC Project Manager

11. ABSTRACT (200 words or less)

Probabilistic fracture mechanics calculations were performed to assess the significance of the revised fatigue curves. Failure probabilities and associated core-damage frequencies were estimated for RPV and piping components of five pressurized water reactor and two boiling water reactor plants. These calculations were made possible by the development of a new version of the pc-PRAISE probabilistic fracture mechanics code that simulates the initiation of fatigue cracks in combination with the growth of these cracks. The calculations indicate that the critical components with the highest probabilities of failure can have through-wall crack frequencies that are on the order of about  $5 \times 10^{-2}$  per year. These components show little or no increase in the failure frequency from 40 years to 60 years. Other components with lower failure probabilities can have their failure frequencies increased by a factor of about 10 over this same 20-year time period. Changing to a reactor water environment from an air environment increased the calculated failure probabilities by a factor of about 100. Contributions to core damage frequencies have also been estimated for each of the vessel and piping components. The maximum calculated contributions are on the order of  $10^{-6}$  per year. An appendix to this report describes sensitivity calculations that evaluate the effects of the many uncertainties of concern.

12. KEY WORDS/DESCRIPTORS (List words or phrases that will assist researchers in locating the report.)

Fatigue, Probabilistic Fracture Mechanics, Reactor Piping, Reactor Pressure Vessel

13. AVAILABILITY STATEMENT

unlimited

14. SECURITY CLASSIFICATION

(This Page)

unclassified

(This Report)

unclassified

15. NUMBER OF PAGES

16. PRICE



**Federal Recycling Program**

**UNITED STATES  
NUCLEAR REGULATORY COMMISSION  
WASHINGTON, D.C. 20555-0001**



**SPECIAL STANDARD MAIL  
POSTAGE AND FEES PAID  
USNRC  
PERMIT NO. G-67**